



TRC0902

**Evaluation of the  
Enhanced Integrated Climatic Model  
for the  
Arkansas State Highway and  
Transportation Department**

John S. McCartney, R. Panneer Selvam, Josh King, Ali Khosravi

Final Report

2010

**TRC-0902: Evaluation of the Enhanced Integrated Climatic Model for the  
Arkansas State Highway and Transportation Department**

John S. McCartney, Ph.D.

Barry Faculty Fellow and Assistant Professor

Department of Civil, Environmental, and Architectural Engineering

University of Colorado at Boulder

R. Panneer Selvam, Ph.D, P.E., ASCE Fellow

James T. Womble Professor of Computational Mechanics

and Nanotechnology Modeling

Director of Computational Mechanics Lab, Adjunct Faculty Electrical Engineering

Assist. Director of Microelectronics & Photonics & Member of HiDEC

Department of Civil Engineering

University of Arkansas

Josh King

Undergraduate Research Assistant

Department of Civil Engineering

University of Arkansas

Ali Khosravi

Graduate Research Assistant

Department of Civil, Environmental, and Architectural Engineering

University of Colorado at Boulder

June 30, 2010

**ABSTRACT**

Analysis of water and heat flow through layered pavement systems is an important part of the site-specific design of pavements. For instance, the temperature and water content are closely associated with the mechanical properties of the pavement soils which govern deformation response under traffic loading, and the predicted water pressures from a flow analysis can be used to design the pavement drainage system. The Enhanced Integrated Climatic Model (EICM) is the component of the Mechanistic-Empirical Pavement Design Guide (ME-PDG) that involves analysis of water and temperature flow through pavement layers. The goal of the ME-PDG is to provide a quantitative, site-specific assessment of the pavement section needed to resist the traffic loading for a given lifetime, and the EICM plays an important role in defining the material properties used in this design guide. AASHTO has recommended that the ME-PDG be used by state departments of transportation in pavement design. However, the Arkansas State Highway and Transportation Department (AHTD) has noticed that use of the ME-PDG in design has led to the prediction of thinner pavement sections than obtained through current design approaches, indicating that it may potentially be under-conservative. Accordingly, AHTD has commissioned several research projects to evaluate the ME-PDG. This study is specifically focused on an in-depth evaluation of the EICM in order to reduce the sources of uncertainty in the ME-PDG design results.

The first step in the evaluation of the EICM was to compare its predictions for a set of baseline cases with those of a well-calibrated model for flow of temperature and water through unsaturated soils, VADOSE/W. Because the EICM incorporates an empirical model to consider the impact of the asphalt layer on infiltration and evaluation, the baseline cases were defined to assess how the EICM considers infiltration and evaporation boundary conditions. Comparison with the results from VADOSE/w indicates that the EICM responds reasonably to precipitation rates less than a certain threshold (0.0001 ft/hr), but shows the same boundary condition for higher precipitation rates. In addition, the EICM showed no response to changes in the boundary conditions leading to evaporation (relative humidity and temperature).

The next step of this project involved comparison of EICM predictions with measured temperature and pore water pressure distributions beneath pavement systems located in different climatic zones of Arkansas. An innovative approach to measure pore water pressure and temperature profiles in pavements was developed, in which sensors were placed into a borehole in the subgrade beneath the asphalt. This approach was found to provide satisfactory results over the course of a year for 7 sites, which were consistent with weather data obtained from locations close to the sites. Comparison of the EICM and VADOSE/W model results with the field measurements indicate that the EICM did not provide an adequate representation of the changes in pore water pressure in the subgrade layers. Strategies were

developed to obtain the best results from the EICM, which are presented in the recommendations chapter. VADOSE/w provided reasonable representation of the changes in pore water pressure, although the VADOSE/w model did not consider the impact of the asphalt layer on water flow. Both the EICM and VADOSE/w provided reasonable estimates for the temperature profile in the soil layer.

The experiences gained through the modeling of the field sites were not only summarized in the recommendations chapter, but a user's manual was developed to ensure the most effective use of the EICM in site-specific water flow analyses. A major recommendation was the use of Level 2 parameters for the soil hydraulic properties used in the analysis. Several months of testing were required to obtain the hydraulic properties of the clay soils from the different sites in Arkansas, and the results did not lead to a significant change in the output of the EICM. Another major recommendation was to use level 3 site geometry and weather data in the pavement analyses to obtain the most accurate estimate of the water and temperature flow for a given site.

**Table of Contents**

Chapter 1: Introduction	1.1
Chapter 2: Background	2.1
Chapter 3: Baseline Case Evaluation	3.1
Chapter 4: Field Sites	4.1
Chapter 5: Model-Field Comparison	5.1
Chapter 6: Recommendations	6.1
Chapter 7: References	7.1
Appendix A: Soil Characterization	A.1
Appendix B: Weather Data	B.1
Appendix C: Theory of Water and Heat Flow	C.1
Appendix D: EICM Boundary Condition Manual	D.1
Appendix E: EICM User's Manual	E.1

## 1. INTRODUCTION

### 1.1 Motivation

The goal of a pavement system is to redistribute loads from vehicle traffic to an underlying soil subgrade, which minimizes differential strains associated with eventual rutting or cracking. This goal is primarily achieved through the construction of a densely compacted, stiff aggregate base layer overlain by asphalt or concrete driving surface. After construction, these layers have very high elastic compression moduli, which means that applied stresses will only lead to small strains. However, the moduli of pavement materials tend to change over time due to environmental interaction and application of loads greater than the elastic yield point of the pavement materials. This study is focused on improving our understanding of environmental interaction with pavement systems to better predict the changes in pavement moduli over time.

In pavement performance analyses, the water content and temperature of the different pavement materials (asphaltic concrete, aggregate base, and subgrade soil) are important variables to consider. The water content is closely related with the deformation response of soils. The modulus of soils, a parameter that governs the deformation response of the soil under traffic loading, is particularly sensitive to the water content (Drumm et al. 1998; Miller et al. 2008; Khosravi and McCartney 2009, 2010). Dynamic traffic loading of soils with high water contents close to saturation can lead to a generation of excess pore water pressure, leading to a reduction in effective stress or migration of fine particles (pumping) from the subgrade into the base (or vice versa). Some types of clay subgrade soils have the potential to swell or shrink in response to water flow, which may cause strain in the pavement system causing cracking of the surface treatment. The temperature also has important impacts on the deformation response of the asphaltic concrete and soils. At high temperatures, bituminous binders have a higher viscosity and lower strength which can lead to a reduction in the resilient modulus of asphaltic concrete (Fu and Harvey 2007). Reductions in resilient modulus of asphaltic concrete will eventually lead to rutting of the pavement surface. With respect to soils, freezing temperatures can lead to movement of water into the pavement system by capillarity, causing heave as well as subsequent losses in strength during thawing.

The Enhanced Integrated Climate Model (EICM) was developed by integrating several previous models in order to predict the site-specific flow of water and temperature through layered pavement materials. However, due to the multiple phenomena considered by this model

and the complexity of the boundary conditions, the results from the EICM model are not well understood. Further, the impact of selecting different input parameters for the model on pavement performance is not well understood. Accordingly, the goals of this study are to (1) review the different physical processes in the EICM to better understand the results obtained from this model, (2) develop and analyze baseline cases to assess the EICM, and (3) analyze site-specific water and temperature flow through several pavement cross-sections in different climatic zones in Arkansas. With respect to the last goal, data has been collected in from different sites throughout Arkansas for comparison with the EICM, which can be used to validate the software. Once validated, the results from the EICM can be used with more confidence to predict the lifetime of pavements.

## **1.2 Problem Statement**

Climatic interaction can have a significant impact on the performance of pavements, especially in Arkansas where the subgrade often consists of poorly-draining, fine-grained soils. At present, the effects of climatic interaction on pavement material properties are predicted using the Enhanced Integrated Climate Model (EICM). The EICM is a component of the Mechanistic-Empirical Pavement Design Guide (MEPDG) and is used to predict the flow of water and temperature in the soil layers beneath pavements. The MEPDG uses the output from the EICM to predict the lifetime of pavements under typical traffic loading. There is a potential need to implement the ME-PDG in pavement design due to FHWA requirements. Because of the significant impact that the EICM results can have on the predicted pavement lifetime, the Arkansas State Highway and Transportation Department (AHTD) has decided to validate the EICM for use in Arkansas.

The EICM was developed in 1989 to integrate several previously developed models that simulate drainage and climatic effects on the mechanical properties of pavement layers. Specifically, the EICM combines a statistical model of published weather databases, a hydraulic model for gravity drainage of water from soil, a surface heat transfer model, and a one-dimensional diffusion model for coupled temperature and moisture flow (Lytton et al. 1989; Larson and Dempsey 2003). These different models can be combined to simulate climatic conditions at a road location (surface temperature and precipitation), drainage of the aggregate base from initially saturated conditions, changes in moisture content and internal temperature distributions due to weather fluctuations, and the likelihood of freeze-thaw conditions. This

information has been found to be useful for sizing of drainage and hydraulic barrier systems in design. However, it has also be combined with empirical relationships between temperature, moisture content (or suction), and compression modulus. Using this secondary information, temporal fluctuations in the moduli of the asphaltic concrete, base, and subgrade layers of the pavement can be predicted for use in mechanistic-empirical pavement design.

Validation of an integrated climate model is critical for Arkansas because of the state's unique topographical, geological, and geographical settings. Arkansas has several microclimates, a large spatial variation in subgrade soils, and a range in roadway geometries used in design for rural and urban applications. This state-specific information is currently not incorporated into databases and empirical relationships used in the EICM. Without validation, use of the EICM for pavement design in Arkansas will either lead over-design, resulting in high construction costs, or under-design, resulting in premature pavement failure. Independent validation of the EICM has been attempted in several other states in the U.S., including New Jersey, Minnesota, Idaho, and Ohio. Despite the important goals of the EICM, all of these states have encountered difficulties in matching its predictions of moisture content, temperature, and compressive moduli values with field observations. This is partially due to the inherent complexity of the model, resulting from (1) the contrasting motivations behind the original developments of the component models; (2) the empirical nature of several of the components of the model (making them less applicable to the entire country); (3) the large number of required inputs (mechanical and hydraulic properties of soils and asphaltic concrete, climatic variables, empirical "fitting" parameters) that may be difficult to define for a location without site-specific monitoring; (4) inconsistent integration of the different physical processes considered by the different components of the model; and (5) consideration of only one dimensional moisture and temperature flow processes. Another major shortcoming of the EICM lies in its outdated consideration of moisture and temperature transport processes in pavements. For instance, the EICM does not consider coupling between temperature and moisture flow, which neglects water vapor flow, an important transport phenomenon in unsaturated soils. Also, the databases of empirical relationships between moisture content changes, volume change, and compressive moduli in the EICM were only defined for a limited range of subgrade soils, aggregate base material, and asphaltic concretes that may not be representative of those in Arkansas.



Due to the variety of issues that limit validation of the EICM, other integrated climate models need to be assessed for use in Arkansas. Numerical modeling of water flow through soils in response to climatic boundary conditions has undergone significant improvements in the technical literature since the development of the EICM in 1989 (Lytton et al. 1989) and its most recent update 2003 (Larson and Dempsey 2003). This is in part through advancements in the field of landfill cover systems (Zornberg and McCartney 2006). There has been a significant effort to develop advanced integrated climate models such as VADOSE/W, HYDRUS-2D, and SOILVISION that can better consider climatic boundary conditions, new soil constitutive models, complex 2-dimensional geometry, and coupled flow phenomena. The current version of EICM has not considered these updates, and as it is a black-box these improvements cannot be incorporated. At the same time, an advantage of the EICM over recently developed integrated climate models is that the EICM permits synthesis of moisture content and temperature data to predict modulus values. However, as the validation process of an integrated climate model for pavements will most certainly involve measurement of relationships between moisture content, temperature, and modulus, this information can be combined with results from the other models.

### **1.3 Research Objectives**

The goal of this research is the validation of integrated climate models that can be used to assess the effects of moisture infiltration and temperature change on the long-term performance of pavements in Arkansas. The use of integrated climate models plays a key role in recent developments in the Mechanistic-Empirical Pavement Design Guide (MEPDG). Validation of these models involves consideration of the impact of incorporating Arkansas-specific climate variables, soil properties, and pavement geometry information into the models on comparisons between predicted values of moisture, temperature, and modulus changes with those measured in pavement sections in different regions of Arkansas. Further, validation also involves improvement of different components of the models to improve consideration of the constitutive relationships relating moisture, temperature, and modulus, climate interaction with the pavement, and coupling between temperature and moisture flow. Experience with existing integrated climate models for pavements indicate that they are difficult to use, with several required inputs that may be difficult to quantify for some pavement designs. Accordingly, particular efforts will be made to increase the accessibility of the models to make them more user-friendly for design engineers in Arkansas. The specific objectives of this study are listed as follows:

**Objective 1:** Evaluate the importance of the different input and output variables from integrated climate models through a literature review of the physical processes guiding moisture and temperature flow, including governing equations, climatic boundary conditions, and soil constitutive models, including evaluation of previous validation attempts.

**Objective 2:** Characterize the geometry, soil properties, and climate characteristics of seven pavement sections in the different climate zones of Arkansas that will be considered in the EICM validation process.

**Objective 3:** Measure the time-variation in important variables governing environmental interaction with pavement sites located in different regions of Arkansas, including moisture content and temperature of the subgrade soil, global compression modulus of the pavement, and climatic data.

**Objective 4:** Perform simulations of suction and temperature variations for the sites in different regions of Arkansas with the Enhanced Integrated Climate Model and an advanced integrated climate model (VADOSE/W).

**Objective 5:** Compare the predicted values of moisture, temperature, and modulus obtained from the climate interaction models with those measured at the six pavement sections throughout Arkansas.

**Objective 6:** Refine the consideration of input parameters, constitutive models, and boundary conditions to better match the output of the integrated climate models with field observations.

**Objective 7:** Develop recommendations for the use and implementation of climate interaction modeling in the design of pavements in different regions of Arkansas.

## **1.4 Scope**

Chapter 2 includes an in-depth evaluation of how the EICM considers water flow processes, boundary conditions, initial conditions, soil hydraulic properties. Of these different considerations, the boundary conditions are perhaps the most important to evaluate critically because they incorporate the interaction between the site-specific weather conditions and the amount of water entering or exiting the pavement system. Unfortunately, the EICM is not well documented, so the details of the how the model quantifies the applied boundary conditions are not certain.

Chapter 3 includes an evaluation of a series of baseline cases to assess the way that the EICM and VADOSE/W incorporate infiltration and evaporation boundary conditions. The goal of the baseline cases is to help identify how EICM considers environmental boundary conditions so that it can be used as effectively as possible in replicating field conditions.

Chapter 4 includes the monitoring of matric suction and temperature profiles at pavement sites in seven different regions in Arkansas and comparing predicted data computed from the EICM to measured field data. The seven sites are located near the towns of Marked Tree (Mississippi Embayment), Murfreesboro (Ouachita Mountains), Malvern (Central Arkansas), Plumerville (Arkansas River Valley), Camden (South-Central Arkansas), Lake View (South-East Arkansas), and Greenland (Ozark Mountains). Each of these sites has unique weather aspects due to the topography and unique subgrade types due to the local geology. This chapter includes a description of the field monitoring system as well as the results that have been measured over the course of this project.

Chapter 5 includes a comparison between the predictions of EICM and VADOSE/W in evaluating the site-specific variation in water content and temperature in the subgrade soils. The comparison of these results was synthesized to make recommendations on how to best use the EICM in pavement analysis which are described in Chapter 6. The references cited are listed in Chapter 7.

This report also includes several appendices. Appendix A includes a description of the procedures and specific results from characterization tests used to quantify the hydraulic conductivity, soil-water retention curve, and thermal conductivity of the soils obtained from Shelby tube samples at each of the sites. Appendix B includes a presentation of the weather data (precipitation, temperature, wind speed, relative humidity) from 2005 to 2010 collected from nearby weather stations. Appendix C includes an overview of the theory of water and heat flow in general and Appendix D includes a description of how the EICM implements this theory. Appendix E includes a user's manual for the EICM with screen-by-screen instructions on how to perform an analysis.

## 2. BACKGROUND

### 2.1 Interaction of Water and Heat with Pavements

Water and temperature are climatic variables that are well known to affect the modulus of soils and asphalt (Yoder and Witczak 1972; Thompson and Robnett 1979). Accordingly, long-term assessments of pavement performance (*i.e.*, strains) under repeated loading require long-term assessments of water and temperature flow in pavement systems. However, this is a complex task that requires synthesis of experience from soil physics, geotechnical engineering, transportation engineering, physics, and climatology. As research from these fields has been integrated, there has been a steady evolution in modeling capabilities for climate interaction in pavements. This evolution extends from early work conducted at the University of Illinois and the US Army Corps Cold Regions Experimental Laboratory in the late 1970's and early 1980's, to work done at Texas A&M in the late 1980's. Since this time, there have been parallel advances in soil-climate modeling for vadose-zone applications (Fayer 1990) and alternative landfill cover systems (Zornberg and McCartney 2006). However, only recently have these advances in other fields been integrated into pavement models (Gupta *et al.* 2007; Roberson and Seikmeier 2002).

The goal of a climate model for pavements is to quantify the transient flow of water and temperature through a layered pavement system in response to climatic boundary conditions. Figure 2.1 illustrates some of the 2-dimensional phenomena that must be considered to properly assess water and temperature flow. Water can infiltrate into soils by a combination of advective flow, capillary rise, molecular diffusion, and water vapor flow. Depending on the permeability of the different materials in the pavement and the hydrologic setting, one or more of these pathways for water flow may dominate. Heat can flow into the pavement due to solar radiation, which can be affected by surface reflections as well as wind. Climatic boundary conditions at the ground surface are complex, and may vary on a minute-by-minute basis. Further, the pavement surface may initially be impermeable, but may gradually become more so as cracks form.

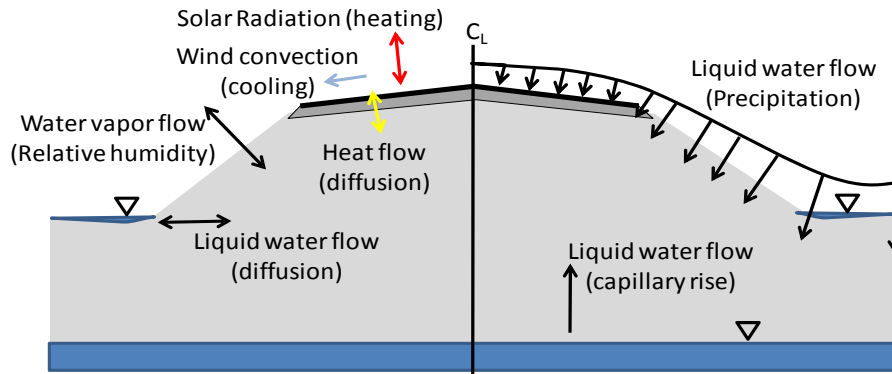


Figure 2.1: Pathways for water and heat migration in pavements

## 2.2 Enhanced Integrated Climate Model (EICM)

A flow chart of the enhanced integrated climate model is shown in Figure 2.2, and was developed under contract to Federal Highway Administration by Lytton *et al.* (1989) and refined by Witzcack *et al.* (2000). The EICM is composed of four component models: the Precipitation (PRECIP) Model, the Infiltration and Drainage (ID) Model, the Climatic-Material-Structural Model (CMS) Model and the U.S. Army Cold Regions Research and Engineering Laboratory (CRREL) Model for Frost Heave-Thaw Settlement. As can be seen from the flow chart, these four models are all interrelated, often with common inputs and outputs. Overlap occurs because the models were developed as separate entities before they were integrated into the EICM.

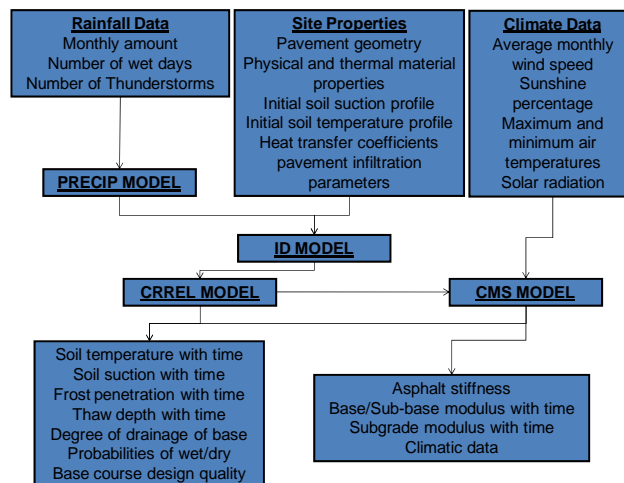


Figure 2.2: Inputs and outputs for different components of the EICM (Lytton *et al.* 1998)

The PRECIP model, developed by Liang and Lytton (1989), uses a deterministic algorithm involving average climatic data and probability theory to simulate rainfall patterns that are considered acceptable for design purposes. Output data from the Precipitation Model consists of a prediction of the amount of rainfall, the day on which it occurs, the number of thunderstorms,

the likelihood of having a wet or dry day. Using simulated rainfall data ensures that rainfall during the design period will be equal to or greater than the long-term climatic average. The intention of this model is to develop worst-case predictions of weather variables for pavement design. This model is not used in the EICM when actual precipitation data is used to model extreme rainfall events or when comparing modeled data to measured data over a given time period. In this case, the actual precipitation data can be entered directly into the EICM. The original EICM model incorporated Arkansas into a large region, as shown in Figure 2.3. A recent update to the EICM (version 3.4) includes options to include site-specific data or to obtain data from internal databases. Nonetheless, the impact of comparing different weather conditions that occur throughout a state has not been thoroughly investigated.

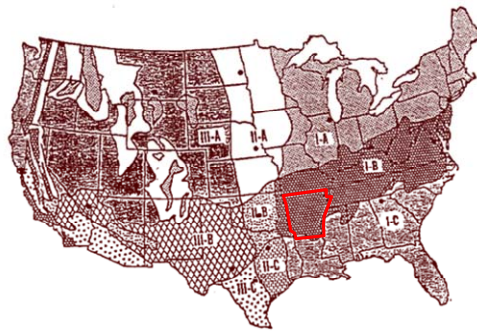


Figure 2.3: Climate regions considered in the original EICM model (Lytton et al. 1998)

The Infiltration and Drainage Model (ID), developed by Liu and Lytton (1985), performs several tasks in evaluating the effect of precipitation on a pavement profile. These tasks include drainage analysis, infiltration analysis and pavement design evaluation. The ID model uses an analytical relationship to compute the degree of drainage (via lateral drainage) versus time of an initially saturated granular base course layer overlying a permeable or impermeable subgrade. The geometry of this layer can be input by the user. This analysis assumes that the base course is a free draining material, and that water cannot enter the subgrade. Further, this simplified analysis does not account for drainage or hydraulic barriers in the pavement system. Unfortunately, this model does not account for how the pavement becomes fully saturated in the first place, so it may be an over-conservative situation to use in design. The pavement evaluation module of the ID model uses an empirical procedure to evaluate the relative adequacy of the base course design in terms of the amount of time that is required to reach a critical degree of saturation. The more rapidly the base course can drain, the more effective it will be as a load

carrying member of the pavement structure under wet conditions. The ID model contains empirical coefficients to account for flow through cracked pavements, which are difficult to define logically. The output of ID model includes the degree of saturation of the base course, the degree of drainage over consecutive dry days and the probability of a dry/wet base course. The results presented in this study indicate that the ID model may be the component of the EICM which is most in need of updating, as it controls the hydraulic boundary condition atop the subgrade. Although it may be a simple conceptual model useful for preliminary design, the ID model does not permit simulation of the actual hydraulic interaction between a pavement system and the atmosphere.

Temperatures throughout the pavement structure in response to changes in atmospheric conditions at the surface are predicted using the Climatic-Materials-Structures model (CMS), developed by Dempsey *et al.* (1985). The CMS model estimates the heat flux at the surface to calculate the temperature profile through the pavement layers. The main input for the CMS model are the thermal conductivity and specific heat capacity of the pavement layers. The CMS model considers radiation, convection, conduction, and the effects of latent heat, but it does not consider plant transpiration, condensation, evaporation, or sublimation. These last mechanisms of heat flux are not considered because their impact was found to be relatively small compared to the other mechanisms. Heat fluxes caused by water infiltration of water (which usually is colder than the subgrade) into the pavement system were also neglected, which implies that the CMS model is not completely integrated with the other models of the EICM. The comparison of the field and EICM results in Chapter 5, as well as in results published by other studies, indicates that the EICM provides acceptable predictions of temperature profiles in pavement systems.

The United States Army Cold Regions Research and Engineering Laboratory (CRREL) Frost Heave and Thaw Settlement Model, developed by Guyman *et al.* (1986), is a one-dimensional, coupled heat and water flow model in the subgrade layer of the pavement system with capabilities to evaluate the effects of freezing conditions. The variation in the matric suction profile with depth and time in the subgrade layer is predicted in the CRREL is predicted using a one-dimensional diffusion analysis. Advective water flow due to gravity drainage, infiltration, or from ponding is neglected in this model, because these mechanisms of water flow are not consistent with the ID model, which dictates the matric suction boundary condition applied to the top of the subgrade layer in the CRREL model. The lack of consideration of advective water

flow is valid for relatively low permeability clays, as long as the initial suction profile in the clay is known. If the initial suction profile is not known, then the entire analysis period of the EICM (1 year maximum) may involve equilibration of the suction profile with the initial boundary conditions, rather than response of the suction profile to daily changes in the boundary conditions. The lack of gravity drainage and advective water flow in the CRREL model may be one of the reasons for the poor fit between the suction profiles measured in the field and those predicted by the EICM predictions presented in Chapter 5.

The value for the temperature at the bottom of the asphalt layer from the CMS model is used as an input to the Frost Heave and Thaw Settlement Model for the soil temperature predictions. The CRREL Model uses the temperature profile through the pavement layers as established by the CMS Model to compute changes in the soil temperature profile, and thus frost penetration and thaw settlement. The phase change of water to ice is computed using the CRREL model, so it can be used to estimate frost heave. The freezing zone may range in thickness from a few millimeters to many meters, and wherever it occurs it controls the movement of water due to ice segregating and partially blocking the pores in the soil against water movement. The nature of this blockage is handled in the model by reducing the hydraulic conductivity of the soil. This model uses the output of the ID model along with temperature boundary conditions to predict the temperature variation and the depth of frost heave in the pavement.

After development of the EICM, studies by Lytton *et al.* (1989) and Larson and Dempsey (1997) used to the model to match field data. As the model did not initially match the field results well, the authors adjusted several of the material properties and physical phenomena using “fitting” factors until the predictions matched the field data. This fitting process may have serious implications on the validation of the model. If the model does not well represent the physical phenomena governing water content and temperature flow, then it would be very difficult to determine adequate “fitting” parameters for each site in the country.

### **2.3 Validation Process of an Integrated Climate Model**

The outline of the validation process for an integrated climate model is shown in Figure 2.4. This outline provides a structure for the research that will be performed as part of this study, as well as its implementation into pavement engineering practice. Weather and soil data from a particular site in Arkansas must first be collected and discretized for use in an integrated climate model (ICM). The model can be used to predict the temporal variation in water content, pore



water pressure, and temperature, which can be compared with field monitoring results. If these results do not match, each of the previous steps can be refined, until the model and its inputs are calibrated for use in Arkansas. The ICM results can then be used with confidence in MEPDG.

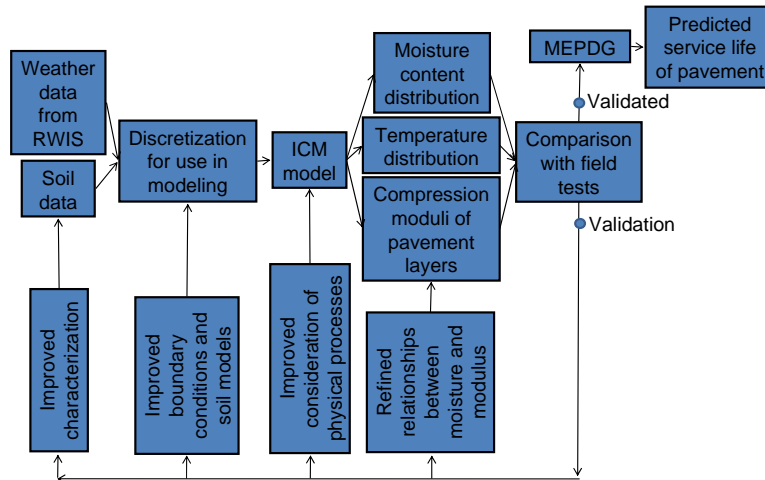


Figure 2.4: Framework for validation of integrated climate models for use in pavement design in Arkansas

## 2.4 Results of Previous Validation Efforts

Several states have encountered difficulties in efforts to validate the EICM for local weather and soil conditions. Most of these efforts have been made in the past three years due to the recent impetus to use mechanistic-empirical design for pavements. These issues will help guide the validation for the EICM in Arkansas, and may indicate the benefit gained by complementing the information from EICM with other integrated climate models in pavement design.

### 2.4.1 New Jersey

New Jersey has undergone a significant amount of validation testing and modeling (Ahmed *et al.* 2005; Zaghoul *et al.* 2006). Some of the results from these two studies are summarized below in Figure 2.5. One observation is that the EICM does not do a good job of modeling fluctuations in water content at depth in the pavement. Although the results in Figure 2.5(c) indicate that the temperature predictions follow the same trends as measured values, the actual profiles of temperature may differ greatly at the soil surface. This is the most critical place to accurately model temperature, as temperature has the greatest effect on the asphalt modulus.

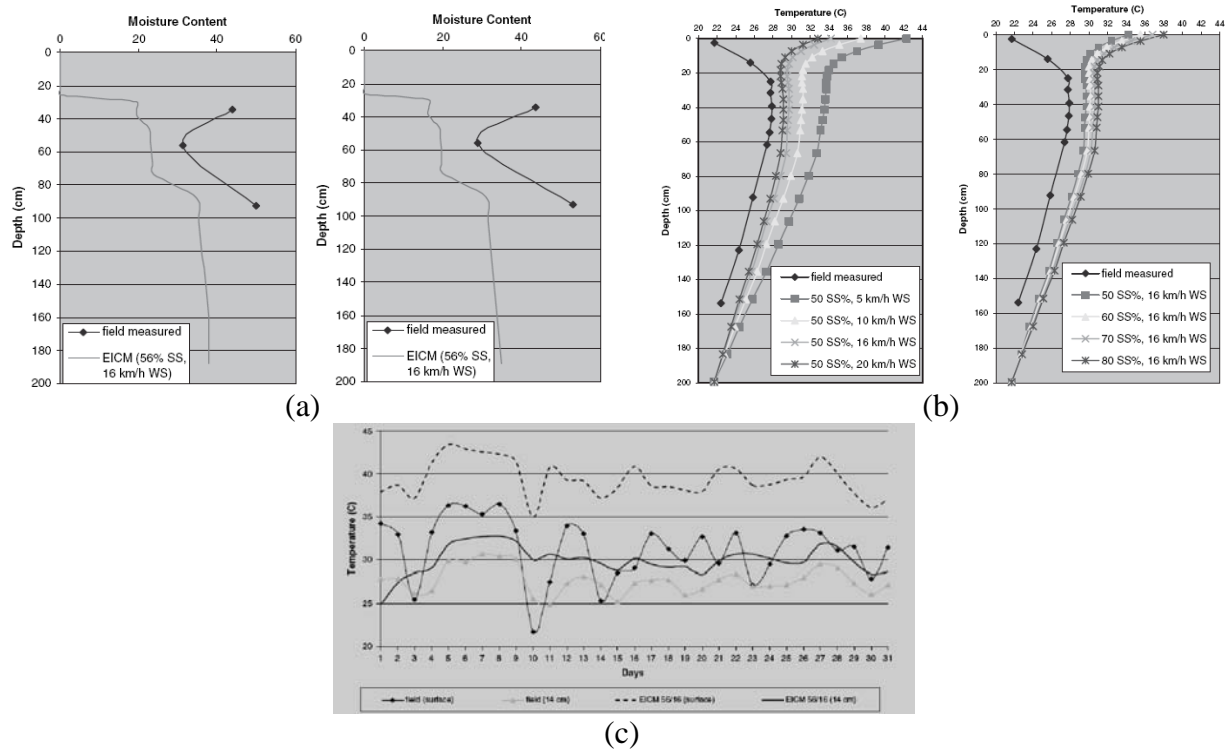


Figure 2.5: Comparison between measured and predicted (EICM) results; (a) Water content profiles; (b) Temperature profiles for different wind speeds; (c) Temperature fluctuations at different depths

### 2.4.2 Minnesota

Minnesota has made significant investments into the validation of the EICM because of the important role of frost heave in pavements (Roberson and Seikmeier 2002; Birgisson *et al.* 2007; Gupta *et al.* 2007). Birgisson *et al.* 2007 focused on comparison of EICM results with water content and FWD modulus results. This is one of the only independent studies in the literature that has made these comparisons, shown in Figure 2.6. Although the validated model was capable of matching the water content and stiffness in relatively wet conditions, it did a poor job of modeling the pavement in dry conditions (zero water content and a modulus that was 1 order of magnitude too high). Nonetheless, at least the model followed the trends in the data.

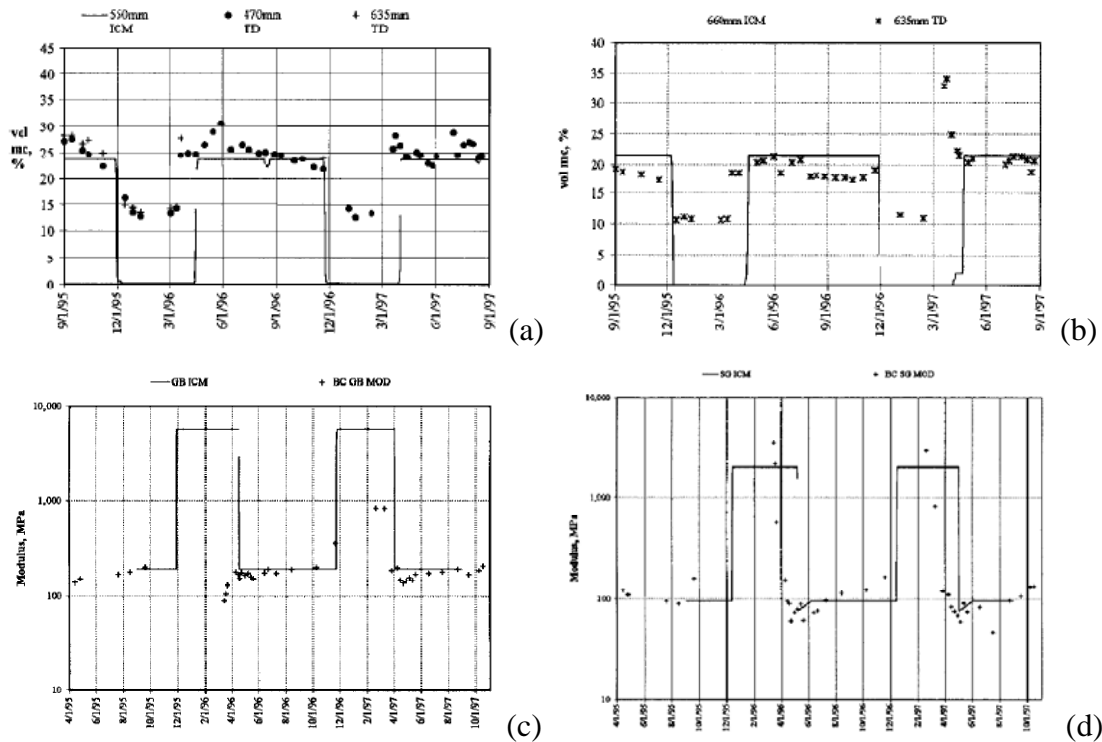


Figure 2.6: Comparison between measured and EICM results in Minnesota: (a) Water content in aggregate base; (b) Water content in aggregate base; (c) Modulus of aggregate base; (d) Modulus of subgrade

Minnesota DOT has moved away from using the semi-empirical EICM to calculate water flow in pavements. Instead, MnDOT is investigating the use of finite element models such as SEEP/W (a companion program to VADOSE/W without climatic boundary conditions) that can solve water flow problems in unsaturated soils (Robertson and Siekmeier 2002). The advantage of such models is that they can consider actual 2-dimensional pavement geometries, as shown in Figure 2.7. An advantage that would have been gained by using VADOSE/W instead of SEEP in this application is that actual weather boundary conditions could be used instead of the simplified point of infiltration analysis.

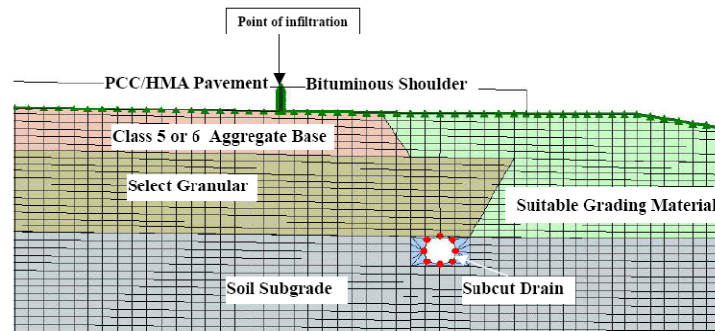


Figure 2.7: SEEP/W mesh used by Minnesota to model water infiltration (Robertson and Siekmeier 2002)

In addition to advanced flow modeling, MnDOT has focused on the improved characterization of the hydraulic and mechanical properties of unsaturated soils. Gupta et al. (2007) made significant advances in determining relationships between matric suction predicted from the EICM or other climate-interaction modeling and the resilient modulus used in the MEPDG.

### 2.4.3 Ohio

Research has been performed in Ohio to match field and laboratory data (Liang 2006; Quintero 2007). Field data was obtained from six pavement sections built with different drainable base materials at I-90 in Ashtabula, Ohio and at U.S. Road 23. Hourly weather data recorded at an automated weather station located at the site were used as input into the EICM. Temperature, frost depth and water content profiles measured in the field were compared with the profiles predicted by the EICM during the same simulation period. Typical results from a comparison of the model and field results from the U.S. Road 23 project are shown in Figure 2.8. The temperature difference chart in Figure 2.8(a) indicates that the EICM was able to predict the temperature within 5 °C, although the difference in the measured and predicted temperatures varied over time. The volumetric water content at a point in Figure 2.8(b) indicates that the EICM is not sensitive to weather fluctuations that may be measured in the field. This is likely due to the way that EICM considers the impact of the asphalt layer on infiltration into the pavement layer. Nonetheless, the predicted and measured volumetric water content have the same magnitude, although this may be a feature of the initial conditions input into EICM. The results indicate that the predicted temperature profile did not match the measured field data, although the range in values predicted by the model can be considered within an acceptable

range. A good match between the predicted and measured frost depth for sections with unbounded base materials was found, but not for those with bounded base materials. The ability of the model to accurately predict water content profile was found to be enhanced by using field material properties instead of laboratory-obtained properties as inputs.

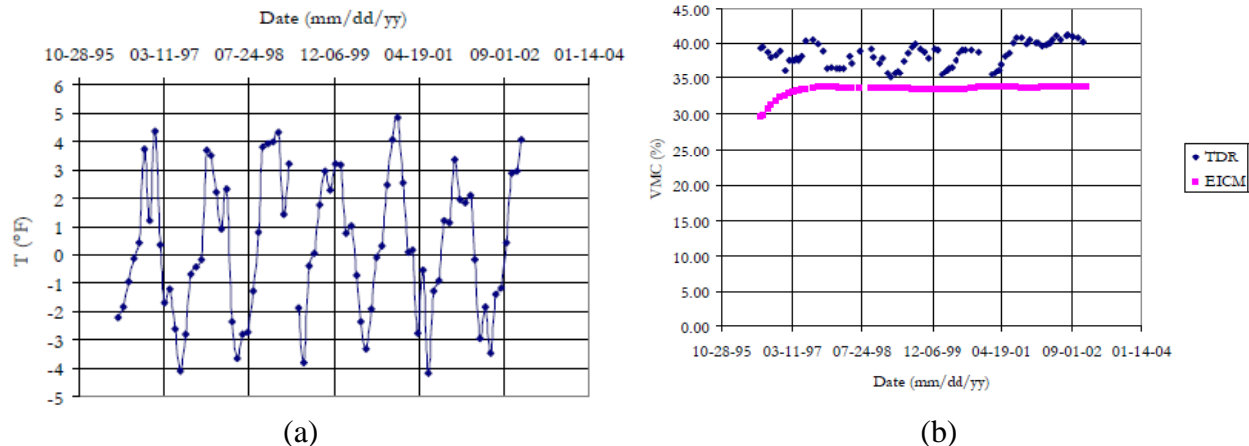


Figure 2.8: Examples of quality of EICM and field predictions from Ohio (Quintero 2007): (a) Temperature difference between field and predicted; (b) Measured (TDR) and predicted (EICM) volumetric water content over time

#### 2.4.4 Idaho

Idaho has recently sponsored a project focusing on validation of the EICM for use in Idaho (Bayomy and Salem 2004). This project involved quantification of the variation of subgrade water and asphalt surface temperature at various sites in Idaho and determine their effects on the structural capacity of the pavement layers. The project included instrumentation of five pavement sites throughout Idaho to measure water content (using Time Domain Reflectometry), temperature (using thermistors), groundwater level, and frost penetration (using resistance probes). The capacity of the road was evaluated using Falling weight Deflectometer. Information was collected for three years. This project involved development of correlations between resilient modulus measured in the field and water variations, and used the EICM to predict the water and temperature fluctuations. Results of a mechanistic analysis conducted using the EICM-predicted and measured variations in pavement modulus indicate that the incorporation of the seasonal variation in pavement design process leads to the prediction of significantly shorter pavement service life. The results from this project, shown in Figure 2.9(a), indicate that the EICM did a relatively poor job of matching water content profiles. Similar to the results obtained by New Jersey, the model did a poor job at estimating changes in water

storage deep in the soil profile. The estimates of modulus values predicted from the EICM, shown in Figure 2.9(b), indicate an average error of approximately 30%.

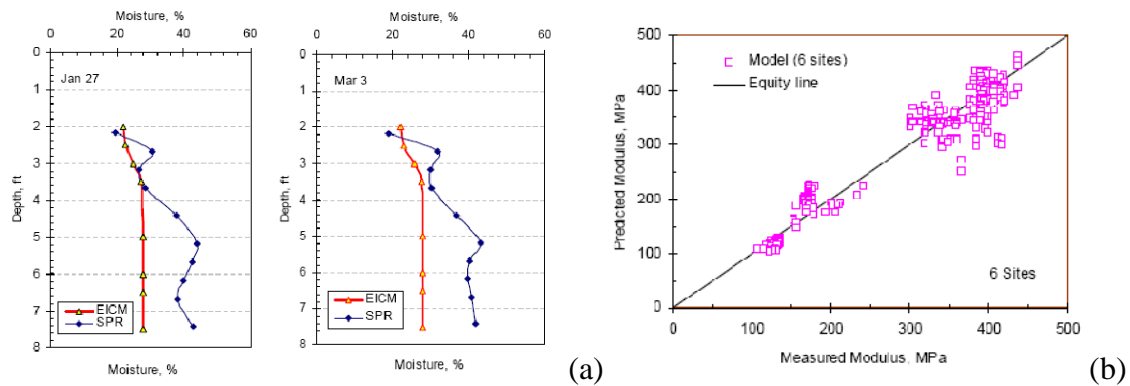


Figure 2.9: (a) Comparison between water content profiles predicted by the EICM model and measured in the field; (b) Comparison between predicted and measured modulus values

#### 2.4.5 NCHRP 602 Study

A national study funded by the NCHRP by Zapata and Houston (2008) was published shortly after this project started. This study involved collection of soils from 30 sites throughout the U.S., collection of weather data from online databases for these sites, and prediction of the water content from these sites using the EICM. The study led to the implementation of several Level 2 empirical relationships for the soil material properties which were input into the most recent version of the EICM. The study involved comparing the predicted water content from the EICM with field measurements. The study used different levels of input parameters in the EICM analysis, including default (Level 1), estimated (Level 2), and user-added (Level 3) inputs. The results of this comparison are shown in Figure 2.10. The study found that use of Level 3 inputs led to the best prediction of the water content, represented by the how close the dark best-fit line was to the 45 degree line (the gray line). The study then proposed modified estimated material property relationships in the EICM (Level 2) to calibrate the model. These relationships have been implemented in the most recent version of the EICM (released in 2007). The most recent version of the EICM which incorporated these relationships was used in this study. However, this study focused only on the impact of using Level 3 inputs for the soils in Arkansas.

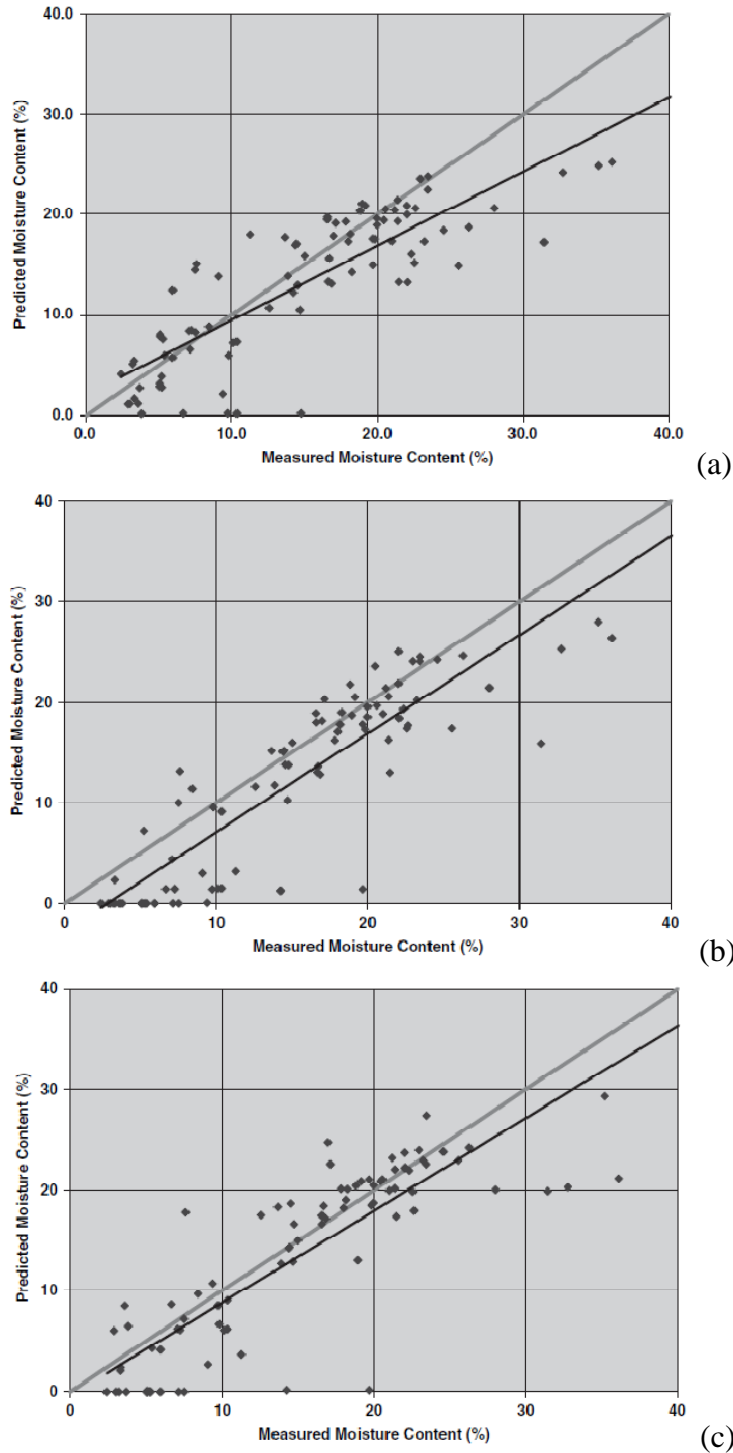


Figure 2.10: Results from Zapata and Houston (2008) showing the impact of different levels of input parameters on the predictions of the water content by EICM: (a) Level 1 (default); (b) Level 2 (estimated); (c) Level 3 (site-specific measurements)

## 2.5 Impact of Site-Specific Inputs for the EICM

The main inputs that must be input by a user (i.e., no default) into EICM are the thicknesses of the different layers. However, these values can be selected based on local experience as part of a design process. The EICM provides default parameters for almost all of the material properties of the different pavement layers, and permits the user to select standard AASHTO soil classifications that can be expected at a site. The EICM results are particularly sensitive to the properties of the asphalt or Portland concrete (PCC) input into the model, because they represent the main interface with the atmosphere. For instance, if the asphalt layer has low thermal conductivity, it will act as an insulator for the underlying soils. The weather data is almost always a Level 3 input, but this data is now readily available in online databases managed by TRB or Weather Underground.

The main input parameters that involve an important decision between Level 2 and 3 inputs are the soil material properties. Zapata and Houston (2008) described the incorporation of new Level 2 inputs into the EICM for the saturated hydraulic conductivity and soil-water retention curve (SWRC), in which easy-to-determine soil index parameters (the plasticity index). The new SWRC relationship for the SWRC is shown in Figure 2.11. The soil properties used in the EICM representing unsaturated conditions (the SWRC) require significant laboratory efforts which may require up to one month of testing for clays. The SWRCs for each of the soils evaluated in Appendix A required at least a month, which implies that Level 2 inputs may be the most practical for pavement design using the EICM. The results of the EICM are not particularly accurate, as will be discussed in the following sections of this chapter, so spending significant time to obtain accurate site-specific soil material properties may not be justified.

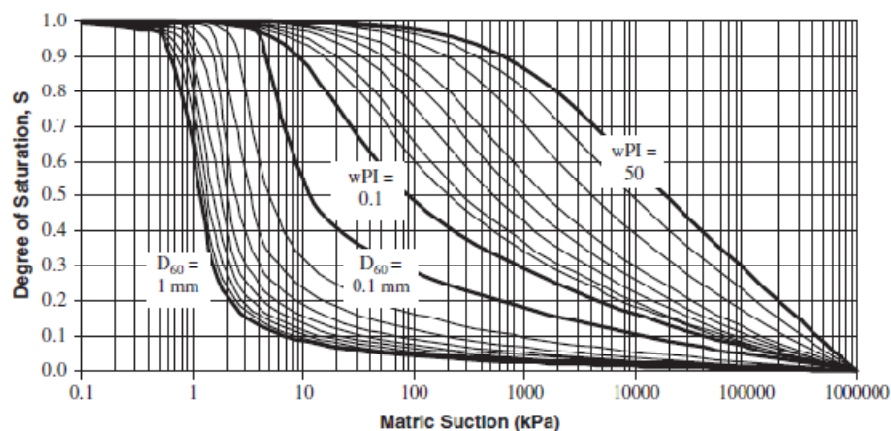


Figure 2.11: Level 2 relationships for the SWRC developed by Zapata and Houston (2008)



### 3. BASELINE CASE EVALUATION OF INTEGRATED CLIMATE MODELS

#### 3.1 Overview of Baseline Analyses

EICM and VADOSE/W both incorporate the same governing equations to understand heat and water flow, but they differ in the way that they consider the boundary conditions for water flow. Accordingly, this chapter includes an evaluation of a set of baseline cases. The goal of evaluating these baseline cases is to understand how infiltration and evaporation are considered in the EICM and VADOSE/W models. Specifically, this study involves comparison of the volumetric water content and pore water pressure profiles with depth in a pavement system predicted from the EICM and VADOSE/W models, with different boundary conditions. The boundary condition that is most important for infiltration is the precipitation rate, while the boundary conditions most important for evaporation are temperature and relative humidity.

Two baseline cases are considered in this chapter. The first case involves the evaluation of different infiltration rates applied to the surface of the pavement system, while the second case involves application of different relative humidity values. In order to isolate the impact of the infiltration rate and the relative humidity, each baseline case considers the same pavement layer geometry and material properties. A summary of the different boundary conditions for each of the baseline cases is shown in Table 3.1.

Table 3.1: Baseline cases considered for analysis

Baseline case name	Analysis Duration (day)	Temperature (°C)		Relative humidity (%)		Max Wind Speed (mps)	Infiltration rate (mm/day)
		Max	Min	Max	Min		
1a	365	21.1	21.1	80	80	0	$6.1 \times 10^{-3}$
1b	365	21.1	21.1	80	80	0	$6.1 \times 10^{-1}$
1c	365	21.1	21.1	80	80	0	$6.1 \times 10$
2a	365	32.2	32.2	50	50	0	0
2b	365	32.2	32.2	60	60	0	0
2c	365	32.2	32.2	80	80	0	0

The volumetric water content and pore pressure profiles from these two models are expected to be different. EICM incorporates empirical relationships to predict the transfer of water through the asphalt and base layers. Although the permeability of asphalt is lower than most soils, water flow primarily occurs through cracks and fissures in the asphalt. Although, the EICM user's

manual requires several input parameters describing the characteristics of the asphalt surface (cracks, joints, etc.), it does not explain the impact of selecting different parameters on the outputs of the EICM. Accordingly, a comparison of the EICM results with those from VADOSE/W, a soil analysis software with well-defined boundary conditions, may be revealing. Specifically, because the EICM and VADOSE/W incorporate the same governing equations for water flow in the pavement soil layers, a comparison between the results of the two models should reveal the impact of the asphalt layer on evaporation and infiltration.

### 3.2 Boundary Conditions and Material Properties used in the Baseline Cases

The boundary conditions used in this analysis are listed in Table 3.2, and include both hydraulic and thermal boundary conditions. In both analyses, the environmental boundary conditions are applied to an initially unsaturated soil layer having a uniform volumetric water content with depth. More explanations about boundary conditions in the EICM model are given in Appendix C. Because VADOSE/W is a 2-D model, no-flow (zero-flux) boundary conditions are required for the sides of the model so that it can be used as a 1-D model.

Table 3.2: Boundary conditions considered in analysis

Type of boundary condition		Location
Hydraulic	Zero pore pressure	Bottom of the model
	Zero total flux	Left and right sides of the model
Thermal	Constant temperature	Bottom of the model
	Zero total flux	Left and right sides of the model
Climate	Climate condition	Surface

The geometry of the model specifications have been summarized in Table 3.3 and schematics of the models are shown in Figure 3.1. To have a more straightforward comparison between EICM and VADOSE/W, VADOSE/W was used as a 1D model. A modeling duration of 1 year was used in the analysis, with an hourly time increment.

Table 3.3: Baseline geometry details

Total depth (m)	1.8
Asphalt layer thickness (m)	0.
Base layer thickness (m)	0.3
Subgrade layer thickness (m)	1.5
Water table depth (m)	1.8

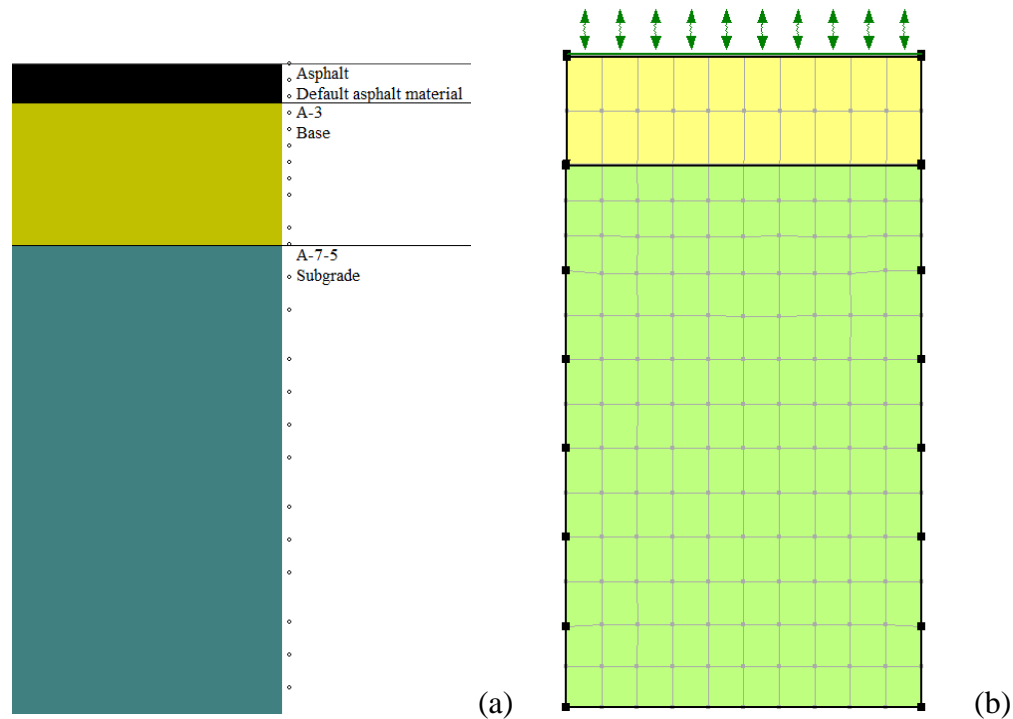


Figure 3.1: Schematic of the model considered for the baseline cases analysis:

(a) EICM; (b) VADOSE/W

The material properties used in the baseline cases are summarized in Table 3.4. The materials used in the analysis were obtained from the defaults in EICM. Specifically, the default asphalt material properties were used as the surface treatment, AASHTO A-3 soil was used as the base course layer material and AASHTO A-7-5 soil was used as the material for the subgrade layer.

Table 3.4: Material properties of pavement soil layers

<i>Layer</i>	Base course	Subgrade
Type of soil	AASHTO A-3 Soil	AASHTO A-7-5 soil
Porosity $n$	0.25	0.39
Saturated permeability $K_{sat}$ (m/day)	$2.56 \times 10^{-2}$	$3.13 \times 10^{-5}$
Dry unit weight ( $\text{g}/\text{cm}^3$ )	1.92	1.63
Initial vol. water content ( $\text{m}^3/\text{m}^3$ )	0.17	0.33
Initial temperature ( $^{\circ}\text{C}$ )	22.1	22.1
Plasticity index (PI)	0	24
$D_{60}$ (mm)	0.28	0.03
% Passing #4 Sieve	95.3	94
% Passing #200 Sieve	5.2	70.5
Dry thermal conductivity ( $\text{kJ}/\text{day}\cdot\text{m}\cdot^{\circ}\text{C}$ )	119.52	119.52
Vol. heat capacity ( $\text{kJ}/\text{m}^3\cdot^{\circ}\text{C}$ )	1875	1875

The SWRC and hydraulic conductivity of the soils were defined using the Fredlund and Xing (1994) model. The SWRC equation and the description of the different parameters for the Fredlund and Xing (1994) SWRC are presented in Appendix A. The SWRC and K-function of the soil layers are shown in Figure 3.2, with parameters summarized in Table 3.5.

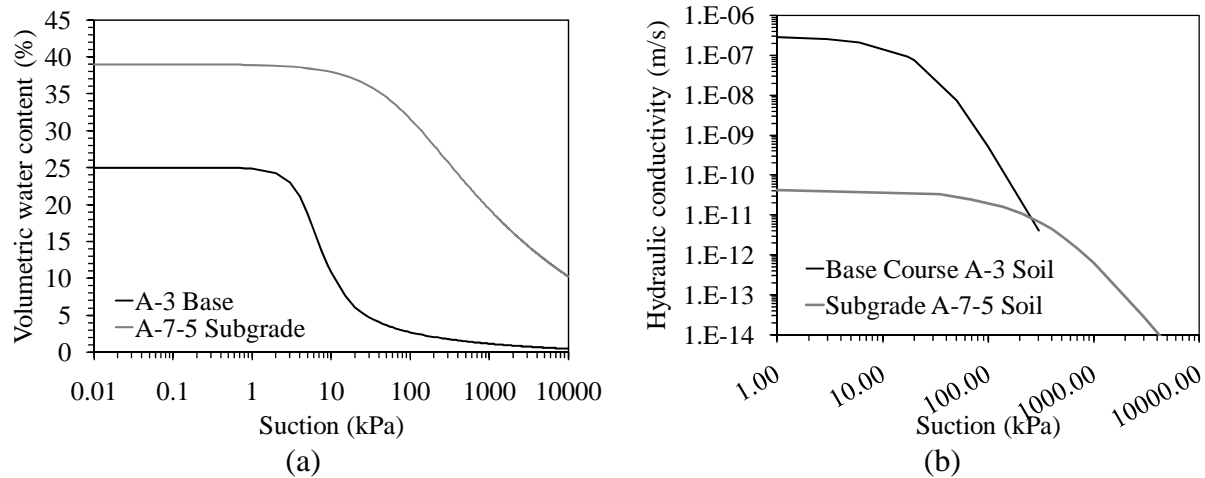


Figure 3.2: Hydraulic properties of soils in the baseline cases: a) SWRC and b) K-function

Table 3.5: Fredlund and Xing (1994) SWRC parameters considered for the soil layers

Fredlund and Xing (1994) parameters	Base course	Subgrade
$\theta_{\text{sat}}$ ( $\text{m}^3/\text{m}^3$ )	0.25	0.39
$a_{\text{FX}}$ (kPa)	34.22	449.70
$n_{\text{FX}}$	2.83	1.03
$m_{\text{FX}}$	1.00	0.50
$h_r$ (kPa)	100	500

The EICM requires inputs concerning the condition of the asphalt layer, which are input into the ID submodel. The inputs for the ID submodel used in the baseline case analyses are shown in Table 3.6. These inputs are the same as those used for the site-specific analyses in the next chapter, since these parameters were found not to have a significant impact on the EICM results.

Table 3.6: Inputs for the ID model

Length of Cracks	100'	Types of Fines in Base		Inert Filler	
Length Surveyed	100'	% Fines in Base	2.5	% Gravel in Base	70
% Sand in Base	27.5	One Side Width	25'	Slope Ratio (%)	1.5

### 3.3 Results from Baseline Case 1

#### 3.3.1 Overview

Baseline case 1 was used to assess the impact of the precipitation rate on the predicted pore pressure and water content profiles in the base and subgrade layers. Each time increment of the analysis was assigned the same weather boundary conditions. Case 1A involves a constant rainfall of 0.00001 in/hr (near zero), Case 1B involves application of a constant rainfall rate of 0.001 in/hr, and Case 1C involves application of a constant rainfall rate of 0.1 in/hr. It is expected that the pore water pressure magnitudes at different time steps will change more significantly for greater infiltration rates. The ID model of the EICM computes the degree of saturation in the base course from the applied rainfall using Ridgeway's model. Ridgeway's model allows for a maximum infiltration rate of  $0.1 \text{ ft}^3/\text{hr}/\text{ft}^2$  (1.2 in/hr) through the asphalt and into the base. Accordingly, increasing the infiltration rate above this limit is expected to have no effect. Baseline Cases 1A to 1C have lower infiltration rates, so this was not expected to be an issue.

#### 3.3.2 Results from Baseline Case 1A

Baseline Case 1A involves a constant, relatively low infiltration rate applied to the pavement surface. The EICM results from Baseline Case 1A are shown in Figure 3.3. The water pressure in the base, shown in Figure 3.3(a), indicates that the entire base layer is unsaturated. The suction at the base course layer starts at approximately 35 kPa, and actually increases to 50 kPa. This increase in suction (corresponding to drying) may be due to numerical issues in the EICM. It also may be due to the initial water content selected for the base, corresponding to an initial suction of 40 kPa. After reaching a suction of 50 kPa, the suction at the bottom of the base remains constant. It is still non-intuitive that the top of the base course layer would be dryer than the bottom during infiltration. The initial water pressure in the subgrade is -550 kPa, corresponding to the initial water content of  $0.33 \text{ m}^3/\text{m}^3$ . The water pressure at different depths in the soil is observed to increase at different rates for different depths in the profile, as shown in Figure 3.3(b). The different rates for different points in the model arise because water is flowing upward from the water table at 1.8 meters, and water is flowing downward from the positive water pressure boundary condition in the base course. This can be observed in this water pressure profiles in Figures 3.3(c) and 3.3(d). These two figures show water pressure profiles for different

times throughout the year. As the EICM can only run for a period of 1 year, the soil layer never reached a steady-state water pressure profile. The temperature results from the model are not shown because the temperature boundary condition is constant.

The VADOSE/W results are shown in Figure 3.4. The water pressure profiles shown in Figure 3.4(a) indicate that the soil layer responds more rapidly to the infiltration boundary condition than in the EICM (due to the lack of the asphalt layer). The base bottom of the base layer actually becomes wetter (lower negative water pressures), before it becomes drier. This is due to equilibration of the initial conditions in the base and subgrade layer with the applied flow process. In other words, the base course is wetter than it wants to be during this infiltration scenario, while the subgrade is dryer than it wants to be during this infiltration scenario. There is a transient process in which the top of the base become saturated, then it gradually becomes unsaturated at its upper surface. When the suctions in the base layer are greater than -600 kPa, they are not shown on the plot because the SWRC for the base shown in Appendix A indicates that this is above the residual water content of the soil. This is the case for all of the profiles in Figure 3.4(a) that end halfway through the base. At steady-state infiltration, the base is unsaturated at the top. Unlike the EICM results, the subgrade reaches a steady-state profile with a suction at the top of the subgrade of 160 kPa. The predicted water content profiles in Figure 3.4(a) indicate that the base is still unsaturated except at the pavement surface.

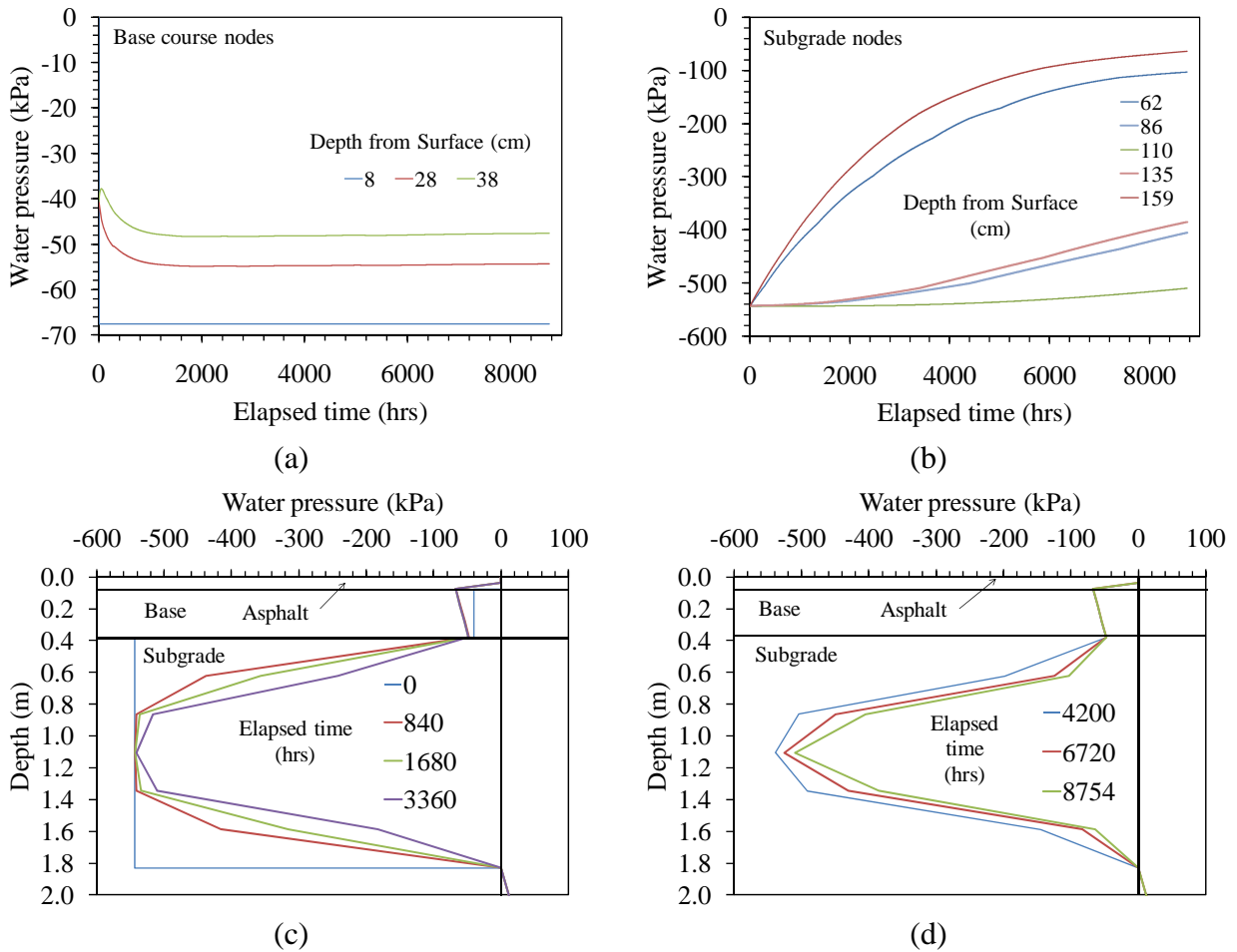


Figure 3.3: Case 1A EICM results: (a) Water pressure in base; (b) Water pressure in subgrade; (c) Water pressure profiles at early times; (d) Water pressure profiles at late times

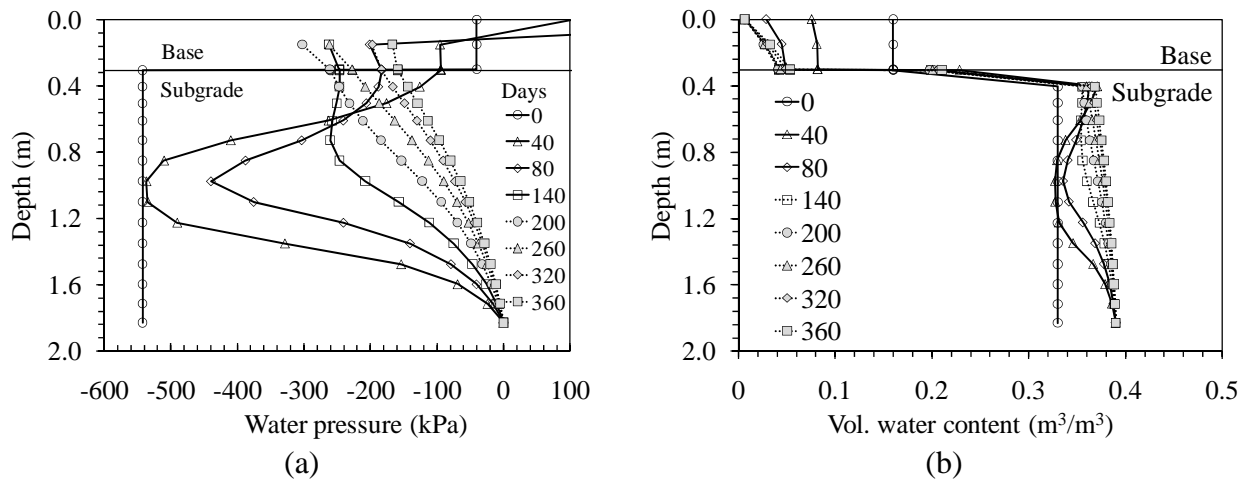


Figure 3.4: Case 1A VADOSE/W results: (a) Suction profiles for different days of analysis; and (b) Vol. water content profiles for different days of analysis

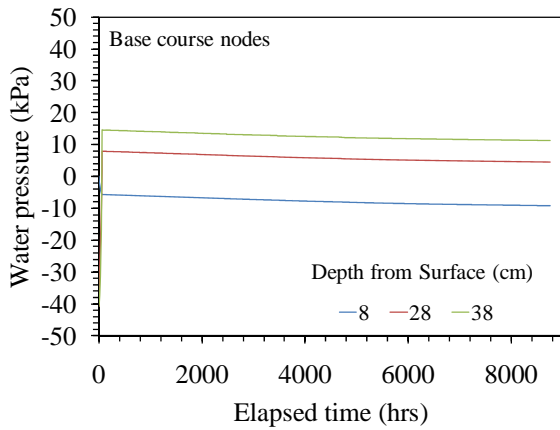




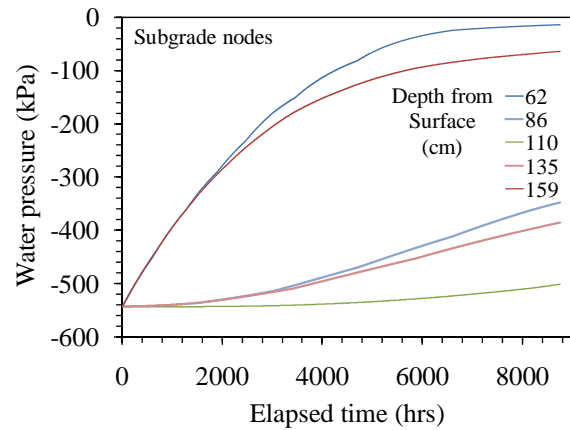
### ***3.3.3 Results from Baseline Case 1B***

Baseline Case 1B involves application of an infiltration rate to the pavement surface that is 100 times greater than in Baseline Case 1A. The EICM results from Baseline Case 1B are shown in Figure 3.6. The water pressure in the base, shown in Figure 3.5(a), indicates that the top of the base is unsaturated, while the bottom of the base is saturated and under positive pressures. This is consistent with the greater infiltration rate applied in this case. This implies that a positive pressure is being applied as the upper boundary condition to the subgrade. These pressures are observed to decrease slightly over time despite the constant infiltration rate, likely due to numerical issues. The water pressure at different depths in the soil is observed to increase at different rates for different depths in the profile consistent with Baseline Case 1A, as shown in 53.6(b). The water pressure at the top of the subgrade layer is positive in this case, consistent with the greater infiltration rate.

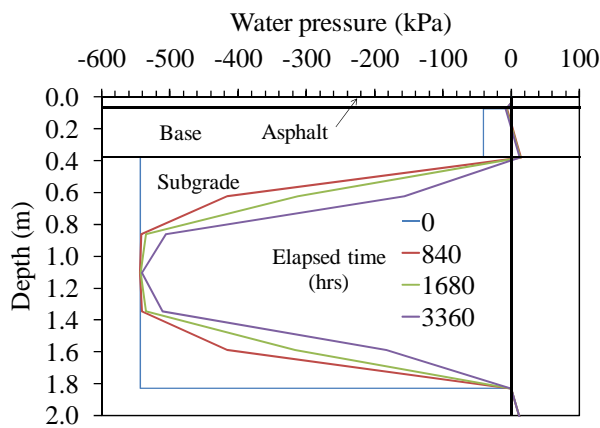
The VADOSE/W results for Baseline Case 1B are shown in Figure 3.6. Consistent with Baseline Case 1A, the base initially experiences positive water pressures. However, after equilibration with the infiltration process, the suction at the bottom of the base is slightly less than that in Baseline Case 1A. The suction at the top of the subgrade at steady-state conditions was 151 kPa. Despite the increase in infiltration rate by 2 orders of magnitude, this change in the suction at the top of the subgrade is not significant (160 kPa in Case 1A). The relatively insignificant change in the suction at the base may be due to the lack of curvature in the hydraulic conductivity of the subgrade soil for these infiltration rates.



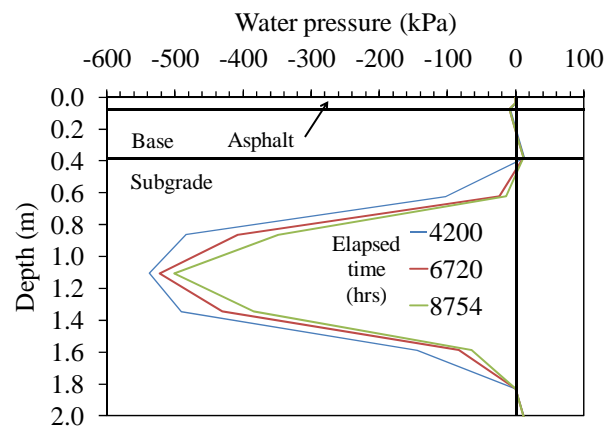
(a)



(b)

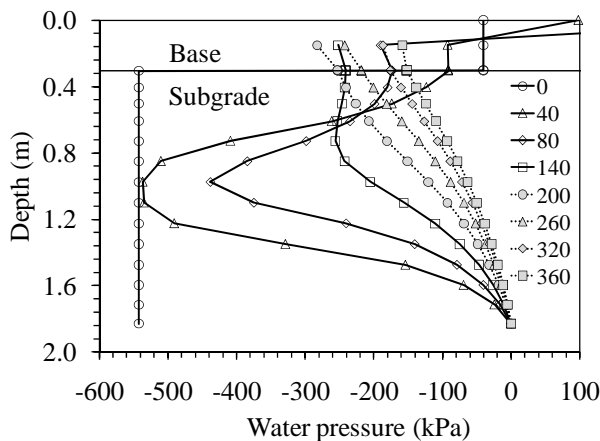


(c)

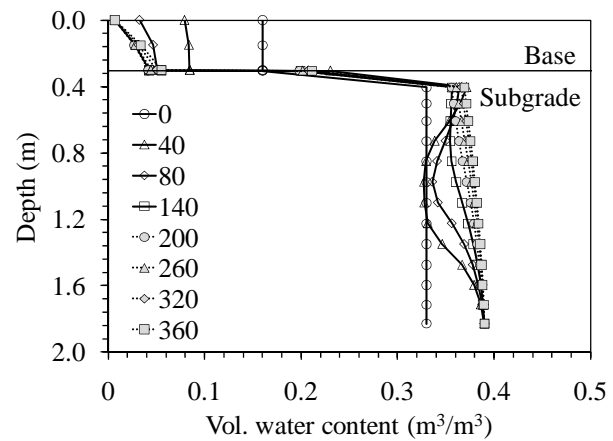


(d)

Figure 3.5: Case 1B EICM results: (a) Water pressure in base; (b) Water pressure in subgrade; (c) Water pressure profiles at early times; (d) Water pressure profiles at late times



(a)



(b)

Figure 3.6: Case 1B VADOSE/W results: (a) Suction profiles for different days of analysis; and (b) Vol. water content profiles for different days of analysis

3.3.4 Results from Baseline Case 1C

Despite the increase in infiltration rate by a factor of 100 to 0.1 in/hr from that in Baseline Case 1B (0.001 in/hr), the results for Baseline Case 1C from the EICM shown in Figure 3.7 are essentially identical to those from Baseline Case 1B in Figure 3.5. This is possibly due to a limitation in the amount of water allowed into the base course layer by the Ridgeway model in EICM, although the cutoff infiltration rate was mentioned to be 1.2 in/hr in the EICM manual. The results from VADOSE/W for Baseline Case 1C are shown in Figure 3.8, which indicate that the soil reaches saturation with depth. The water content of the base course layer is greater than in Baseline Cases 1A and 1B, which means that the greater infiltration rate supplies enough water to keep the base course wet and to provide inflow to the initially unsaturated subgrade.

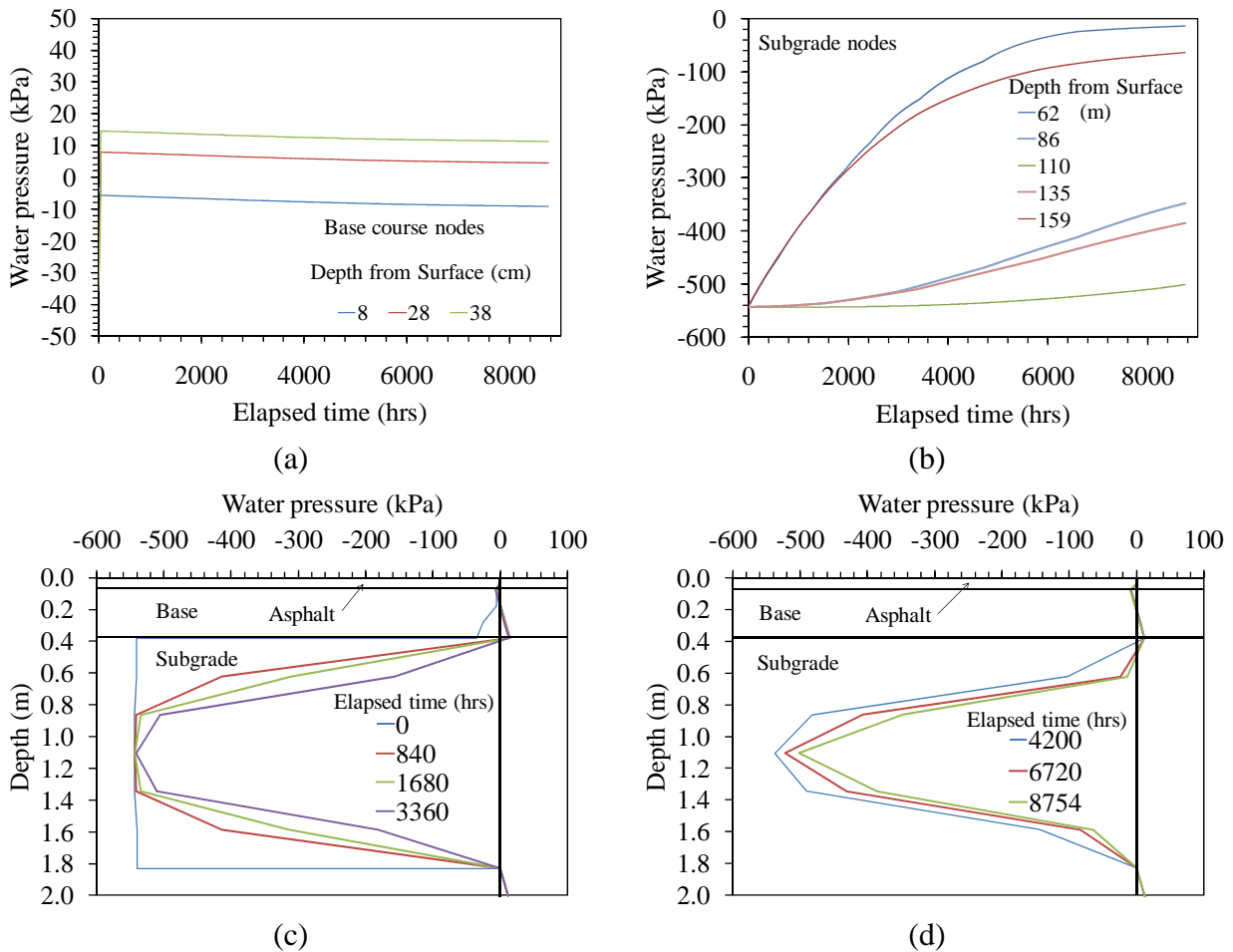


Figure 3.7: Case 1C EICM results: (a) Water pressure in base; (b) Water pressure in subgrade; (c) Water pressure profiles at early times; (d) Water pressure profiles at late times

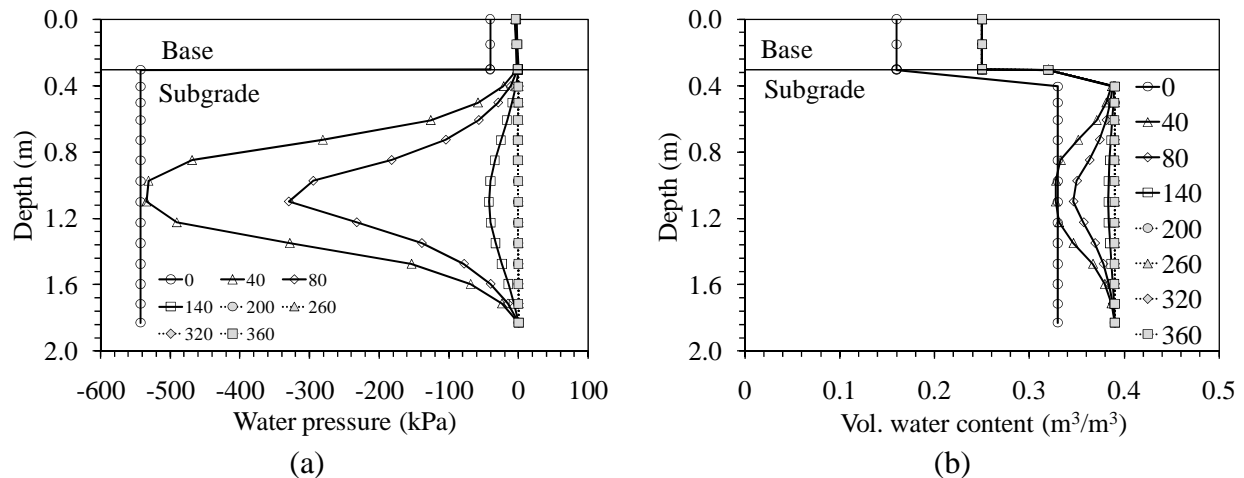


Figure 3.8: Case 1C VADOSE/W results: (a) Suction profiles for different days of analysis; and (b) Vol. water content profiles for different days of analysis

### 3.3.5 Summary of Baseline Case 1 Results

The EICM results from Baseline Case 1 indicate that infiltration rate has some impact on the model results, but only for relatively low infiltration rates. The only impact of this infiltration rate is on the steady-state profile of water pressure in the base layer, which imposes a constant suction boundary on the subgrade layer. The fact that only one year can be modeled by EICM indicates that steady-state conditions may not be reached for some soil profiles.. Lytton et al. (1993) indicates that the EICM calculates the infiltration rate to the base course using the cumulative rainfall data collected over a two week period. This may mean that the total rainfall during any two week period may be greater than the limit set by the Ridgeway model on the amount of water that can enter the base layer. In addition to the infiltration issues, the limitation of the EICM that a constant initial water content must be used for analysis prevents simulation of actual field cases, as discussed in the Chapter 5.

## 3.4 Results from Baseline Case 2

### 3.4.1 Overview of Baseline Case 2

Baseline Case 2 involves evaluation of the effect of evaporation induced by imposing a high temperature and low relative humidity on the pavement surface. Three different relative humidity values of 50, 60 and 80% along with a constant temperature of 32.2 °C were considered for the three cases in Baseline Case 2 (see Table 1). No infiltration was imposed in this case.

3.4.2 Results for Baseline Case 2A

The EICM results for Baseline Case 2A in Figure 3.9 are extremely puzzling. This figure indicates that the results for this case are the same as those for Baseline Cases 1B and 1C, even though no infiltration was imposed. This indicates that the EICM does not consider evaporation in its analysis, likely due to the effect of the asphalt layer. An interesting implication of these results is that this means that the high infiltration rates imposed in Baseline Cases 1B and 1C corresponds to no water entering the subgrade layer. Instead, the base is assumed to remain constantly saturated throughout the year, leading to a decrease in suction in the subgrade. This is a major issue of concern with the EICM. The results from VADOSE/W shown in Figure 3.10 are more consistent with what should be expected. The suction at the top of the subgrade reached a value of 250 kPa (Figure 3.10(a)), while the base was nearly air-dry (Figure 3.10(b)).

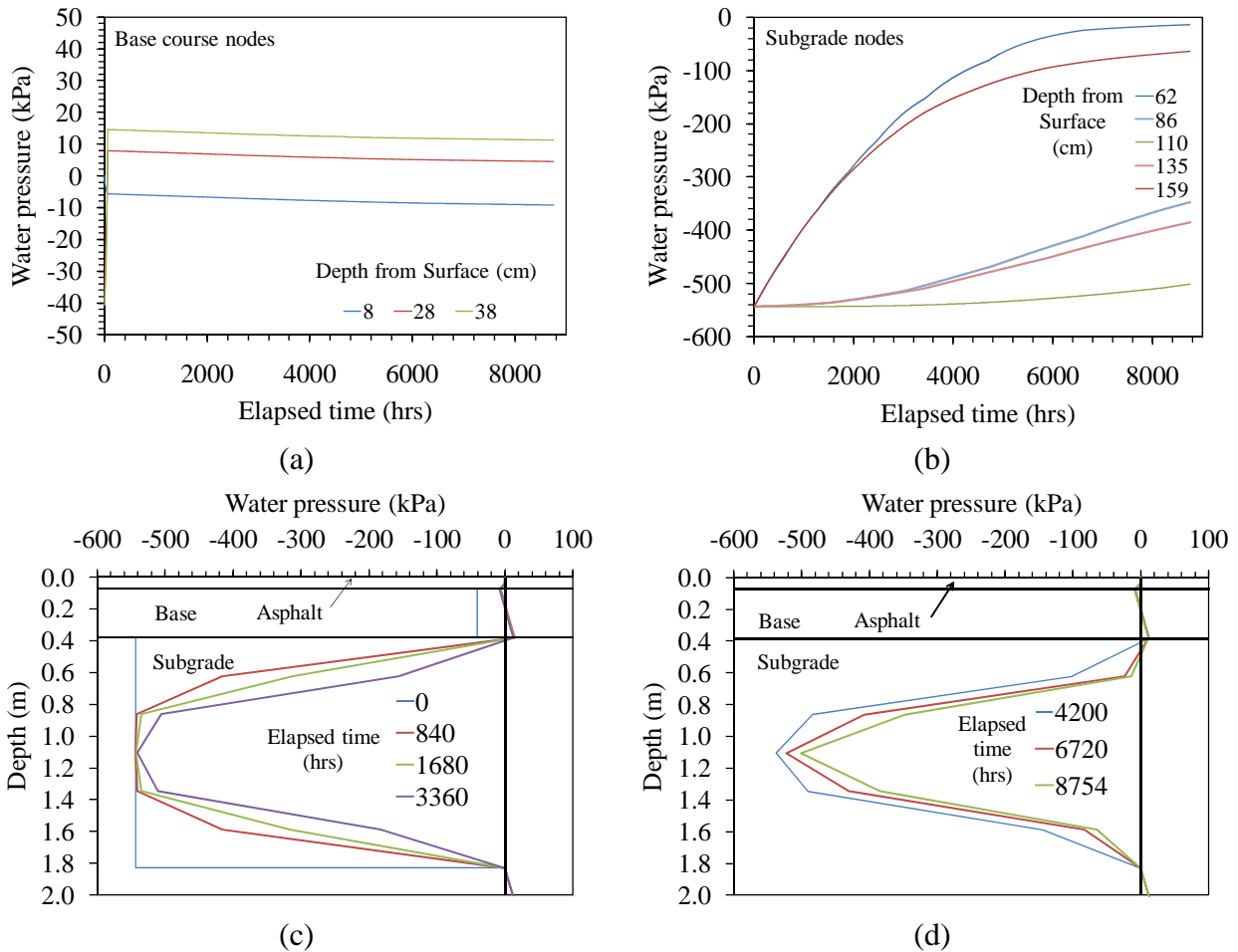


Figure 3.9: Case 2A EICM results: (a) Water pressure in base; (b) Water pressure in subgrade; (c) Water pressure profiles at early times; (d) Water pressure profiles at late times

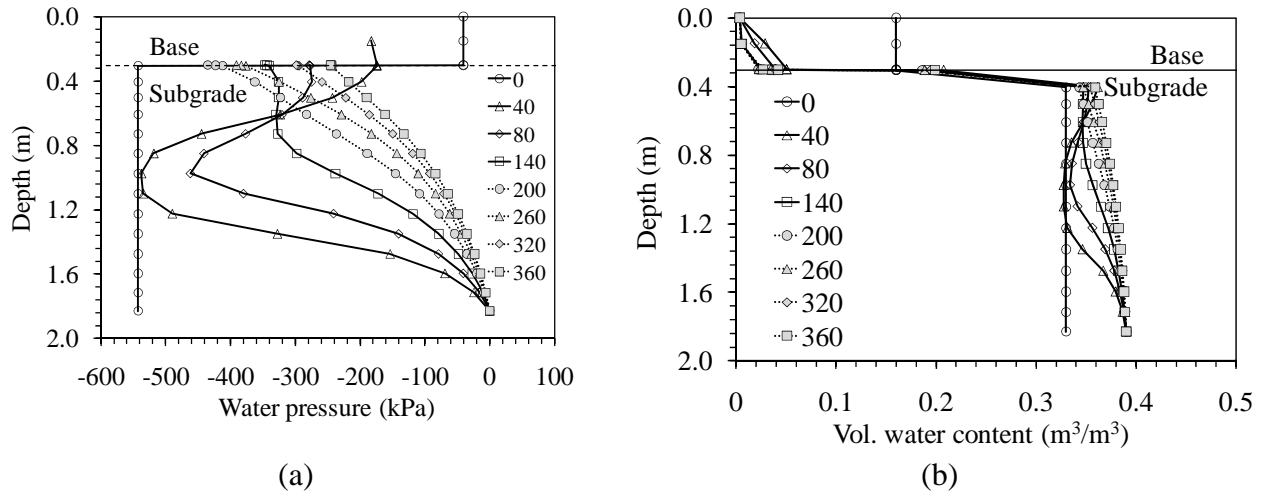


Figure 3.10: Case 2A VADOSE/W results: (a) Suction profiles; and (b) Water content profiles

3.4.3 Results for Baseline Case 2B

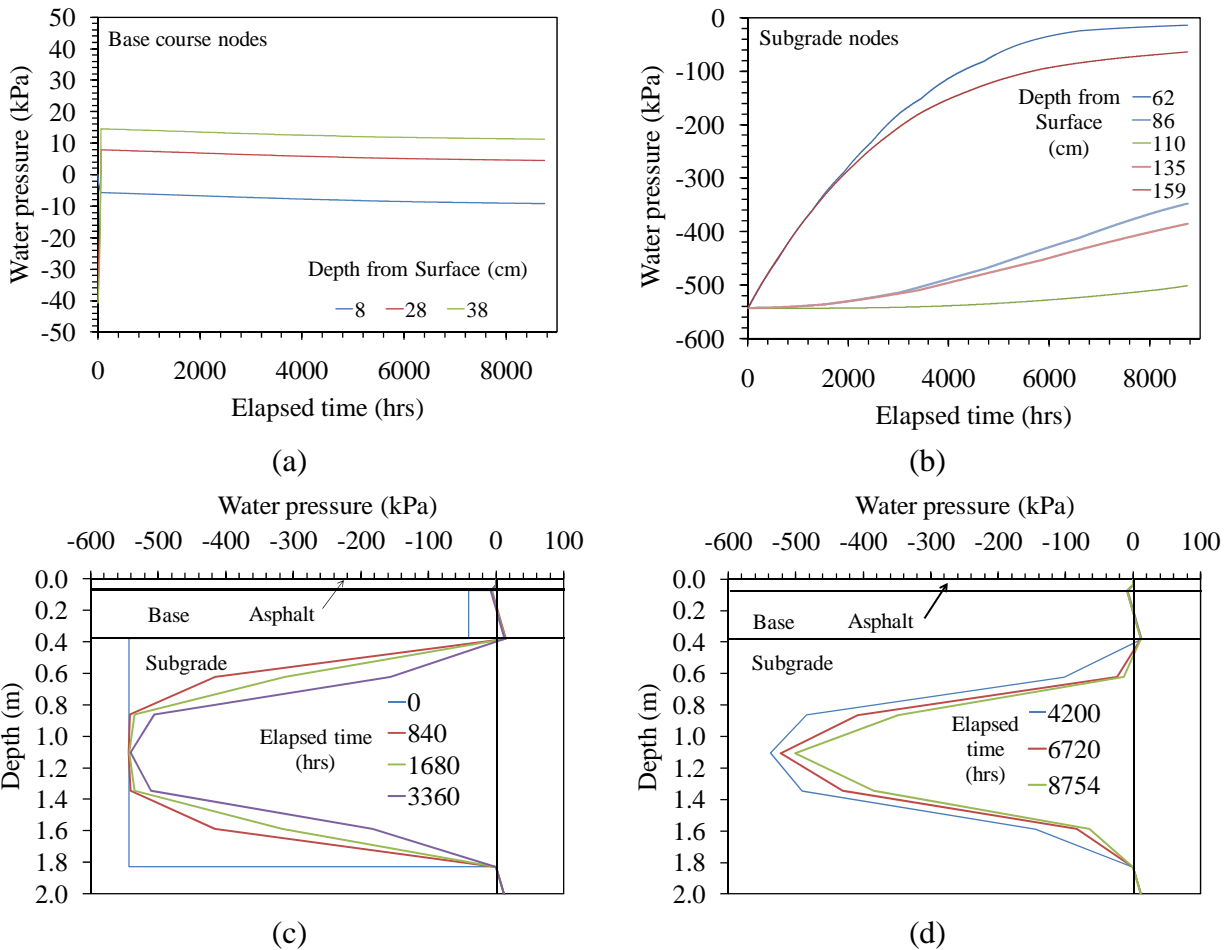


Figure 3.11: Case 2B EICM results: (a) Water pressure in base; (b) Water pressure in subgrade; (c) Water pressure profiles at early times; (d) Water pressure profiles at late times

Again, the EICM results for Baseline Case 2B shown in Figure 3.11 indicate the same results despite the change in boundary condition. The VADOSE/W results in Figure 3.12 are reasonable. The suction at the top of the subgrade layer after a year of evaporation under this higher relative humidity (i.e., less evaporation) is -210 kPa. This is lower than in Baseline Case 2A, which had a higher relative humidity.

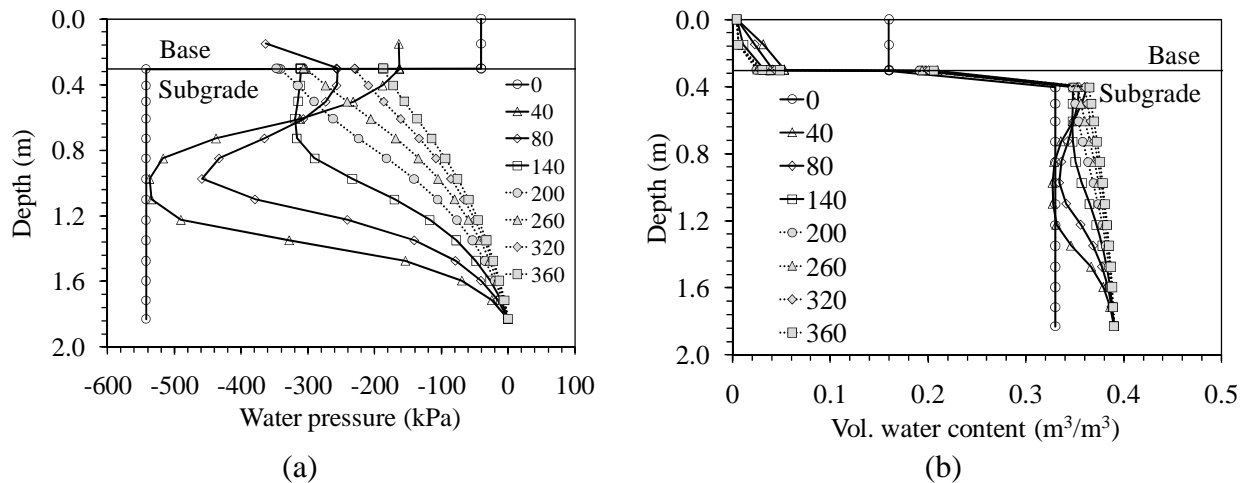
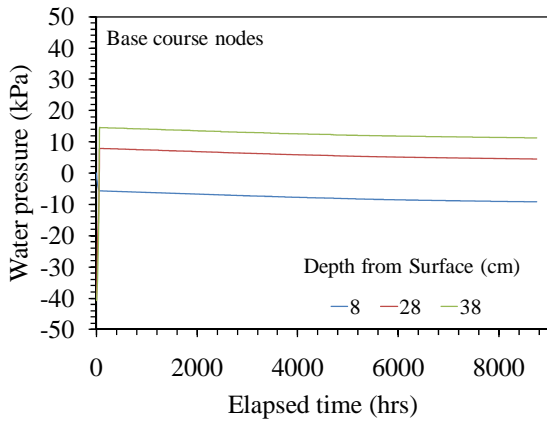


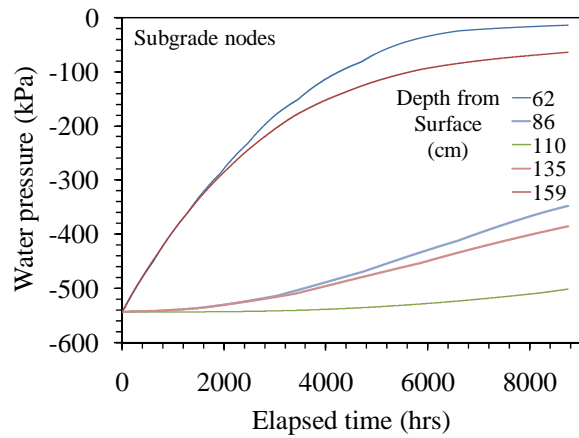
Figure 3.12: Case 2B VADOSE/W results: (a) Suction profiles for different days of analysis; and (b) Vol. water content profiles for different days of analysis

### 3.4.4 Results for Baseline Case 2C

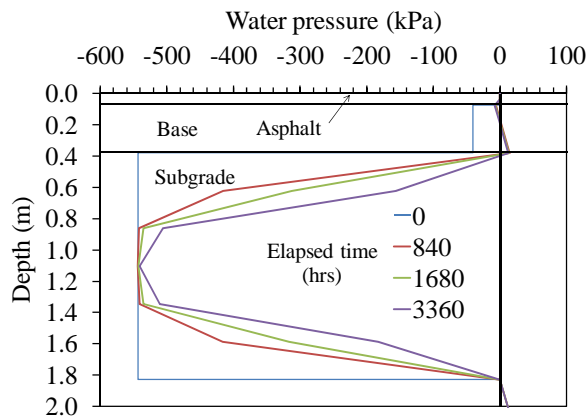
Again, the EICM results for Baseline Case 2C shown in Figure 3.13 indicate the same results despite the change in boundary condition. The VADOSE/W results in Figure 3.14 are also reasonable. The suction at the top of the subgrade layer after a year of evaporation under this relative humidity is -200 kPa. This is only slightly lower than in Baseline Case 2B, which had a slightly higher relative humidity.



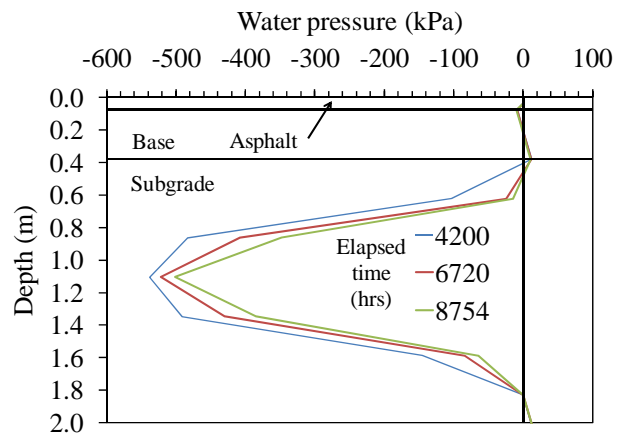
(a)



(b)



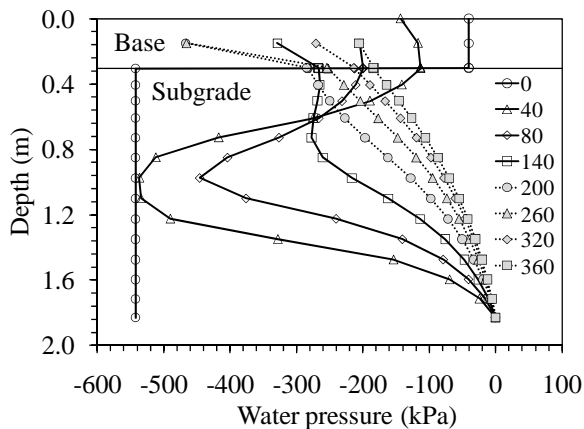
(c)



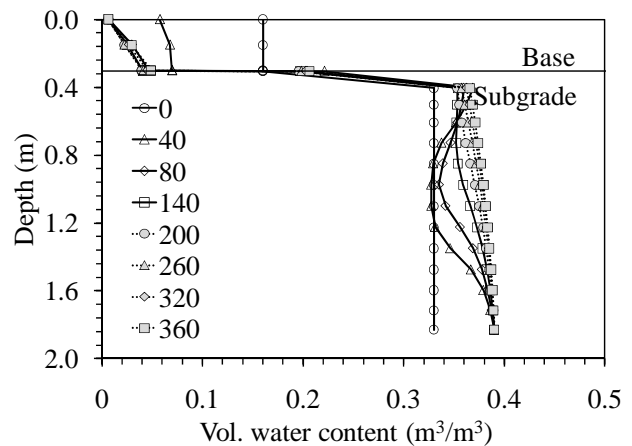
(d)

Figure 3.13: Case 2B EICM results: (a) Water pressure in base; (b) Water pressure in subgrade;

(c) Water pressure profiles at early times; (d) Water pressure profiles at late times



(a)



(b)

Figure 3.14: Case 2C VADOSE/W results: (a) Suction profiles for different days of analysis; and

(b) Vol. water content profiles for different days of analysis



### ***3.4.5 Overview of Baseline Case 2 Results***

The results from Baseline Case 2 indicate that humidity has a negligible impact on the results of the EICM model. However, these results also imply that infiltration rates greater than 0.00001 in/hr may have a negligible impact on the infiltration process. The fact that wetting of the occurred in the EICM results when no infiltration was applied to the pavement was initially confusing. However, the VADOSE/W results indicate that the soil profile became wetter than the initial suction over time, because the relative humidity meant that water vapor was flowing into the initially dry soil. Nonetheless, the fact that the EICM showed the same results for each relative humidity indicates that the algorithm for the water content of the base is not sensitive to the relative humidity.

## 4. FOCUS SITES IN ARKANSAS AND FIELD MONITORING PROGRAM

### 4.1 Focus Regions in Arkansas

There are six distinct regions of Arkansas having different topographic, climatic, and geographic settings, shown in Figure 4.1. In general terms, the Ozark plateau is relatively dry due to its elevation with freezing temperatures through most of the winter, the Arkansas river valley is more temperate due to the river and lower elevation, the Mississippi embayment is relatively humid with warmer temperatures throughout the year, Northeast Arkansas has weather patterns affected by the contrast in elevation from the embayment due to Crowley's ridge, the west gulf coastal plain is relatively humid with temperatures similar to Louisiana, the Ouachita mountains have a blend in climate between the Ozarks and the west gulf coastal plain.

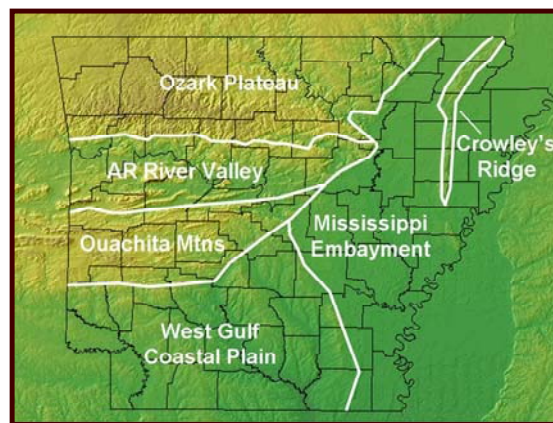


Figure 4.1: Regions of Arkansas with distinct climates

Seven pavement sites in each of these regions were selected as test sites to validate the predictions of the EICM, shown in the map in Figure 4.2. The sites were selected to have the same surface treatment (*i.e.*, asphalt concrete), geometry (*i.e.*, embankment slopes, drainage ditch shape), performance (*i.e.*, lack of cracking or rutting), and topographical settings (*i.e.*, a flat section of road). A summary of the sites and geometries is shown in Table 4.1.

Table 4.1: Summary of locations in Arkansas for suction-temperature monitoring

Site	Region	Asphalt thickness (cm)	Base thickness (cm)
Greenland	Ozark Mountains	8.9	17.8
Plumerville	Arkansas River Valley	7.6	17.8
Malvern	Central Arkansas	5.1	17.8
Murfreesboro	Ouachita Moutains	8.3	30.5
Camden	West Gulf Coastal Plain	15.2	35.6
Lake Village	Mississippi Embayment	11.4	34.3
Marked Tree	Northeast Arkansas	6.0	22.0



Figure 4.1: Regions of Arkansas with distinct climates

The weather data for each site was collected from a publically-available online database (Weather Underground), from a weather station within 10 miles of each site. The weather is summarized in Appendix B. A summary of the maximum, minimum, and average annual values of temperature, humidity, and precipitation for each of the sites is shown in Table 4.2.

Table 4.2:

Site	Temperature (°C)			Relative humidity (%)			Average daily precipitation
	Max	Mean	Min	Max	Mean	Min	
Greenland	20.1	14.0	7.9	91.7	71.4	46.8	0.3
Plumerville	22.1	15.7	9.4	92.8	71.8	45.4	0.3
Murfreesboro	23.5	16.8	10.1	93.7	70.2	46.0	0.3
Malvern	22.7	17.1	11.3	86.7	66.2	45.2	0.4
Camden	21.8	16.2	10.4	98.0	77.7	52.5	0.1
Lake Village	23.3	17.6	11.7	89.9	69.9	48.0	0.3
Marked Tree	21.2	15.7	10.1	89.1	69.2	48.3	0.4

Not only is the weather different at each of the sites, but the soils are different throughout the state. The soils in the mountain regions of the state are typically The procedures and detailed results for the characterization of the soils from the different sites are presented in Appendix A.

This includes index tests to classify the soils, hydraulic tests to determine the hydraulic conductivity and soil-water retention curve (SWRC), and thermal tests to determine the thermal conductivity. A summary of the soil properties from the different sites which will be used in the EICM and VADOSE/W analyses is shown in Table 4.3.

Table 4.3: Summary of hydraulic properties for Arkansas soils

Site	USCS soil classification	Hydraulic conductivity (m/s)	$\theta_s$ (%)	$\theta_r$ (%)	$a_{FX}$ (kPa)	$n_{FX}$	$m_{FX}$
Greenland	CH	$5.74 \times 10^{-11}$	43.8	0.0	650	1.80	1.50
Plumerville	CH	$4.38 \times 10^{-10}$	36.8	0.0	1600	1.20	1.75
Malvern	CH	$8.47 \times 10^{-10}$	27.2	0.0	1200	1.10	1.98
Murfreesboro	CL	$2.23 \times 10^{-11}$	37.6	0.0	350	1.50	0.40
Camden	CH	$1.19 \times 10^{-9}$	33.2	0.0	750	1.70	1.00
Lake Village	CL	$3.2 \times 10^{-11}$	41.3	0.0	300	1.70	1.00
Marked Tree	CH	$5.63 \times 10^{-11}$	42.9	0.0	1100	1.20	1.50

## 4.2 Field Monitoring Program

In addition to characterization of the geometry, soil properties, and pavement conditions at each of these six sites located in Arkansas, a monitoring plan is proposed to measure site-specific fluctuations in matric suction and temperature in the subgrade layers. Field monitoring of water content and temperature in pavements is not a simple exercise due to the complications in placing sensors beneath existing roads. Approaches that have been used in the past are pit installations (Liang et al. 2007) and trenches (Gupta et al. 2008). However, pit installations cannot be installed beneath the asphalt and are limited in depth. Trenches are destructive, and are only suitable for new pavement construction. Accordingly, a new field monitoring approach was developed in this study.

This new approach consists of inserting sensors into boreholes constructed through cores through the asphalt layer, backfilling the borehole with soil having high hydraulic conductivity, and sealing the surface with an asphalt cap. Decagon EC-TM sensors (Figure 4.3) were used in this project, as they are capable of simultaneously measuring temperature and water content, have relatively long battery life (2-3 years), and are robust and suitable for field deployment.

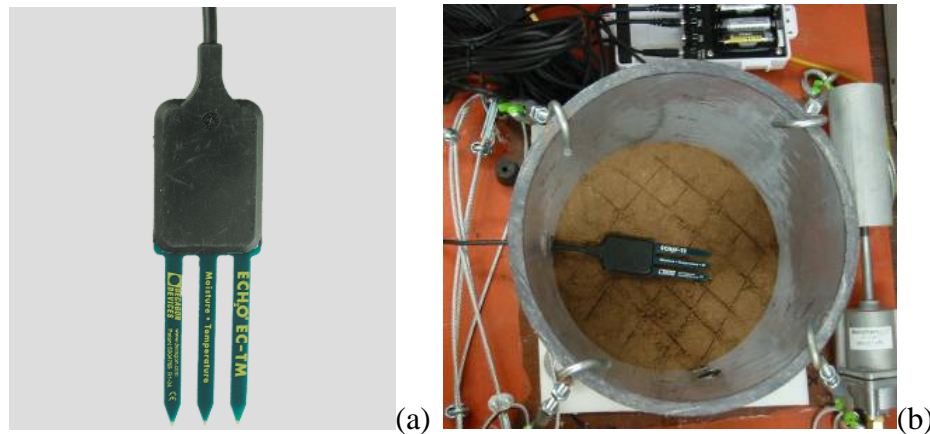


Figure 4.3: (a) EC-TM temperature-water content sensor; (b) Calibration of EC-TM sensor

The same monitoring program was implemented at all seven sites in Arkansas. A schematic of the typical monitoring installation at a site is shown in Figure 4.4. The goal of this monitoring approach was to evaluate the fluctuations in water content near the edge of the pavement, underneath the asphalt layer, as this is where the greatest fluctuations in matric suction are expected.

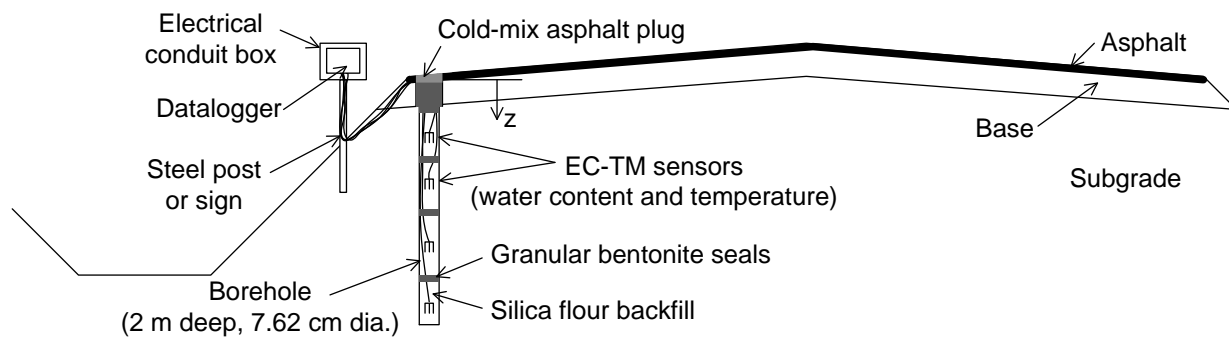


Figure 4.4: Schematic of the field installation setup

The first step in the installation is to create a 6 inch core through the asphalt layer. This core is used to determine the as-built thickness of the asphalt layer. The next step is to auger through the base course layer and the top of the subgrade, as shown in Figure 4.5(a). After subgrade soil starts to come up on the augur, the auguring was stopped and the hole was cleaned. The as-built depth of the base course layer was then measured. Next, a thin-walled 3 ft-long Shelby tube was pushed into the subgrade to obtain a sample of soil. A second Shelby tube was then pushed to obtain a second sample of subgrade. This sampling process resulted in a borehole with a depth of approximately 6 ft. Intact Shelby tube samples of soil from each site were transported to the University of Colorado at Boulder for geotechnical characterization (see Appendix A).

The next step of the installation was to use an asphalt saw to create a channel in the asphalt to the edge of the shoulder as shown in Figure 4.5(b). This channel is used to pass the wires of the sensors from the borehole to a datalogger box in the shoulder. The final channel is shown in Figure 4.5(c).

The next step was to drape an EC-TM sensor into the borehole, after which a silica flour backfill was poured into the borehole. Silica flour is essentially crushed rock, and is typically used in pottery applications. It was used in this study because it has high hydraulic conductivity when unsaturated, and because a consistent soil structure is obtained when pouring it into the borehole. The site-soils were all clays, so it was not possible to replace this soil back into the borehole and ensure adequate contact between the subgrade and EC-TM sensors. A picture of the wire of several EC-TM sensors and silica flour (white powder) in the borehole is shown in Figure 4.5(d).

After placement of one layer of silica flour around a dielectric sensor, a layer of granular bentonite clay was placed atop the silica flour. Due to the low hydraulic conductivity of the bentonite, it acts as a hydraulic barrier between the lower layer of silica flour and another layer of silica flour placed atop the bentonite layer. This approach can be used to create individual “pockets” of silica flour. The dielectric sensors in each pocket can be used to infer the suction at different depths in the soil layer, using an approach that will be discussed later in this section. The bentonite also helps to avoid seepage of water along the sensor cables. After all of the sensors have been installed in the subgrade, section of the hole at the depth of the base course was filled with bentonite. The sensor cables were passed through a flexible electrical conduit for protection, which was passed through the channel in the asphalt. The conduit was buried in the subgrade soil and was attached to a metal box which contains the datalogger.

Cold mix asphalt was used to fill the top inches of the bore, as shown in Figure 4.5(d). The metal box holding the datalogger was secured to a street sign or metal post, as shown in Figure 4.5(e), in order to protect the datalogger from water, traffic, animals, and mowers.



Figure 4.5: Field monitoring system installation pictures: (a) Auguring through base course; (b) Creating channel through asphalt; (c) Final channel in asphalt running to the edge of the shoulder; (d) installation of sensors and backfilling with silica flour; (e) Cold-mix patch on surface; (f) Datalogger box in shoulder attached to metal post

As mentioned, the silica flour was used due to its relatively high permeability when unsaturated, which means that water will be readily transmitted from the subgrade soil to the silica flour around the sensor during changes in soil suction due to environmental interaction. The EC-TM sensors measure the water content of the silica flour, not that of the surrounding soil. Although the soil at the interface with the silica flour may have a significantly different water content, the matric suction at the interface is continuous. This means that the EC-TM sensors are used to infer the matric suction in the soil by way of measuring the water content of

the silica flour. The SWRC for the silica flour is shown in Figure 4.6 along with that of a typical clay soil (see Appendix A for more details). These SWRCs can be used to explain the concept of suction measurement using the EC-TM sensors. For instance, if the EC-TM sensor indicates that the volumetric water content in the silica flour is 25%, the suction within the silica flour for this volumetric water content can be determined using the silica flour SWRC to be 50 kPa. As the suction is continuous between the silica flour and surrounding soil, the suction within the soil must also be 50 kPa. At this suction, the SWRC for the soil can be used to determine that the water content in the soil is 38%. The thermal conductivity of silica flour is similar to that of soils, so the temperature measurements from the EC-TM sensors were not modified.

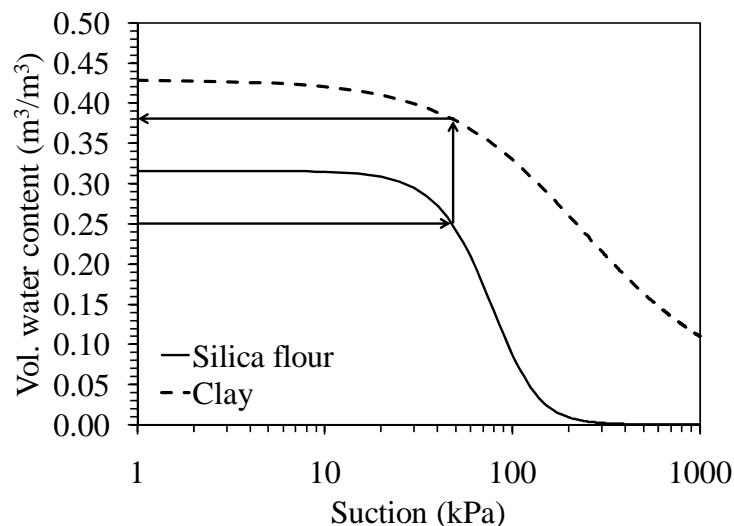


Figure 4.6: SWRCs of silica flour and a clay soil showing the concept of suction measurement

### 4.3 Suction and Temperature Monitoring Results

The measured suction and temperature data for each of the seven sites are shown in Figures 4.7 through 4.14. Each of these figures shows the variation in suction and temperature with time, as well as profiles of suction and temperature with depth. The time-series figures for suction indicate that it required approximately 2 months for the sensors to equilibrate with the subgrade soil (see Figure 4.7(a) for a good example). Although some of the sensors appear to be malfunctioning over time (especially those from Marked Tree), the sensors provide reasonable results. The suction profiles indicate that the suction decreases with depth, which is expected for a shallow water table. The greatest fluctuations in suction occur in the sensor closest to the surface. One strange observation was that the measured temperatures vary more for deeper sensors than for the shallow ones, except at Camden. This will be discussed in the next chapter.



4.4.1 Greenland Data

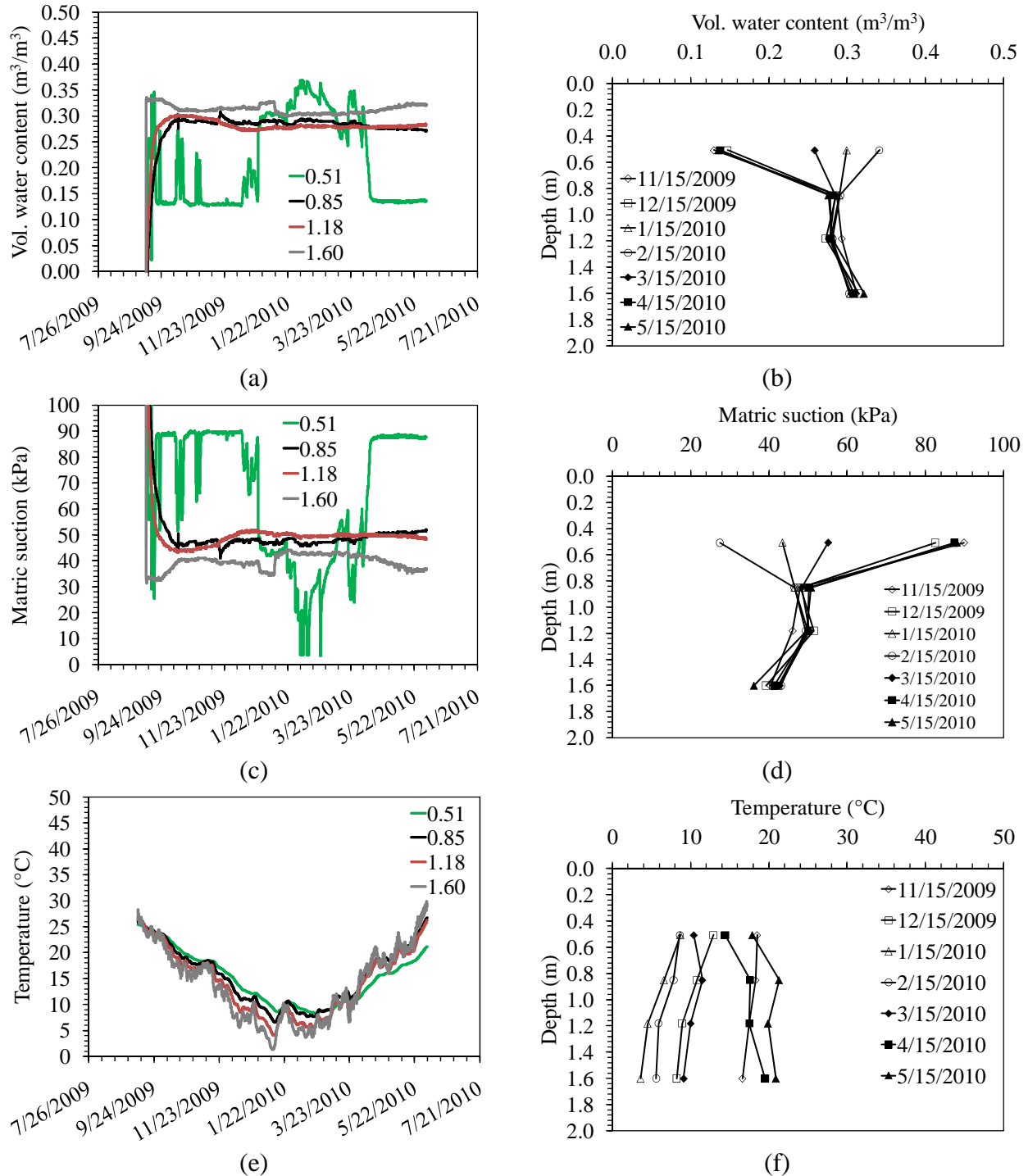


Figure 4.7: Field monitoring data for Greenland: (a) Silica flour water content; (b) Silica flour water content profiles; (c) Matric suction; (d) Matric suction profiles; (e) Temperature; (f) Temperature profiles

4.3.2 Plumerville Data

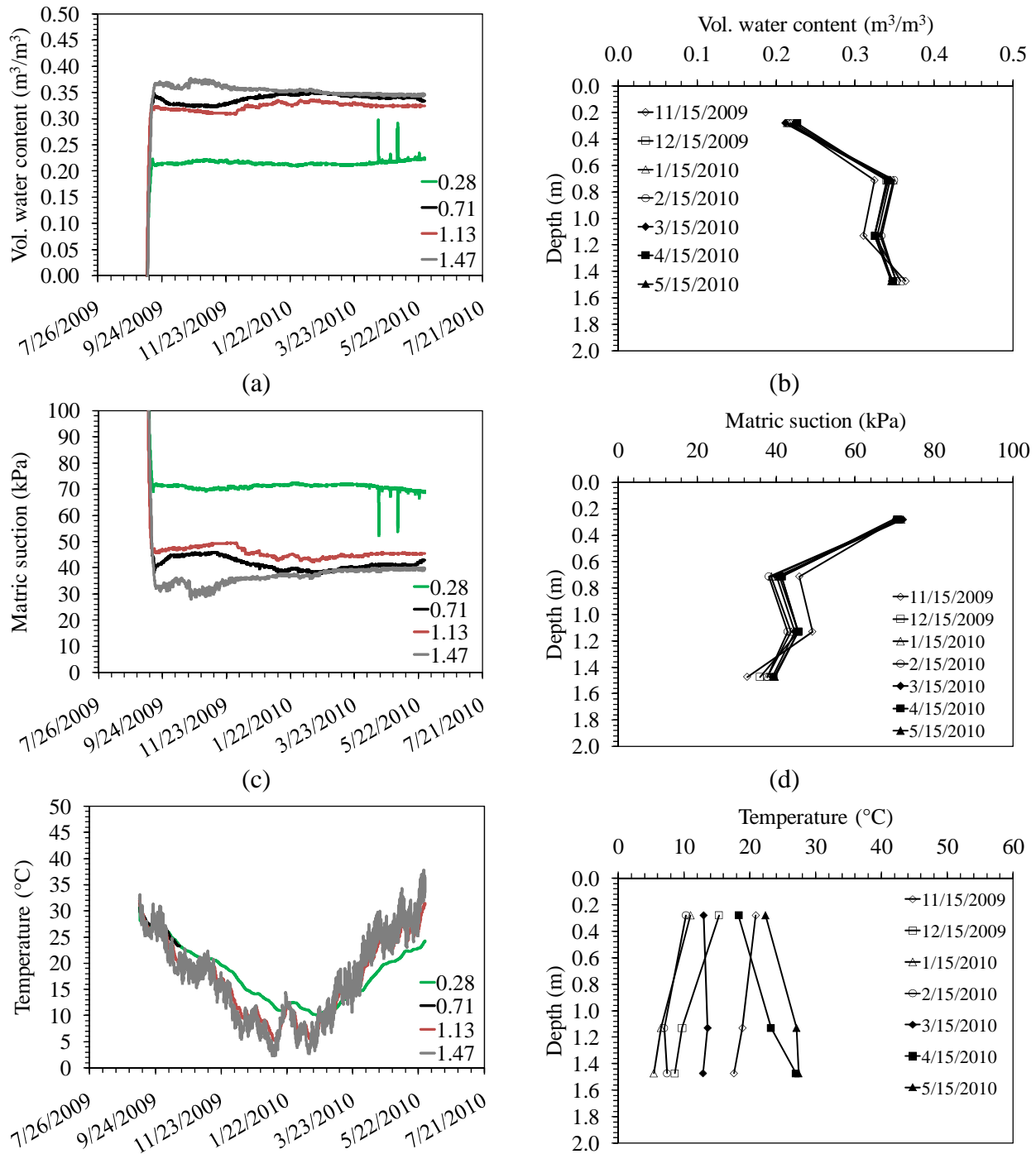


Figure 4.8: Field monitoring data for Plumerville: (a) Silica flour water content; (b) Silica flour water content profiles; (c) Matric suction; (d) Matric suction profiles; (e) Temperature; (f) Temperature profiles

4.3.3 Malvern Data

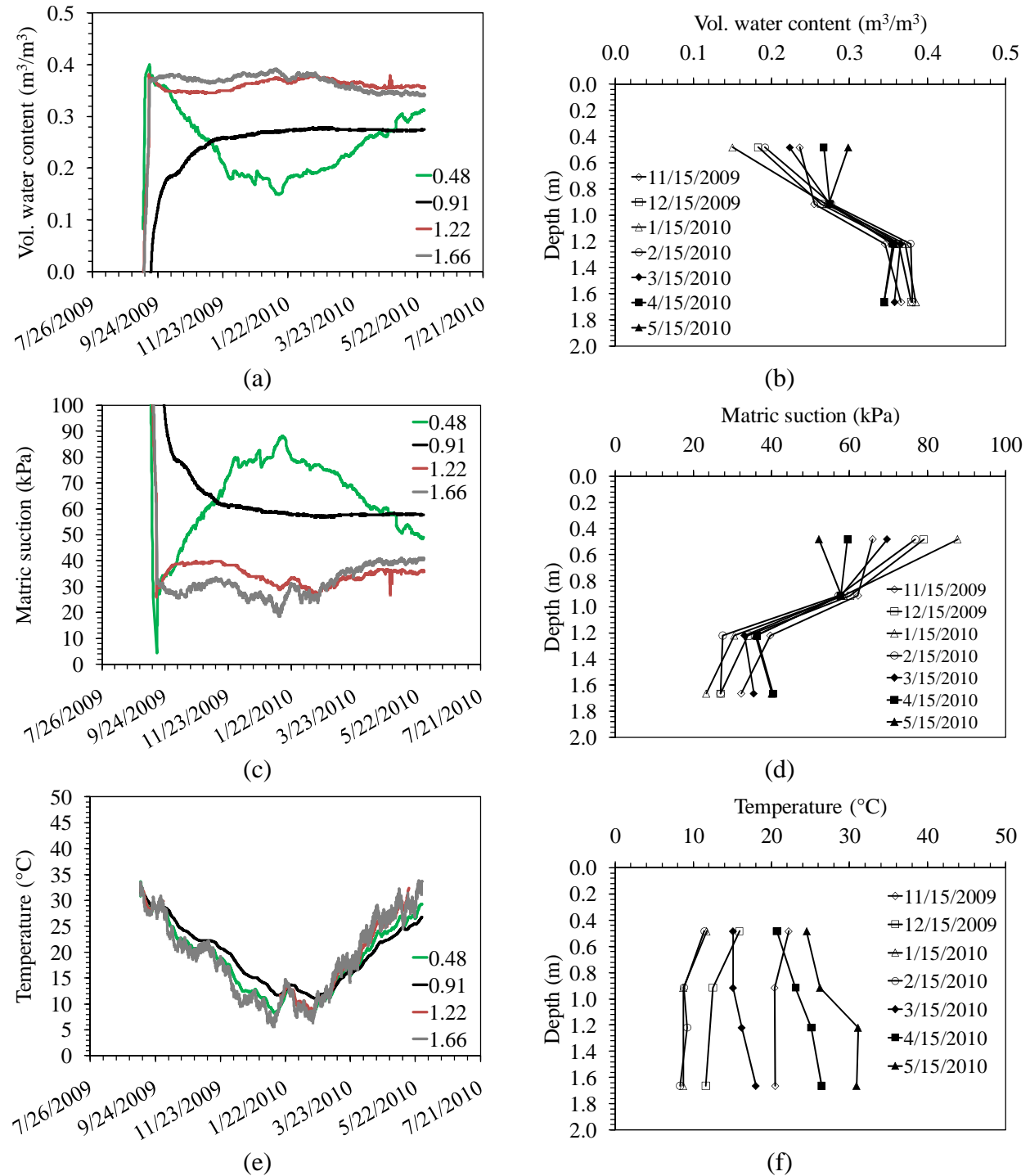


Figure 4.9: Field monitoring data for Malvern: (a) Silica flour water content; (b) Silica flour water content profiles; (c) Matric suction; (d) Matric suction profiles; (e) Temperature; (f) Temperature profiles

4.3.4 Murfreesboro Data

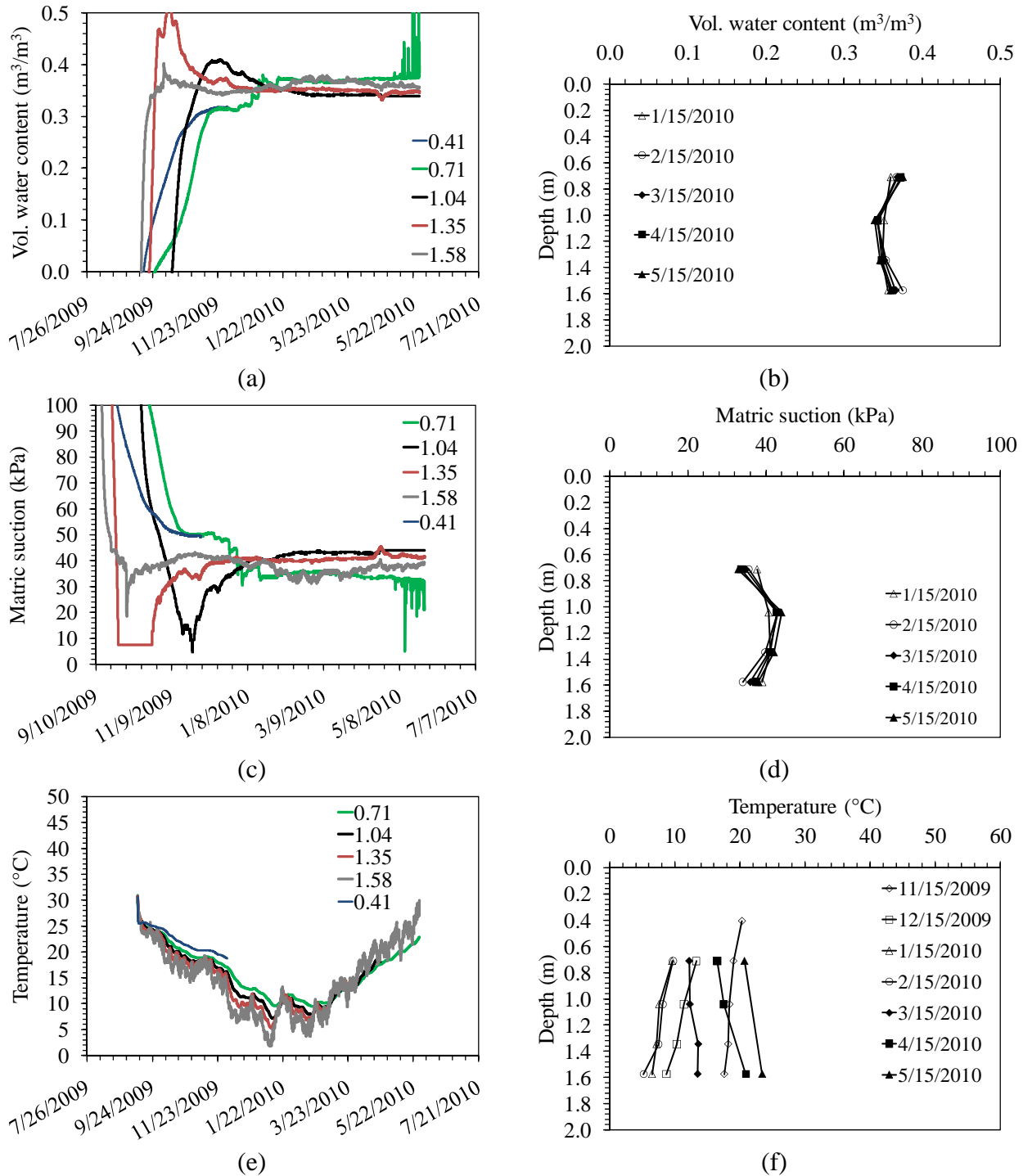


Figure 4.10: Field monitoring data for Murfreesboro: (a) Silica flour water content; (b) Silica flour water content profiles; (c) Matric suction; (d) Matric suction profiles; (e) Temperature; (f) Temperature profiles

4.3.5 Camden Data

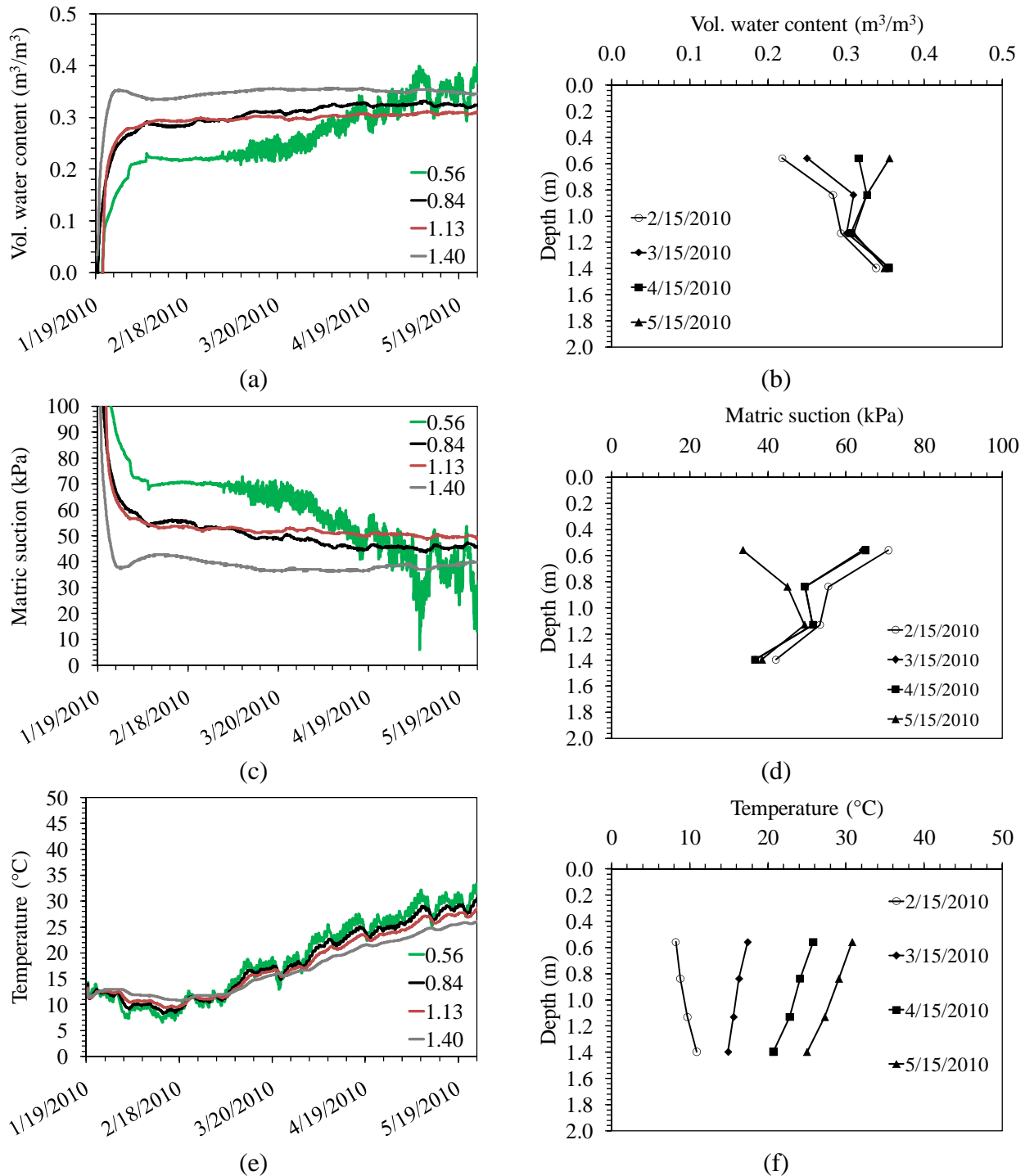


Figure 4.11: Field monitoring data for Camden: (a) Silica flour water content; (b) Silica flour water content profiles; (c) Matric suction; (d) Matric suction profiles; (e) Temperature; (f) Temperature profiles

4.3.6 Lake Village Data

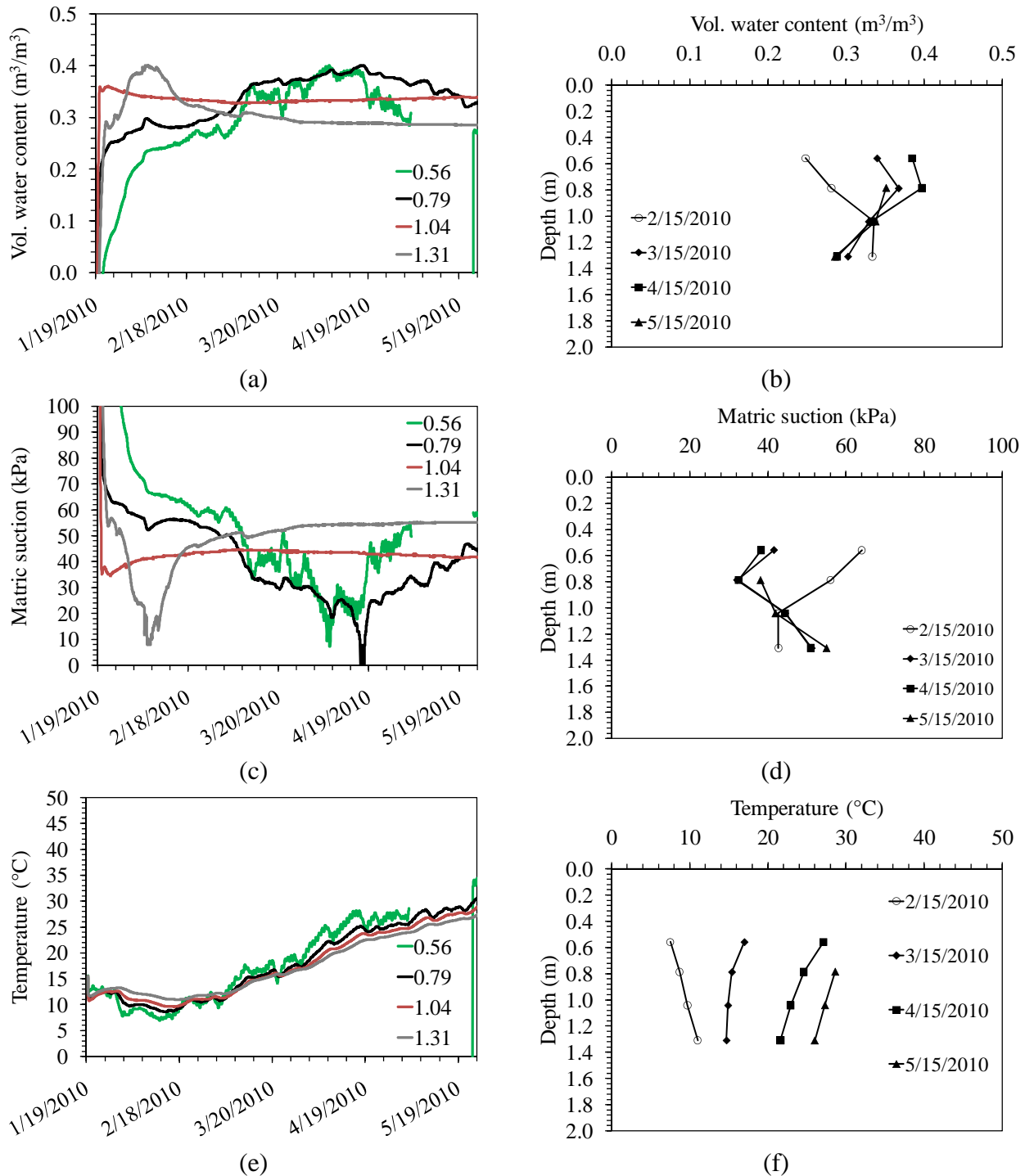


Figure 4.12: Field monitoring data for Lake Village: (a) Silica flour water content; (b) Silica flour water content profiles; (c) Matric suction; (d) Matric suction profiles; (e) Temperature; (f) Temperature profiles

4.3.7 Marked Tree Data

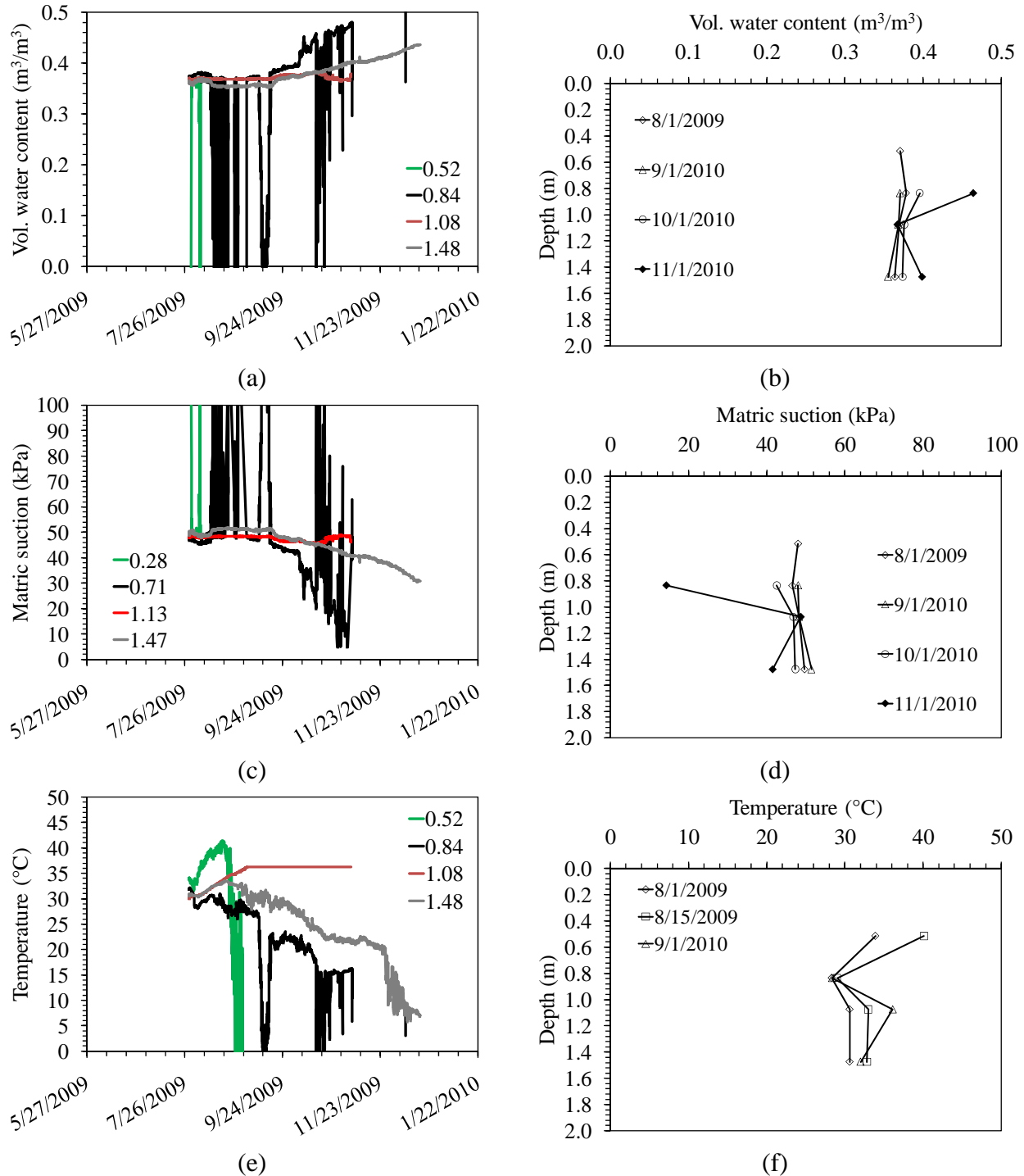


Figure 4.14: Field monitoring data for Marked Tree: (a) Silica flour water content; (b) Silica flour water content profiles; (c) Matric suction; (d) Matric suction profiles; (e) Temperature; (f) Temperature profiles

## 5. COMPARISON OF MODEL PREDICTIONS WITH FIELD MEASUREMENTS

### 5.1 Overview

This chapter involves a comparison between the EICM and VADOSE/W predictions of the matric suction and temperature profiles at the seven sites in Arkansas using Level 3 inputs for the subgrade soil and weather data, and Level 1 inputs for the asphalt and base layers. The asphalt layer is an important component in pavement systems. The results from the two models are not expected to be the same, but their relative performance in matching the field data is expected to be different. The EICM has the advantage over VADOSE/W in that it considers the asphalt in the hydraulic analysis. Although empirical, the quantification of how water is transferred through the asphalt into the base and subgrade is complex. Although the asphalt likely varied from site to site, the default asphalt properties in the EICM was used. The compacted aggregate base course was assumed to be an AASHTO A-3 soil for all of the sites. The thicknesses of the asphalt and base layers were set to be the same as those measured in the field. The subgrade soils are all represented using the material properties presented in Appendix A.

Interaction between the atmosphere and the pavement soil layers was modeled using EICM and VADOSE/W. Specifically, one-dimensional, coupled flow of heat and water were simulated for the soil in the shoulder area of the pavement using atmospheric boundary conditions. The asphalt layer was not considered in this analysis, so the results are representative of the shoulder of the pavement. During field visits to each of the sites, the water table was observed to coincide with the drainage ditch throughout much of the year, which is at a depth of approximately 2 m from the shoulder of the pavement. Accordingly, a depth of 2 meters was used for the water table at all of the sites. A total depth of 10 meters was used in the temperature analysis, as this was the depth to which fluctuations in temperature were observed. A total depth of 2 meters was used in the suction analysis, to ensure that the models had as many nodes as possible in the subgrade layer.

The initial temperature profile used in the analysis was defined as the average annual air temperature for each of the sites. For the EICM analyses, the initial water content in the subgrade was set to be the water content from the SWRC at which the soil started to desaturate. This was selected to give a reasonable starting point for the analysis. This is reasonable as the water table at all of the sites is relatively close to the surface, so the soil is nearly saturated. For the VADOSE/W analyses, the initial suction profile was defined by running the model with weather



data from 2005-2010, and observing the suction profile around which suction fluctuates on a seasonal basis. A similar approach was used by Weeks and Wilson (2005) in modeling tailing covers to obtain more reliable matching of model results and field measurements of suction.

A comparison of the EICM and field results is shown in Figures 5.1 through 5.21. The predicted suction profiles at the sites were generally reasonable, but only because the initial suction in the subgrade layers was defined as described above. The charts of suction as a function of time indicate that the predicted suction in all of the soil layers did not change significantly. Although the measured pore water pressures from the sites indicate that there were not significant changes with time after the sensors reached equilibrium, there was more of a change than that predicted by the EICM, especially closer to the pavement surface. Another important issue is that the EICM does not predict any significant fluctuations in the base course layer in response to climate interaction. Despite the lack of success in modeling the pore water pressure at the sites, the temperature profiles at the sites were consistent with the field measurements. However, the field measurements often showed a greater fluctuation in temperature for deeper points. This field observation is not physically intuitive, and may be due to fluctuations in the ground water temperature at the sites.

A comparison of the VADOSE/W and field results is shown in Figures 5.22 through 5.42 for each of the sites. The suction profiles from the VADOSE/W model seem to provide a better fit to the experimental data, with greater fluctuations in suction near the ground surface than deeper in the soil profile. This could be attributed to the lack of an asphalt layer in the flow analysis, meaning that all infiltration is able to enter the base and subgrade layers readily. The temperature profile predictions are consistent with EICM and the field measurements.

Overall, comparison of the EICM, VADOSE/W and field results indicates that EICM provides a relatively good prediction of the temperature profiles. However, it will likely not provide an acceptable long-term prediction of the suction profiles in the subgrade layer. This is especially the case for the low permeability subgrade clays present in Arkansas. Consistent with the baseline case evaluation, the results shown in this chapter indicate that the EICM should not be used to predict water flow in pavement systems until further sophistication is incorporated to change the role of the asphalt and base course layers in pavement-atmosphere interaction.

## 5.2 EICM and Field Comparison

### 5.2.1 Greenland

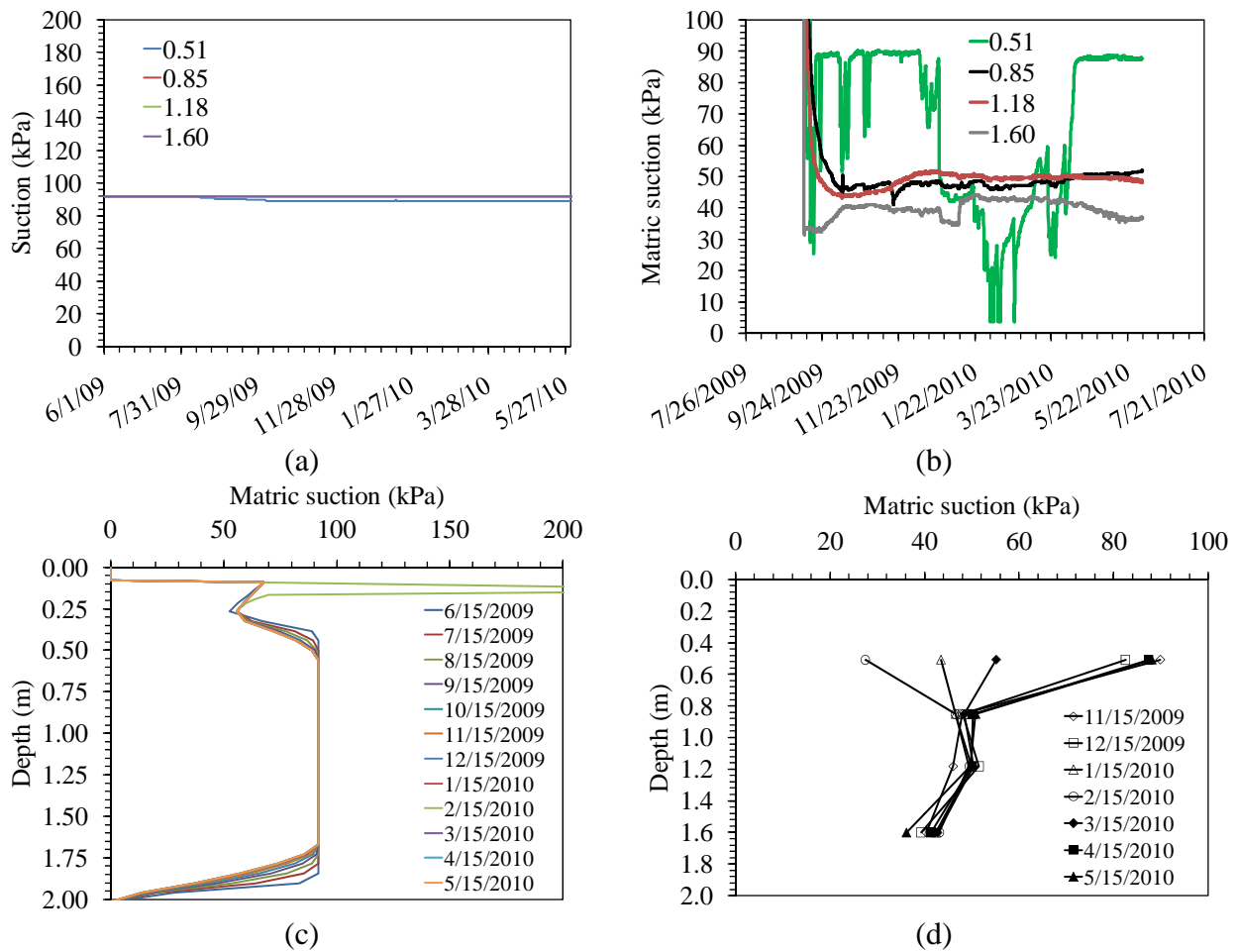


Figure 5.1: Suction: (a) EICM chart; (b) Field chart; (c) EICM profiles; (d) Field Profiles

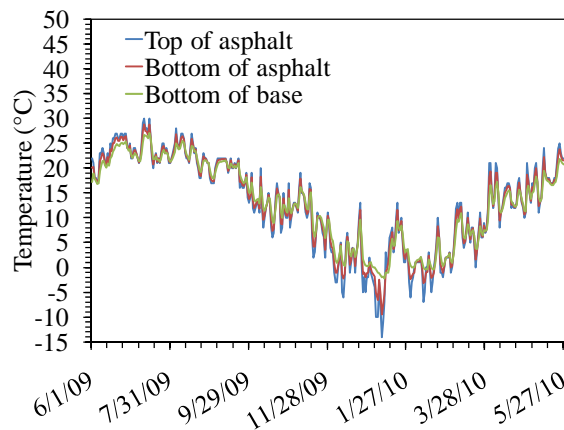


Figure 5.2: Predicted temperature in asphalt and base layers from EICM

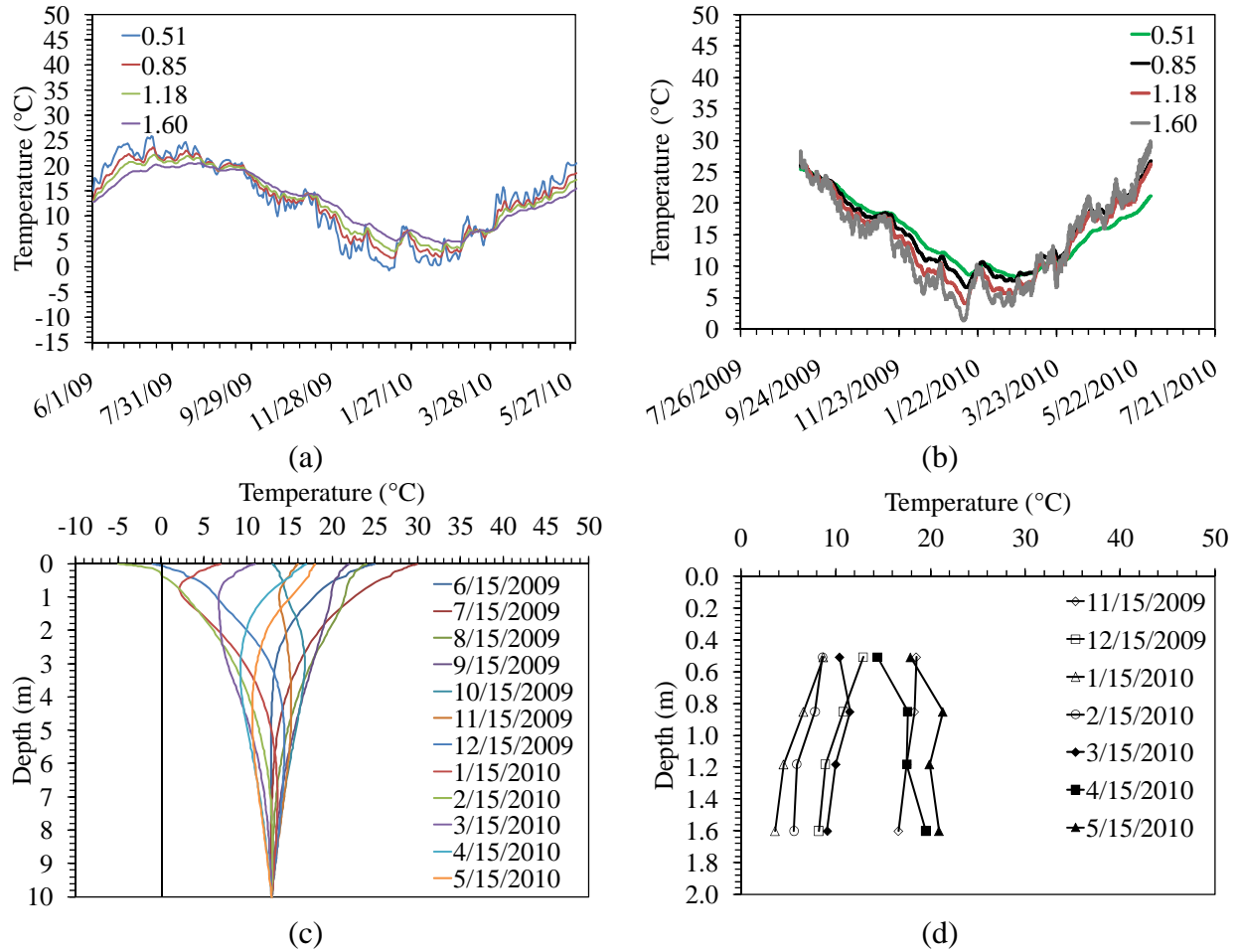


Figure 5.3: Temperature: (a) EICM chart; (b) Field chart; (c) EICM profiles; (d) Field Profiles

5.2.2 Plumerville

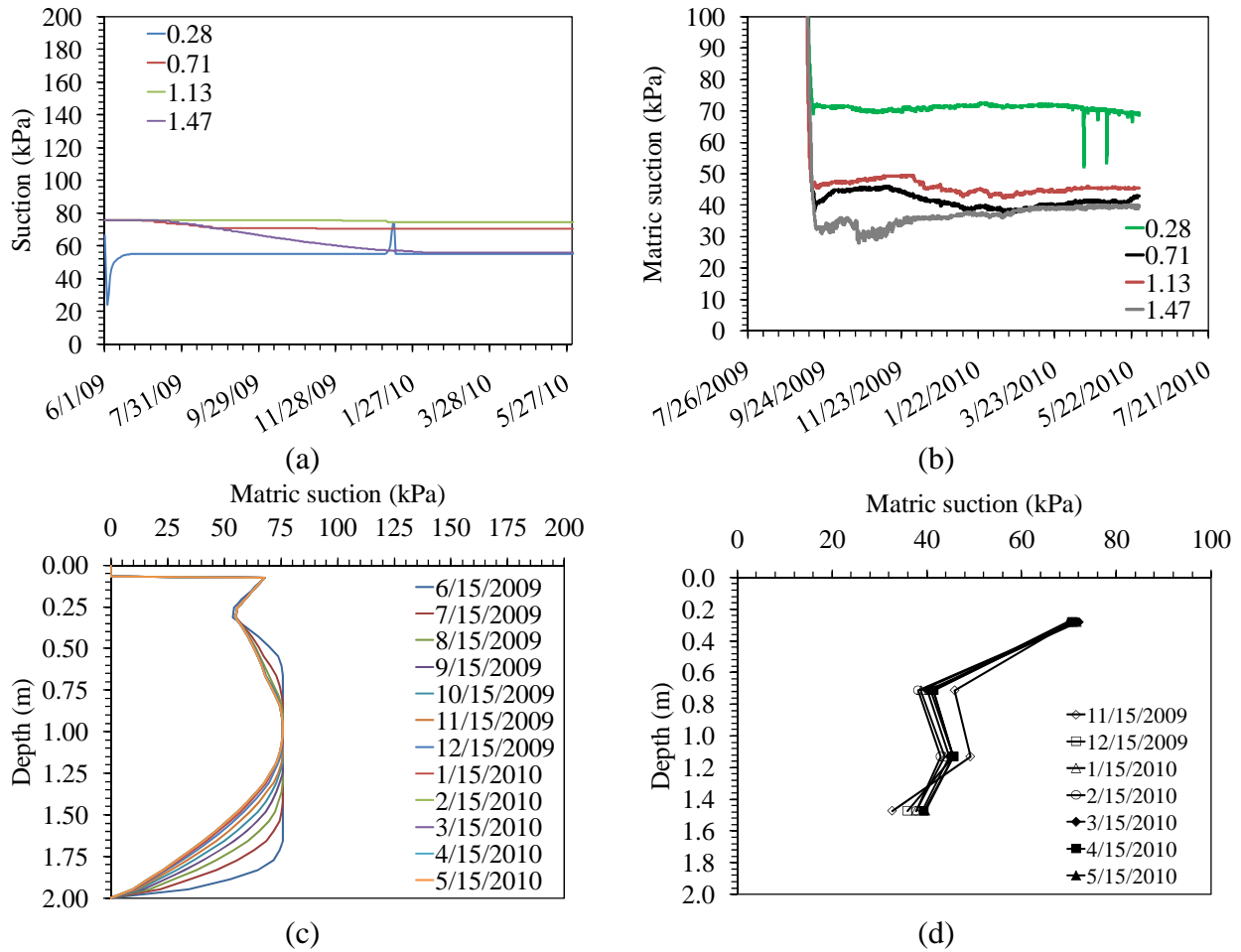


Figure 5.4: Suction: (a) EICM chart; (b) Field chart; (c) EICM profiles; (d) Field Profiles

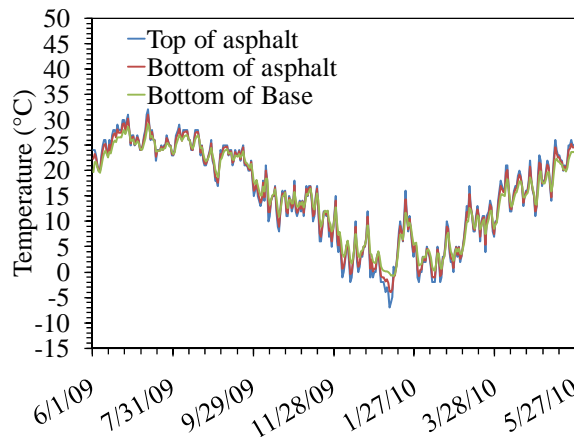


Figure 5.5: Predicted temperature in asphalt and base layers from EICM

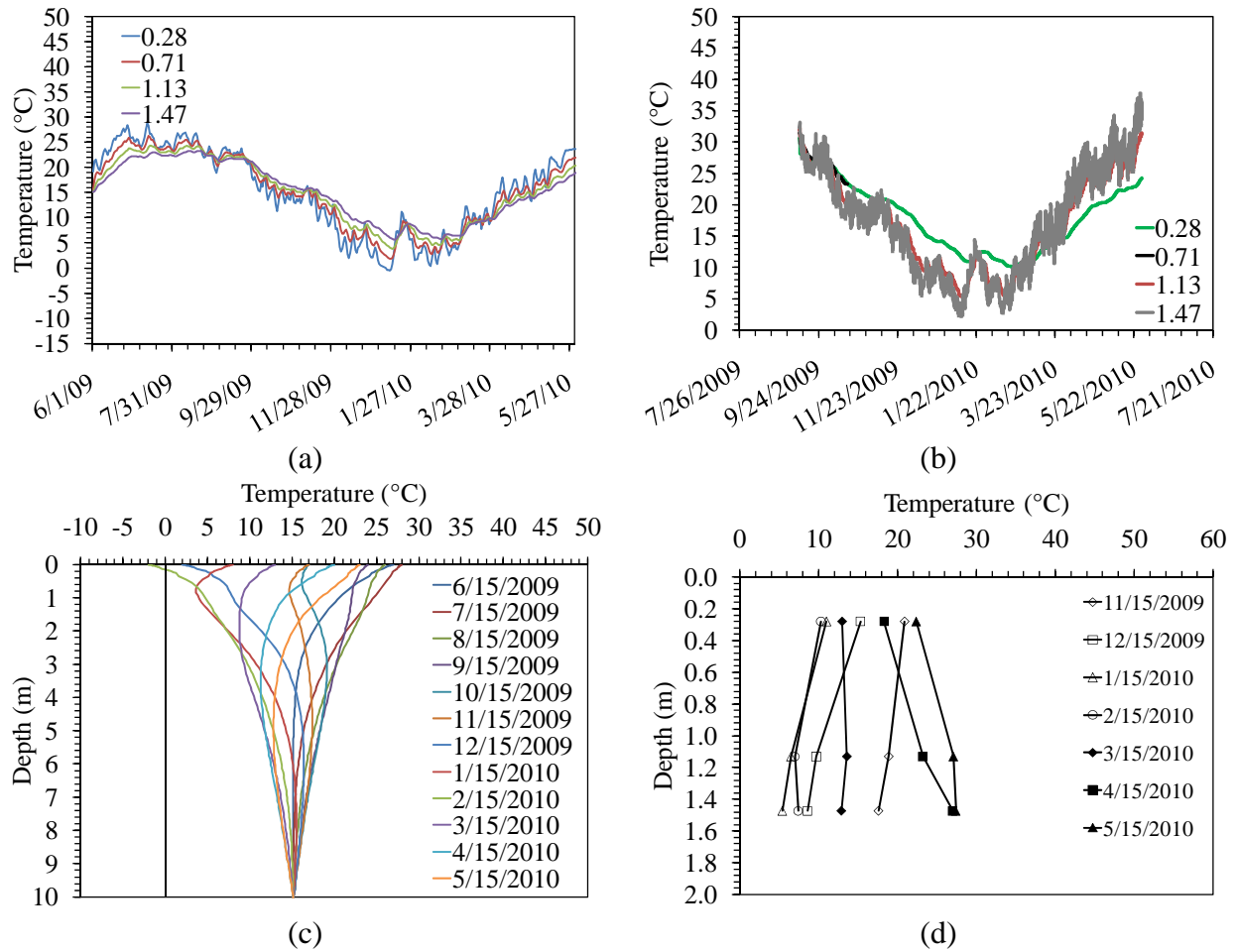


Figure 5.6: Temperature: (a) EICM chart; (b) Field chart; (c) EICM profiles; (d) Field Profiles

5.2.3 Malvern

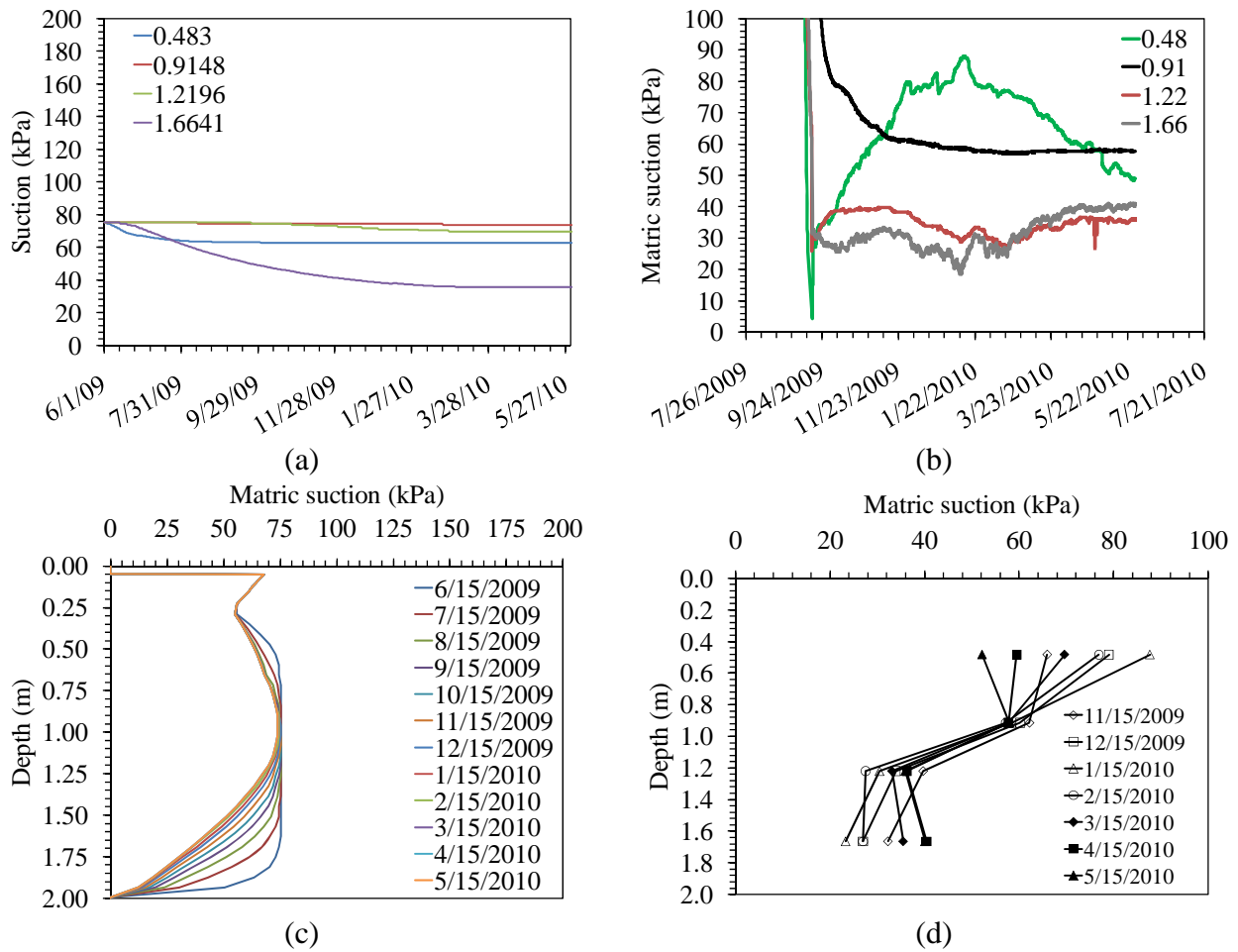


Figure 5.7: Suction: (a) EICM chart; (b) Field chart; (c) EICM profiles; (d) Field Profiles

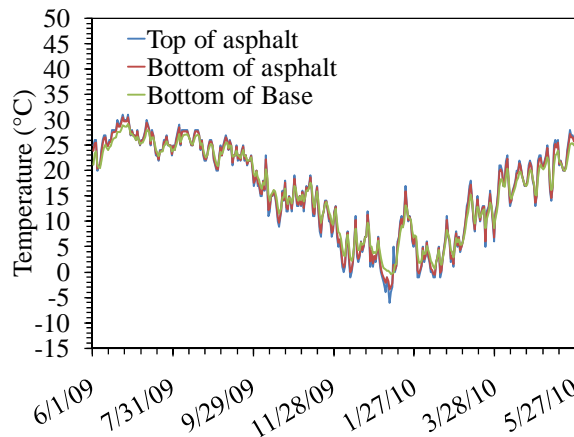


Figure 5.8: Predicted temperature in asphalt and base layers from EICM

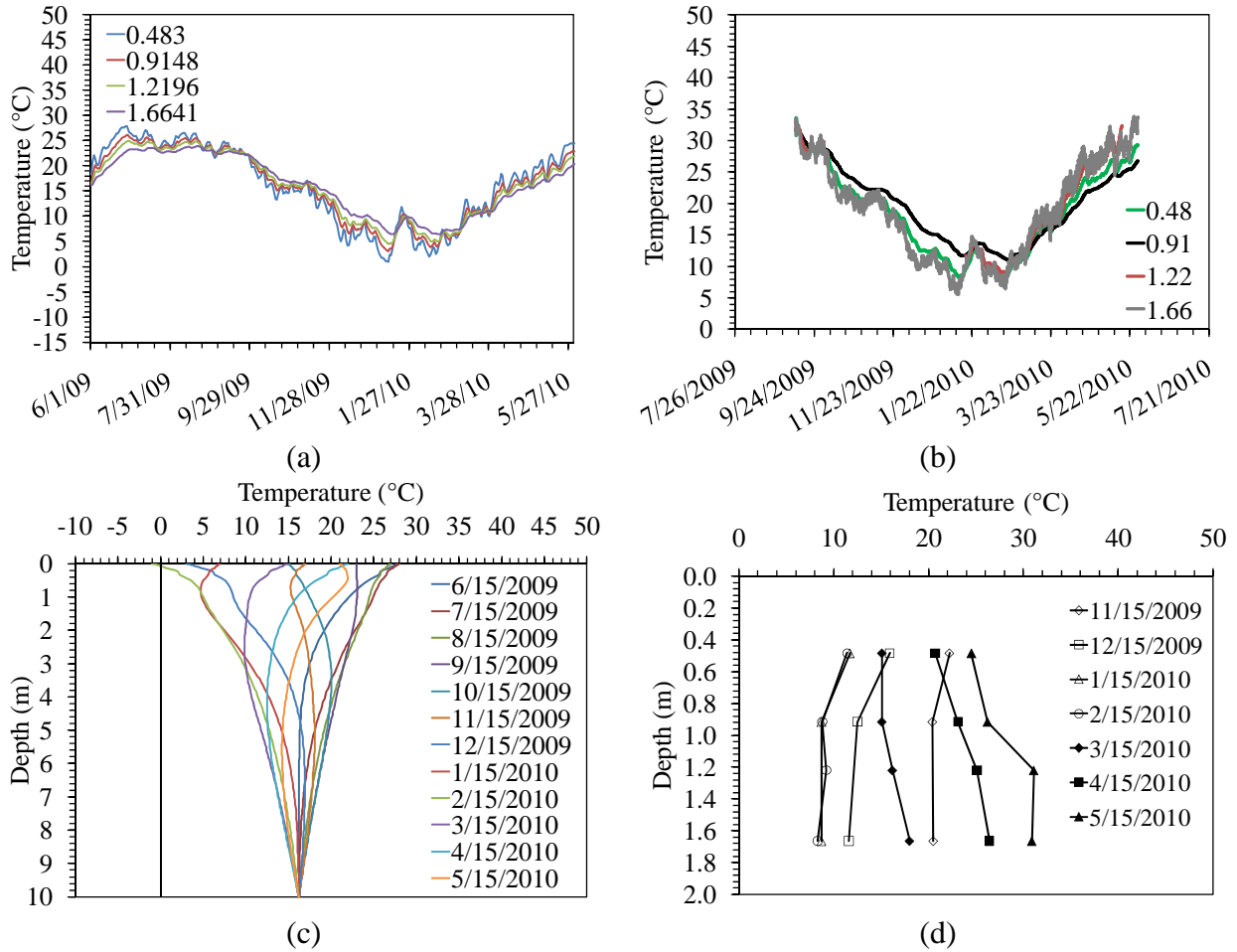


Figure 5.9: Temperature: (a) EICM chart; (b) Field chart; (c) EICM profiles; (d) Field Profiles

5.2.4 Murfreesboro

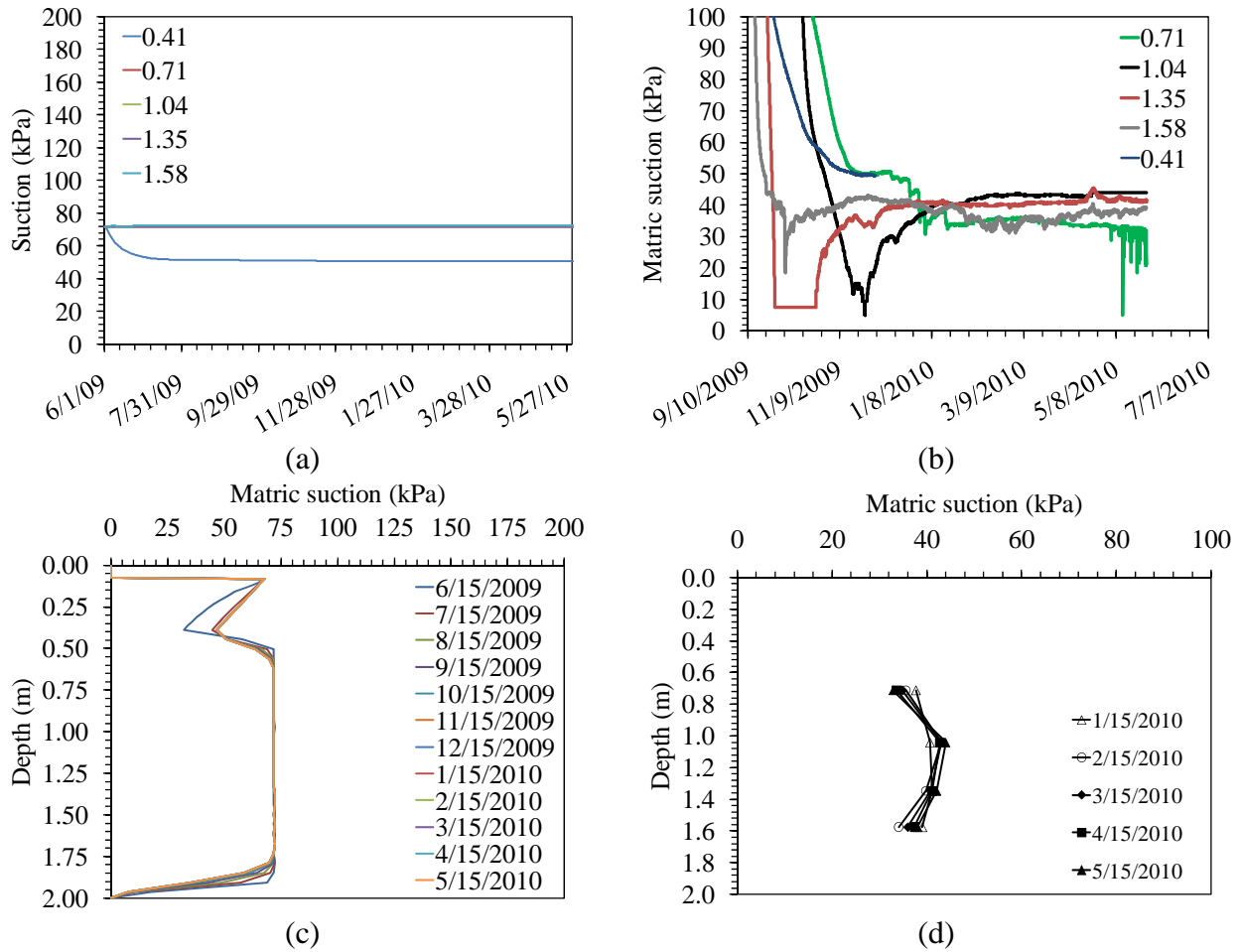


Figure 5.10: Suction: (a) EICM chart; (b) Field chart; (c) EICM profiles; (d) Field Profiles

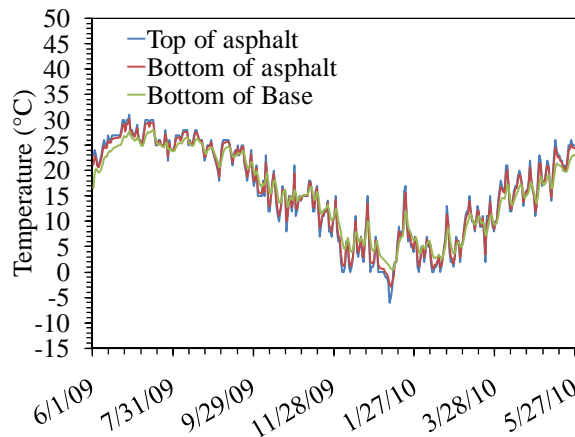


Figure 5.11: Predicted temperature in asphalt and base layers from EICM



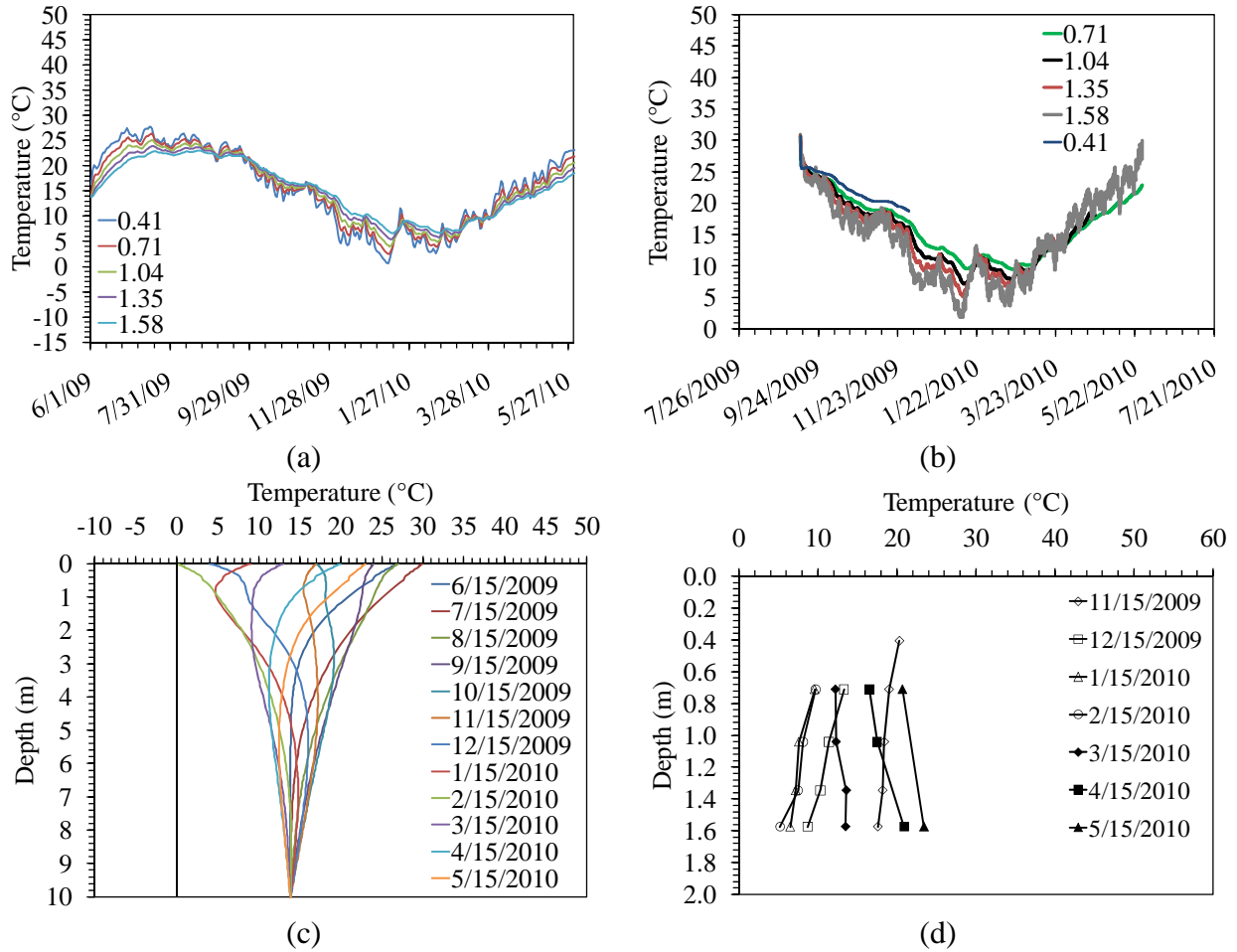


Figure 5.12: Temperature: (a) EICM chart; (b) Field chart; (c) EICM profiles; (d) Field Profiles

5.2.5 Camden

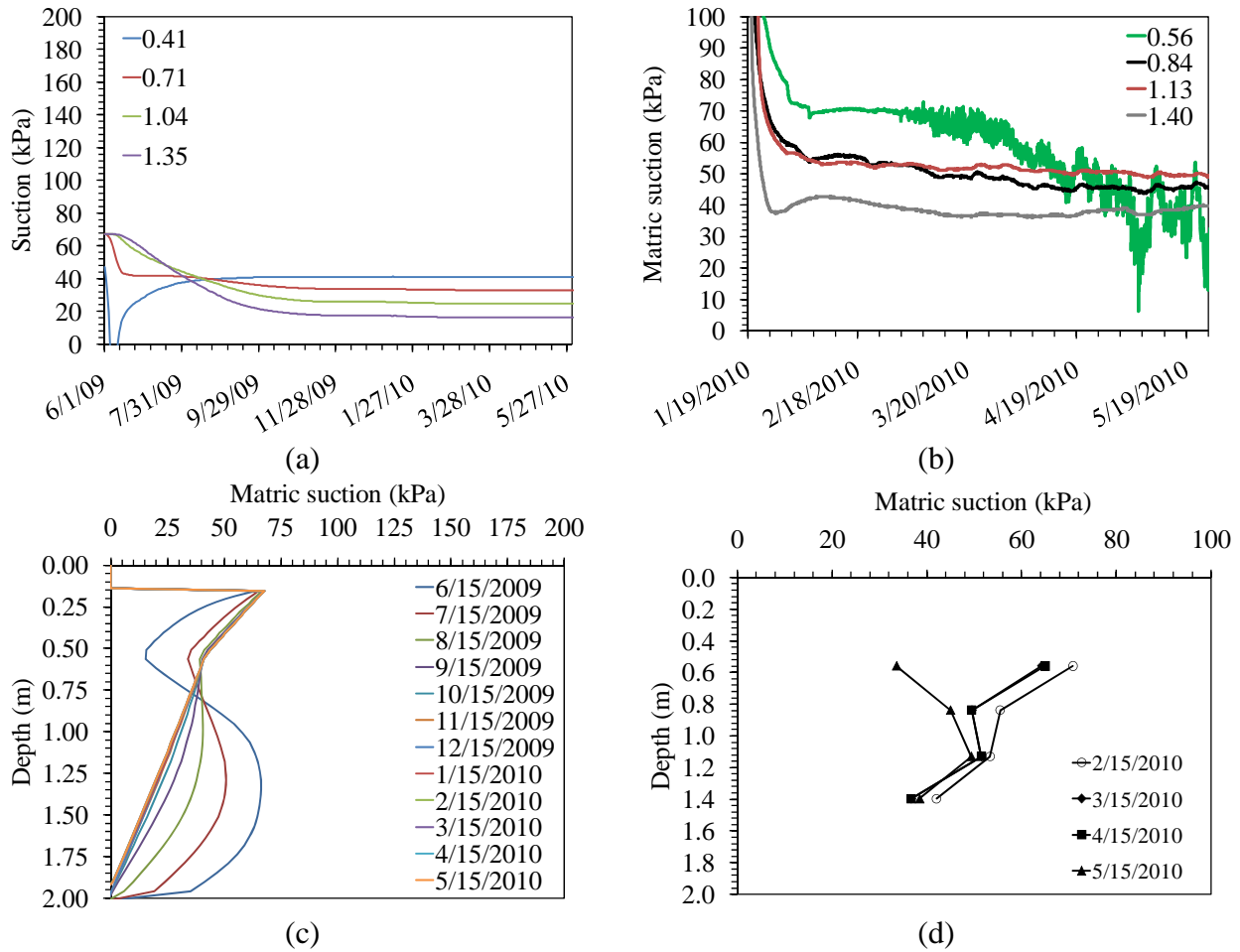


Figure 5.13: Suction: (a) EICM chart; (b) Field chart; (c) EICM profiles; (d) Field Profiles

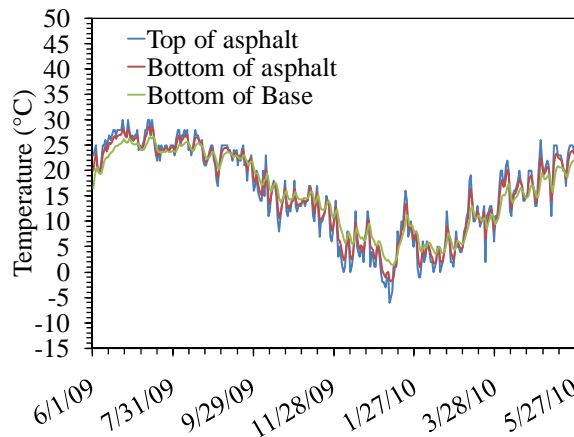


Figure 5.14: Predicted temperature in asphalt and base layers from EICM

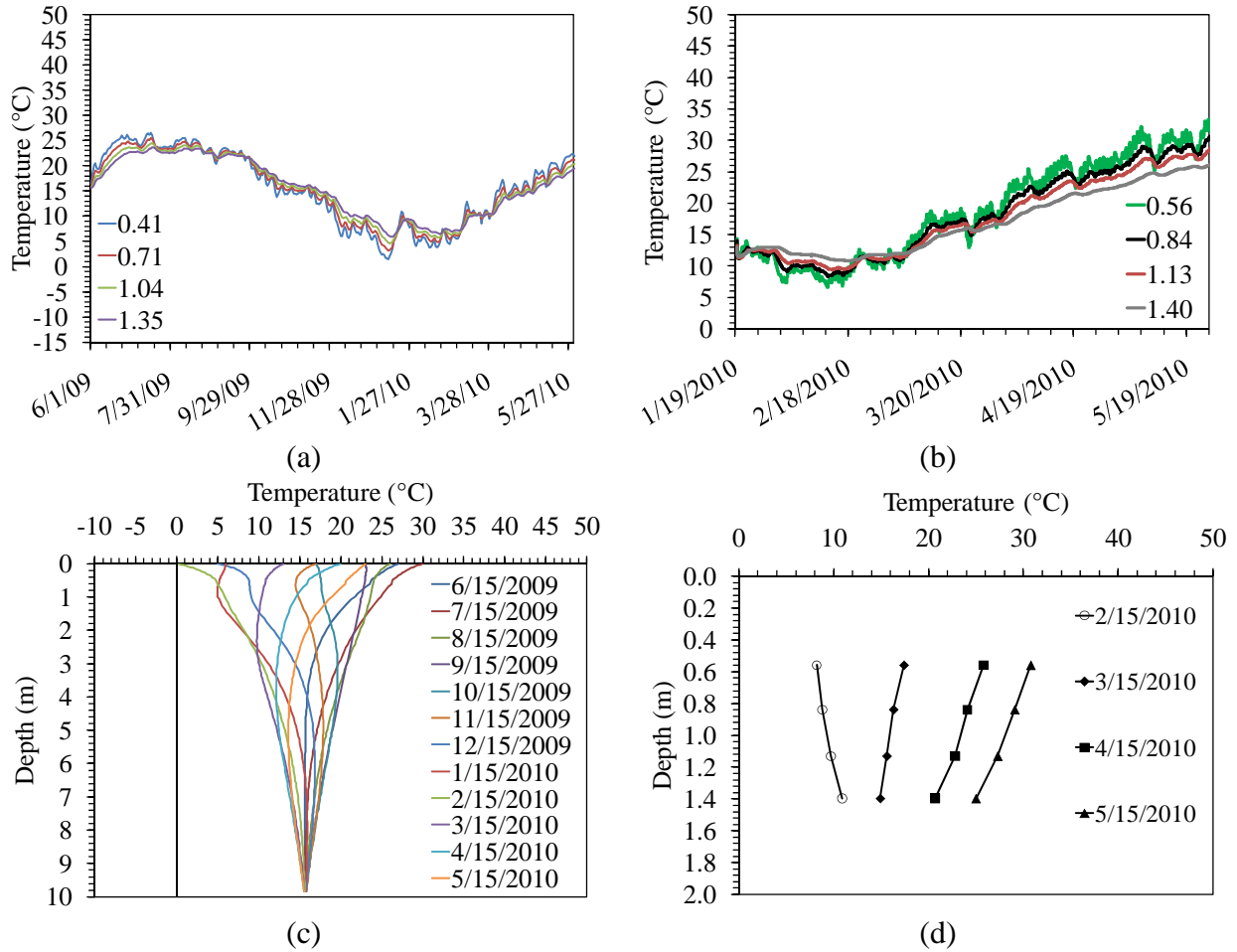


Figure 5.15: Temperature: (a) EICM chart; (b) Field chart; (c) EICM profiles; (d) Field Profiles

5.2.6 Lake Village

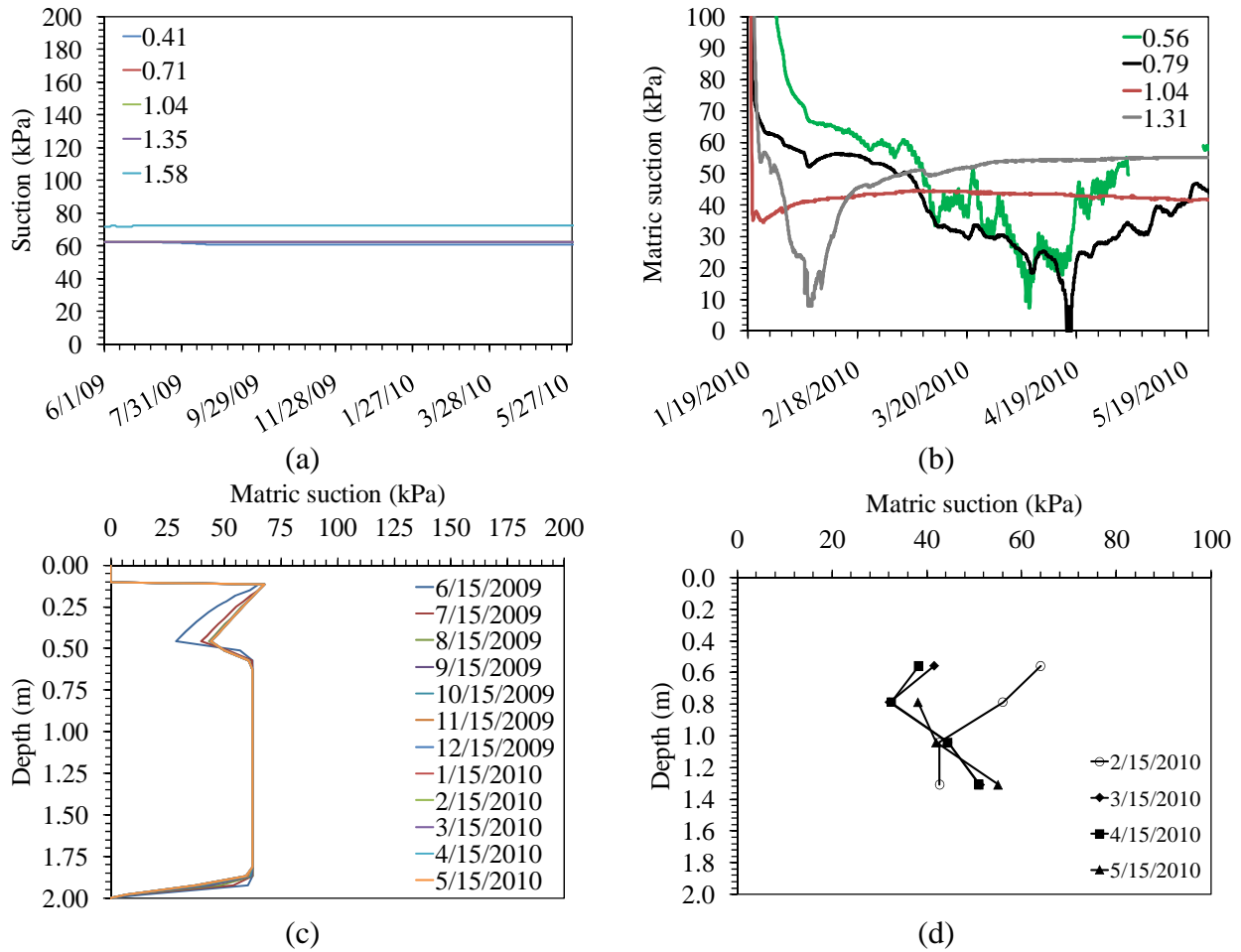


Figure 5.16: Suction: (a) EICM chart; (b) Field chart; (c) EICM profiles; (d) Field Profiles

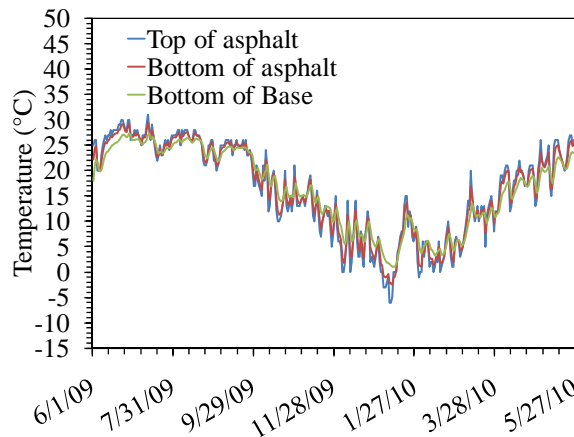


Figure 5.17: Predicted temperature in asphalt and base layers from EICM

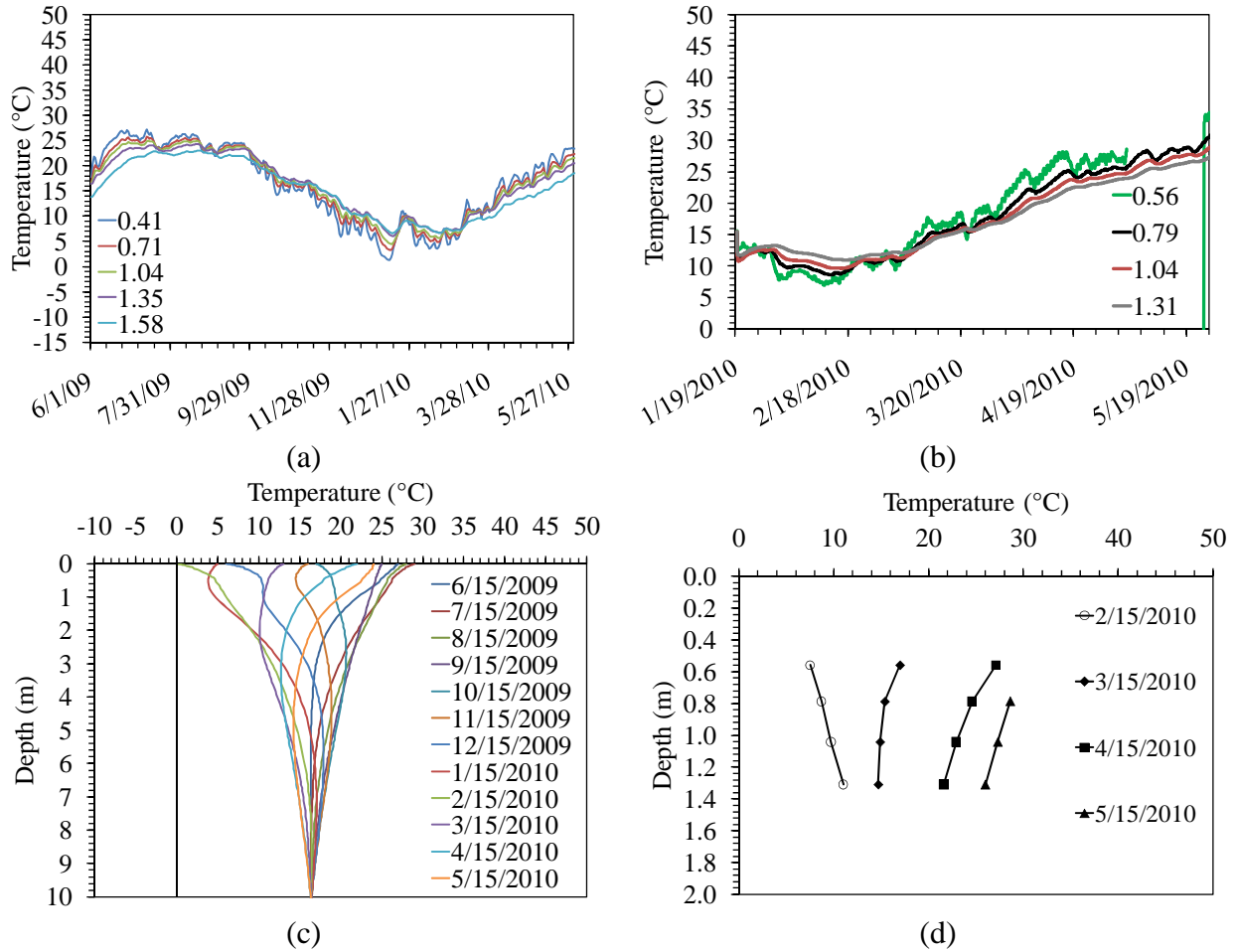


Figure 5.18: Temperature: (a) EICM chart; (b) Field chart; (c) EICM profiles; (d) Field Profiles

5.2.7 Marked Tree

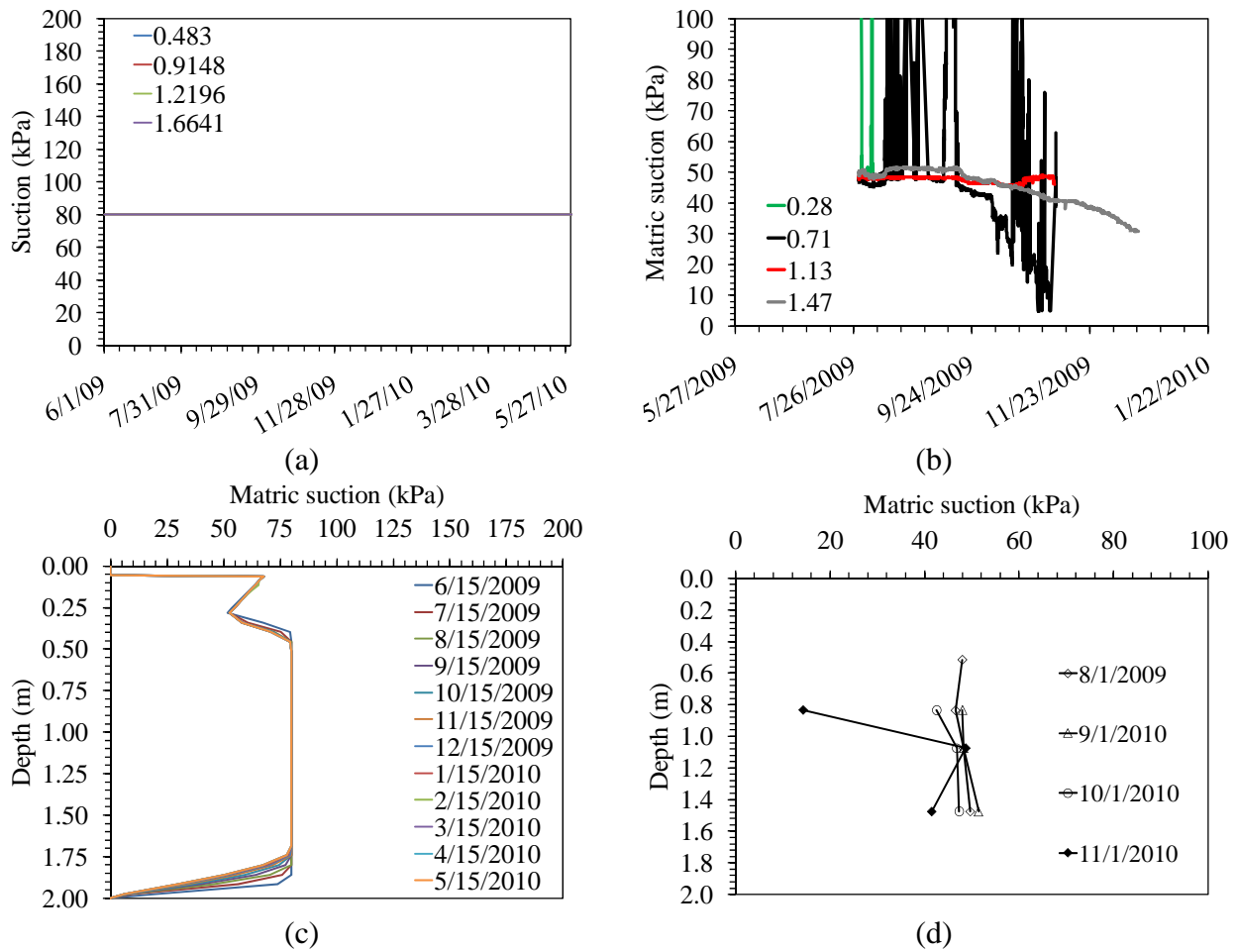


Figure 5.19: Suction: (a) EICM chart; (b) Field chart; (c) EICM profiles; (d) Field Profiles

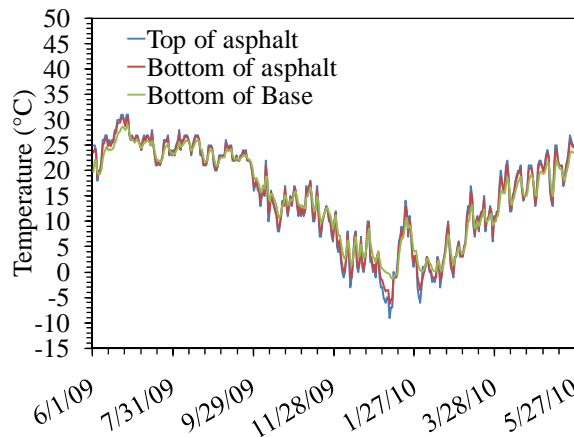


Figure 5.20: Predicted temperature in asphalt and base layers from EICM

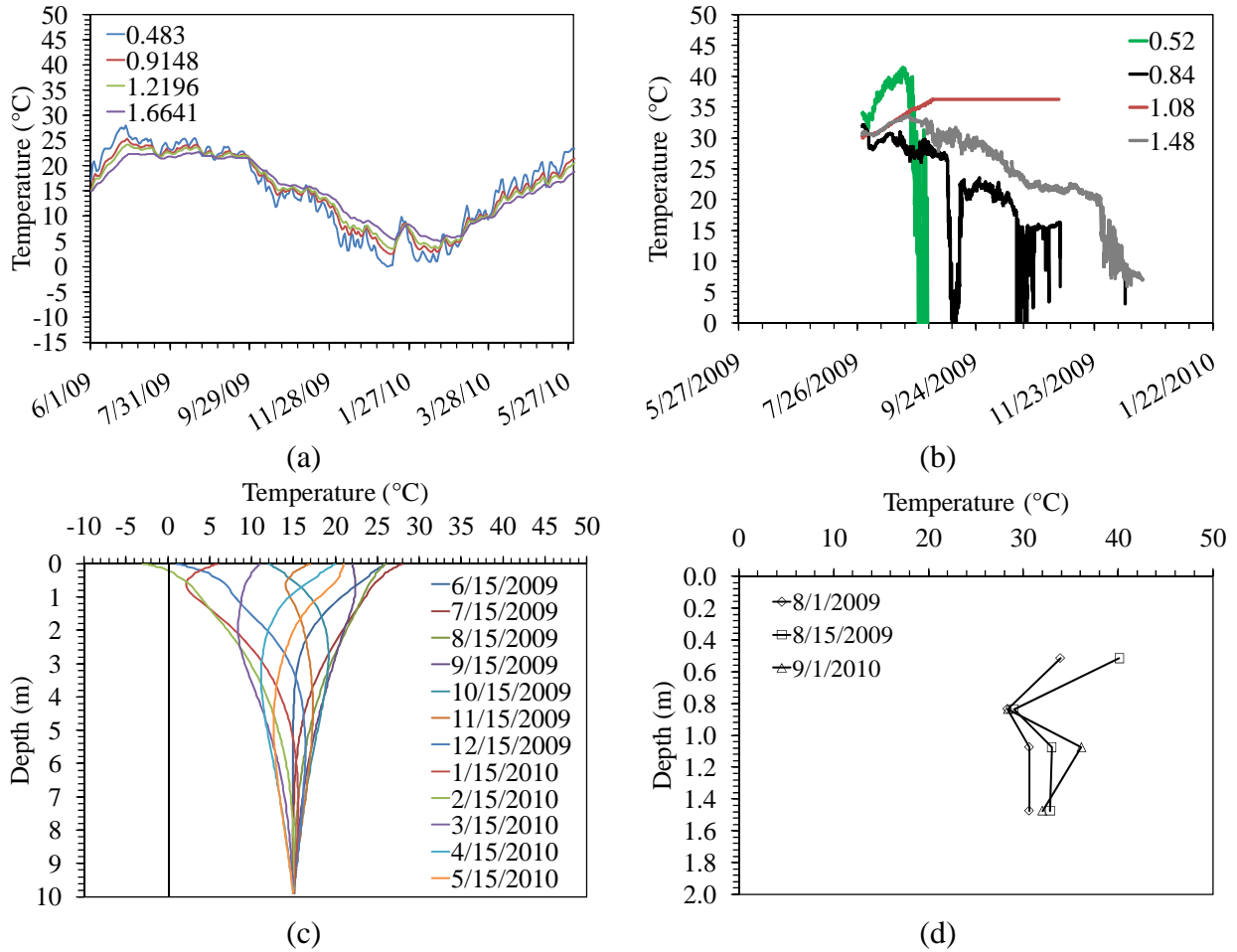


Figure 5.21: Temperature: (a) EICM chart; (b) Field chart; (c) EICM profiles; (d) Field Profiles

### 5.3 VADOSE/W and Field Comparison

#### 5.2.1 Greenland

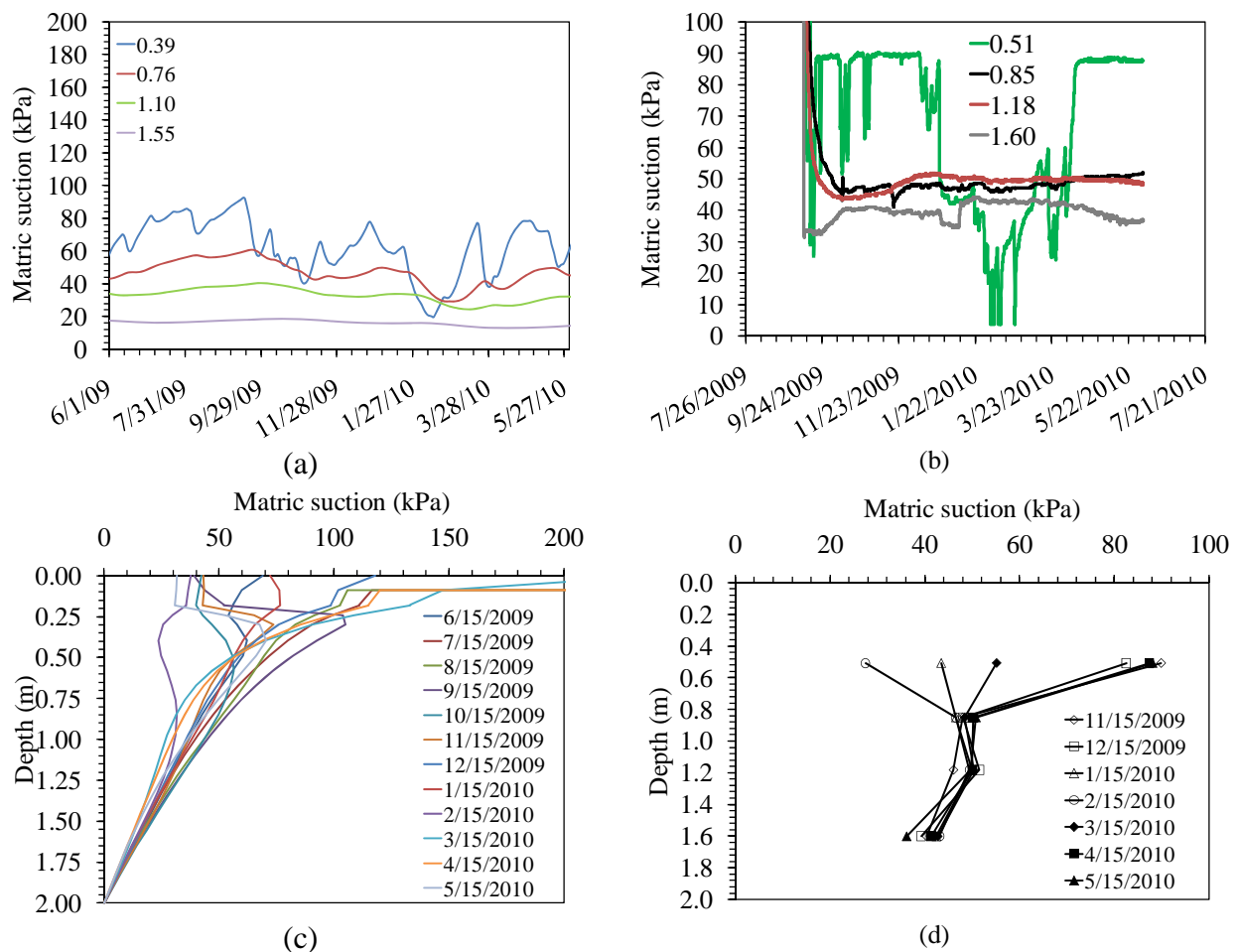


Figure 5.22: Suction: (a) VADOSE chart; (b) Field chart; (c) VADOSE profiles; (d) Field Profiles

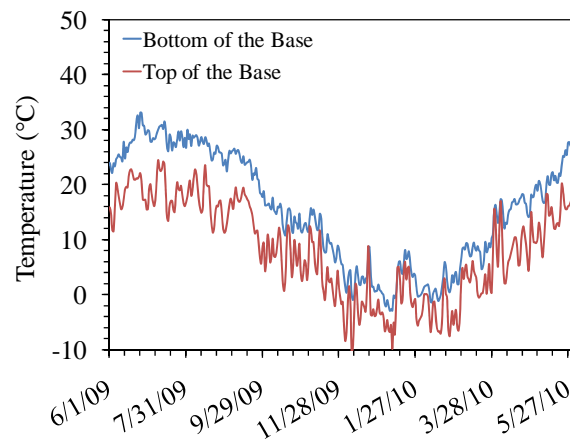


Figure 5.23: Predicted temperature in asphalt and base layers from EICM



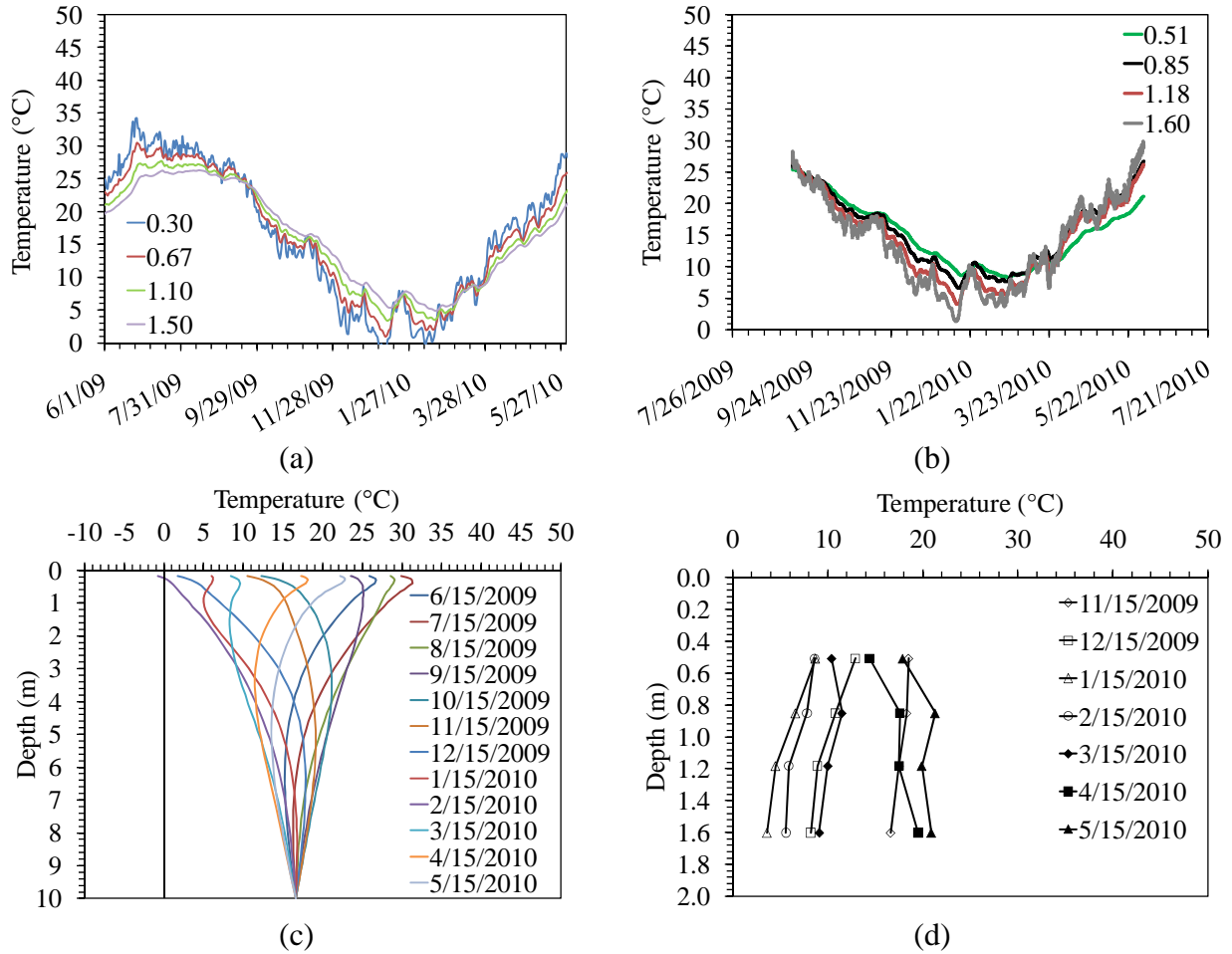


Figure 5.24: Temperature: (a) VADOSE chart; (b) Field chart; (c) VADOSE profiles; (d) Field Profiles

5.2.2 Plumerville

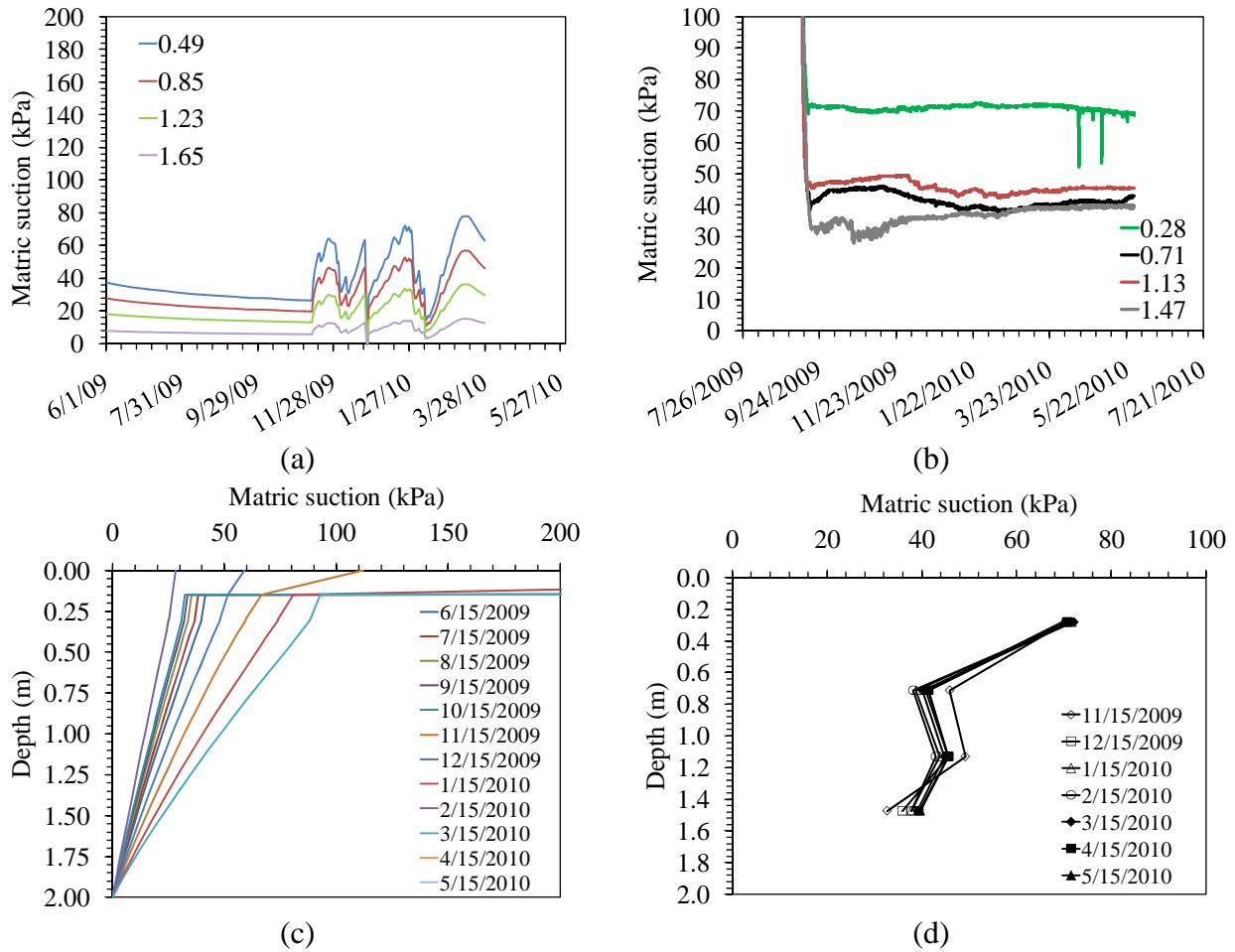


Figure 5.25: Suction: (a) VADOSE chart; (b) Field chart; (c) VADOSE profiles; (d) Field Profiles

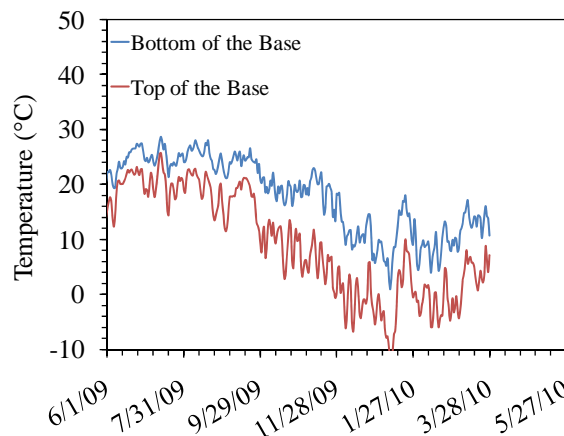


Figure 5.26: Predicted temperature in base layers from VADOSE

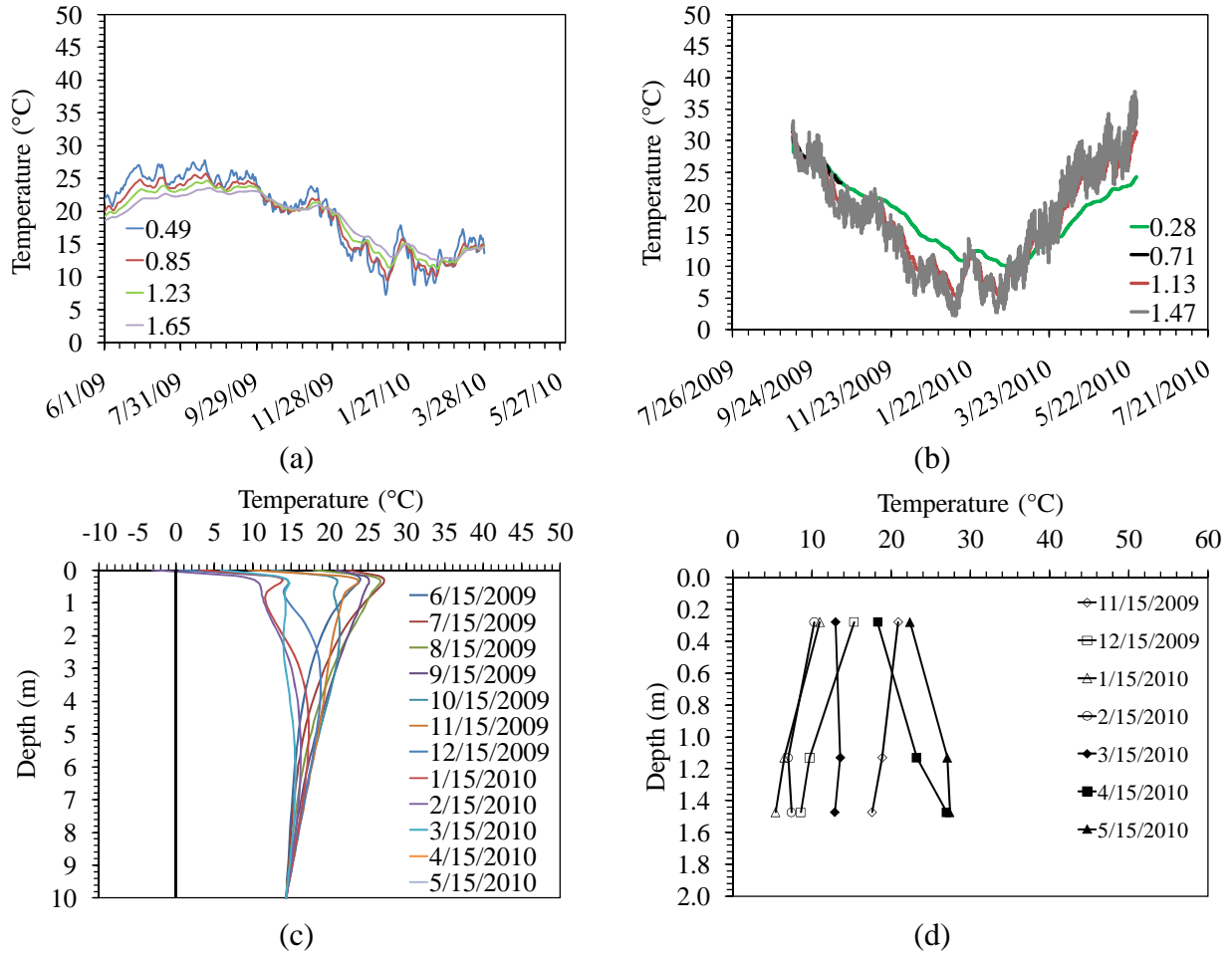


Figure 5.27: Temperature: (a) VADOSE chart; (b) Field chart; (c) VADOSE profiles; (d) Field Profiles

5.2.3 Malvern

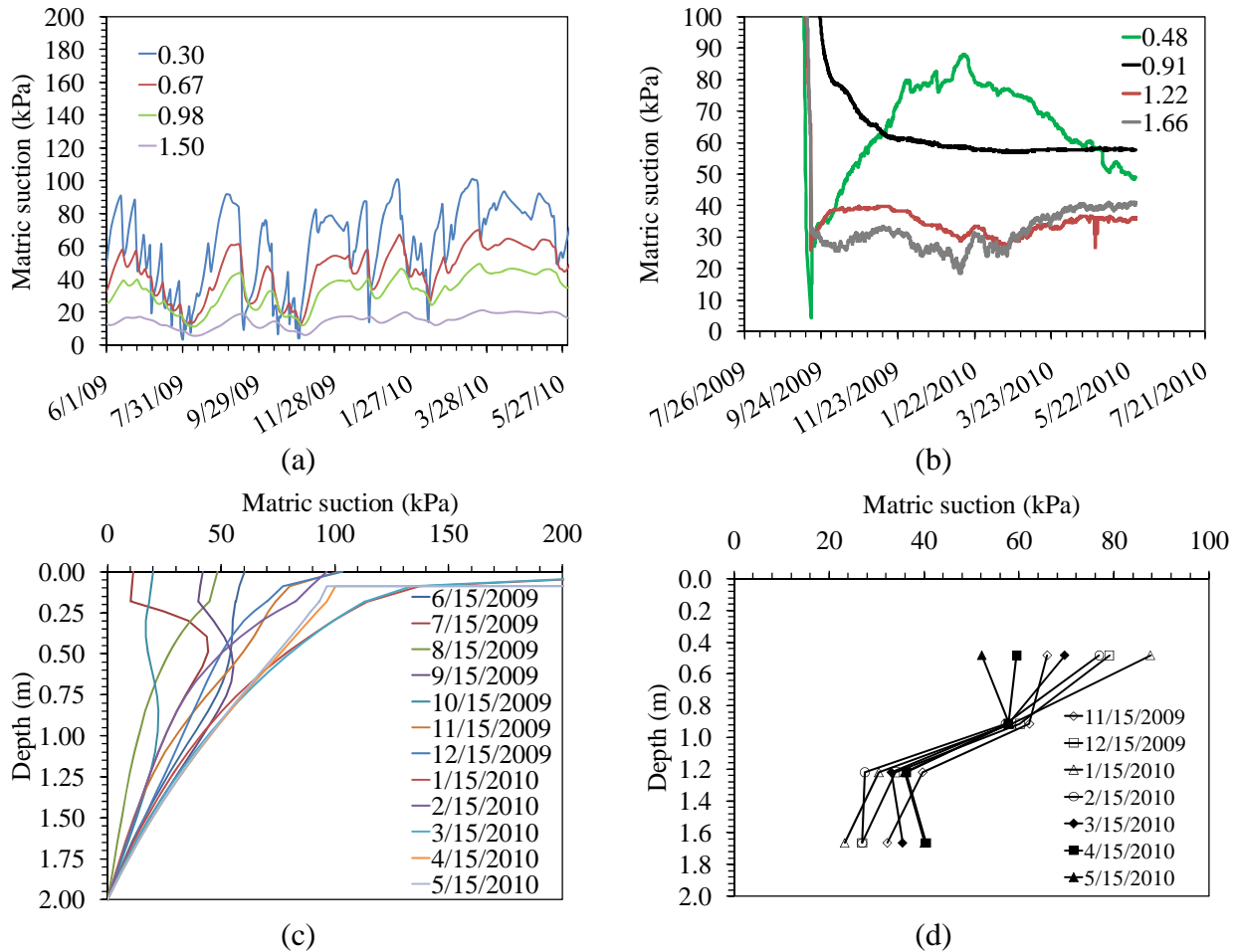


Figure 5.28: Suction: (a) VADOSE chart; (b) Field chart; (c) VADOSE profiles; (d) Field Profiles

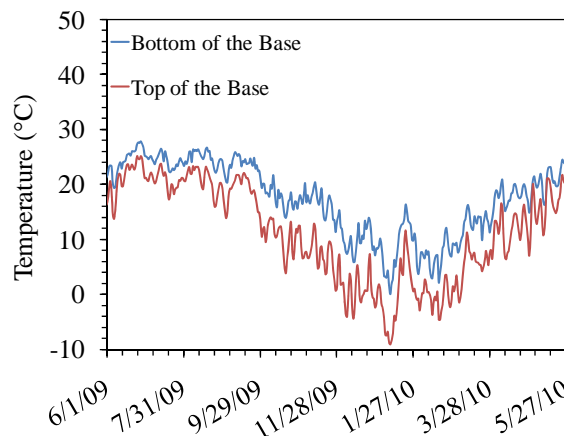


Figure 5.29: Predicted temperature in base layers from VADOSE

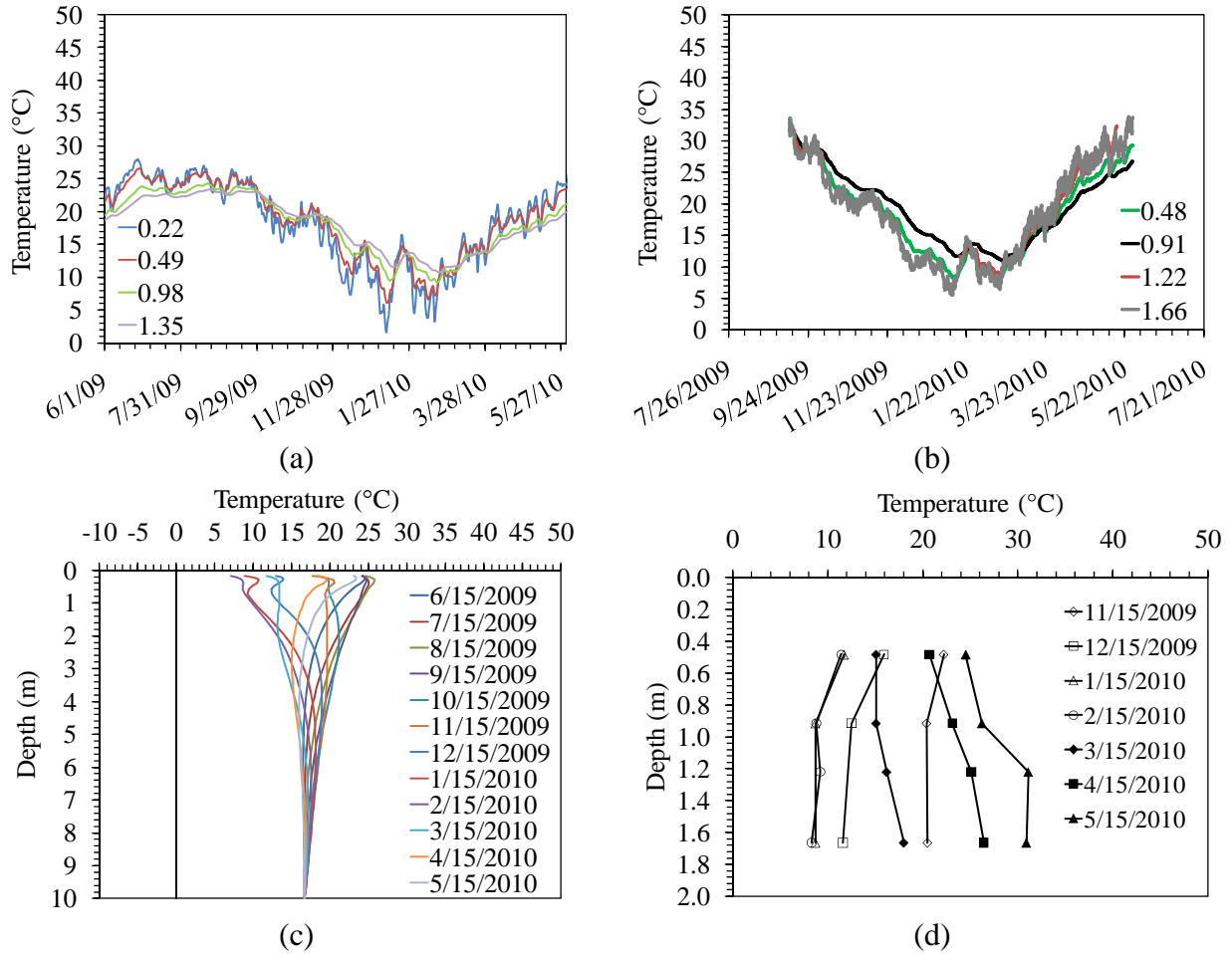


Figure 5.30: Temperature: (a) VADOSE chart; (b) Field chart; (c) VADOSE profiles; (d) Field Profiles

5.2.4 Murfreesboro

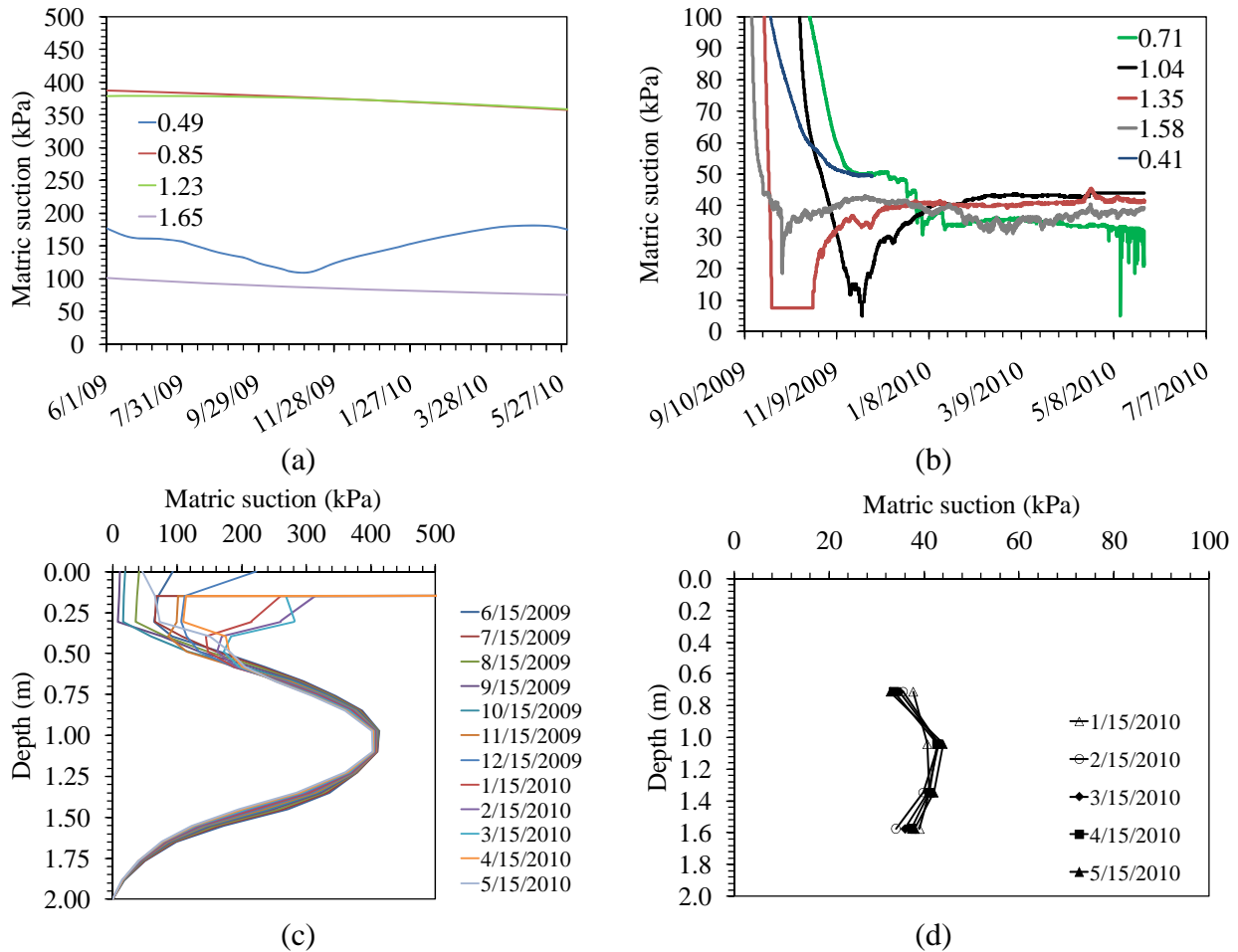


Figure 5.31: Suction: (a) VADOSE chart; (b) Field chart; (c) VADOSE profiles; (d) Field Profiles

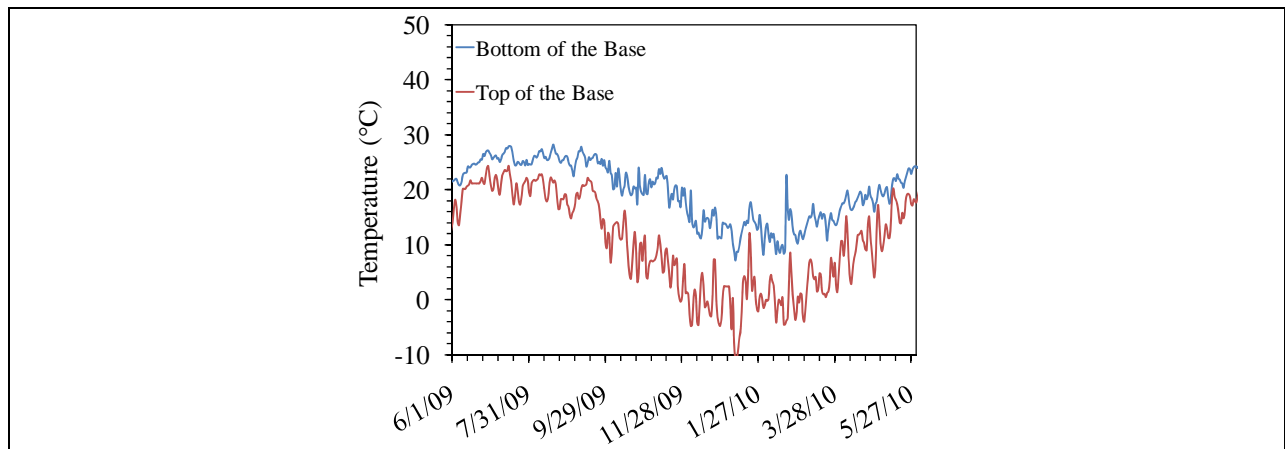


Figure 5.32: Predicted temperature in base layers from VADOSE

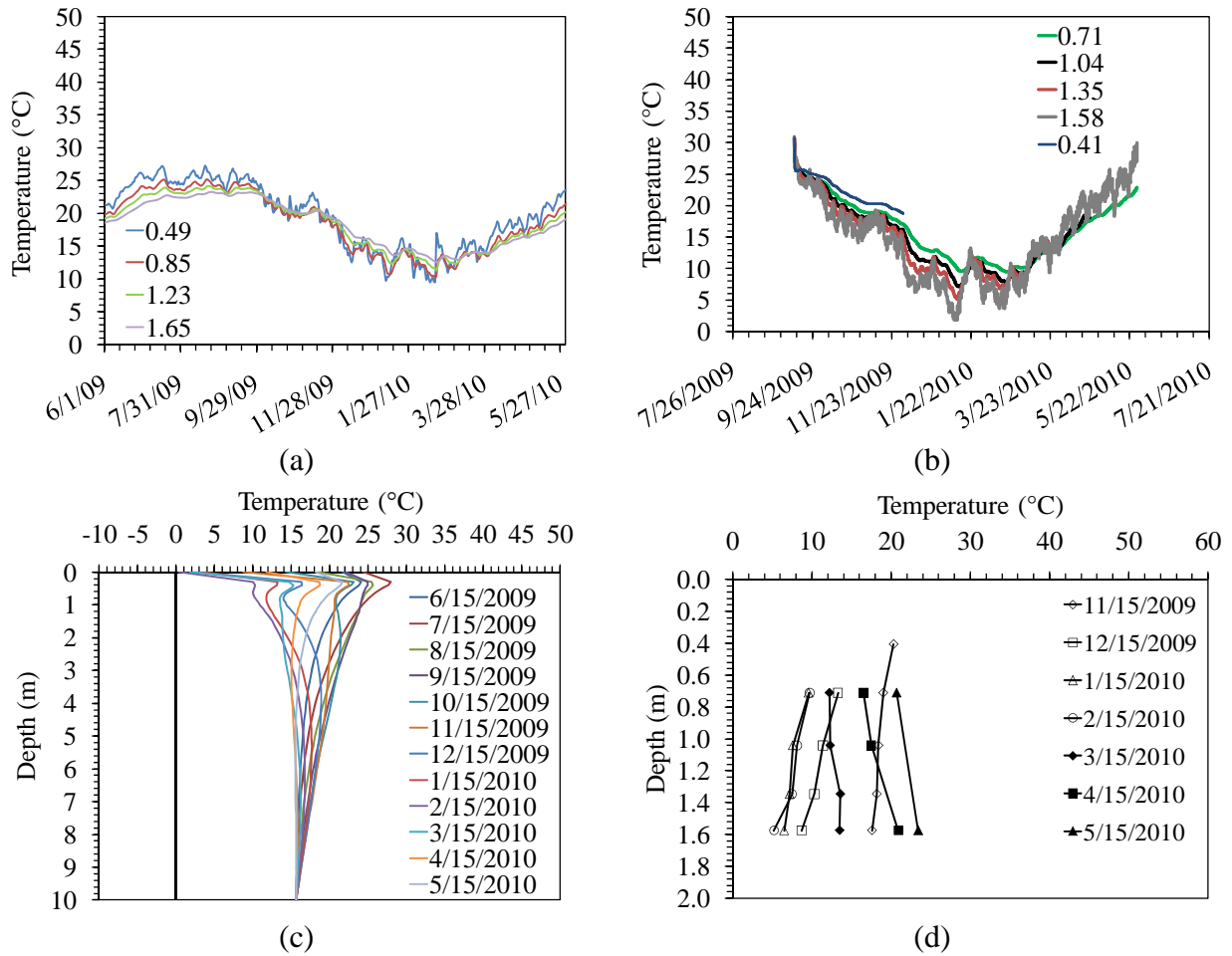


Figure 5.33: Temperature: (a) VADOSE chart; (b) Field chart; (c) VADOSE profiles; (d) Field Profiles

5.2.5 Camden

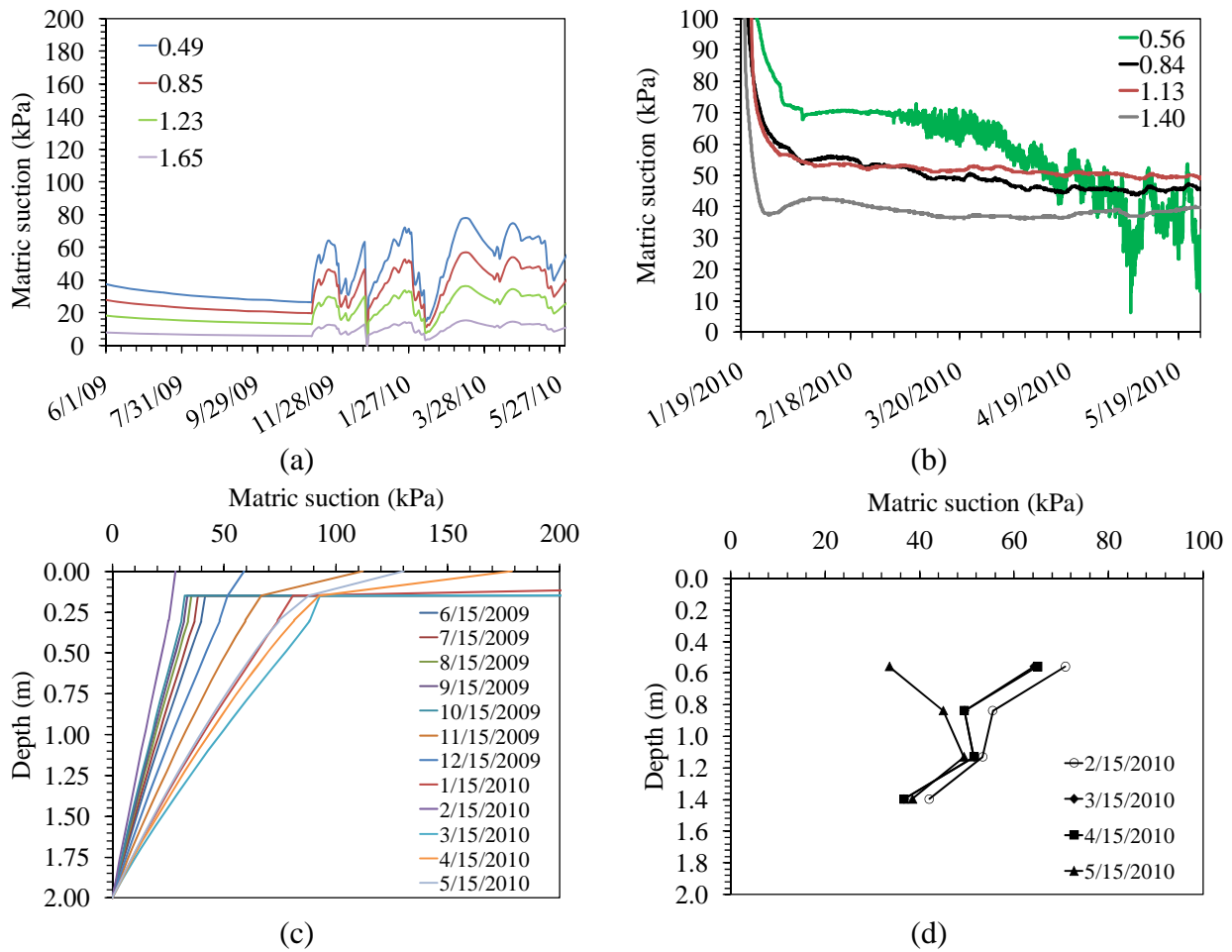


Figure 5.34: Suction: (a) VADOSE chart; (b) Field chart; (c) VADOSE profiles; (d) Field Profiles

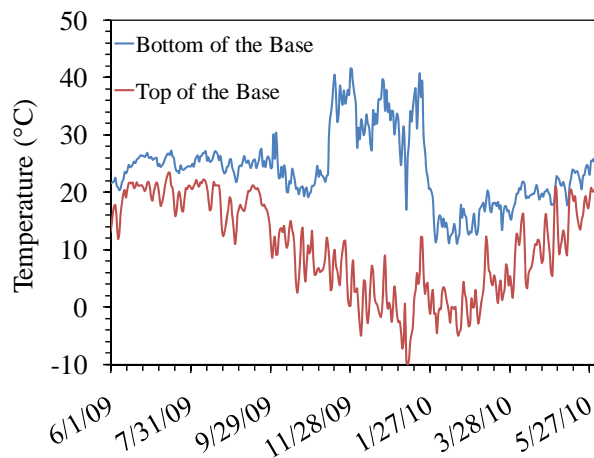


Figure 5.35: Predicted temperature in base layers from VADOSE



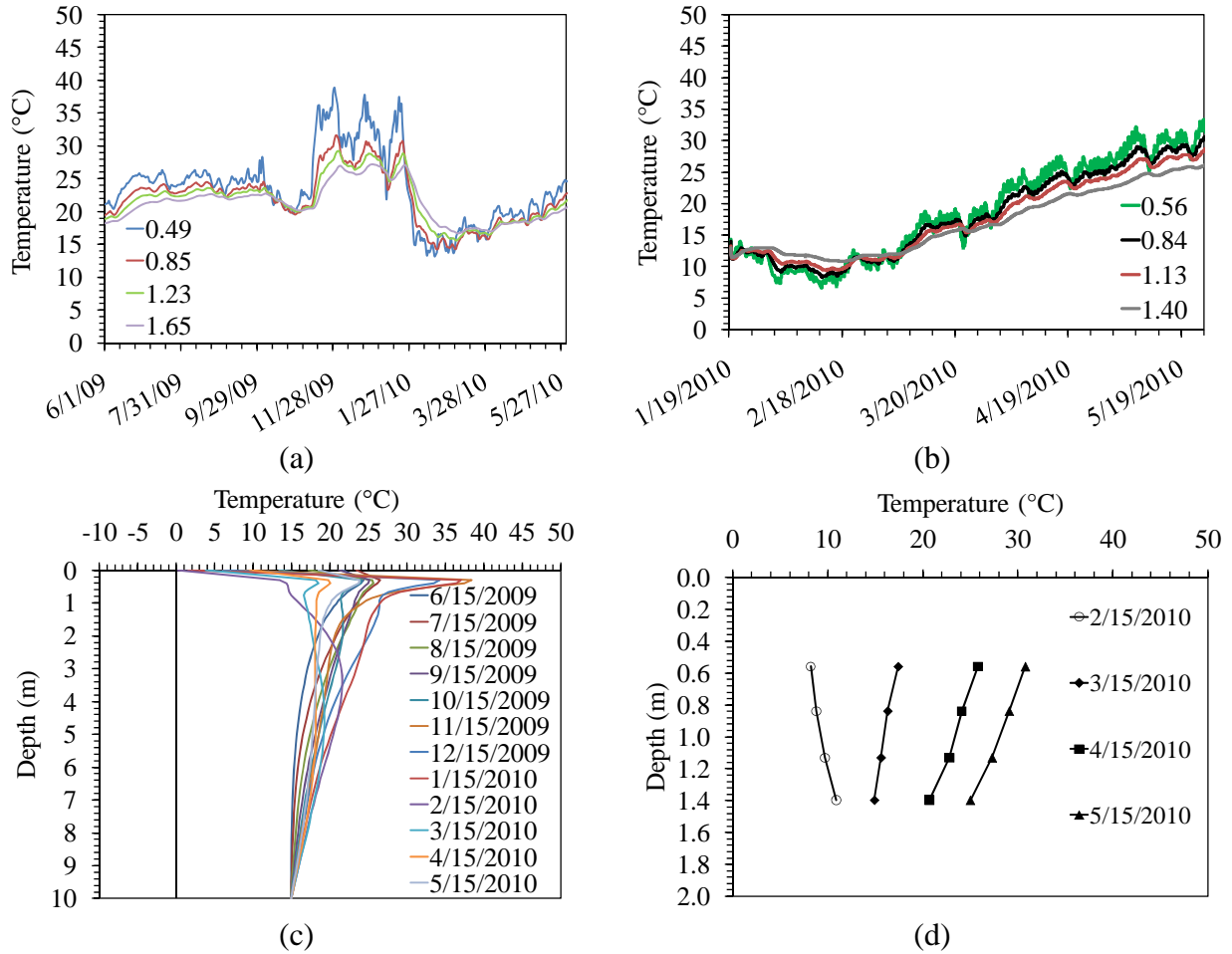


Figure 5.36: Temperature: (a) VADOSE chart; (b) Field chart; (c) VADOSE profiles; (d) Field Profiles

5.2.6 Lake Village

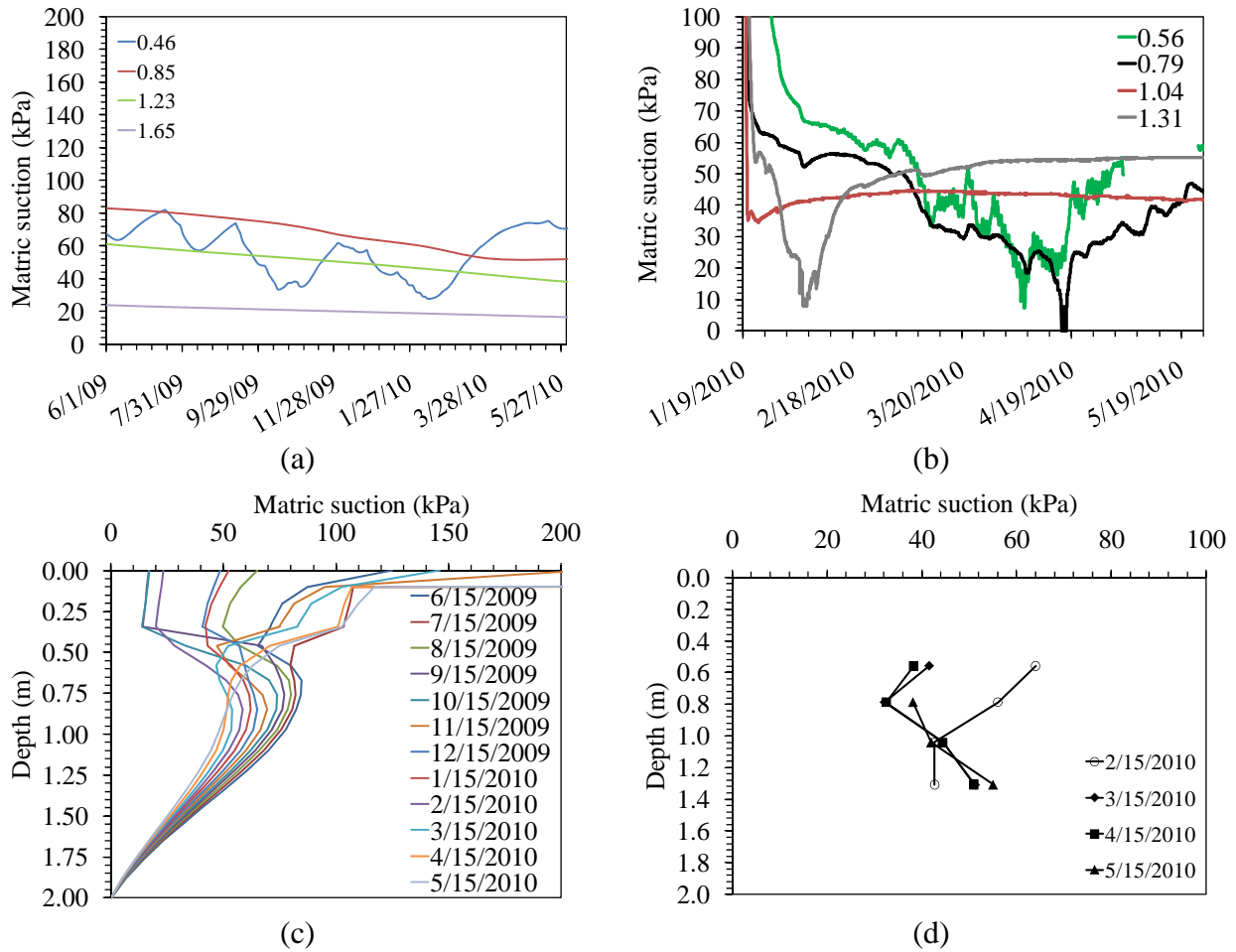


Figure 5.37: Suction: (a) VADOSE chart; (b) Field chart; (c) VADOSE profiles; (d) Field Profiles

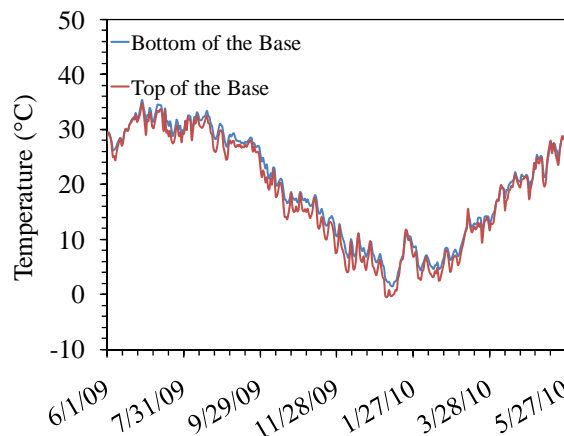


Figure 5.38: Predicted temperature in base layers from VADOSE

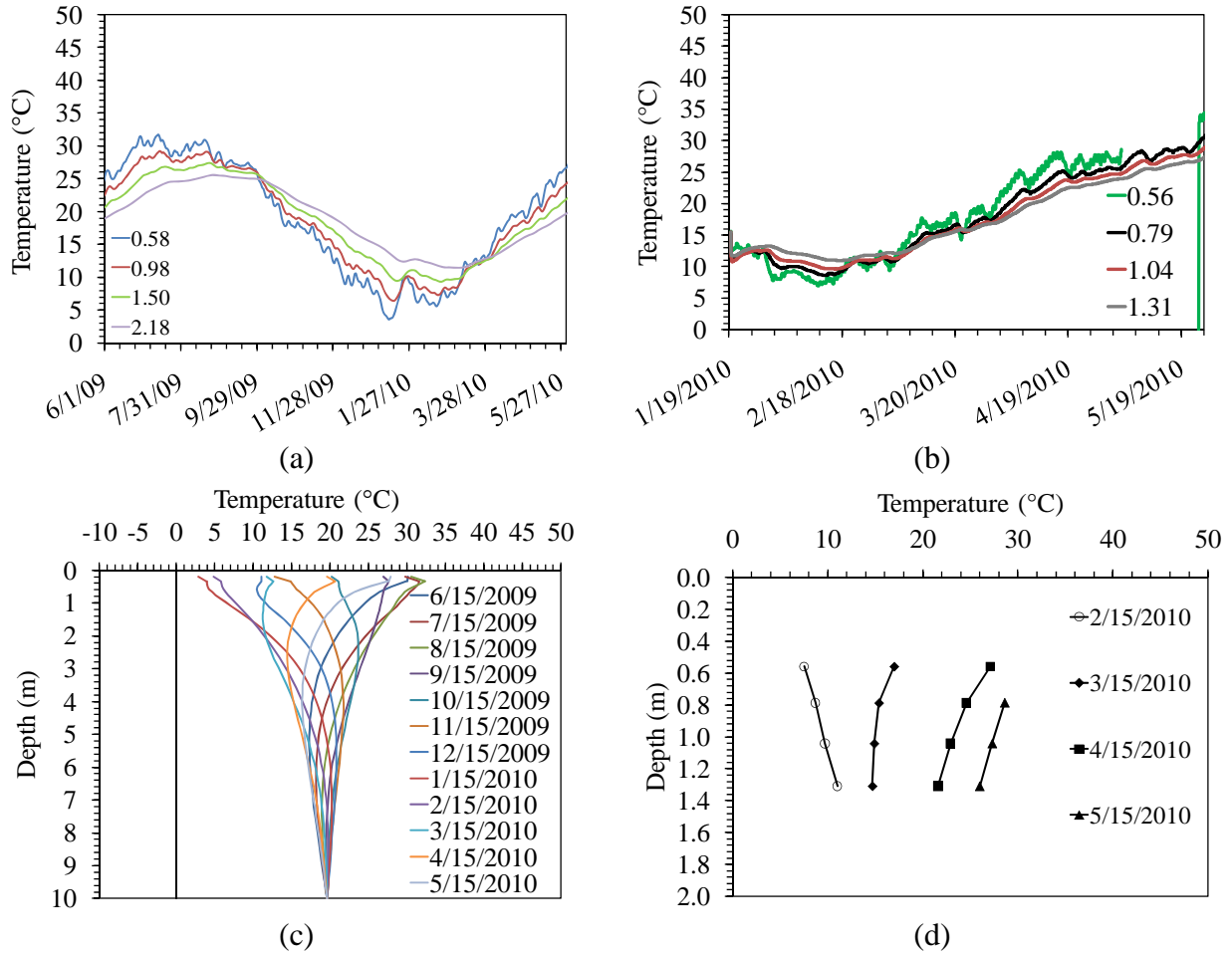


Figure 5.39: Temperature: (a) VADOSE chart; (b) Field chart; (c) VADOSE profiles; (d) Field Profiles

5.2.7 Marked Tree

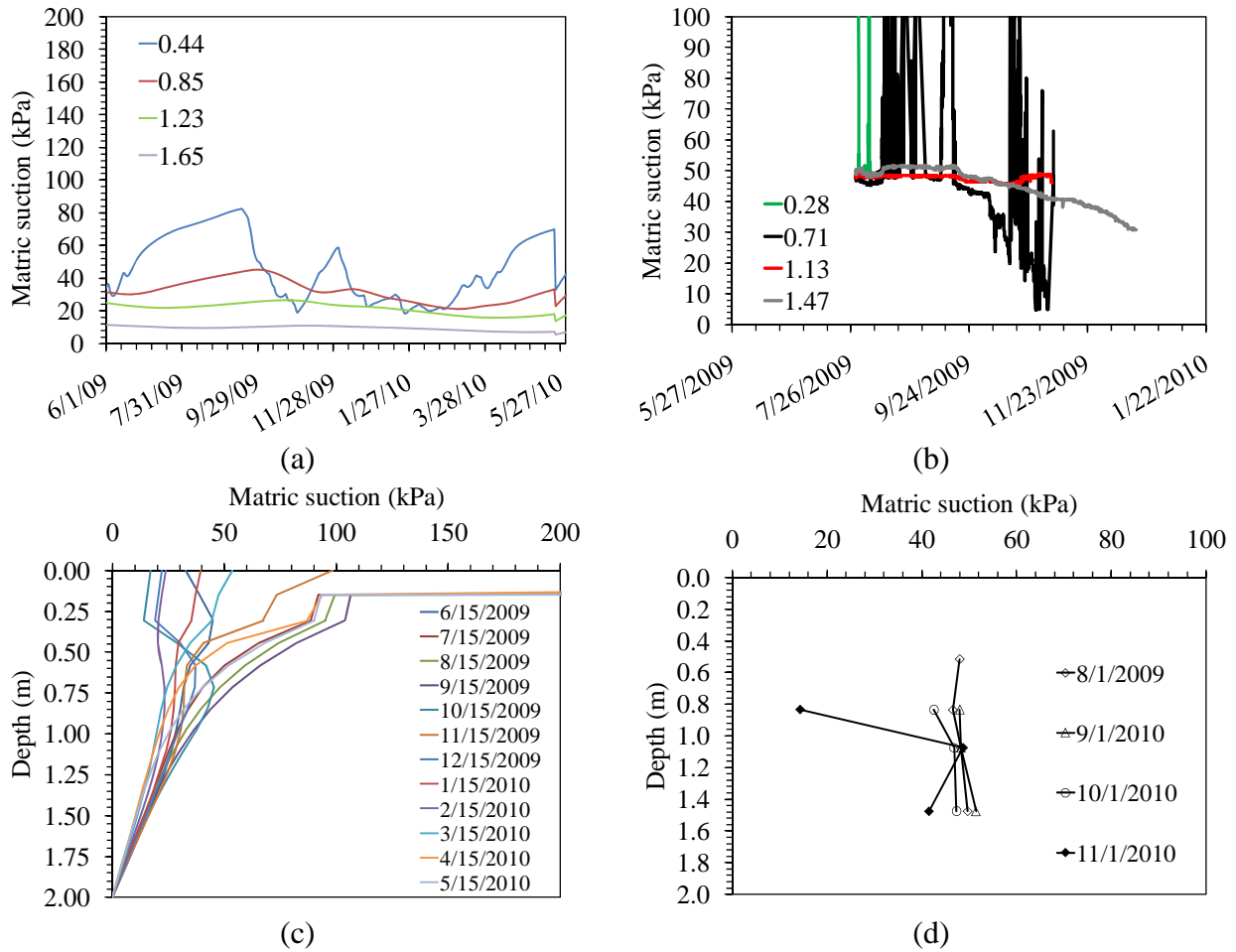


Figure 5.40: Suction: (a) VADOSE chart; (b) Field chart; (c) VADOSE profiles; (d) Field Profiles

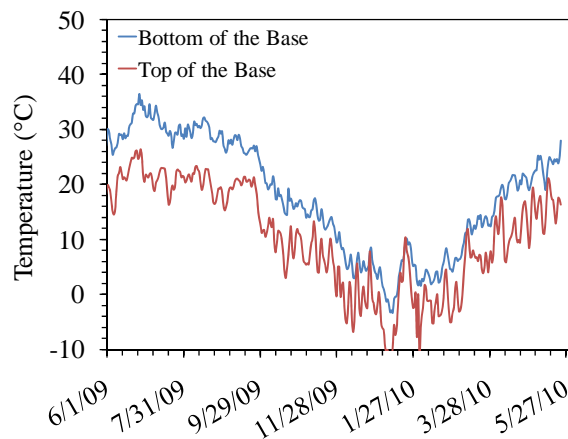


Figure 5.41: Predicted temperature in base layers from VADOSE

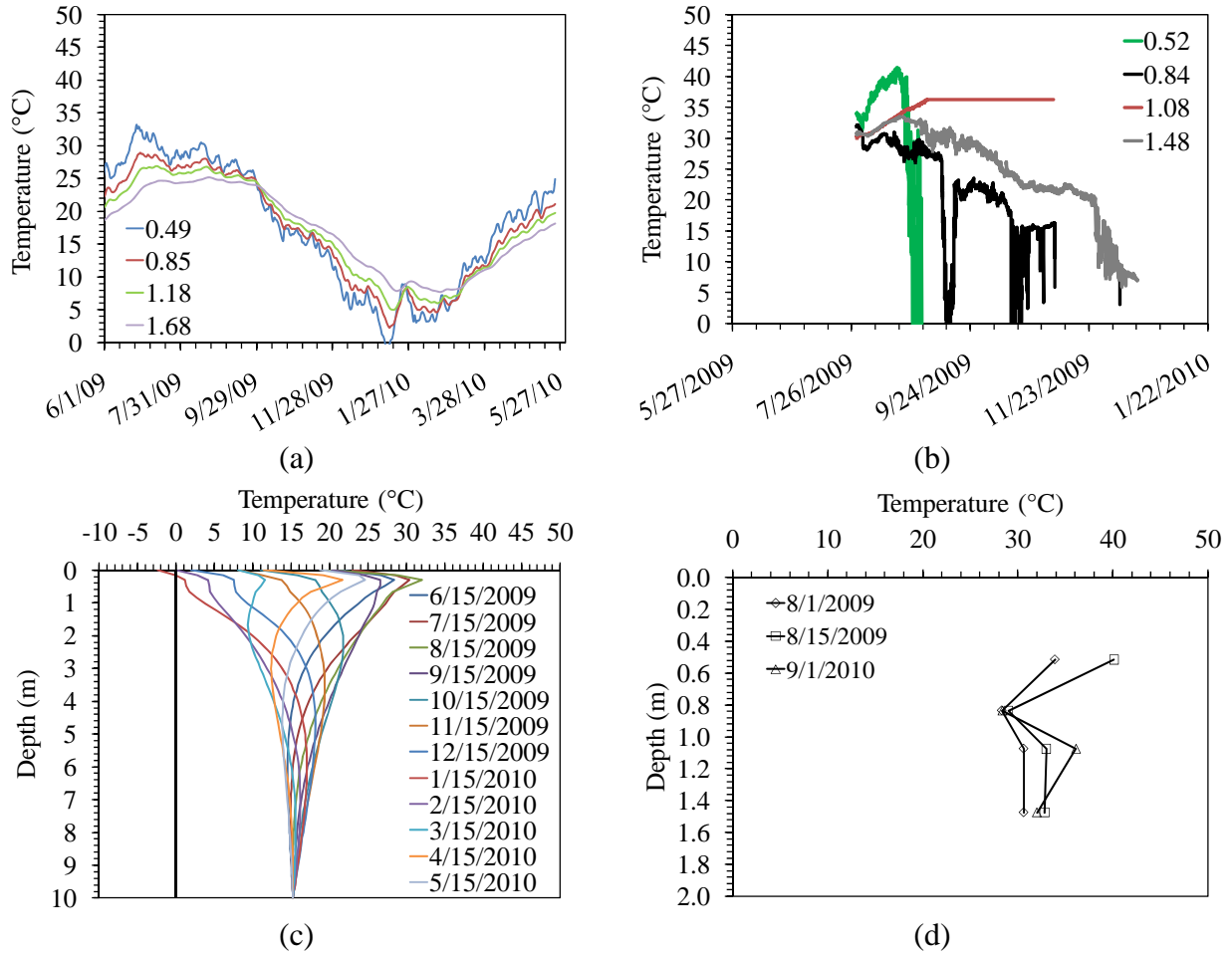


Figure 5.42: Temperature: (a) VADOSE chart; (b) Field chart; (c) VADOSE profiles; (d) Field Profiles

## 6. RECOMMENDATIONS AND CONCLUSIONS

### 6.1 Implementation of this Research

This research program provided Arkansas-specific climatic and soil related inputs suitable for use in developing estimations of the variations in water content and temperature of different pavement layers (asphaltic concrete, aggregate base, and subgrade soil) that can be used in the analysis of pavement performance with the EICM. One of the main conclusions from this project is that the EICM does not provide acceptable predictions of the changes in pore water pressure in the subgrade layer during pavement-atmosphere interaction. This is a major shortcoming of the model. Nonetheless, the EICM provides a reasonable prediction of heat flow in the layered pavement system.

A user's guide for the EICM program was developed, and is shown in Appendix E. This user's guide includes recommendations as to how to easily implement the EICM for pavement design as part of a MEPDG analysis for Arkansas. The main recommendations beyond those for implementation of the model include those focused on the "Levels" which should be used to define the different input variables for the model. The time required in this study to define the SWRCs was prohibitive for design purposes. Accordingly, it is recommended to define the hydraulic properties of the subgrade soils using the empirical (Level 2) relationships developed by Zapata and Houston (2008). Unless available in a design project, it is recommended to use database (Level 1) values for the material properties of the asphalt and base. It is recommended to use site-specific (Level 3) weather data as opposed to database weather, because the EICM only permits a short time period of 1 year. Accordingly, the weather data for a specific time period of interest should be used. For the initial conditions, it is recommended to use experience-based default estimates (Level 1) for the water content of the soil layers corresponding to the value at the air-entry suction for the soils. This value was observed to provide the best results for the flow analyses because the soil has a permeability close to that at saturation, which means that it will respond relatively quickly to boundary conditions. This was also found to be a good strategy because the water table at the sites in Arkansas is relatively close to the pavement surface (i.e., 2 meters below the asphalt level). It is recommended to use site-specific (Level 3) input parameters for the geometry of the soil layers at the sites because the geometry has an important impact on both temperature and water flow. A good estimate of the water table at the different sites is also important to provide reasonable water flow results in the soil profile.

## 6.2 Issues Needing Improvement in EICM

### 6.2.1 Water Flow Model

The results of the Baseline Case analyses indicate that the EICM does not intuitively consider the impact of infiltration and evaporation on the pavement layer. The impact of the asphalt and base layers on the infiltration and evaporation processes needs further improvement. In addition to the hydraulic properties, the EICM uses very simplified representations of the governing equation for water flow in unsaturated soils. In fact, there are two separate water flow conditions modeled in the EICM. The first is gravity drainage of an initially saturated, inclined, base course layer. A phreatic surface is assumed to form as water drains laterally, and the time required for the water to drain is estimated using an analytical technique. This approach makes several simplifying assumptions concerning the hydraulic properties of the soil (considers saturated properties to model an unsaturated condition) and the boundary conditions for flow (the base is assumed to freely drain laterally, but not into the subgrade). Most significantly, the EICM does not ascertain how the soil reached a fully-saturated condition in the first place.

The boundary conditions used by the EICM simplify actual weather boundary conditions by imposing a series of constant suction values to the base course-subgrade interface. The function used to consider this boundary condition is not particularly sensitive to the weather data for a given site. This approach may simplify the input weather conditions so far that they may be significantly different from site-specific weather data. In low permeability soils like clay, the majority of water flow into and out a soil may be due to water vapor flow rather than advective or diffusive flow of liquid water. Although the EICM does a relatively good job of monitoring temperature profiles in pavements, it neglects the effect that temperature gradients have on water vapor flow. Overall, the over-simplified consideration of the different mechanisms of water flow in the EICM is likely a primary cause of its inability to adequately model changes in water content.

A flow chart of how an alternative integrated climate model can be used to obtain a similar range of results is shown in Figure 6.1. It is important to note that due to recent advances in computational techniques and physical modeling, all of the processes considered by different models in the EICM can be considered in a single, truly integrated model instead of several separate simulation models incorporated into the current version of the model.

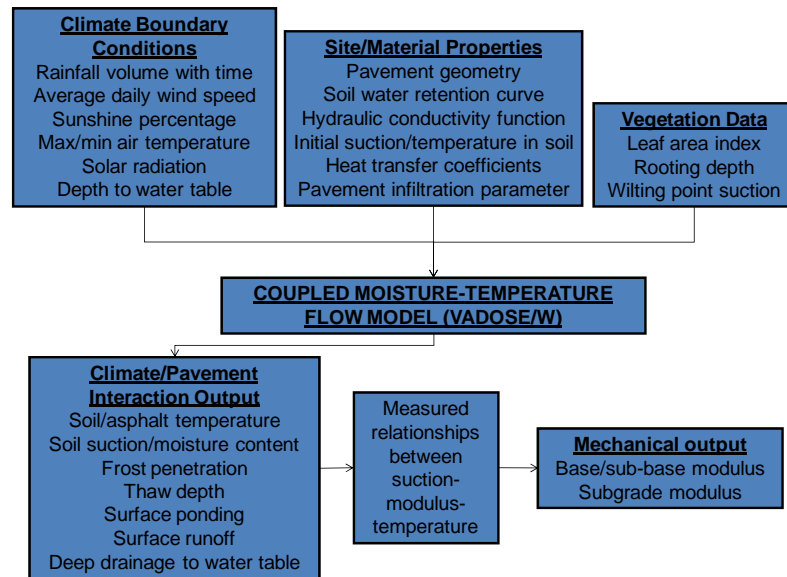


Figure 6.1: Flow chart for the use of a truly integrated climate model

Simulation programs such as VADOSE/W successfully integrate climate boundary conditions, site material properties, and vegetation into a coupled water-temperature flow model, which was observed to match well with field monitoring results. However, in order to consider pavement structures with these simulation programs, a strategy to consider the asphalt layer must still be implemented. One option would be to consider the asphalt layer as impermeable. The finite element mesh for a 2-D simulation in VADOSE/W is shown in Figure 6.2(a). The black asphalt layer was assumed to be impermeable, so all precipitation touching the pavement surface ran off onto the shoulders, where it infiltrated into the pavement. Water content and temperature contours shown in Figures 6.2(b) and 6.2(c) indicate that water content and temperature fluctuations during the modeled infiltration event were isolated to the edges of the pavement. The data from this simulation was used to predict the spatial distribution in inflow (Figure 6.3(a)), the development of ponding in the drainage ditches with time (Figure 6.3(b)), and water content distribution (Figure 6.3(c)).



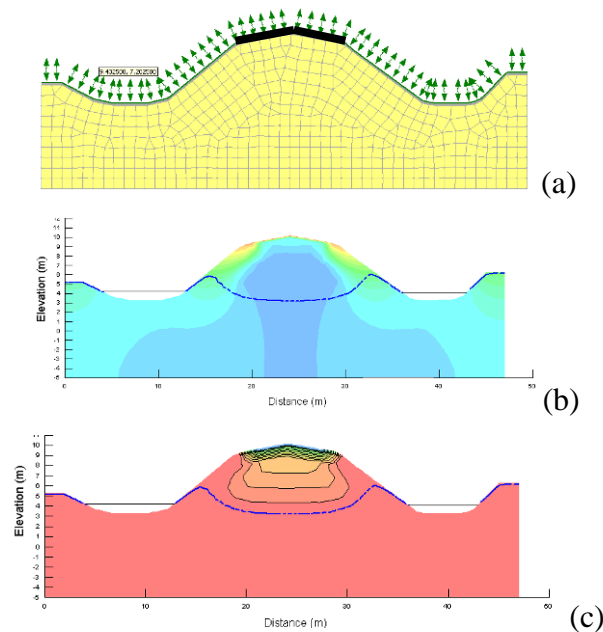


Figure 6.2: (a) Model used to investigate infiltration into a 2-D pavement system in VADOSE/W (Note: Arrows denote an infiltration-evaporation boundary condition); (b) Water content contours in the pavement profile during infiltration; (c) Temperature profiles during infiltration

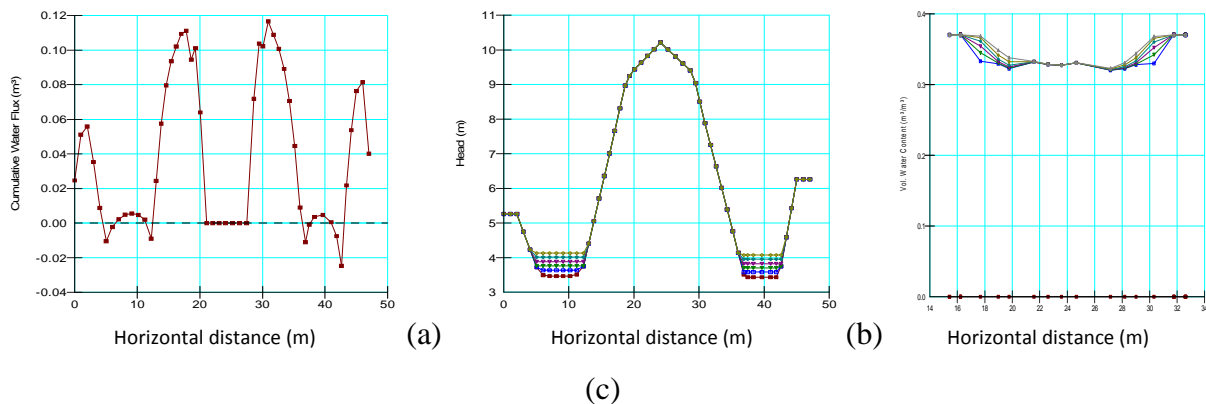


Figure 6.4: Example of results from VADOSE/W analysis: (a) Infiltration with length along the pavement; (b) Ponding heights in the drainage ditch with time during steady infiltration; (c) Water content changes in the pavement during steady infiltration

### 6.2.2 Relationships Linking Hydraulic and Mechanical Coupling

Although this study did not evaluate the linkage between water flow and the mechanical properties of pavement layers (resilient modulus), this is one of the main applications of the EICM results in a ME-PDG analysis. The current EICM uses empirical relationships between the

modulus of compacted soils and the water content. The empirical relationships that depend on temperature (i.e., those for the asphalt) are likely to provide results that show realistic trends with time, while those that depend on the water content are likely not to show realistic trends (because the EICM does not adequately predict water flow in unsaturated pavement systems).

Nonetheless, research indicates that the relationships in EICM may need further improvement due to their lack of consideration of the stress-state in the unsaturated soils and the role of wetting and drying (hysteresis). Early studies on resilient modulus looked at the influence of the degree of saturation (Thompson and Robnett 1979), with typical results shown in Figure 6.5(a). Although this figure shows fitted relationships (that are commonly used in design), the scatter reflects the fact that the degree of saturation is not the primary variable affecting the resilient modulus. A decreasing trend in resilient modulus with degree of saturation was also observed by Drumm *et al.* (1997) in Figure 6.5(b), but this trend varied significantly for different soils. More recent studies have focused on the stress state in the unsaturated soil. The stress state is closely tied to the relationships between the pore air pressure, pore water pressure, and the confining pressure. The difference between pore air pressure and pore water pressure is referred to as the matric suction. Figure 6.5(c) shows the variation in resilient modulus for a base course with matric suction, measured for a constant confining pressure (Gupta *et al.* 2007). This figure shows a more revealing upward trend in resilient modulus with increasing matric suction. The degree of saturation and suction are related through the water retention curve, but because this curve is different for every soil (and for the same soil when compacted to different densities) the degree of saturation for different soils at the same suction may be very different. Another important variable that affects the resilient modulus is the temperature. This is because formation of ice will lead to an increase in volume. However, for a fully saturated soil, the compression of the soil will be resisted by the ice. The trend observed in resilient modulus for temperatures below zero is shown in Figure 6.5(d) (Guymon *et al.* 1986).

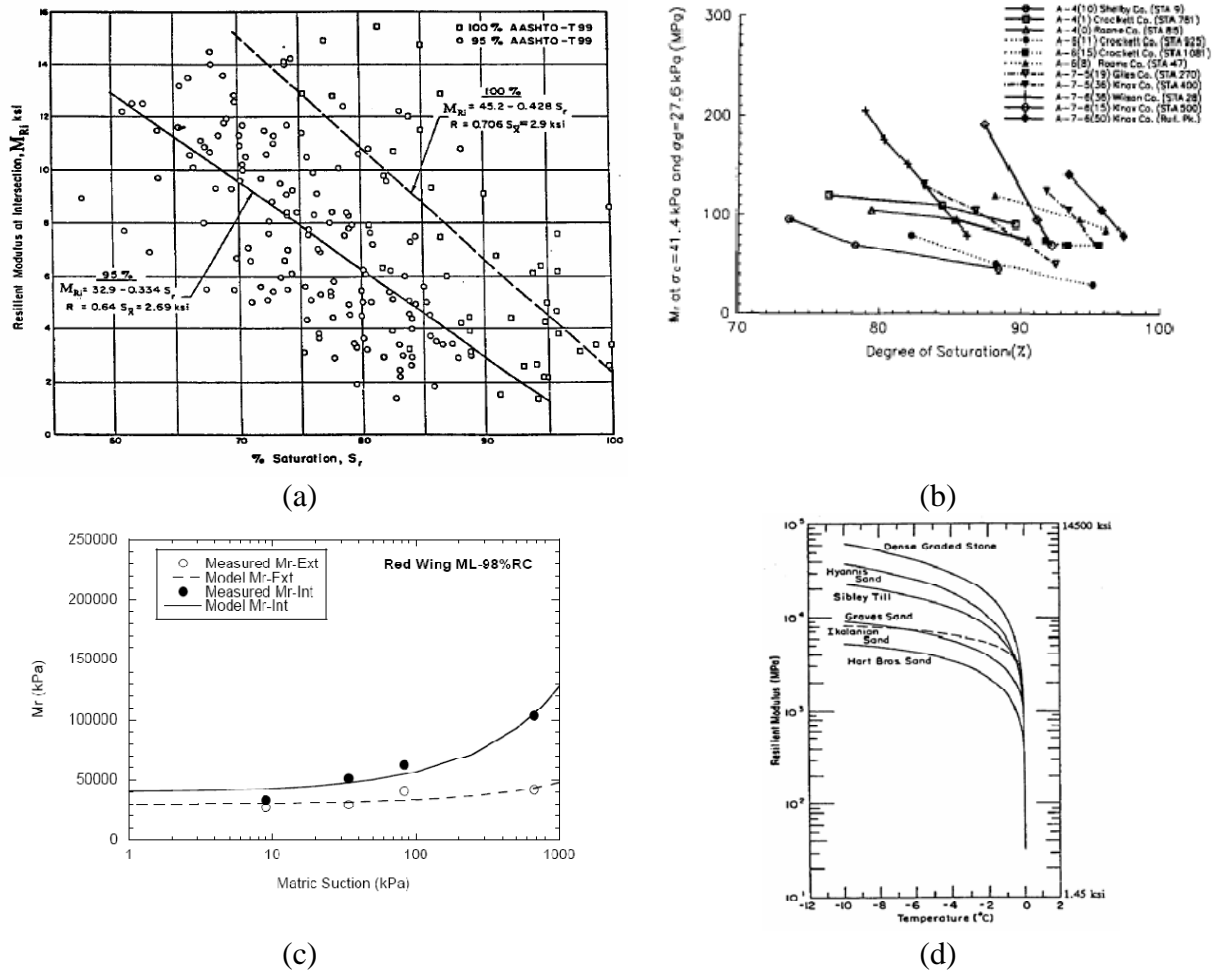


Figure 6.5: Resilient modulus variation with: (a) Degree of saturation (Thomson and Robnett 1979); (b) Degree of saturation (Drumm et al. 1997); (c) Matric suction (Gupta et al. 2007); (d) Temperature

The prediction of volume change due to water movement in clays of high plasticity is another important output from an integrated climate model. Although the CRREL model predicts the surface heave of the pavement due to frost instruction, it does not predict the surface heave expected in soils that change in volume due to shrinkage and swelling as water moves out and into the subgrade, respectively. The amount of volume change expected in a pavement will likely vary depending on the plasticity of the subgrade soil. This may be relevant to regions of Arkansas such as Malvern and Texarkana, which have geologic deposits of smectite soils having high shrink-swell potential.

## 7. REFERENCES

- Ahmed, Z., Marukic, I., Zaghoul, S., and Vitillo, N. (2005). "Validation of enhanced integrated climatic model predictions with New Jersey seasonal monitoring data." *Transportation Research Record*. 1913, 148-161.
- Alshibli, K.A., Abu-Farsakh, M. and Seyman, E. (2005). "Laboratory evaluation of the Geogauge and Light Falling Weight Deflectometer as construction control tools." *Journal of Materials in Civil Engineering*, 17(5). 560-569.
- Applied Research Associates (ARA). (2009). ICM Software. <http://www.ara-tracker.com/~glarson> . (August 30, 2009).
- ASTM D4318. (2010). Standard Test Methods for Liquid Limit, Plastic Limit, and Plasticity Index of Soils. ASTM International. West Conshohocken, PA.
- ASTM D5334. (2008). Standard Test Method for Determination of Thermal Conductivity of Soil and Soft Rock by Thermal Needle Probe Procedure. ASTM International. West Conshohocken, PA.
- ASTM D6836. (2008). Standard Test Methods for Determination of the Soil Water Characteristic Curve for Desorption Using a Hanging Column, Pressure Extractor, Chilled Mirror Hygrometer, and/or Centrifuge. ASTM International. West Conshohocken, PA.
- Bjorn, B., Ovik, J. and Newcomb, D. (2007). "Analytical Predictions of Seasonal Variations in Flexible Pavements: Minnesota Road Research Project Site." *Transportation Research Record* 1730. Pg. 81-90.
- Bayomy, F. and Salem, H. (2005). "Monitoring and modeling subgrade soil moisture for pavement design and rehabilitation in Idaho. Phase III: Data collection and Analysis." ITD Project No. SPR-0010(27) 124. 251 pp.
- Birgisson B., and Roberson, R. (2000). "Drainage of Pavement Base Material: Design and Construction Issues". *TRB Transportation Research Record* 1709.
- Brandon, T.L. and Mitchell, J.K. (1989). "Factors influencing the thermal resistivity of sands." *Journal of Geotechnical Engineering*. ASCE. 115(12), 1683-1698.
- Dempsey, B., Herlach, W., and Patel, A. (1985). "The Climatic-Materials-Structural Pavement Analysis Program." Final Report, FHWA/RD-84/115. Vol 3. FHWA. Washington, D. C.
- Dempsey, B.J. and Robnett, Q.L. (1979). "Influence of Precipitation, Joints, and Sealing on Pavement Drainage." *TRB Transportation Record* 705.

- Drumm, E., Reeves, J., Madgett, M., and Trolinger, W. (1997). "Subgrade resilient modulus correction for saturation effects." *Journal of Geotechnical and Geoenvironmental Engineering*. ASCE. 123(7), 663-670.
- Fayer, M.J. (2000). "Unsaturated Soil-Water and Heat Flow Model, Version 3.0." US DOE.
- Fu, P., and J.T. Harvey. (2007). "Temperature Sensitivity of Foamed Asphalt Mix Stiffness: Field and Lab Study." *International Journal of Pavement Engineering*, 8(2), 137-145.
- Gardner, W. (1958). "Some Steady-State Solutions of the Unsaturated Moisture Flow Equation with Application of Evaporation from a Water Table." *Soil Science*. Vol. 85. pp. 223-232.
- Gupta, G., Ranaivoson, A., Edil, T., Benson, C., Sawangsuriya, A. (2007). "Pavement Design Using Unsaturated Soil Technology." MN/RC-2007-11. Minneapolis, MN. 246 pp.
- Gupta, R., McCartney, J.S., Noguiera, C. and Zornberg, J.G. (2008). "Moisture Migration in Geogrid-Reinforced Expansive Subgrades." *GeoAmericas*. Cancun, Mexico. Mar. 3-5 2008.
- Guymon, G. L., Berg, R. L., and Johnston, T. C. (1986). "Mathematical Model of Frost Heave and Thaw Settlement in Pavements." U. S. Army Cold Regions Research and Engineering Laboratory.
- Khosravi, A. and McCartney, J.S. (2009). "Impact of Stress State on the Dynamic Shear Moduli of Unsaturated, Compacted Soils." 4th Asia Pacific Conference on Unsaturated Soils. Newcastle, Australia. Nov. 23-25, 2009.
- Khosravi, A., Ghayoomi, M., McCartney, J., and Ko, H.-Y. (2010). "Impact of Effective Stress on the Dynamic Shear Modulus of Unsaturated Sands." *GeoFlorida 2010*. Feb. 20-24, 2010.
- Larson, G. and Dempsey, B. (1997). "Enhanced Integrated Climate Model, Version 2." Minnesota Road Research Project Report MN/DOT 72114. 99 pp.
- Larson, G., and Dempsey, B. J. (2003). "Enhanced Integrated Climatic Model Version 3.0." Applied Research Associates/ ERES Division Staff, for upgrade with results from NCHRP 1-37 A, the 2002 Guide Development.
- Liang, R. (2006). "Validation of Enhanced Integrated Climatic Model Prediction over Different Drainable Base Materials." *Transportation Research Board Annual Meeting 2006 Paper #06-2529*.
- Liang, H. S., and Lytton, R.L. (1989). "Rainfall Estimation for Pavement Analysis and Design." Presented at 88th Annual Meeting. Transportation Research Board. Washington, D.C.

- Liang, R.Y., Al-Akhras, K. and Rabab'ah, S. (2007). "Field Monitoring of Moisture Variations Under Flexible Pavement." *Transportation Research Record: Journal of the Transportation Research Board*, No. 1967, Transportation Research Board of the National Academies, Washington, D.C., 2006, pp. 160–172.
- Liu, S., Jeyapalan, J. K., and Lytton, R. L. (1983). "Characteristics of Base and Subgrade Drainage Pavements, Subgrade Water." *TRB Transportation Research Record* 945.
- Liu, S. J., and Lytton, R. L. (1985). "Environmental Effects on Pavement-Drainage." Report FHWA-DTFH-61-87-C-00057, Vol. IV, Federal Highway Administration, Washington, D.C.
- Lytton, R., Pufahl, D., Michalak, C., Liang, H., and Dempsey, B. (1989). "An Integrated Model of the Climatic Effects on Pavement." Report No. FHWA-RD-90-033. FHWA, U.S. Department of Transportation. McLean, VA.
- McCartney, J.S. and Zornberg, J.G. (2003). "Assessment of Evapotranspirative Cover Performance using Field Data and Numerical Modeling." IV International Workshop on Applications of Computational Methods in Geotechnical Engineering. Ouro Preto, Brazil. August 17-20, 2003.
- Miller, G.A., Khoury, C.N., Muraleetharan, K.K., Liu, C. and Kibbey, T.C.G. (2008). "Effects of soil skeleton deformations on hysteretic soil water characteristic curves: Experiments and simulations." *Water Resources Research*. 44. 10 pg.
- National Research Council. (2004). *Guide for Mechanistic-Empirical Design of New and Rehabilitated Pavement Structures*. NCHRP Report I-37A. TRB. Washington, D.C.
- Philip, J.R. and DeVries, D. (1957). "Moisture movement in porous materials under temperature gradients." *Transactions of the American Geophysical Union*. 38, 222-232.
- Quintero, N. (2007). "Validation of the Enhanced Integrated Climatic Model (EICM) for the Ohio SHRP Test Road at U.S. 23." M.S. Thesis submitted to the Russ College of Engineering and Technology of Ohio University.
- Richter, C. A., and Witczak, M. W. (2001). "Application of LTPP Seasonal Monitoring Data to Evaluate Volumetric Moisture Predictions from the Integrated Climatic Model." *Transportation Research Board (TRB), 80th Annual Meeting*, Washington, D.C.
- Ridgeway, H. H. (1976). "Infiltration of Water Through the Pavement Surface", *TRB Transportation Record* 616.

- Roberson, R. and Siekmeier, J. (2002). "Determining Material Moisture Characteristics for Pavement Drainage and Mechanistic Empirical Design." MN/DOT Research Bulletin. M&RR 09.
- Thompson, M.R., and Robnett, Q.L. (1979). "Resilient Properties of Subgrade Soils." *Transportation Engineering Journal*, ASCE, Vol. 105, No. TE1, pp. 71-89.
- Transportation Research Board (TRB). (2009). *Mechanistic-Empirical Design Guide Climate Database*. [http://onlinepubs.trb.org/onlinepubs/archive/mepdg/climatic\\_state.htm](http://onlinepubs.trb.org/onlinepubs/archive/mepdg/climatic_state.htm).
- Suwangsurinya, A. Edil, T., and Bosscher, P. (2003). "Relationship Between Soil Modulus Gauge Modulus and Other Test Moduli for Granular Soils." *Transportation Research Record*. 3140, 3-10.
- Wang, X. and Benson, C.H. (2004). "Leak-free pressure plate extractor for the soil water characteristic curve." *ASTM Geotechnical Testing Journal*. 27(2), 1-10.
- Witzcak, M.W., Houston, W.N., Zapata, C.E., Richter, C., Larson, G. and Walsh, K. (2000). "Improvement of the Integrated Climatic Model for Moisture Content Predictions." *Inter-Team Technical Report (Seasonal 4)*, NCHRP 1-37 A.
- Yoder and Witzcak (1975). *Principles of Pavement Design*. John Wiley and Sons. New York.
- Zaghloul, S. Ayed, A. Abd El Halim, A. Vitillo, N, and Sauber, R. (2006). "Investigations of Environmental and Traffic Impacts on Mechanistic-Empirical Pavement Design Guide Predictions." *TRR*. No. 1967, 148-159.
- Zapata, C.E. and Houston, W.N. (2008). *Calibration and Validation of the Enhanced Integrated Climatic Model for Pavement Design*. NCHRP Report 602.
- Zapata, C.E., Houston, W.N., Houston, S.L., and Walsh, K.D. (1999). "Soil-Water Characteristic Curve Variability." *Geotechnical Special Publication No. 99, Advances in Unsaturated Geotechnics, Proc. of sessions of Geo-Denver 2000*, ASCE, Denver, Colorado.
- Zornberg, J.G., and McCartney, J.S. (2005). "Evaluation of Evapotranspiration from Alternative Landfill Covers at the Rocky Mountain Arsenal." *Experus 2005*. Tarantino, A., Romero, E., and Cui, Y.J. (eds). Trento, Italy, 27-29 June 2005. Balkema, Rotterdam.
- Zornberg, J.G., and McCartney. (2006). "Chapter 34: Evapotranspirative Cover Systems." In: *The Handbook of Groundwater Engineering, 2nd Edition*. Jacques W. Delleur (Editor-in-Chief). CRC Press. Boca Raton, Florida.

## A. SOIL CHARACTERIZATION

### A.1 Overview

Well-defined material properties are critical to obtaining a correct estimate of the suction and temperature distributions during heat and temperature flow. Both EICM and VADOSE/W have the same material property inputs, although EICM incorporates empirical parameters which can be used to estimate material properties using easier-to-determine soil index properties (e.g. consistency limits). The properties of the soils from the different sites in Arkansas that were measured in this study include:

- Hydraulic Conductivity
- Soil-Water Retention Curve (SWRC)
- Thermal Conductivity
- Volumetric Heat Capacity

### A.2 Index Properties

The consistency (Atterberg) limits were measured for the soils from the different sites to classify the soils according to the USCS classification scheme. The liquid limit (LL) and plastic limit (PL) of the fine-grained soils were determined according to ASTM D4318. The Plasticity Index (PI) was calculated as the difference between the measured LL and PL. The Atterberg limits for the soils from the different sites are summarized in Table A.1, along with the USCS classification of the soils. All of the soils are clays of varying plasticity. The soil from Lake Village had the lowest plasticity index, likely because the soils from this site are sediments deposited by the Mississippi river.

Table A.1: Index properties of the site soils

Site	PL	LL	PI	USCS Classification
Greenland	28	46	19	CH
Plumerville	24	50	26	CH
Malvern	14	23	9	CL
Murfreesboro	21	54	33	CH
Camden	20	33	13	CH
Lake Village	26	28	2	CL
Marked Tree	37	72	35	CH



### A.3 Hydraulic Conductivity of Saturated Soil Specimens

Flexible-wall permeameters were used to measure the hydraulic conductivity of water-saturated fine-grained soil. The permeability cell is a triaxial cell equipped with double drainage lines connected to the top and bottom of the soil specimen held within a latex membrane. The permeability tests were performed using back pressure to ensure initial saturation of the specimen. Care is taken to be certain that flow is steady state and that the soil is permeated long enough for the water to pass through the soil. Hydraulic gradients of approximately 100 to 130 were used in this study to speed up the measurement of hydraulic conductivity, as the hydraulic conductivity of the soils in this study are all relatively low.

The first step in measurement of the hydraulic conductivity is the saturation of the soil specimen. After the soil specimen is placed within the latex membrane within the permeameter cell, a high vacuum pump is used to apply a vacuum with a magnitude of approximately -80 kPa to the inside of the specimen. The specimen is then permitted to de-air for approximately one hour. During this time, the cell is assembled around the specimen and is filled with water used as the confining pressure. A cell pressure of 35 kPa is applied as a “seating” confining pressure to ensure that the specimen is always under a positive effective stress. De-aired water is then introduced into the bottom platens under atmospheric pressure to saturate, from the bottom up, the ceramic disc, soil specimen, top platen. De-aired water is flushed through both chambers of the pressure transducer, all valves, tubing, and the flow pump in order to ensure that the system is fully water-saturated conditions. The cell pressure and back-pressure are then increased in increments to values of 600 kPa and 565 kPa, maintaining an effective stress of 35 kPa. During this incremental increase in pressures, Skempton’s B-value parameter is measured to infer the initial degree of saturation of the specimen. This parameter is measured by closing the backpressure supply lines, increasing the cell pressure, and measuring the pore water pressure response with a pressure transducer. The specimens tested in this study all had a B-value in excess of 0.96, indicating adequate saturation. After saturation of the soil specimen, the water pressure applied to the bottom of the specimen is reduced to 530 kPa while the water pressure applied to the top of the specimen is maintained at 565 kPa. The pressure difference between top and bottom of the specimen causes the water flow through the soil specimen from the top (higher pressure) to the bottom (lower pressure) of the specimen.

During the test, volume of water inflow from the top and outflow from the bottom are measured. When the steady state flow (inflow equals outflow), the hydraulic conductivity is calculated as:

$$(A.1) \quad K = \frac{VL}{At\Delta h}$$

where  $K$  is the saturated hydraulic conductivity,  $\Delta h$  is the head difference across the top and bottom of the specimen,  $V$  is the volume of flow in a time increment  $t$  at steady-state conditions,  $L$  is the specimen length, and  $A$  is the cross-sectional area of the specimen.

The water flow from the top and bottom of the specimen during the hydraulic permeability tests for the soil specimens from different sites are shown in Figures A.1 through A.7. The value of outflow ( $V/t$ ) at the end of the hydraulic conductivity test was used to define the hydraulic conductivity using Equation A.1. A summary of the hydraulic conductivity values for the saturated soils from the different sites is shown in Table A.2. This table also includes the hydraulic conductivity of saturated AASHTO A-3 crushed aggregate base. The hydraulic conductivity values of the clays from the different sites are extremely low. For comparison, clay that is typically used as a hydraulic barrier in landfill applications has a hydraulic conductivity less than  $10^{-9}$  m/s.

Table A.2: Hydraulic conductivity of saturated soil specimens from the different sites

Site	Hydraulic conductivity (m/s)
Class 7 Base	$2.97 \times 10^{-7}$
Greenland	$5.74 \times 10^{-11}$
Plumerville	$4.38 \times 10^{-10}$
Malvern	$8.47 \times 10^{-10}$
Murfreesboro	$2.23 \times 10^{-11}$
Camden	$1.19 \times 10^{-9}$
Lake Village	$3.2 \times 10^{-11}$
Marked Tree	$5.63 \times 10^{-11}$

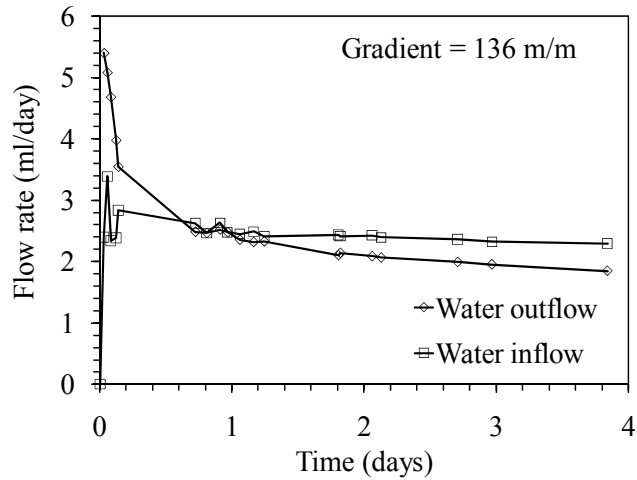


Fig. A.1: Water flow rate with time for saturated soil from Greenland

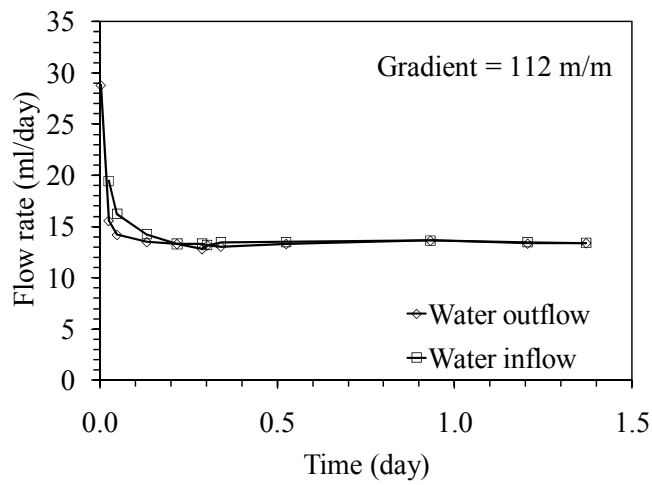


Fig. A.2: Water flow rate with time for saturated soil from Plumerville

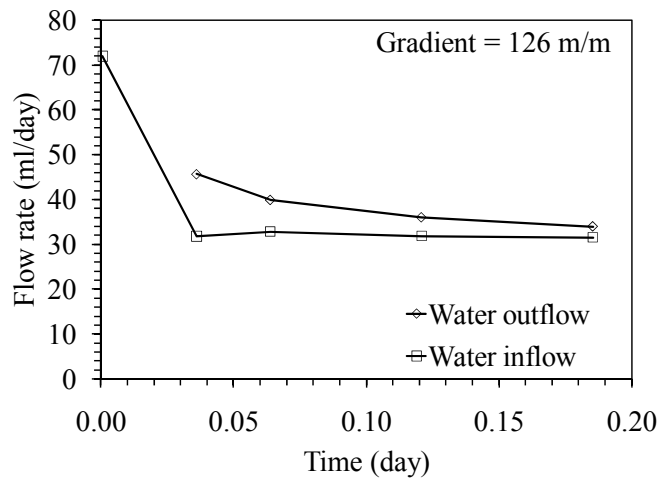


Fig. A.3: Water flow rate with time for saturated soil from Malvern

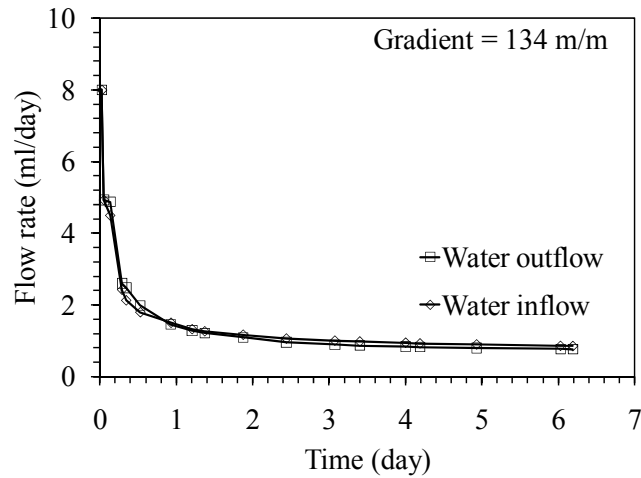


Fig. A.4: Water flow rate with time for saturated soil from Murfreesboro

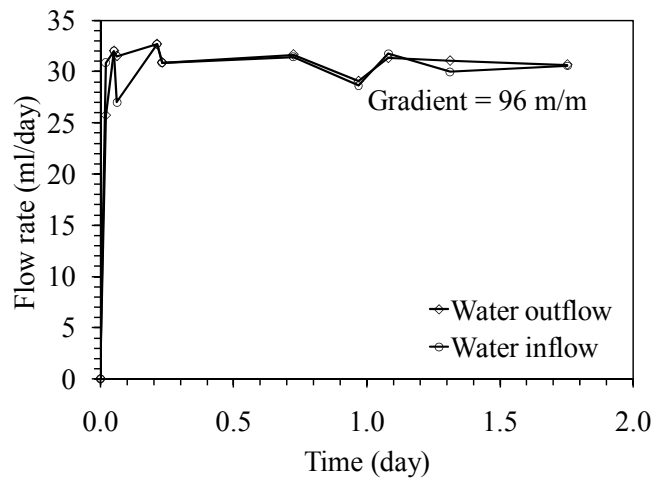


Fig. A.5: Water flow rate with time for saturated soil from Camden

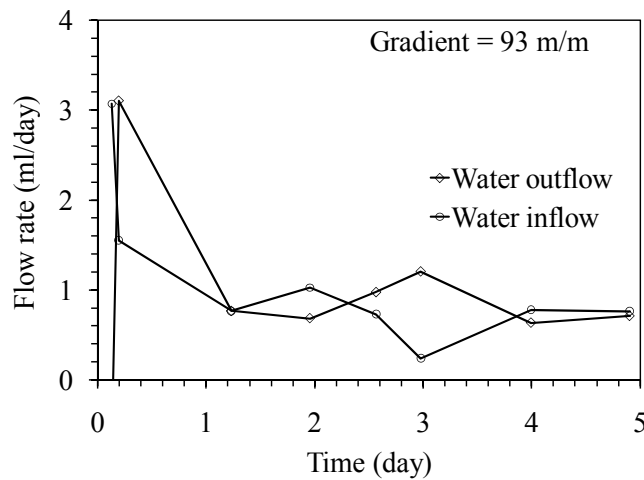


Fig. A.6: Water flow rate with time for saturated soil from Lake Village

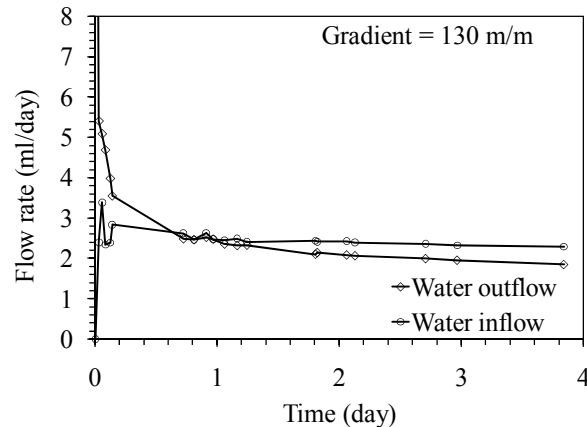


Fig. A.7: Water flow rate with time for saturated soil from Marked Tree

#### A.4 Soil-Water Retention Curves

Soil-Water Retention Curves (SWRCs) describe the relationship between suction and volumetric water content (or degree of saturation). This relationship is critical to analysis of water flow in unsaturated soils such as those found in pavement systems. Several techniques are available to measure the SWRC (ASTM D6836; Wang and Benson 2004) using physical and thermodynamic techniques. Physical techniques involve expulsion of water from a specimen of initially water-saturated soil by imposing a known value of suction on a specimen boundary. Specimens are usually small in size so that the variation in suction within the specimen is minimal. Thermodynamic techniques involve evaporation of water from a specimen inside a closed environment with known relative humidity. In this case, the total suction (i.e., the sum of osmotic pressure and matric suction) within the soil will reach equilibrium with the water vapor pressure in the pore air (related to the relative humidity). However, as water flow is controlled by the matric suction, a correlation must be developed between total and matric suction to use these techniques. In general, physical techniques are used for low suctions (e.g., < 1500 kPa) while thermodynamic techniques are used for higher suctions.

Although the soils in this study are all clays, which are known to retain water up to very high suctions, a physical technique (typically used for low suctions) was used in this study. The goal of the SWRC measurements in this study was to identify the air-entry suction (i.e., the suction at which the soil starts to desaturate), and to identify the slope of the desaturation portion of the SWRC. This means that the shape of the SWRC was not measured at high suctions in this study. This was done because the water table at the different sites is relatively high, and suctions close to saturation are expected throughout the year.

An axis translation technique was used to measure the SWRC in the same flexible wall permeameter setup used in the hydraulic conductivity testing. A schematic of the test setup is shown in Fig. 2.

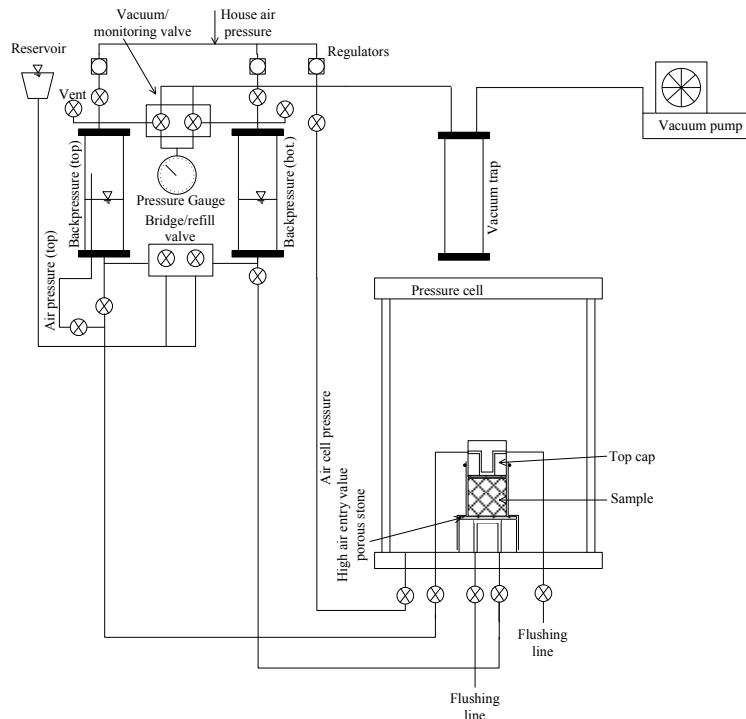


Fig. A.7: Schematic of the permeameter setup with axis translation for SWRC measurement

The axis translation technique takes advantage of the fact that the suction is equal to the difference between the pore air and water pressures. Axis translation permits the control of the suction in the specimen by applying (or measuring) a difference in air and water pressure across a soil specimen resting atop a high-air entry ceramic disc or porous membrane. The high air-entry ceramic disc permits independent control of the pore water pressure on the boundary of the specimen as only water is transmitted through the ceramic for suction values less than the air-entry suction of the ceramic. The pore water pressure in the axis translation technique needs not be zero as the suction is equal to the difference in the air and water pressure. Accordingly, backpressure saturation can be used to initially saturate the specimen by dissolving entrapped air bubbles. The axis translation technique with backpressure permits improved accuracy of outflow measurements from unsaturated materials. Outflow from the specimen during application of increments of suction values is typically measured using visual observation of the water level in a graduated burette connected to the water drainage line from the specimen.

The main difference in the setup for the SWRC testing in the flexible wall permeameter is that the specimen was placed atop the high-air entry ceramic disc. After the soil specimen and disc are placed within the latex membrane in the flexible wall permeameter, a high vacuum pump is used to apply a vacuum to the inside of the specimen, with a magnitude of approximately -80 kPa. The system is then permitted to de-air for approximately one hour. The specimen is then saturated using the same approach described for the saturated hydraulic conductivity test. After saturation of the soil specimen, the cell pressure applied is 600 kPa, while the back-pressure applied to the top and bottom of the specimen is 565 kPa. Air is flushed from the top platen of the specimen while maintaining an air pressure of 565 kPa. The water pressure at the bottom of the specimen is still also 565 kPa, so no flow occurs through the specimen during this flushing period. The difference in air and water pressures is the same across the specimen, so the suction is 0 kPa (corresponding to saturated conditions). De-saturation can be started by decreasing the water pressure at the bottom of the ceramic disc while maintaining the air pressure on top of the specimen constant. A higher air pressure at the top of the specimen will cause water flow from the bottom of the specimen, and the lower water pressure than the air pressure implies that the soil is under suction.

The first suction increment is not expected to desaturate the specimen. In other words, the first suction applied is expected to be less than the air-entry suction of the specimen. However, when a suction is applied that is greater than the air-entry suction, air will enter the top of the specimen (displacing water), and the specimen will start to de-saturate. The SWRC of soil is determined by imposing different increments of suction to the specimen, and recording the volume of water withdrawn from the specimen until reaching equilibrium (no flow) conditions. The change in volumetric water content can be determined by calculating the dividing the outflow of water during an increment by the total volume of the specimen. The SWRC is defined by correlating the volumetric water content at the end of an increment with the applied suction.

This experimental approach leads to the definition of discrete points on the SWRC. However, a continuous function is needed to represent the SWRC in numerical models such as the EICM or VADOSE/W. Accordingly, a continuous function can be fitted to the discrete data points. The EICM uses the continuous SWRC function proposed by Fredlund and Xing (1994), given by the following equation:

$$(A.2) \quad \theta = C_{\psi} \frac{\theta_s}{\left[ \ln \left( e + \left( \frac{\psi}{a_{FX}} \right)^{n_{FX}} \right) \right]^{m_{FX}}}$$

where  $a_{FX}$ ,  $n_{FX}$  and  $m_{FX}$  are fitting parameters,  $\psi$  is the matric suction applied to the soil,  $\theta$  is the volumetric water content,  $\theta_s$  is the saturated volumetric water content (equal to the porosity), and  $C_{\psi}$  is a correction function to account for residual conditions:

$$(A.3) \quad C_{\psi} = 1 - \frac{\ln \left( 1 + \frac{\psi}{h_r} \right)}{\ln \left( 1 + \frac{10^6}{h_r} \right)}$$

where  $h_r$  is the matric suction corresponding to the residual water content, which is the water content at which the SWRC flattens at high suctions. The correction factor  $C_{\psi}$  forces the suction at zero volumetric water content to be  $10^6$  kPa.

The  $a_{FX}$  parameter is related to the air entry suction of the soil, which is the suction at which air can enter the soil pores. Variations in this parameter will cause the SWRC to move to the left or right. In the EICM, two of the Fredlund-Xing SWRC model parameters,  $a_{FX}$  and  $h_r$  are labeled as dimensionless parameters. This is incorrect as inspection of Equations A.1 and A.2 indicates that both of these parameters must have the same units as suction. The impact of inadvertently considering the  $a_{FX}$  parameter dimensionless when converting a SWRC from metric to English units is shown in Figure A.8. It is recommended that when defining the SWRC of the soil in EICM, the SWRC should be first defined in kPa, and then the suction units can be converted to psi if English units are used in the analysis.

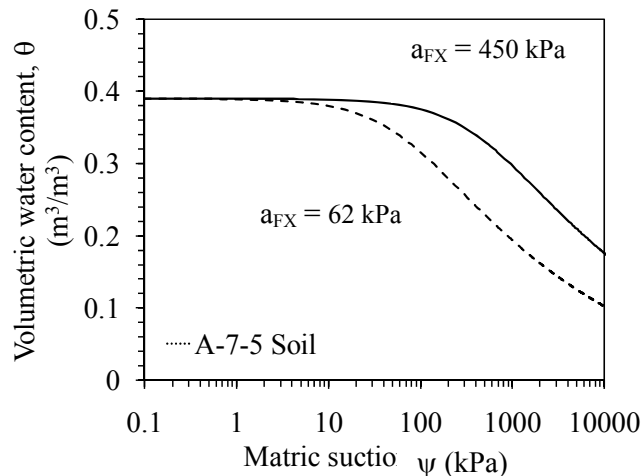
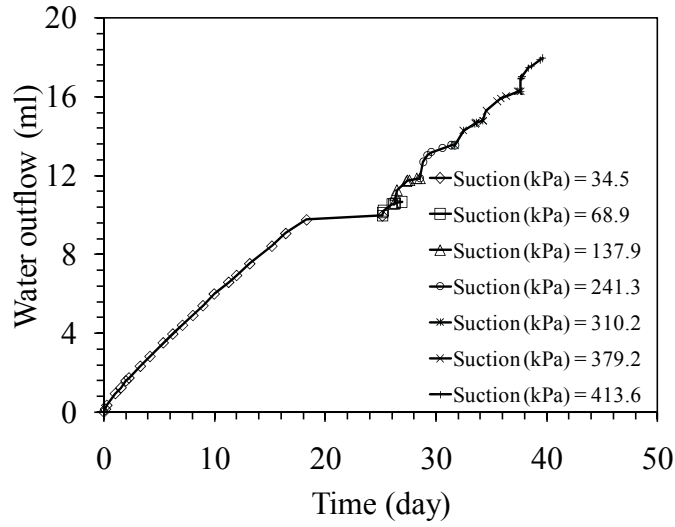


Figure A.8: Impact of using the wrong units for  $a_{FX}$  on the shape of the SWRC

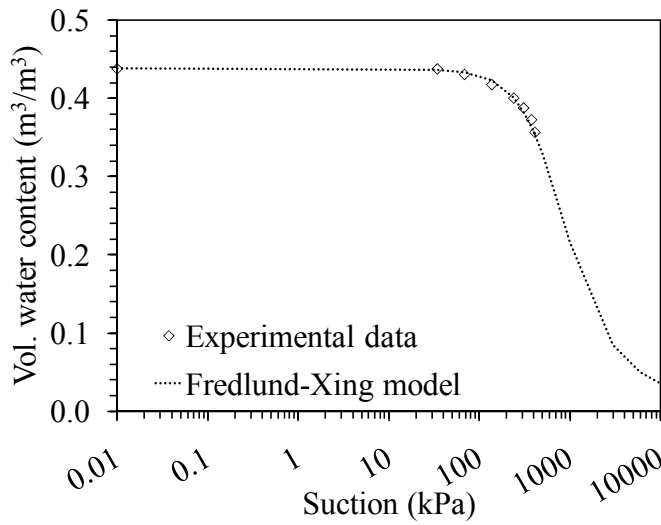


The fitted SWRC equation can be used to estimate the hydraulic conductivity of the unsaturated soils. As a soil specimen desaturates, the hydraulic conductivity to water will decrease because the cross-sectional area available for water in the specimen will decrease. Accordingly, the relationship between hydraulic conductivity and suction is referred to as the K-function. This is another important input for the EICM and VADOSE/W. Although techniques are available to measure the hydraulic conductivity function, a predictive approach was used to estimate the K-function, as described by Fredlund and Xing (1994). This prediction requires the measured saturated hydraulic conductivity and the parameters of the SWRC.

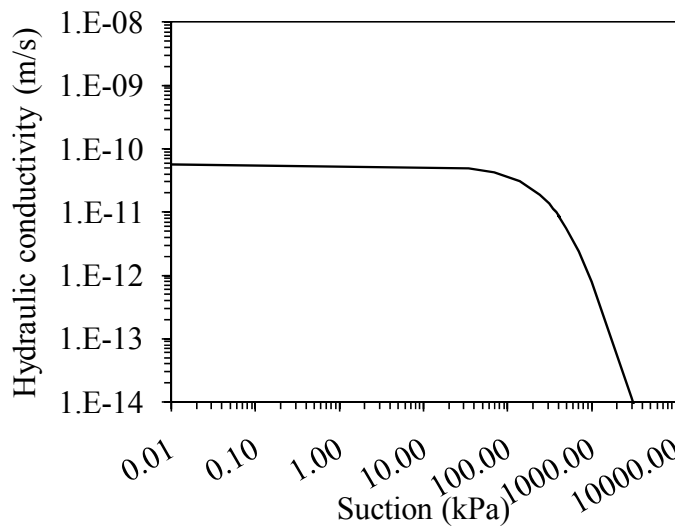
The data from the SWRC tests is shown in Figures A.9 to A.15 for the soils from the seven sites in Arkansas. This includes the outflow during each of the increments of suction, the discrete and fitted SWRC results, and the predicted K-functions. In general, the shapes of the SWRCs for the different soils are similar, with an air-entry suction in the range of 100 kPa. The water content at the air-entry suction was found to be a good parameter to use as the initial suction in the subgrade soil profile in the EICM analyses. This is because before reaching this air-entry suction, the specimen is water-saturated and the hydraulic conductivity is close to the value at saturation.



(a)



(b)



(c)

Figure A.9: SWRC results for the soil specimen from Greenland: (a) Outflow for different suction stages; (b) Experimental and fitted Fredlund-Xing SWRC; (c) Predicted K-function

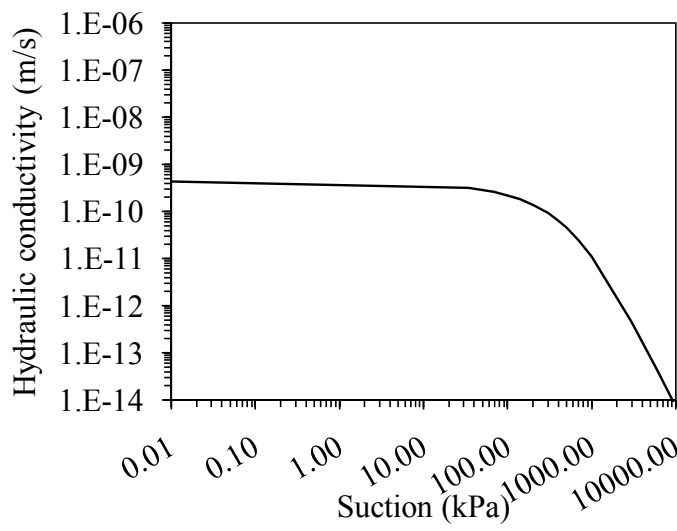
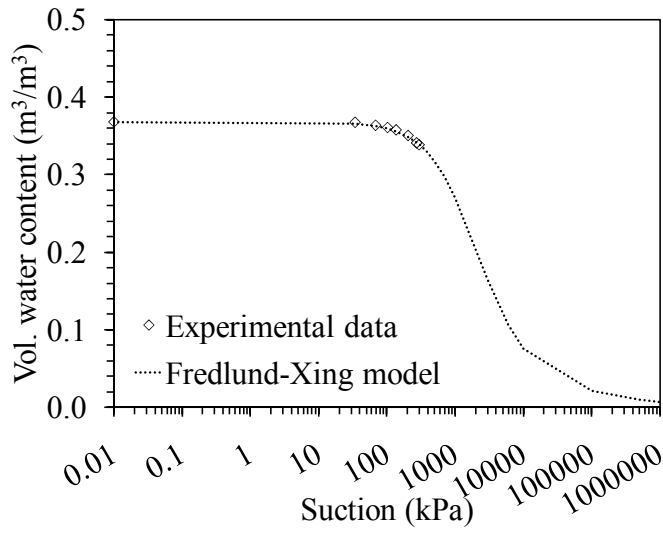
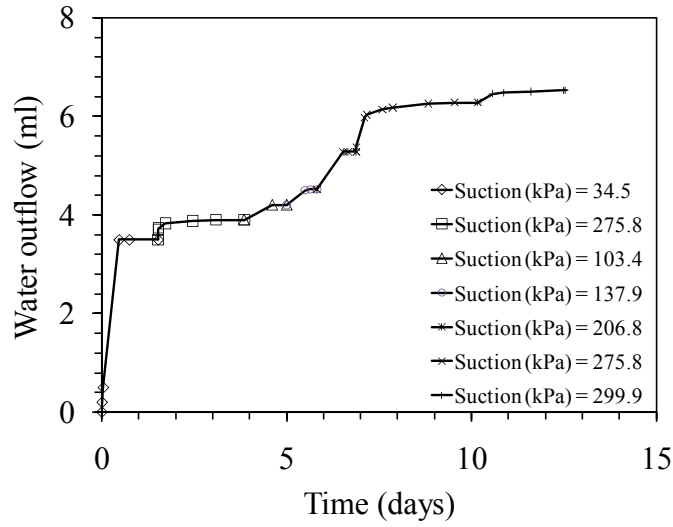
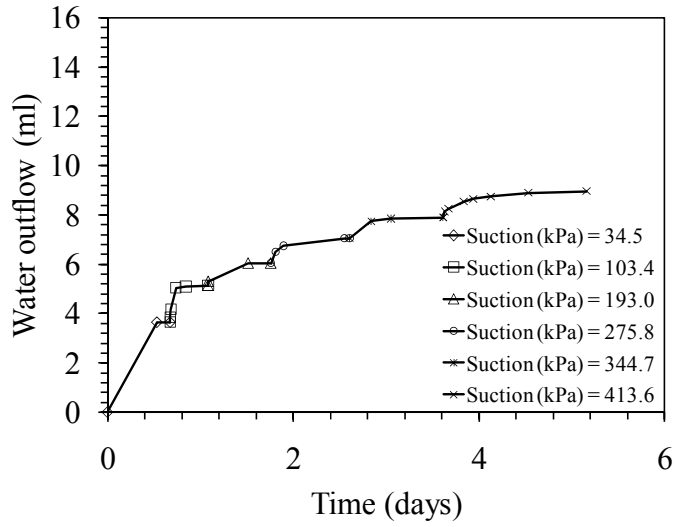
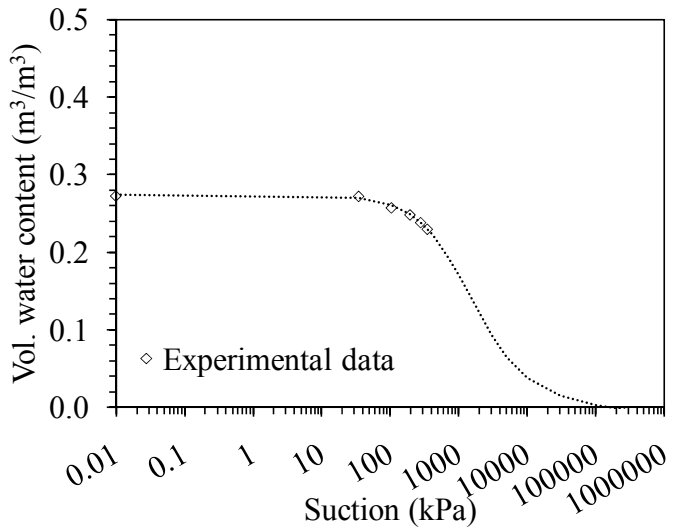


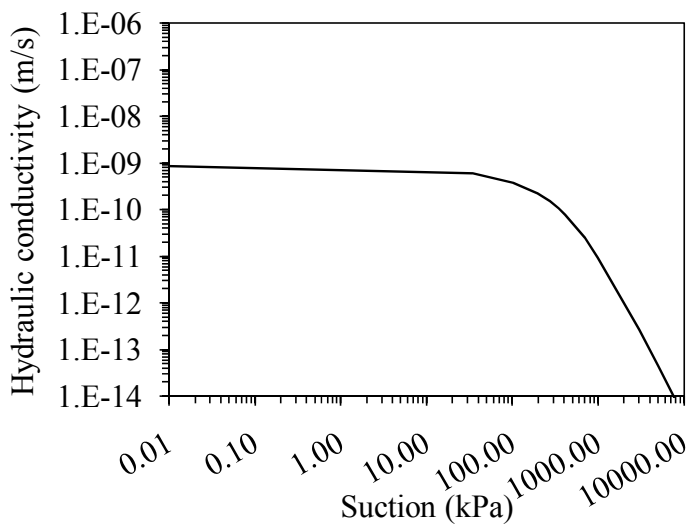
Figure A.10: SWRC results for the soil specimen from Plumerville: (a) Outflow for different suction stages; (b) Experimental and fitted Fredlund-Xing SWRC; (c) Predicted K-function



(a)

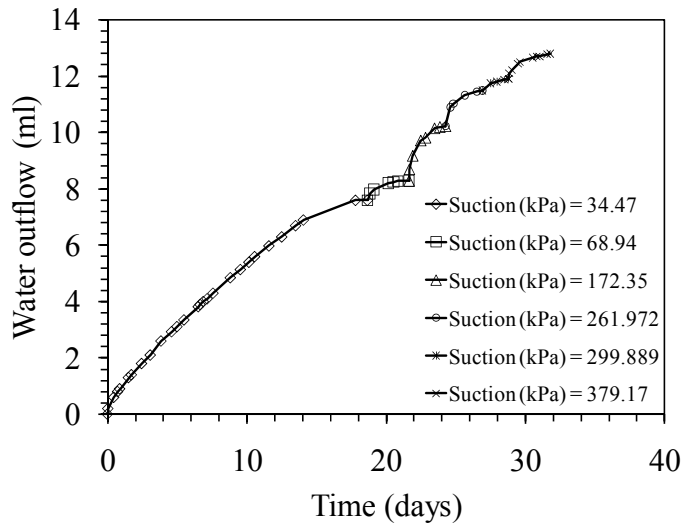


(b)

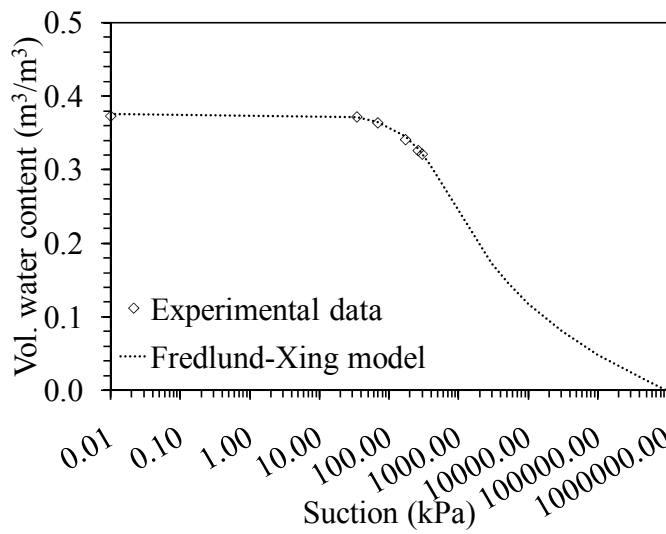


(c)

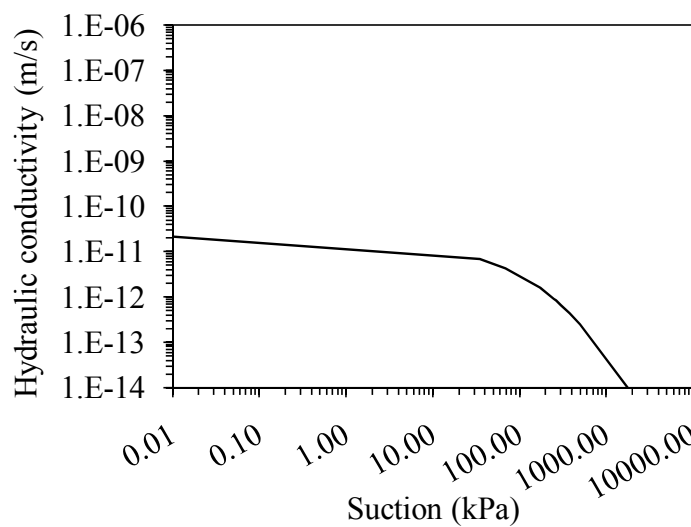
Figure A.11: SWRC results for the soil specimen from Malvern: (a) Outflow for different suction stages; (b) Experimental and fitted Fredlund-Xing SWRC; (c) Predicted K-function



(a)

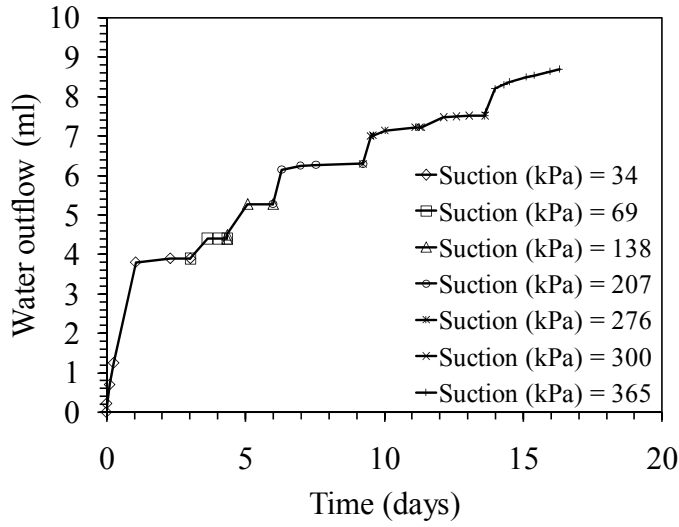


(b)

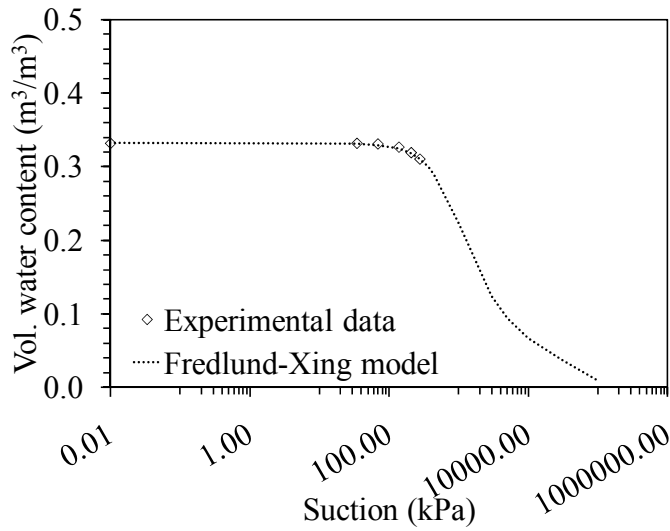


(c)

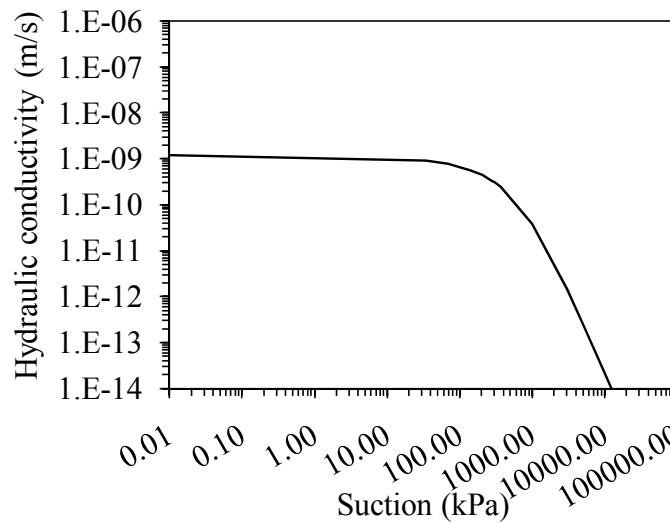
Figure A.12: SWRC results for the soil specimen from Murfreesboro: (a) Outflow for different suction stages; (b) Experimental and fitted Fredlund-Xing SWRC; (c) Predicted K-function



(a)

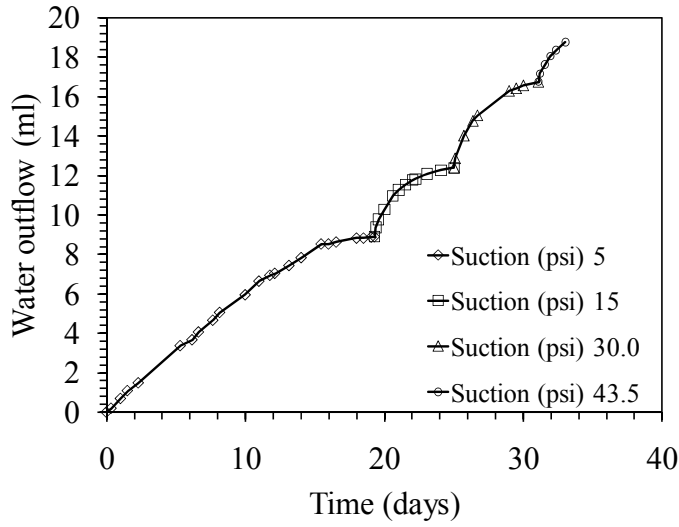


(b)

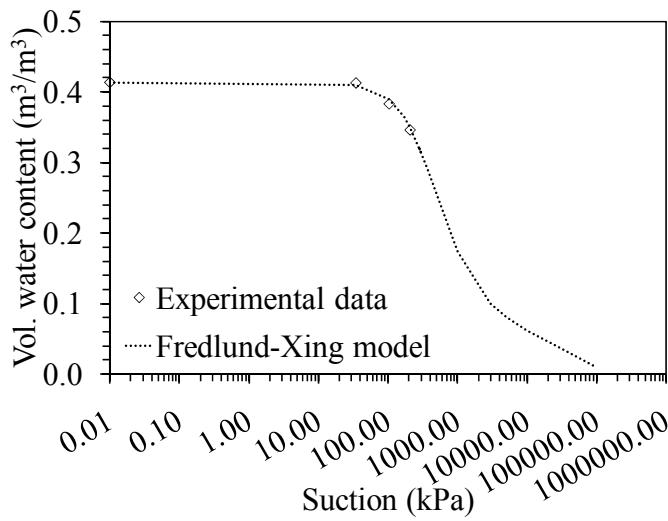


(c)

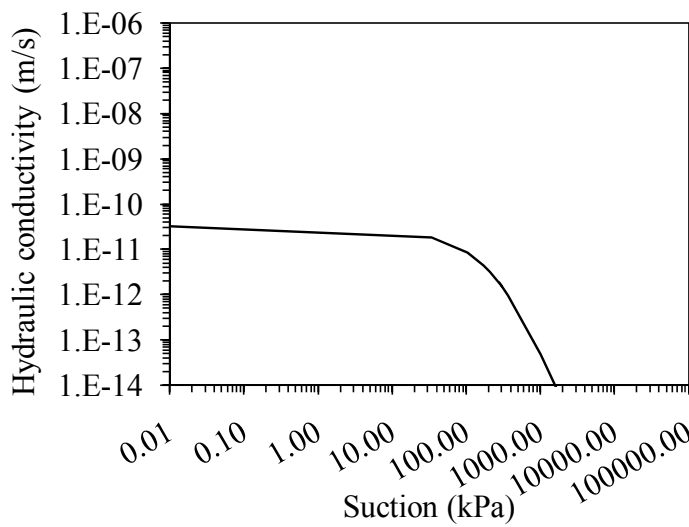
Figure A. 13: SWRC results for the soil specimen from Camden: (a) Outflow for different suction stages; (b) Experimental and fitted Fredlund-Xing SWRC; (c) Predicted K-function



(a)

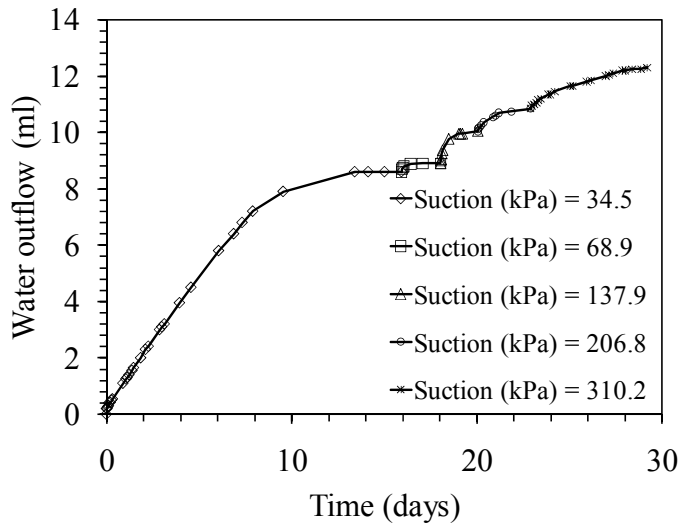


(b)

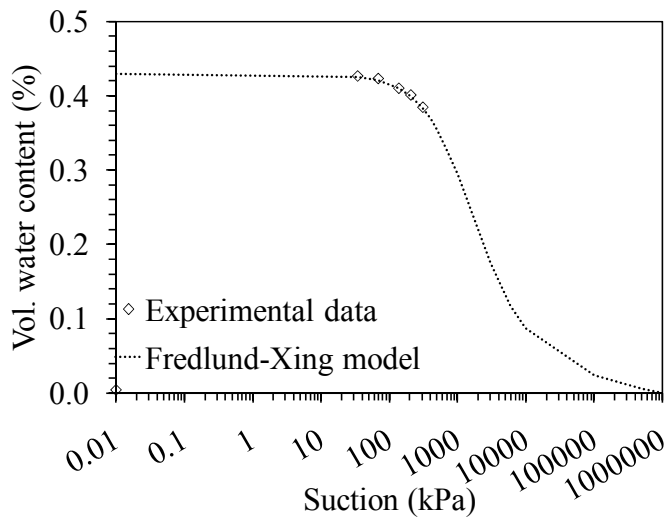


(c)

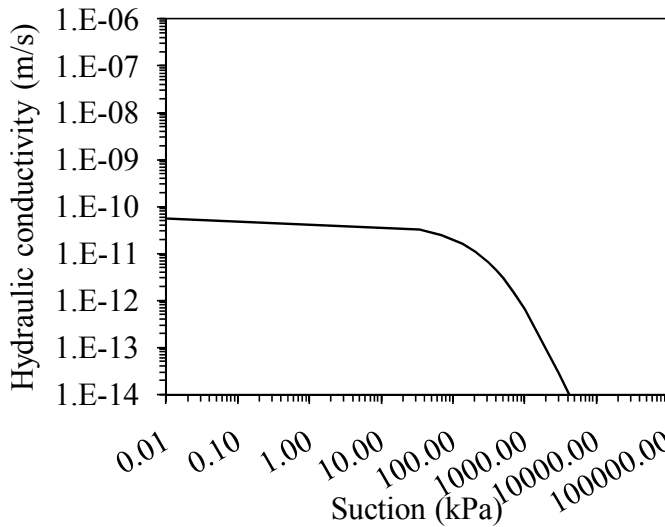
Figure A.14: SWRC results for the soil specimen from Lake Village: (a) Outflow for different suction stages; (b) Experimental and fitted Fredlund-Xing SWRC; (c) Predicted K-function



(a)



(b)



(c)

Figure A.15: SWRC results for the soil specimen from Marked Tree: (a) Outflow for different suction stages; (b) Experimental and fitted Fredlund-Xing SWRC; (c) Predicted K-function



The SWRC of the base course soil and silica flour were measured using the axis-translation technique, but in a rigid-wall permeameter, shown in Figure A.16. This test was used as saturation of these coarser soils is easier, and because the preparation of these soils in a flexible mold is more difficult. In the case of silica flour, sample preparation was performed by pouring the silica flour inside the retaining ring in its loosest condition. This method for the sample preparation was chosen to have a better simulation of the site condition. Saturation of the specimen is an important part of the test that is performed by keeping the water level in the Mariotte burette at the same level as the surface of the specimen. This will cause the water flow from the burette into the specimen resulting in the saturation of the specimen. In the case of silica flour, a considerable settlement was observed during saturation. The dimensions of the specimen after saturation were considered for the back calculation of water content. The air pressure in the vessel is then increased, and the water pressure on the other side of the saturated ceramic is maintained constant. Application of air pressure to the soil in the vessel will cause air to enter the pores and displace water, which will flow from the soil through the saturated ceramic. The air-entry pressure of the ceramic disc must be higher than that of the soil, and should be higher than the maximum air pressure applied to the pressure vessel. The water pressure at the base of the ceramic disc is usually kept at atmospheric pressure, and outflow is measured using a constant-head Mariotte burette.

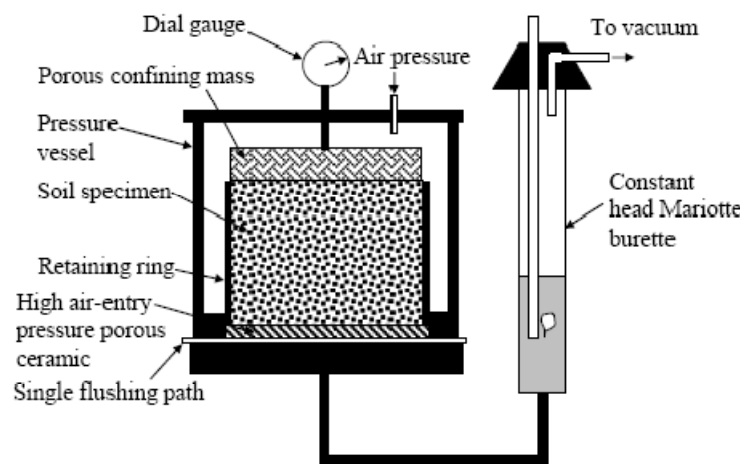


Fig. A.16: Schematic of the rigid-wall permeameter for axis-translation testing

The water level in a constant-head Mariotte burette can change during outflow from the specimen while maintaining the same water pressure at the base of the ceramic. After outflow is negligible, the system is in equilibrium under the imposed matric suction. The total volume of

outflow can be measured for this pressure increment. This approach can be repeated for higher air pressure increments, which will cause gradual drainage of the specimen. After reaching equilibrium at the highest pressure increment, the pressure may be decreased; hysteresis can be investigated by permitting water from the constant-head Mariotte burette to flow back into the specimen. At the end of testing, the final volumetric moisture content can be estimated from the gravimetric water content and the dry density. The volumetric moisture content at each increment can then be back-calculated from the outflow measured throughout the test. The range of suction for this test is limited by the air-entry value of the porous ceramic disc, which is typically between 100 and 500 kPa. More details for axis translation testing can be found in ASTM D6836. The SWRC and predicted K-function for the base are shown in Figure A.17, while those for the silica flour are shown in Figure A.18.

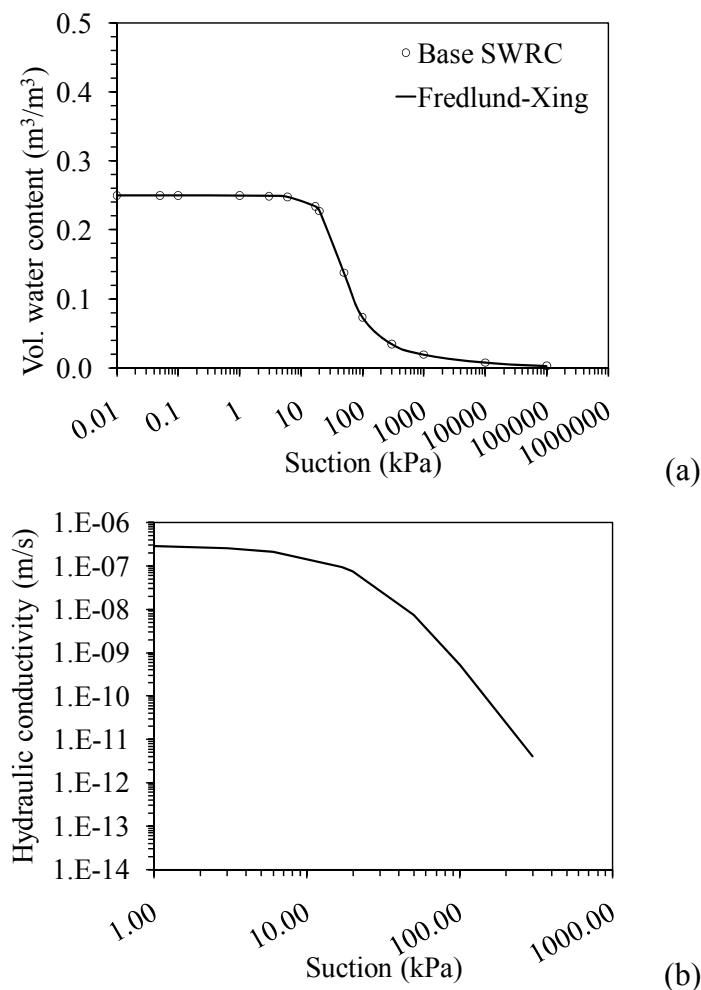


Figure A.17: Base course: (a) SWRC data with fitted Fredlund-Xing SWRC; (b) K-function

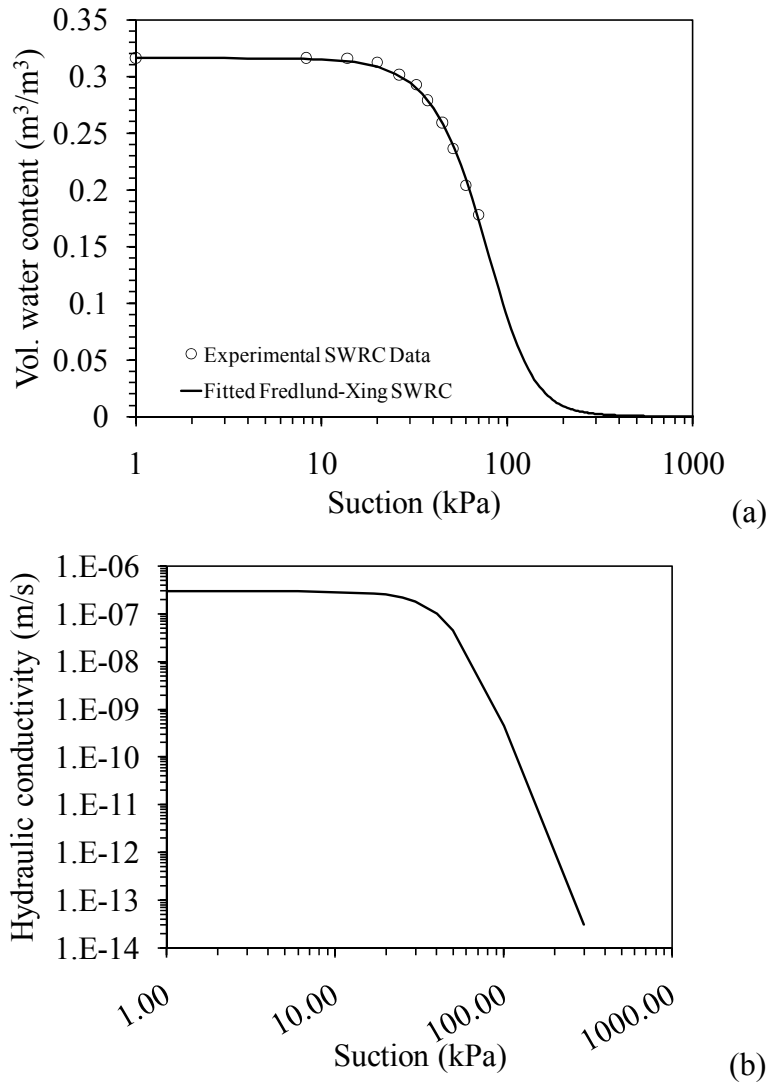


Figure A.18: Silica flour: (a) SWRC data with fitted Fredlund-Xing SWRC; (b) K-function

### A.5 Thermal Conductivity

The thermal needle technique was used to measure thermal conductivity according to ASTM D5334. The thermal needle used in this study was part of the KD2Pro Setup obtained from Decagon Devices of Pullman, Washington, shown in Figure A.19. The thermal needle incorporates a heater coil and a thermocouple. The thermal needle test involves applying a constant thermal load to the needle for a period of thirty seconds. The temperature rise in the soil measured by the thermocouple in the needle can be related with the thermal conductivity through an analytical solution to the cylindrical heat flow equation, as shown in Figure A.20. Soils with a high thermal conductivity dissipate heat away from the needle to the soil further away from the needle, while soils with low thermal conductivity will act as insulators and keep the heat pulse

close to the needle. More details on thermal conductivity measurement with the thermal needle approach can be obtained from Brandon and Mitchell (1989). The thermal needle test was performed on the intact soil specimens obtained from the Shelby tubes brought from the different sites in Arkansas. The thermal conductivity values for the soils from the different sites are listed in Table A.3.



Figure A.19: KD2Pro test setup with the thermal needle used to determine the thermal conductivity

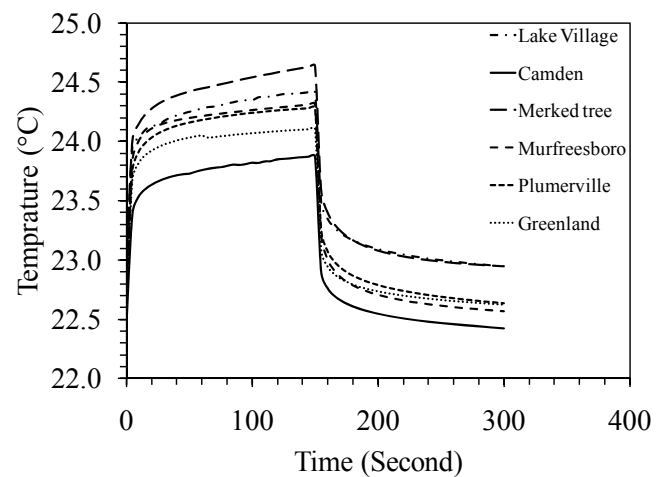


Figure A.20: Changes of temperature of specimens with time during thermal needle testing for the soils from different sites

Table A.3: Thermal conductivity values measured for the soils from different sites

Site	$\lambda$ W/(m·K)	Initial test temperature °C
Greenland	2.770	22.61
Plumerville	1.973	22.67
Malvern	2.010	22.50
Murfreesboro	2.131	22.71
Camden	2.039	22.42
Lake Village	1.644	22.89
Marked tree	1.539	22.91

## B. WEATHER DATA FOR FOCUS SITES IN ARKANSAS

### B.1 Weather Data Overview

The weather data used in the EICM and VADOSE/W includes the maximum, mean, and minimum daily values of temperature, relative humidity, barometric pressure, and mean daily values of windspeed, percent sunshine, and precipitation. This data was obtained from an online weather database ([www.wunderground.com](http://www.wunderground.com)), populated from publically available weather stations. The weather stations for each of the sites and the distance from the sites are summarized in Table B.1.

Table B.1: Weather stations used to collect weather data for the different sites

Site	Weather station	Distance (miles)
Greenland	Fayetteville airport	5.2
Plumerville	Plumerville	2.5
Malvern	Little Rock	52
Murfreesboro	DeQueen	37
Camden	Camden airport	6
Lake Village	Greenville, MI	15
Marked Tree	Jonesboro	31

The weather data for all of the sites from January 2005 to June 2010 are shown in Figures B.1 through B.7. A summary of the annual weather data for each of the sites is summarized in Table B.1. The sites are all relatively similar in an average sense, although it is clear that the northern soils have a slightly lower temperature. All of the sites have relatively high amounts of precipitation, with Camden having the lowest amount.

Table B.2: Summary weather information for the different sites in Arkansas

Site	Temperature (°C)			Relative humidity (%)			Average daily precipitation
	Max	Mean	Min	Max	Mean	Min	
Greenland	20.1	14.0	7.9	91.7	71.4	46.8	0.30
Plumerville	22.1	15.7	9.4	92.8	71.8	45.4	0.33
Malvern	22.7	17.1	11.3	86.7	66.2	45.2	0.37
Murfreesboro	23.5	16.8	10.1	93.7	70.2	46.0	0.28
Camden	21.8	16.2	10.4	98.0	77.7	52.5	0.07
Lake Village	23.3	17.6	11.7	89.9	69.9	48.0	0.32
Marked Tree	21.2	15.7	10.1	89.1	69.2	48.3	0.35

**B.2 Weather data**

**B.2.1 Greenland**

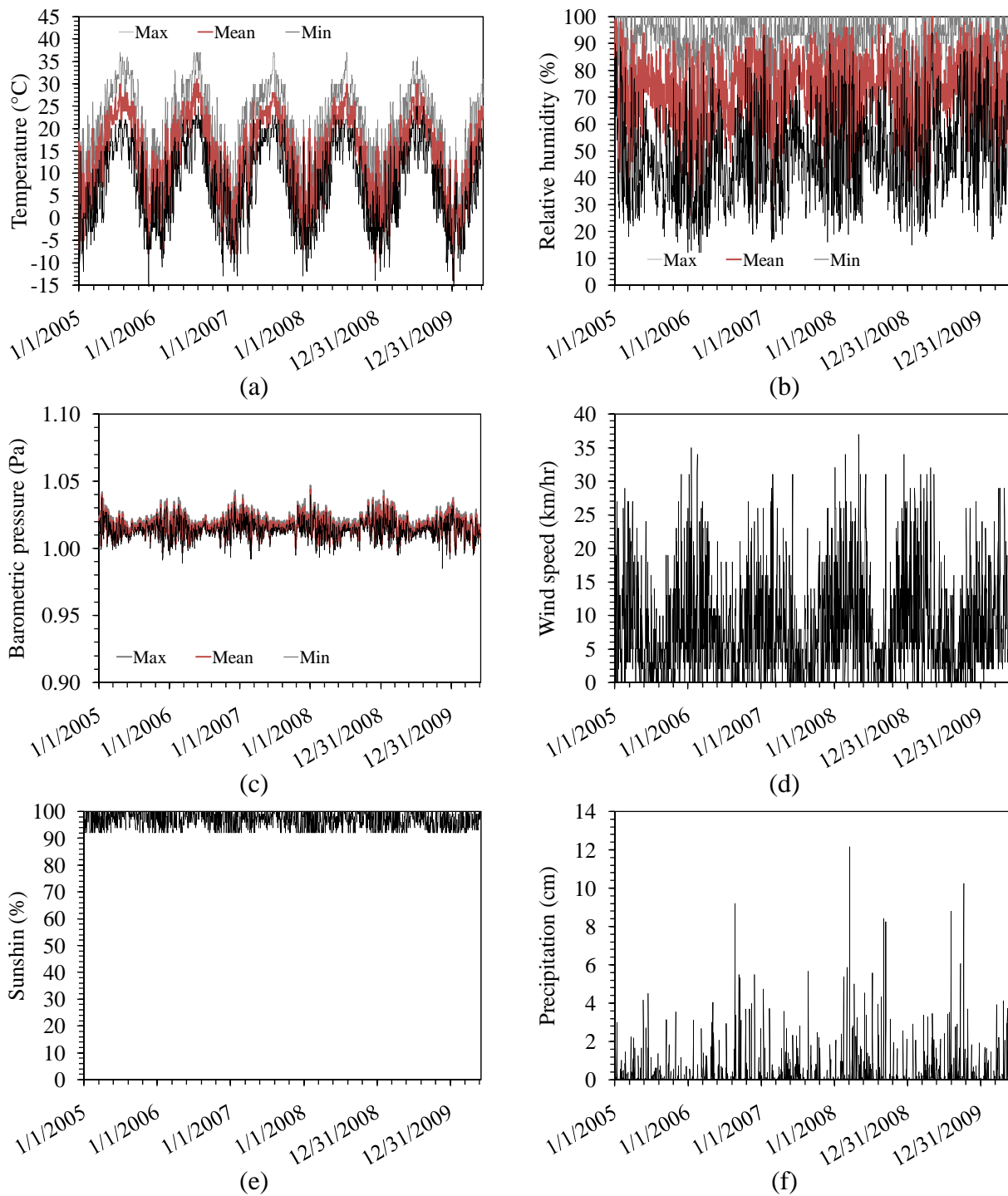


Figure B.1: Weather data for Greenland

**B.2.2 Plumerville**

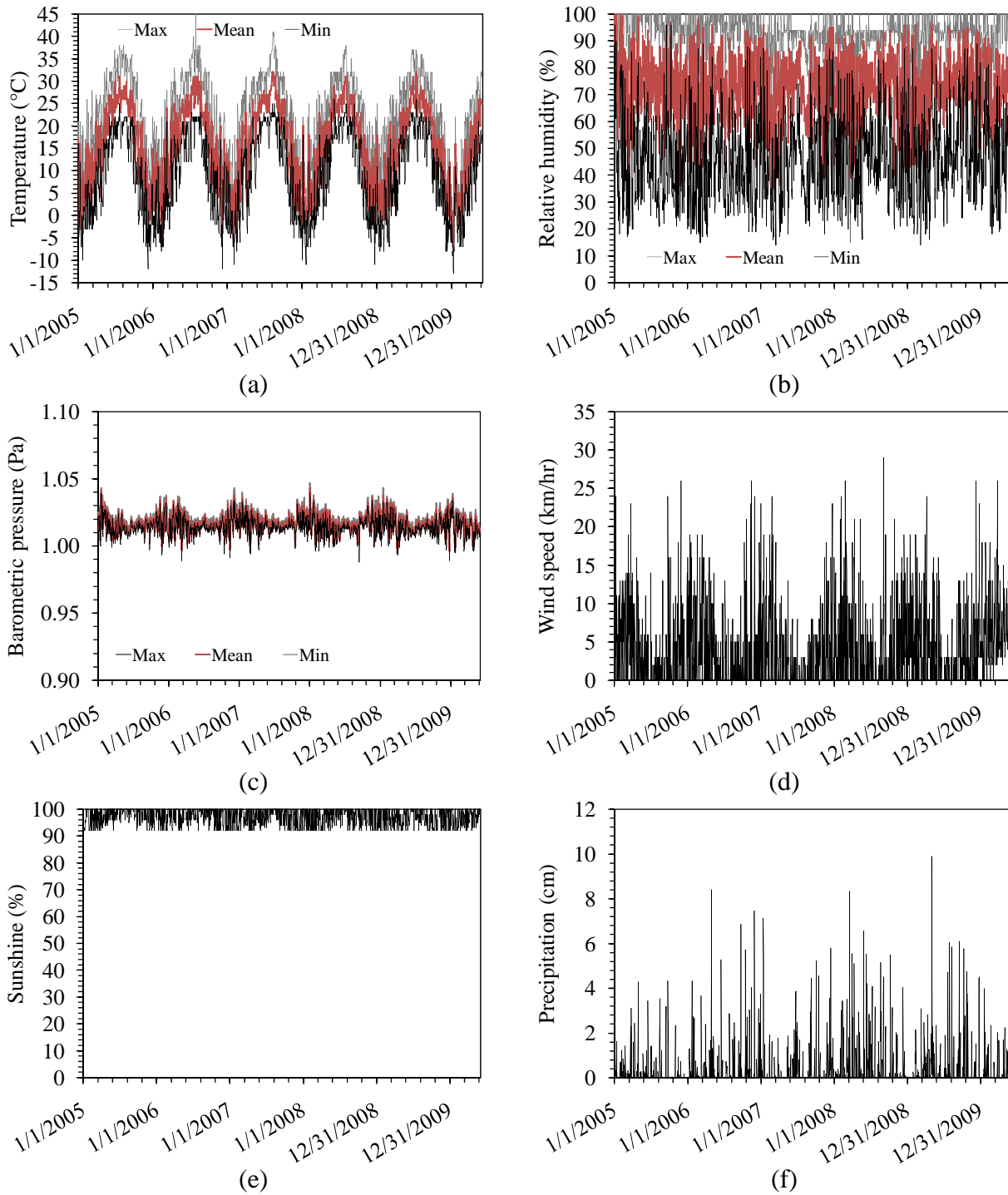


Figure B.2: Weather data for Plumerville

**B.2.3 Malvern**

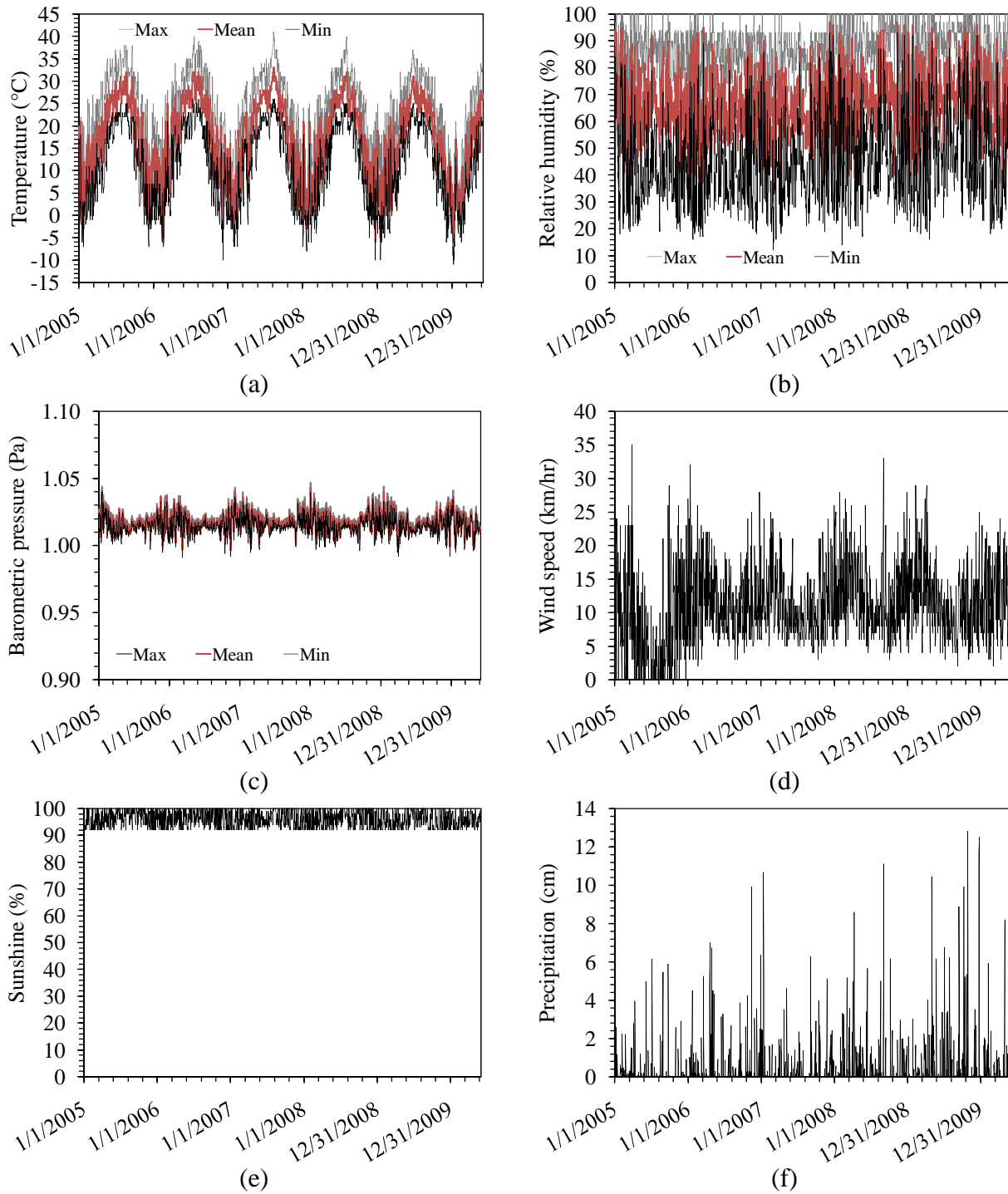


Figure B.3: Weather data for Malvern



**B.2.4 Murfreesboro**

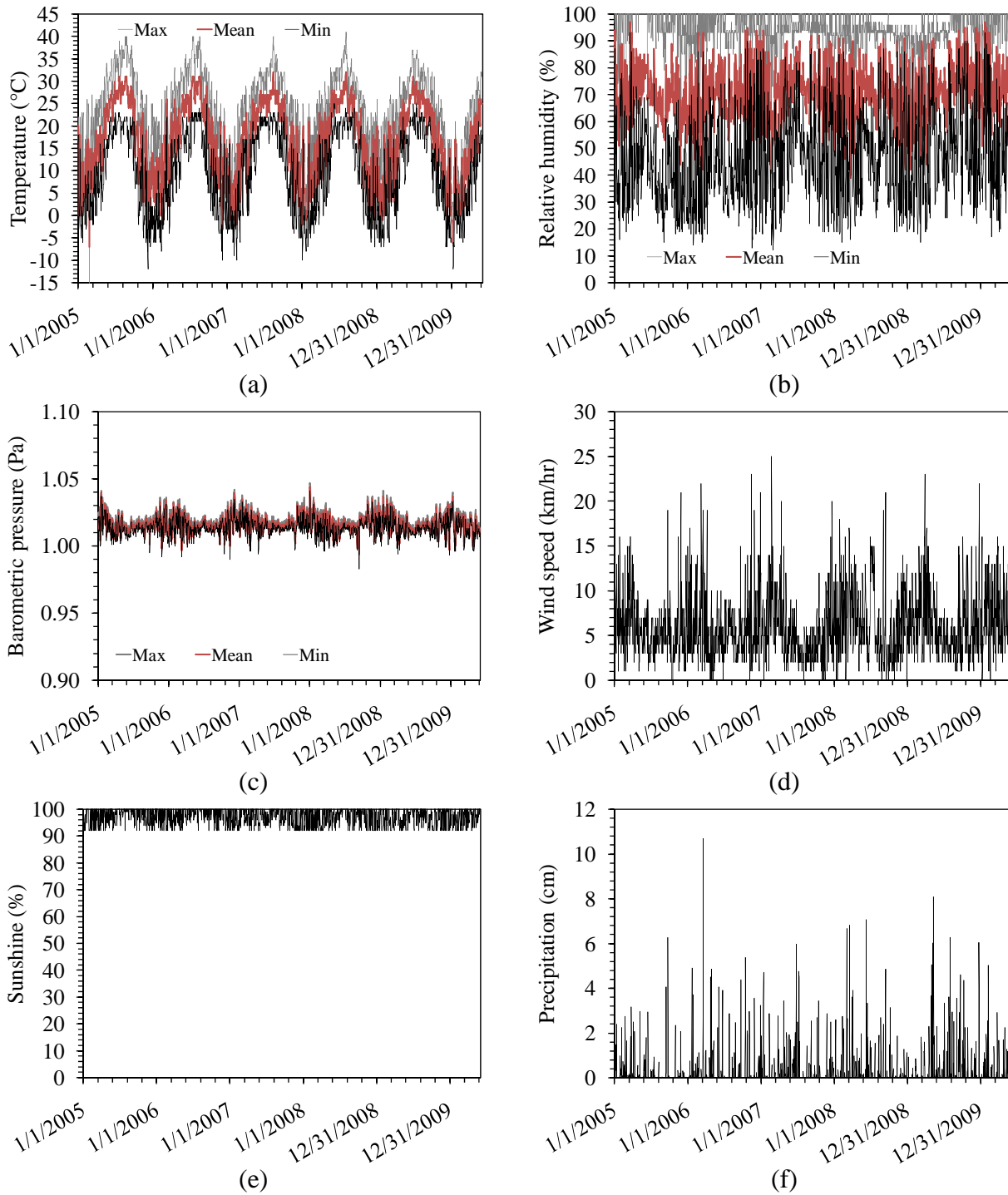
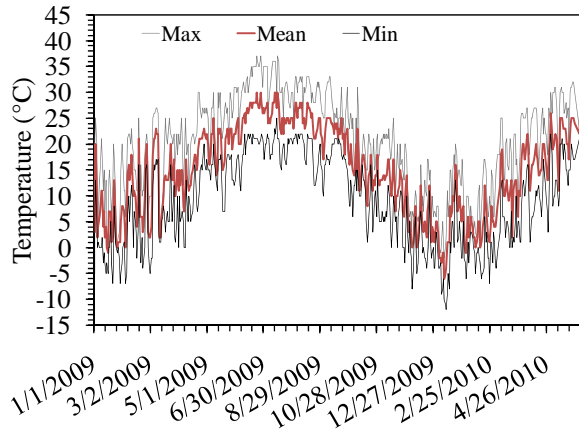
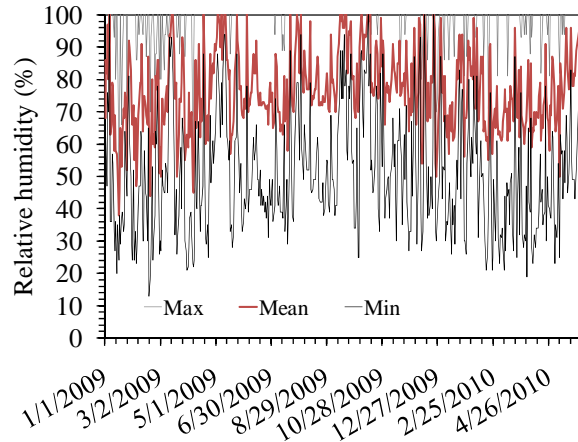


Figure B.4: Weather data for Murfreesboro

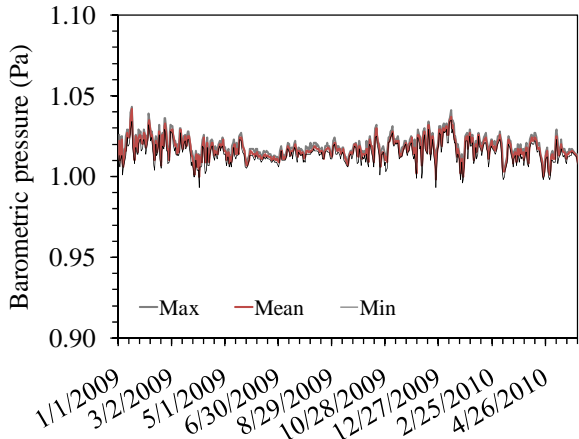
**B.2.5 Camden**



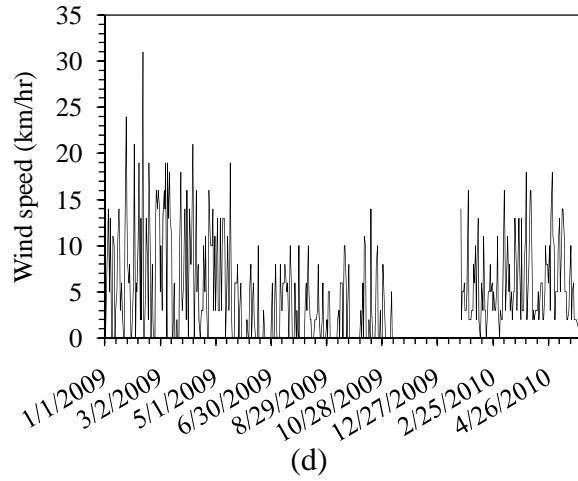
(a)



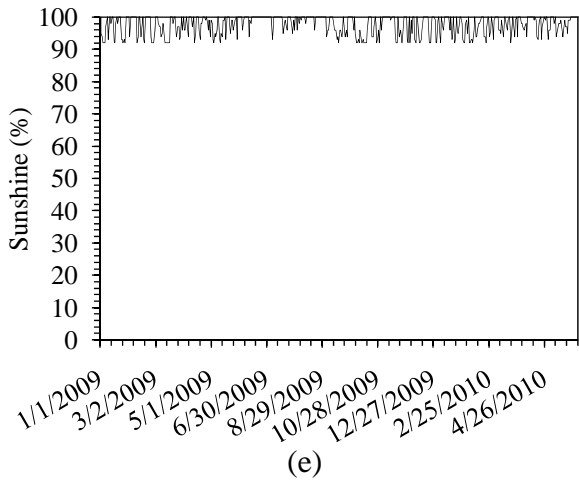
(b)



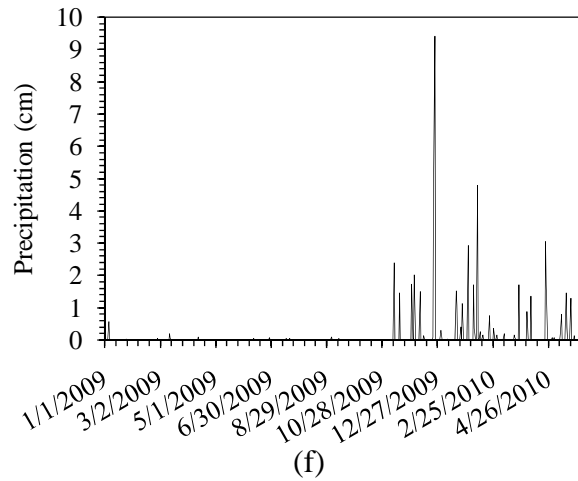
(c)



(d)



(e)



(f)

Figure B.3: Weather data for Camden

B.2.6 Lake Village

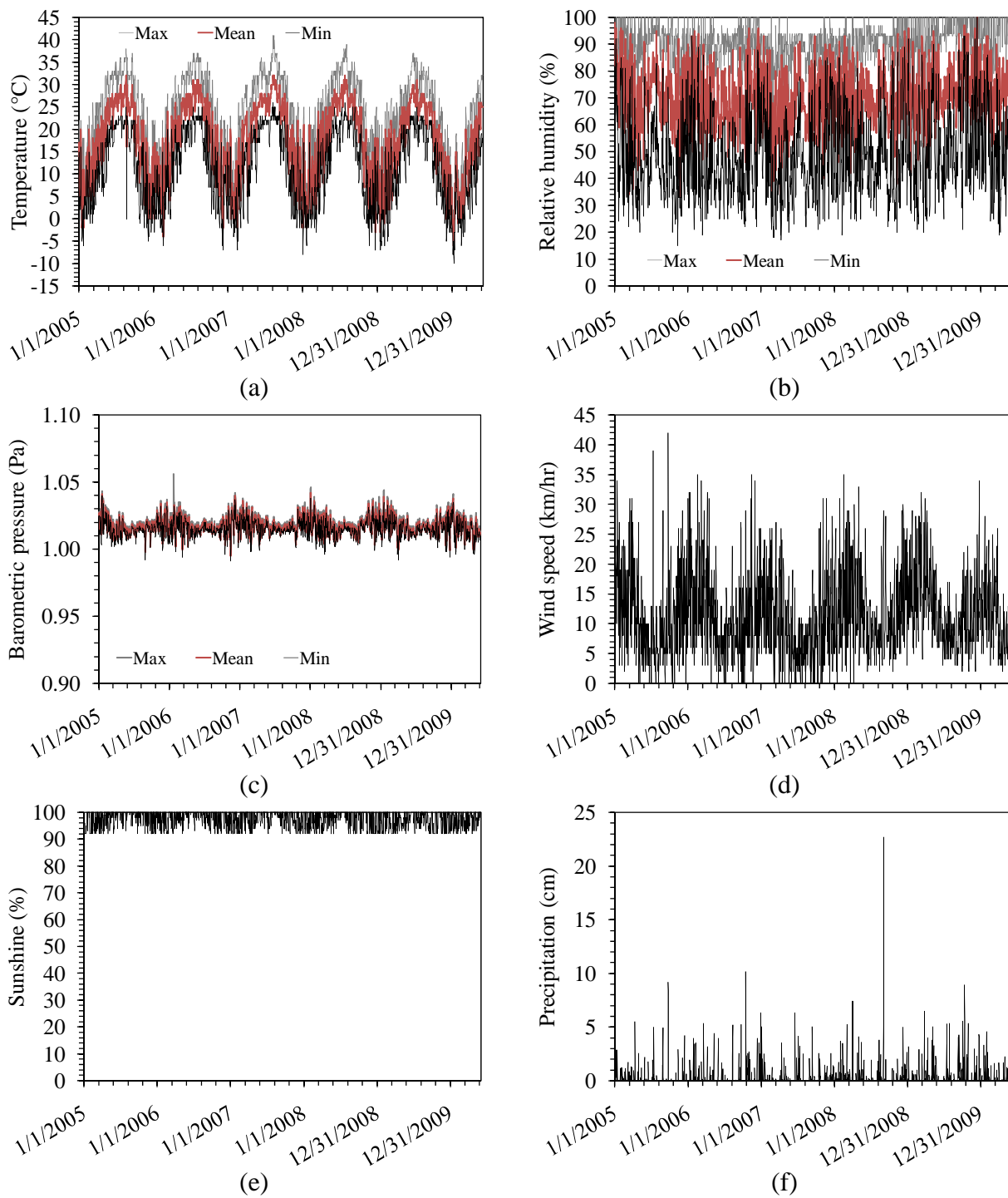


Figure B.6: Weather data for Lake Village

**B.2.7 Marked Tree**

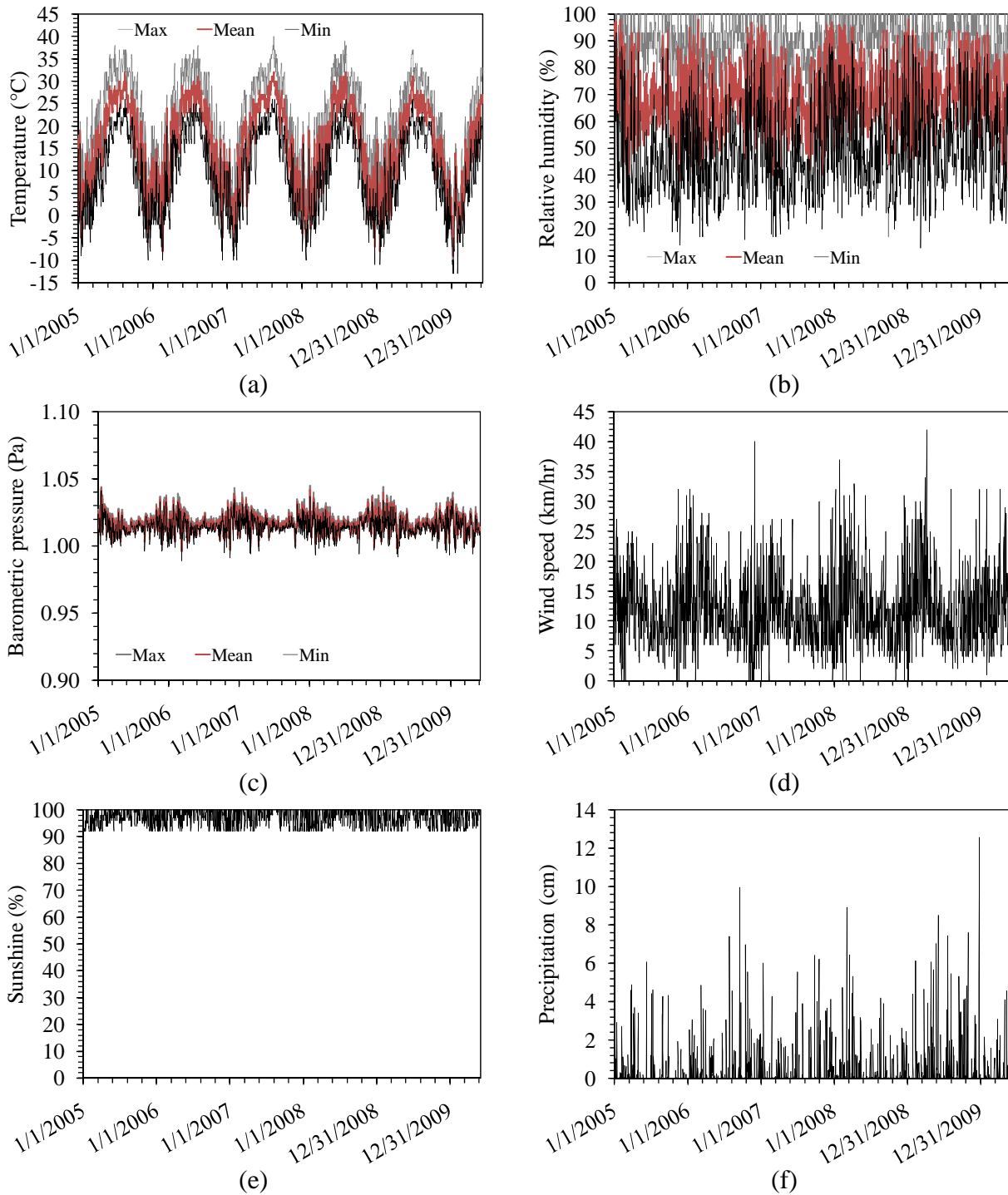


Figure B.7: Weather data for Marked Tree

## C. GENERAL CONCEPTS OF WATER AND HEAT FLOW IN SOILS

### C.1 Flow of Water in Soils

This chapter includes a review of the governing equations for water and heat flow in pavement materials. These equations are implemented into both EICM and VADOSE/W. The main difference between these programs is in how the atmospheric boundary conditions are implemented into their analysis. More information on boundary conditions for the EICM can be found in Appendix D.

In this report, water content refers to the volumetric amount of water in a soil (volume of water divided by the total volume of the soil). The volumetric water content ( $\theta$ ) is different from the gravimetric water content ( $w$ ), which refers to the amount of water in the soil on a mass basis (mass of water divided by mass of solids). The volumetric water content is equal to the product of the gravimetric water content and the ratio of the dry density to the density of water. The maximum value of the volumetric water content is the porosity (the volume of voids divided by the total volume). Phenomena such as pumping, faulting, and spalling are more apt to occur when the soil is close to saturation (when the volumetric water content is close to the porosity). The stiffness of unsaturated soils is greater than that of water-saturated or dry soils due to capillarity (Qian et al. 1990).

Water can flow into the pavement system by infiltration during precipitation or flooding events, an increase in the level of the groundwater table, or due to a malfunctioning drainage system. Due to the negative effects of water mentioned above, if water enters the pavement system it is critical that it be removed from the pavement system via the drainage system. Water flow through pavement materials can occur in either liquid or vapor form. Liquid water flow is important to consider for soils with relatively high permeability (compacted aggregate base, silt or sand subgrade soils), while vapor flow is important for soils with low permeability (clay subgrade soils).

Liquid water flow through soils is described by Darcy's law. Darcy's law represents the relationship between the rate of water flow through soil and the gradient in total hydraulic head. For one-dimensional vertical flow in the  $z$ -direction, Darcy's law is defined as:

$$(C.1) \quad q = -K \frac{\partial H}{\partial z}$$

where  $q$  is the flux density of water (m/s),  $K$  is the hydraulic conductivity (m/s),  $z$  is the length coordinate (m), and  $H$  is the total hydraulic head (m). Combination of Darcy's law with the continuity equation ( $\partial\theta/\partial t = -\partial q/\partial z$ ) yields the governing equation for one-dimensional flow of water in the  $z$ -direction.

$$(C.2) \quad \frac{\partial\theta}{\partial t} = \frac{\partial}{\partial z} \left( K \left( \frac{\partial H_p}{\partial z} + 1 \right) \right)$$

where  $t$  is time and  $H_p$  is the water pressure head (equal to the negative of the matric suction head).  $\partial\theta/\partial t$  can be replaced by  $C(H_p)(\partial h/\partial t)$ , where  $C(H_p)$  represents the slope of the relationship between  $q$  and  $H_p$  ( $\partial\theta/\partial H_p$ ), which is referred to as the Soil-Water Retention Curve. Equation (C.2) can be written as:

$$(C.3) \quad C(H_p) \frac{\partial H_p}{\partial t} = -\frac{\partial}{\partial z} \left( K \left( \frac{\partial H_p}{\partial z} + 1 \right) \right)$$

Water flow through soils in vapor form is described by Fick's law, defined as follows:

$$(C.4) \quad q_v = -\frac{D}{\rho_w} \frac{\partial \rho_v}{\partial z}$$

where  $q_v$  is the flux density of water vapor,  $D$  is the vapor diffusivity,  $\rho_w$  is the density of water, and  $\rho_v$  is the vapor density. When applied to soils, adjustments must be made to account for the meandering path available for flow. The common adjustments applied are included by writing the diffusivity term as:

$$(C.5) \quad D = \alpha(\theta_s - \theta)D_a$$

where  $\alpha$  is a factor to account for the tortuosity of the flow path,  $\theta_s$  is the saturated water content, and  $D_a$  is the diffusivity of water vapor in air. Inserting Equation (C.5) into Equation (C.4), and using the chain rule to account for changes in vapor pressure with temperature, leads to a modified version of Fick's law:

$$(C.6) \quad q_v = -\frac{D}{\rho_w} \frac{\partial \rho_v}{\partial H_p} \frac{\partial H_p}{\partial z} - \frac{D}{\rho_w} \frac{\partial \rho_v}{\partial T} \frac{\partial T}{\partial z}$$

where  $T$  is temperature. Many researchers propose that vapor is transported through the liquid phase by condensation and evaporation in each pore. These phenomena led some researchers to implement an enhancement factor " $\eta$ " (Philip and de Vries 1957). Implementing  $\eta$  into the second term in Equation 6, leads to the modified equation:

$$(C.7) \quad q_v = -\frac{D}{\rho_w} \frac{\partial \rho_v}{\partial H_p} \frac{\partial H_p}{\partial z} - \frac{D}{\rho_w} \eta \frac{\partial \rho_v}{\partial T} \frac{\partial T}{\partial z}$$

Also, the vapor density can be defined as the product of the saturated vapor density ( $\rho_{vs}$ ) and the relative humidity ( $H_r$ ), leading to the following equation:

$$(C.8) \quad q_v = -\frac{D}{\rho_w} \frac{\partial(\rho_{vs}H_r)}{\partial H_p} \frac{\partial H_p}{\partial z} - \frac{D}{\rho_w} \eta \frac{\partial(\rho_{vs}H_r)}{\partial T} \frac{\partial T}{\partial z}$$

The relative humidity and water pressure head are related as follows:

$$(C.9) \quad H_r = \exp \left[ -H_p \frac{MG}{RT} \right]$$

Incorporating Equation (C.9) into Equation (C.8) leads to the following equation for the flow of vapor in soils:

$$(C.10) \quad q_v = -\frac{D}{\rho_w} \rho_{vs} \frac{Mg}{RT} H_r \frac{\partial H_p}{\partial z} - \frac{D}{\rho_w} \eta H_r \frac{\partial \rho_{vs}}{\partial T} \frac{\partial T}{\partial z}$$

where  $\rho_{vs}$  is the saturated vapor density ( $\rho_{vs} = \rho_v/H_r$ ),  $H_r$  is the relative humidity,  $M$  is the molecular weight of water,  $g$  is the gravitational constant,  $R$  is the universal gas constant, and  $\eta$  is an enhancement factor. This relationship accounts for the effect of temperature gradients and enhanced vapor diffusion. The first term in the law is referred to as the isothermal vapor flux density ( $q_{vh}$ ). The second term is referred to as the thermal vapor flux density ( $q_{vT}$ ). These two terms are similar to the liquid flow equation and some of the parameters can be combined to form the conductivity equations.

$$(C.11) \quad K_{vh} = \frac{D\rho_{vs}Mg}{\rho_w RT} H_r$$

and

$$(C.12) \quad K_{vT} = \frac{D\eta H_r}{\rho_w} \frac{\partial \rho_{vs}}{\partial T}$$

where  $K_{vh}$  is the isothermal vapor conductivity and  $K_{vT}$  is the thermal vapor conductivity. The final form of the equation representing coupled water flow (liquid and vapor) can be written as:

$$(C.13) \quad C(h) \frac{\partial h}{\partial t} = -\frac{\partial}{\partial z} \left( K_t(h) \frac{\partial h}{\partial z} + K_L(h) + q_{vT} \right)$$

where  $K_t = K_L + K_{vh}$  and  $K_t$  is the total hydraulic conductivity.

## C.2 Flow of Heat in Soils

Temperature links environmental effects on bound and unbound layers. The temperature is the cause of the resilient modulus drastically changing during freeze-thaw and also the resilient

modulus of the asphalt is reduced in hot temperatures. The effects of temperature change are evident in thermal cracking and rutting. The types of heat transfer include conduction, and latent heat. Conduction is the transfer of heat through physical contact. Latent heat includes the effects of temperature change due to the vapor and liquid flow. The heat conduction equation is given as:

$$(C.14) \quad q_{h1} = -K_h \frac{\partial T}{\partial z}$$

where  $q_h$  is the heat flux density and  $K_h$  is the thermal conductivity. The latent heat can be calculated from the vapor and water sections of this report where  $q_v$  is calculated. This equation is given by:

$$(C.15) \quad q_{h2} = -L_0 q_v + C_{hv}(T - T_0)q_v + C_{hw}(T - T_0)q_L$$

where  $L_0$  is the volumetric latent heat of vaporization,  $q_v$  is the flux density of water vapor,  $C$  is the volumetric heat capacities,  $T$  is temperature, and  $q_L$  is the flux density of water. The combination of conduction and latent heat is described by the following equation:

$$(C.16) \quad q_h = -K_h \frac{\partial T}{\partial z} + L_0 q_v + C_{hv}(T - T_0)q_v + C_{hw}(T - T_0)q_L$$

The boundary conditions used to solve these different equations in the EICM are described in Appendix D.



## **D. EICM THEORY MANUAL**

### **D.1 EICM Overview**

The EICM model version 3.4, developed by the Applied Research Associates (ARA) lab at the University of Illinois under Dr. Gregg Larson, was used in this study (ara-tracker.com). The EICM claims accuracies in the area of predicting water and thermal flow through porous media under asphalts. The program computes pore pressure, water content, temperature, and frost depth by solving governing equation in a minor amount of time. A full year with a large amount of nodes (20) can be modeled very quickly (less than a minute). Along with these computations, the software predicts whether or not the subgrade and design are acceptable. The speed of these rapid computations can be contributed to simplifications within the program. A large simplification the program assumes is that there is no flow of water in the vapor form. This assumption is not realistic and inflicts error, but the time saved is large. Computations made are based on the soil-water retention curves (SWRC) and the permeability functions of the soil. Using the SWRCs and permeability functions, the software performs a semi-accurate set of computations.

The original version of the EICM was developed at Texas A&M University and the Texas Transportation Institute in 1989 combining the Climatic/Materials/Structures (CMS) model, Infiltration and Drainage (ID) Model, CRREL Frost Heave and Thaw Settlement Model, and a rainfall precipitation model (PRECIP). Each sub-model was analyzed in this study, and the inputs and outputs were reviewed. Each submodel in the EICM includes computations involving different layers of the pavement. The typical layers of the pavement are the asphalt, base, subbase, and subgrade. The subbase layer is often not incorporated in new pavements, but can be an important layer in rehabilitated pavements. The individual layers which are involved in computations by the submodels in the EICM are summarized by Table 1. The Precipitation submodel, which was used to develop a set of climate data for a given site, is no longer used in the EICM and is not shown in Figure 1. Instead, historical databases of actual weather data from different sites throughout the country are incorporated into the EICM calculations as part of the ID model. This hourly climatic data can be downloaded and incorporated into the user input climatic section of the program.

Table D.1: Summary of the pavement layers involved in individual submodel calculations

	ABOVE FREEZING		BELOW FREEZING	
	WATER	TEMPERATURE	WATER	TEMPERATURE
ASPHALT	USER INPUT	CMS	0	CMS
BASE	ID	CRREL	CRREL	CRREL
SUBBASE	CRREL	CRREL	CRREL	CRREL
SUBGRADE	CRREL	CRREL	CRREL	CRREL

## D.2 Infiltration and Drainage (ID) Model

The ID model is used by the EICM for several functions. These functions include drainability and infiltration. For the drainage analysis, a numerical technique is used to compute the time to drain an initially saturated base (Larson and Dempsey 1997). In this technique, water is able to freely drain from the base course by gravity to a relatively low degree of saturation. The time for gravity drainage of an initially saturated base course was initially calculated from the work of Casagrande and Shannon (1951), and was further developed by Liu, et al. (1983). Based on this analysis, if the water content remains at a degree of saturation of 0.85 or greater for more than 5 hours, the base course is considered a marginal base for design purposes (EICM help). Further, if the water content remains at a degree of saturation of 0.85 or greater for more than 10 hours, the base course is not suitable for use in pavements.

The infiltration analysis in the ID model uses Ridgeway's model or the Dempsey-Robnett model based on the information input to the EICM. Each analysis assumes an infiltration rate to compute the degree of saturation in the base course layer. The degree of saturation in the base course is used to calculate the head applied to the top of the subgrade layer in the drainage analysis. Lytton et al. (1993) recommends that the Thornthwaite Water Index (TMI) should be used to estimate the degree of saturation in the base course over time for domains where the

groundwater table in the subgrade has a depth greater than 25 ft below the pavement surface. If the TMI model is used in the EICM, the ID model is not used. The TMI model uses a time-dependent empirical factor related to the variation in climate for different zones of the country to calculate the average degree of saturation in the base course layer. Due to the empirical nature of the TMI approach, it can lead to greater uncertainty than the ID model. Specifically, the entire state of Arkansas is grouped into a single TMI zone.

When performing the drainability of the base course, the ID model uses a numerical technique to compute the degree of drainage (drained area / total area in percent) versus time of an initially saturated granular base course with lateral drainage (Lytton et al. 1993)(which assumes the drainage as a two dimensional problem). The analysis of infiltration includes a three-step process to calculate the degree of saturation (or water content) in the base. First, the equilibrium suction profile is determined by assuming hydrostatic conditions, with a water table located at a user defined depth. Next, the shape of the soil-water retention curve is estimated using empirical equations. Finally, the water contents in the base course layer are computed from the SWRD.

There are two options for calculating the degree of saturation in the base course: (a) Ridgeway's model; or (b) the Dempsey-Robnett model. Both of these programs use historic weather records involving precipitation and duration. Ridgeway's model is activated in the program by inputting a number for linear cracks in the pavement. The amount input is irrelevant to the program. Inputting the number 0 for linear cracks will activate the Dempsey-Robnett model. The two programs are described below. The ID model currently estimates the increase in water content of the base course layer based on how much water is entering the base, how fast the base is draining, and how much storage capacity the base has above hydrostatic conditions.

Ridgeway's model assumes water to infiltrate into the base course layer at a rate of 0.1 ft<sup>3</sup>/hr for bituminous pavements and 0.03 ft<sup>3</sup>/hr for PCC pavements. This model calculates the amount of water in the base course based on the volume of rainfall entering the base course layer. The rainfall volume is computed in Ridgeway's model as follows:

$$(D.1) \quad R = k(t_R)^{1-n} t_p^x / SF$$

where R is the volume of rainfall in inches,  $t_R$  is the duration of rainfall in minutes,  $t_p$  is the return period of the storm, k, n, and x are empirical constants, and SF is a shape factor which describes the intensity of a rainfall event. The values of k, n, x, and SF are assumed to be 0.25,

0.75, 0.3, and 1.65 in the ID model, and cannot be changed by a user. These values are assumed to be “appropriate” for the eastern United States. Additional values for these variables are provided in the American Society of Civil Engineers (ASCE) Hydrology Handbook.

The Dempsey-Robnett model does not require a length of cracks in order to estimate the increase in the volume of water in the base course layer. In order to use this model the user must input 0’ for length of cracks on pavement. Dempsey and Robnett (1979) developed empirical equations by measuring the volume of flow through drainage layers for rainfall events having a different intensity and duration. The volume of water entering the base course is estimated using this model as follows:

$$(D.2) \quad R = 0.48PV + 0.32$$

where R is the outflow volume in inches and PV is the precipitation volume in inches. The amount of drainage in the base course is calculated from the degree of saturation. The degree of saturation is represented as follows:

$$(D.3) \quad S_r = 1 - (PD)U$$

where  $S_r$  is the degree of saturation, PD is an index representing the ability of a certain base course to drain water, and U is the decrease in the degree of saturation due to drainage. The ID model uses the information in Table 2 to estimate the value of PD for a given soil.

Table D.2: PD values used by the ID model

Amount of Fines	<2.5%			5%			10%		
	Inert Filler	Silt	Clay	Inert Filler	Silt	Clay	Inert Filler	Silt	Clay
Gravel	70	60	40	60	40	20	40	30	10
Sand	57	50	35	50	35	15	25	18	8

### D.3 Climatic/Materials/Structure (CMS) Model

Temperatures in the asphalt layer of the pavement system are calculated using the CMS model. The upper boundary condition in the program is calculated using the equation proposed by Dempsey (1985). The CMS model only calculates temperatures in the asphalt layer.

The one dimensional heat conduction equation is used to changes in temperature of the asphalt layer over time. The heat conduction equation (Fourier's law) is given as follows:

$$(D.4) \quad \frac{\partial^2 T}{\partial z^2} = \frac{1}{\alpha} \frac{\partial T}{\partial t}$$

where  $T$  is the temperature and  $\alpha$  is the thermal diffusivity.  $\alpha$  is equal to  $\lambda C / \gamma_d$  where  $\lambda$  is the thermal conductivity,  $C$  is the mass specific heat, and  $\gamma_d$  is the dry density. The CMS model solves the heat conduction equation using the finite difference solution as follows:

$$(D.5) \quad T_{(i,t+\Delta t)} = T_{(i,t)} \frac{K \Delta T}{\gamma_d C} T_{(i+1,t)} + T_{(i-1,t)} - 2T_{(i,t)}$$

The boundary conditions required to solve this equation are the temperatures at the asphalt surface and the temperature at the top of the base layer. More information on the temperature boundary condition can be found in Dempsey et al. (1985).

There is no direct relationship between air temperatures and surface temperatures. For this reason it is very difficult to establish a boundary condition for temperature. Without a proper representation of the temperature, the amount of frost/thaw of water in the layers cannot be determined potentially leading to unexpected failure. The temperature boundary can be obtained through a heat balance:

$$(D.6) \quad 0 = q_i - q_r + q_a - q_e + q_c$$

where  $q_i$  is the incoming short wave radiation,  $q_r$  is the reflected short wave radiation,  $q_a$  is the incoming long wave radiation,  $q_e$  is the outgoing long wave radiation, and  $q_c$  is the sensible or convective heat transfer. The incoming short wave radiation can be estimated using the following equation:

$$(D.7) \quad q_i - q_r = aR \left( A + B \left( \frac{S}{100} \right) \right)$$

where  $a$  is the absorptivity of the pavement surface,  $R$  is the extraterrestrial radiation incident on a horizontal surface (function of latitude, typical found in Paltineanu 2002),  $A$  and  $B$  are constants accounting for diffuse scattering (0.202 and 0.539 respectively for the Midwest), and  $S$  is the percent sunshine. The incoming long-wave radiation can be estimated using the following equation:

$$(D.8) \quad q_a = \sigma T \left\{ G - \frac{J}{10^{(PP)}} \right\}$$

where  $\sigma$  is the Stefan – Boltzmann constant equal to  $1.72 \times 10^{-7}$ ,  $T$  is the temperature of the air,  $G$  is a constant equal to 0.77,  $J$  is a constant equal to 0.28,  $p$  is a constant equal to 0.074, and  $P$  is equal to the vapor pressure of the air. The vapor pressure of the air can be estimated as  $6.1078 \times 10^{7.5 * T / (237.3+T)}$ . The outgoing long wave radiation can be estimated using the following equation:

$$(D.9) \quad q_e = \sigma \epsilon T_s^4$$

where  $\epsilon$  = emissivity,  $T$  = surface temperature. The sensible or convective heat transfer can be estimated using the following equation:

$$(D.10) \quad q_c = H(T_{air} - T_s)$$

where  $H$  can be estimated as:

$$(D.12) \quad 122.93 [0.00144 V_m^{0.3} W_v^{0.7} + 0.00097 (T_s - T_{air})^{0.3}]$$

where  $V_m$  is the average of surface and air temperatures in degrees K and  $W_v$  is the average daily wind velocity in m/s. The lower boundary condition is given by the empirical relationship:

$$(D.13) \quad T = nT_a$$

where  $n$  is the surface type coefficient and  $T_a$  is the air temperature.  $n$  is assumed to be equal to 1 for snow, 0.9 for asphalt, and 0.5 for turf.

#### **D.4 Cold Regions Research and Engineering Labs (CRREL) Model**

The temperatures and water contents in the subbase and subgrade layers are calculated using the Cold Regions Research and Engineering Laboratory (CRREL) model. Unlike the other models, the CRREL model uses a finite element solution to the governing equations for water flow and temperature flow to calculate the changes in temperature and water content with time and space. The governing equation for water flow in unsaturated subgrade soils is referred to as the Richards equation, while the governing equation for temperature flow in soils is referred to as the Fourier equation. To solve the governing equations, boundary conditions are supplied from the CMS and ID models while the user must input initial temperatures and water contents for each node in the finite element analysis. Thermal and hydraulic soil properties are required for each soil strata in order to perform computations. The thermal soil properties include the thermal conductivity and specific heat capacity, while the hydraulic soil properties include the hydraulic conductivity and the Soil Water Retention Curve (SWRC). The SWRC is a curve which relates the degree of saturation (or water content) in the soil with the matric suction.

The CRREL model uses temperatures through the asphalt to compute the temperatures through each soil strata. Along with this the model uses properties of the soil (assumed to be constant) to calculate the water and/or ice content. Calculations are made for each node input by the user for each time step. Calculations are simplified to a great extent in order to reduce calculation time. Simplifications include: all water calculations include liquid phase water flow only, water content is constant with respect to temperature, volume changes are neglected outside of frozen zones, and soil constants are invariant with time (Lytton et al. 1993). For each time step the water content is calculated before the temperature. The differential equations were developed for one dimensional analysis using the general form of the Galerkin method (Guyman et al. 1986). A generalized form of Richards equation and the heat conduction equation can be used to calculate the distribution in total hydraulic head or temperature in the subgrade layer, as follows:

$$(D.14) \quad \frac{d}{dz} \left( k_1 \frac{dc}{dz} \right) - \frac{d}{dz} (k_2 c) - k_3 \left( \frac{dc}{dt} \right) = 0$$

In the case of water flow,  $k_1$  = unsaturated permeability,  $k_2 = 0$ ,  $k_3$  = slope of the soil water retention curve,  $c$  = total hydraulic head. This same equation is also used for temperature flow, but in this case  $k_1$  = thermal conductivity,  $k_2$  heat capacity (water) multiplied by the velocity (a constant),  $k_3$  = heat capacity of soil,  $c$  = temperature

The initial water content is input by the user for each soil. From this, the software calculates the initial suction from the Fredlund-Xing (1994) equation below.

$$(D.15) \quad \theta = C(h) * \frac{\theta_{sat}}{\ln \left( \exp(1) + \left( \frac{h}{a_f} \right)^{b_f} \right)^{c_f}}$$

$$(D.16) \quad C(h) = 1 - \frac{\ln \left( 1 + \frac{h}{h_r} \right)}{\ln \left( 1 + \left( \frac{10^6}{h_r} \right) \right)}$$

where  $h_{rx}$ ,  $a_{fx}$ ,  $b_{fx}$ , and  $c_{fx}$  are parameters used to fit the Fredlund-Xing model to the measured SWRC for a given soil. Although the EICM notes that  $a$  and  $h_r$  are dimensionless, they actually have units of suction (psi for an English unit analysis). This is important to note as most SWRCs are defined using metric units.

The boundary conditions for water flow in the CRREL model depend on the results of the analysis for the base course. Using the ID model gives the option of a flux internal boundary condition or a constant head boundary condition. The selection identifies the base/subgrade interface boundary condition. A constant suction is easier to model but simplifies the calculations within the model. A flux boundary condition would account for precipitation on various days. When the air temperature is below freezing, the CRREL model assumes the upper boundary condition is  $dh/dz = 0$ . This simplification is made by omitting the ID model and using the CRREL model for calculations in the base course. For analysis where the temperature is above freezing, the ID model offers the option of using the TMI, flux, or constant head at the base/subgrade interface. Choosing a constant head will allow for easier computations, however the flux choice will model a more realistic situation. For analysis where the groundwater table is greater than 25 feet deep, the TMI option is recommended in the EICM manual, but the basis for this recommendation has not been fully established.

The flux suction at the interface of base/subgrade layer boundary can be represented using the following equation:

$$(D.17) \quad \frac{dh}{dz} = -r \left( \frac{p}{\gamma} - h_s \right)$$

where  $r$  is the pore pressure transfer coefficient controlled by the permeability values of the soils.  $p/\gamma - h_s$  is the difference in pressure between the base and subgrade. In the case that constant suction at the interface of base/subbase layers boundary condition is assumed, the following equation is used to estimate the boundary suction:

$$(D.18) \quad h = h_n - h_0$$

where  $h_n$  is the negative pore pressure in the base and  $h_0$  is the head corresponding to overburden pressure. The constant suction boundary condition can be determined from the infiltration data from the equation given by Lytton (1993) as follows:

$$(D.19) \quad \theta = \frac{n}{(1 + A_w \text{abs}(h)^a)}$$

Rearranging this equation for  $h$  yields the lower boundary condition, as follows:

$$(D.20) \quad h = \left[ \frac{\frac{n}{\theta} - 1}{A_w} \right]^{\frac{1}{a}}$$



where  $A_w$  and  $a$  are constants from the SWRC curve and  $n$  is the porosity of the subgrade. If the Thornthwaite Water Index is used in the ID model, the boundary conditions are implemented at several depths. The program will automatically assume a subbase layer if the user does not input the layer. This implementation yields the boundary conditions as follows:

The base/subbase interface boundary condition can be defined in the TMI method as follows:

$$(D.21) \quad h = \alpha \left[ \exp \left[ \frac{\beta}{TMI + 101 + \gamma} \right] + \partial \right]$$

The subbase/subgrade interface boundary condition can be defined in the TMI method as:

$$(D.22) \quad h = \alpha + \exp[\beta + \gamma(TMI + 101)]$$

The boundary condition at the groundwater table is defined as  $h = 0$ . For temperature flow, the upper boundary condition is given by the empirical relationship  $T = nT_a$ , where  $n$  is the surface type coefficient and  $T_a$  is the air temperature. As mentioned,  $n$  is assumed to be 1 for snow, 0.9 for asphalt, and 0.5 for turf. The lower boundary condition is input by the user as the lowest node temperature, and is recommended to be equal to the mean yearly temperature.

### 3.4 SUMMARY OF BOUNDARY CONDITIONS

The boundary conditions used in the different models are summarized in Table 3.

Table 3: Boundary conditions in the different submodels.

	WATER			TEMPERATURE
	ID MODEL		TMI	
ASPHALT	USER INPUT (0 WATER BELOW FREEZING)			$dt/dz = T_s$  CMS
BAS	FLUX	CONSTANT	TMI	$T = nT_a$
SUBBASE	$dh/dz = -r$ $(p/\gamma - h_s)$  (dh/dz = 0 BELOW FREEZING)	$h = [(n/\theta - 1)/A_w]^{1/a}$	$h =$ $\alpha[e[\beta/(TMI+101+\gamma)] + \partial]$	CRREL
SUBGRADE	CRREL		$h =$ $\alpha[e[\beta/(TMI+101+\gamma)] + \partial]$	
	h=0	h=0	h=0	$T = T_{avg}$

## E. EICM USER'S GUIDE

The following set of steps in this user's guide can be followed to execute an analysis in the EICM model. Under options, there are two important settings which should be set before starting: units and time (hourly or daily). It is recommended to use the EICM in English units, because there are several inconsistencies in the labeled units when metric units are selected. Further, it is recommended to use an hourly analysis, even when only daily weather data is available. This EICM was not able to run with daily data. Hourly data can be obtained from daily data by assuming that the weather throughout the day is the same for each hour. This will lead to short-term inaccuracies in the model results, but it will lead to reliable seasonal trends. The seasonal trends are more important for making decisions for pavement performance evaluation. To insert layers first click "Edit-Add Layer", select Layer 0 on the left side of the window, and the material to be added on the right side, as shown in Figure E.1.

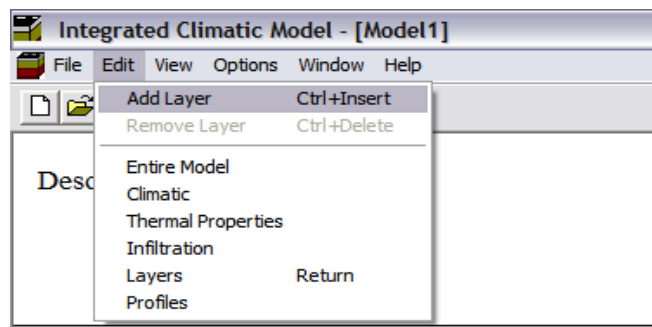


Figure E.1: Step 1 - Enter layers

The top layer of the profile must either be a PCC or Asphalt pavement. Soil materials may not be used for the top layer. Only one asphalt layer may be included in a pavement profile. Although only one PCC layer may be included in a pavement profile, a pavement profile may have a PCC layer with an Asphalt overlay. To select a new layer, click on the highest layer number in the window on the left, and then click the next layer on the right, as shown in Figure E.2. In other words, after the asphalt layer is added, select it in the window on the left, then click the base course in the window on the right.

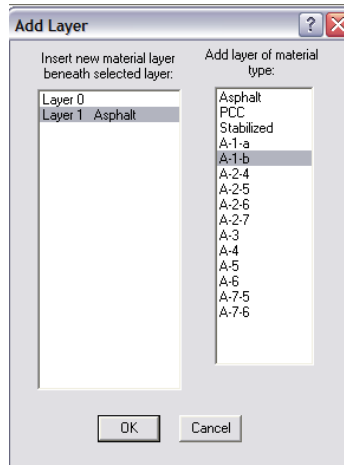
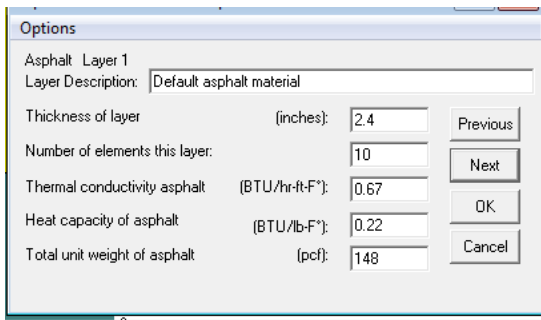
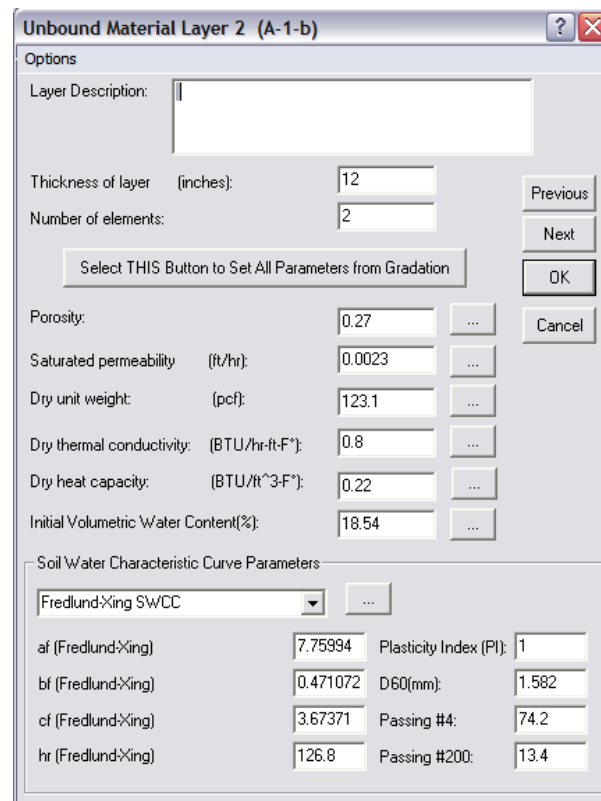


Figure E.2: Adding a base course layer

After each layer is selected from the list in Figure E.2, a window asking for the material properties and layer geometry appears, as shown in Figure E.3. There are different windows for asphalt and soils.



(a)



(b)

Figure E.3: Layer property input windows for: (a) Asphalt; (b) Soils

An important item which is asked in these layer property input windows are the number of nodes. The maximum number of layers allowed in a pavement profile is 30. After each layer is

added, the software will ask for properties of the layer. One of the important things that is asked is the number of nodes per layer. The maximum number of nodes per layer is 100, while the maximum number of nodes for the entire model is 300. If more nodes are selected by a user, the analysis will be more accurate. Although more nodes implies that the program will run more slowly, this is not a significant issue as most EICM runs require 5 minutes or less. If there are not enough nodes, then the output from the model will be too coarse, and will look choppy. The minimum element size (i.e., length of layer divided by the number of elements in the layer) depends on the layer. More elements are allowed in the asphalt than in the soil layers. In the soils, a minimum element spacing of 1 inch is allowed.

For the depth of the subgrade, the model recommends that the profile extend at least to a depth of 240 inches, even if the water table is above this level. This is because the temperature at a site often varies up to the depth. Because the EICM assumes that the temperature at the bottom of the soil profile is constant, a shallow profile may distort the predicted temperature profiles.

The material properties inserted into the layer property windows are typically obtained from site-specific measurements made as part of the pavement design. However, the EICM also provides default values for use as a starting point. In this study, default values were used for all of the model inputs except those related to the soils, weather, geometry, and analysis details (number of elements, time increments, etc).

The major material properties that should be selected are the hydraulic and thermal properties of the soil. The hydraulic conductivity of the base is required to be greater than that of the underlying subgrade. The Soil-Water Retention Curve (SWRC) parameters are by default defined using the Fredlund-Xing (1994) model. It is advised to use this equation because the EICM includes empirical equations to estimate the SWRC parameters from easy to determine index properties (grain size distribution or Atterberg limits).

After the material properties are inputted into each of the screen, the initialization window should be opened as shown in Figure E.4.

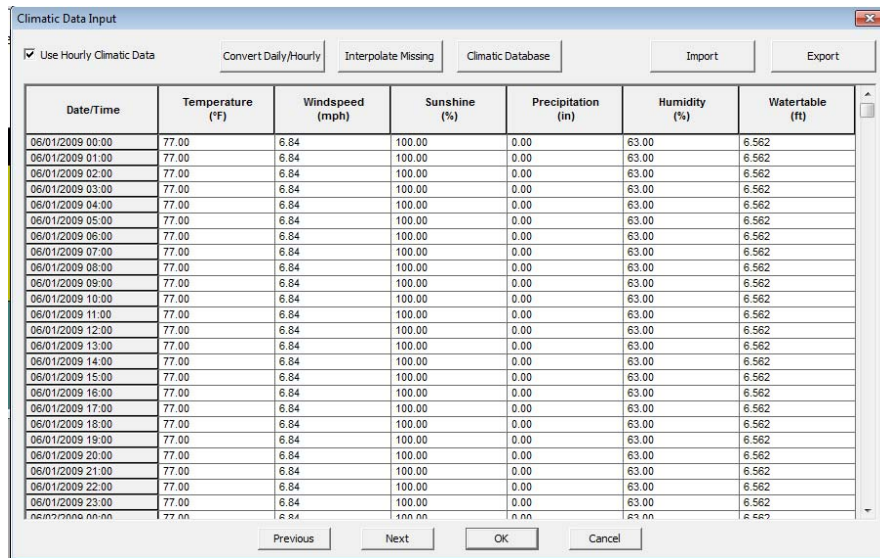


Figure E.4: Step 2 - Click “Edit-Entire Model”

Clicking this button opens the model initialization window, as shown in Figure E.5. The EICM is only capable of running an analysis for a period of one year. However, the EICM can start the analysis from any day of the year. The program recommends starting any analysis on the first day of a month because it provides a monthly weather summary as one of the outputs. The starting time should usually be before the period of interest. The maximum time increment for the output data is every 6 hours. This limit is recommended when performing an annual evaluation. The calculations time increment is recommended to be as small as possible (0.01 hours) to improve the accuracy of the output results. The latitude, longitude, and elevation are associated with a model component which has not yet been implemented in the EICM.

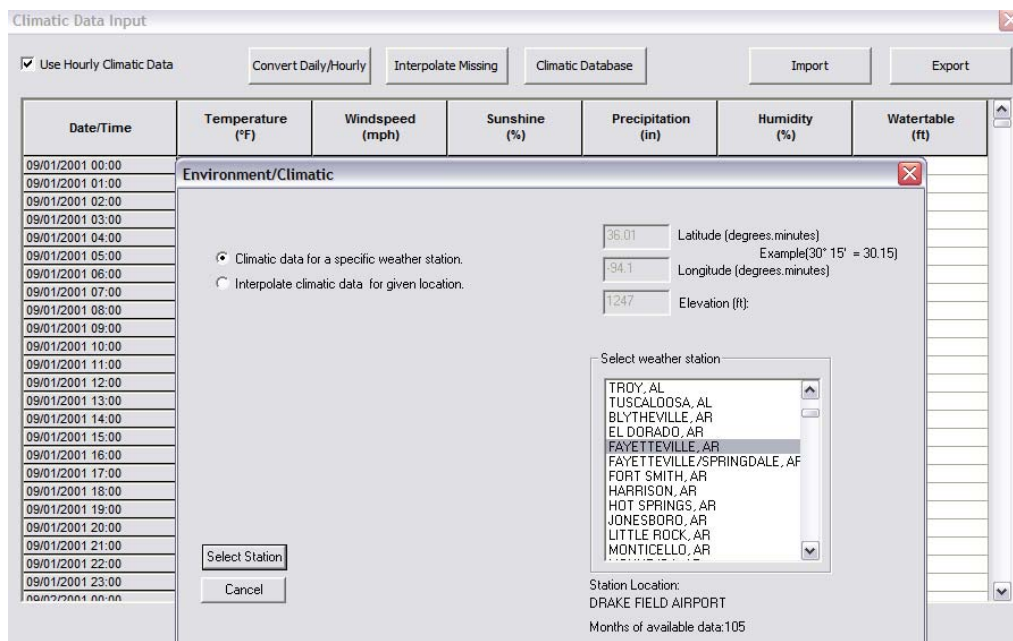
Figure E.5: Step 3 - Insert the time and location details

By clicking next, the user is prompted to enter weather data. It is recommended to develop an Excel file with hourly weather data, then to simply copy and paste the weather data into the window shown in Figure E.6.



Date/Time	Temperature (°F)	Windspeed (mph)	Sunshine (%)	Precipitation (in)	Humidity (%)	Watertable (ft)
08/01/2009 00:00	77.00	6.84	100.00	0.00	63.00	6.562
08/01/2009 01:00	77.00	6.84	100.00	0.00	63.00	6.562
08/01/2009 02:00	77.00	6.84	100.00	0.00	63.00	6.562
08/01/2009 03:00	77.00	6.84	100.00	0.00	63.00	6.562
08/01/2009 04:00	77.00	6.84	100.00	0.00	63.00	6.562
08/01/2009 05:00	77.00	6.84	100.00	0.00	63.00	6.562
08/01/2009 06:00	77.00	6.84	100.00	0.00	63.00	6.562
08/01/2009 07:00	77.00	6.84	100.00	0.00	63.00	6.562
08/01/2009 08:00	77.00	6.84	100.00	0.00	63.00	6.562
08/01/2009 09:00	77.00	6.84	100.00	0.00	63.00	6.562
08/01/2009 10:00	77.00	6.84	100.00	0.00	63.00	6.562
08/01/2009 11:00	77.00	6.84	100.00	0.00	63.00	6.562
08/01/2009 12:00	77.00	6.84	100.00	0.00	63.00	6.562
08/01/2009 13:00	77.00	6.84	100.00	0.00	63.00	6.562
08/01/2009 14:00	77.00	6.84	100.00	0.00	63.00	6.562
08/01/2009 15:00	77.00	6.84	100.00	0.00	63.00	6.562
08/01/2009 16:00	77.00	6.84	100.00	0.00	63.00	6.562
08/01/2009 17:00	77.00	6.84	100.00	0.00	63.00	6.562
08/01/2009 18:00	77.00	6.84	100.00	0.00	63.00	6.562
08/01/2009 19:00	77.00	6.84	100.00	0.00	63.00	6.562
08/01/2009 20:00	77.00	6.84	100.00	0.00	63.00	6.562
08/01/2009 21:00	77.00	6.84	100.00	0.00	63.00	6.562
08/01/2009 22:00	77.00	6.84	100.00	0.00	63.00	6.562
08/01/2009 23:00	77.00	6.84	100.00	0.00	63.00	6.562
08/01/2009 00:00	77.00	6.84	100.00	0.00	63.00	6.562

(a)



Environment/Climatic

Climatic data for a specific weather station.  
 Interpolate climatic data for given location.

Latitude (degrees.minutes): 36.01  
 Longitude (degrees.minutes): -94.1  
 Elevation (ft): 1247

Example(30° 15' = 30.15)

Select weather station:

- TROY, AL
- TUSCALOOSA, AL
- BLYTHERVILLE, AR
- EL DORADO, AR
- FAVETTEVILLE, AR**
- FAVETTEVILLE/SPRINGDALE, AR
- FORT SMITH, AR
- HARRISON, AR
- HOT SPRINGS, AR
- JONESBORO, AR
- LITTLE ROCK, AR
- MONTECELLO, AR

Station Location:  
DRAKE FIELD AIRPORT  
Months of available data:105

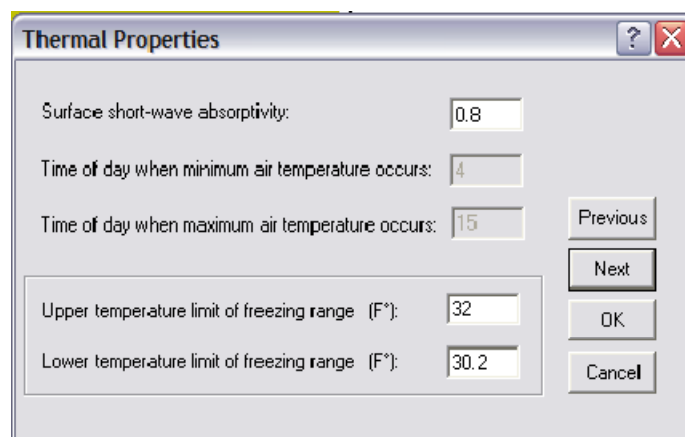
(b)

Figure E.6: Step 4 - Input hourly climatic data: (a) Inserting data from an external database; (b) Using the internal database

For site-specific analyses the weather data can be entered from an external or an internal weather database. The weather data for the seven sites analyzed in this study were obtained from an external database (the Weather Underground website). TRB also has an online climatic database available on the internet containing weather data from several sites throughout the country (TRB 2010). When downloading from the TRB site, the user must move the hourly climatic data file (\*.hcd) to a created folder (with a suffix of \*.hcd) in the EICM program folder. After this, the “Climatic Database” can be accessed in the EICM. The water table is not included

in the \*.hcd files and therefore must be input by the user into the EICM. After inputting data for a single hour the “Interpolate Data” option is available to fill in missing data. When all known information is input, continue to select next for each window correcting default values when necessary. Although not used in this study, the EICM has an internal database of some sites throughout the U.S.

The next step is to insert overall thermal properties for the analysis, as shown in Figure E.7. This includes information about freezing and radiation absorption. The information input in step 5 does not have a large impact on the output data, so the default values can be assumed.



Field	Value
Surface short-wave absorptivity	0.8
Time of day when minimum air temperature occurs	4
Time of day when maximum air temperature occurs	15
Upper temperature limit of freezing range (F°)	32
Lower temperature limit of freezing range (F°)	30.2

Figure E.7: Step 5 - Insert thermal properties

The in-depth details of the base course moisture calculations can be found in Appendix D (the ID model). The base course layer must have a greater value for saturated permeability than the layer immediately below it. Selecting the ME-PDG Thornthwaite Moisture Index Base Course Moisture option activates Equations D.21 and D.22. Specifically, Equation D.21 is used as the boundary condition for the base/subbase interface and equation D.22 is used as the boundary condition for the subbase/subgrade interface. Lytton et al. (1993) recommends this option be used when the groundwater table exceeds a depth of 25 feet. If the TTI Infiltration and Drainage Model is selected, additional information is required. The Dempsey-Robnett Model is activated if a crack length of zero is input. If any number is inserted, the program uses Ridgeway’s model in lieu of the Dempsey-Robnett model. The details of the types and amounts of fines in the base course do not appear to influence the output file. The internal flux or suction boundary condition (i.e., between the base and subgrade) does not seem to have an effect on the output files.



The ICM has two methods for determining base course moisture boundary condition.

The Mechanistic Empirical Pavement Design Guide (ME-PDG) Version 0.900 and later use a method based upon the Thornthwaite Moisture Index calculated from input climate data.

Earlier versions of the ME-PDG (Versions 0.700 and 0.800) and all previous versions of the ICM determined base moisture using an infiltration and drainage model developed by Robert Litton at Texas Transportation Institute.

ME-PDG Thornthwaite Moisture Index Base Course Moisture  
 TTI Infiltration and Drainage Model

Linear length cracks/joints: one side pavement (feet): 100

Total length surveyed for cracks and joints (feet): 100

Type of fines added to base course:  Clay  Silt  Inert filler

Percentage of fines added to base course: 2.5

Percentage of gravel in base course: 70

Percentage of sand in base course: 27.5

One side width of base (feet): 25

Slope ratio/base tangent value (percent): 1.5

Internal boundary condition:  Flux  Suction

Buttons: Previous, Next, OK, Cancel

Figure E.8: Step 6 - Base course moisture model details.

Clicking next will bring the user to the material input screens for the asphalt and soils again. After inputting the different material and geometry properties as discussed above, the next step is to input the initial temperature and water content profiles, as shown in Figure E.9. Unfortunately, the initial water content profile option has been disabled in the current version of the EICM. Instead, the EICM assumes that the water content is initially constant with depth. This is acceptable for compacted soils immediately after construction, but is not accurate for other analyses (especially as the EICM can only be run for a period of 1 year).

The easiest way to insert the initial temperature profile is to insert the mean annual air temperature at the top and bottom of the soil profile, then selecting “generate” and “temperature”. The program will automatically interpolate between these two values. It is important to select each node as an output node. This will allow the user to observe the results for each depth of the pavement profile. This can be done automatically by clicking “generate”, then “output nodes”, and “all nodes”, as shown in Figure E.10.

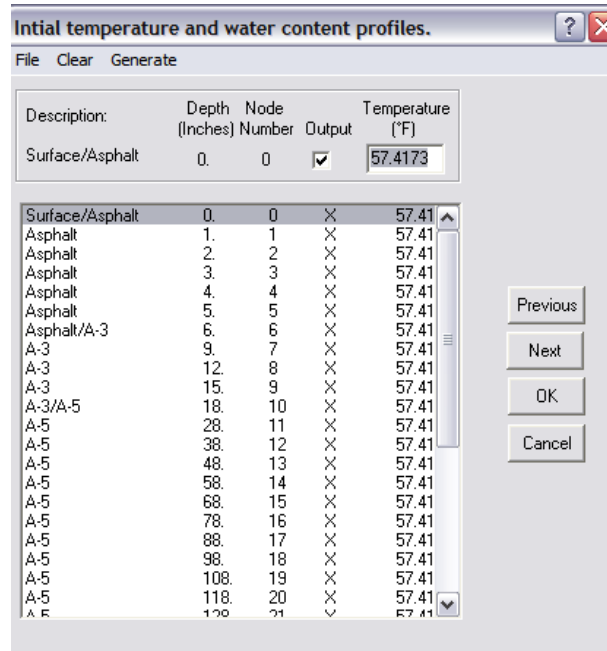


Figure E.9: Step 10 - Insert the initial temperature for each node and select nodes to model

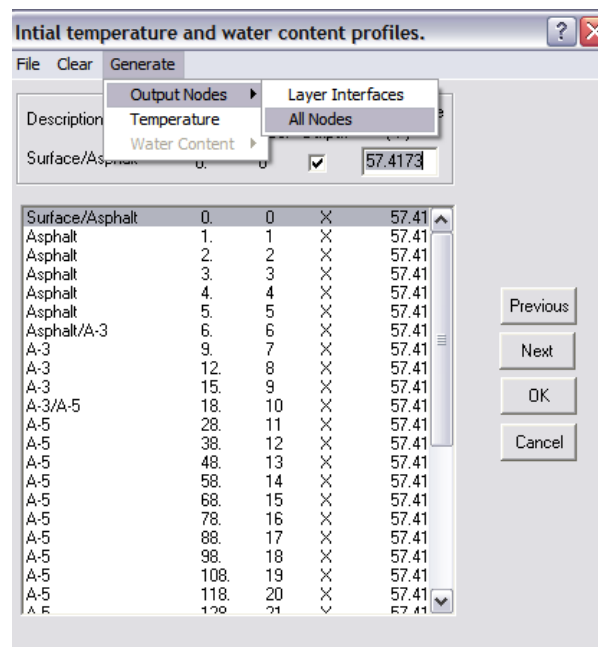


Figure E.10: Node description screen

After this, the EICM model is ready to be run. It can be executed by selecting the “run” command from the file menu. If there are any problems, the program will provide a warning. The main reasons for a warning are:

- Insufficient depth of the model (less than 240 inches)

- Daily weather data instead of hourly data
- Time duration longer than 1 year
- More than 100 elements in one soil layer

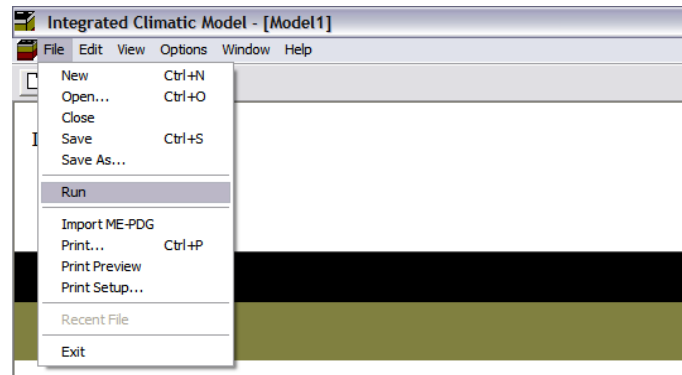


Figure E.11: Step 11 - Execute the model

The program will then run, and will tell the number of days left in the analysis. The model typically requires about 5 minutes to run. After running, the output results can be viewed by clicking “view” and “output files”, as shown in Figure E.12.

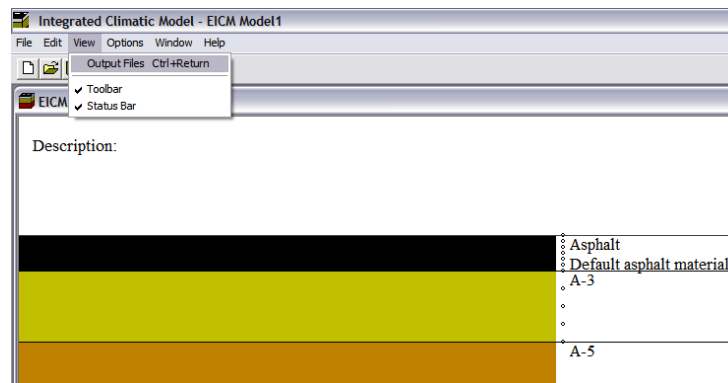


Figure E.12: Selection of output files

Viewing the output files is perhaps one of the bigger challenges of the EICM, but is straightforward after practice. The output file screen is shown in Figure E.13. The first step is to select whether the nodal or profile data is to be evaluated. The nodal data shows the variation in a parameter at a certain depth over the course of a certain time. The profile data shows the variation in a parameter with depth for a given time. To obtain a nodal plot, click “nodal”, then click a parameter (temperature, water content or pore water pressure, then click different depths (holding the control button to select multiple depths), then clicking multiple times (holding the shift button to select a range of dates). Then click “add”, then “tables only”. This will cause a file

to be created in the output files directory. This directory may be difficult to find. It is often easiest to search the computer for “\*.tem”, as this is one of the output files. To obtain a profile plot, click “profile”, then one or more of the parameters, then specific dates.

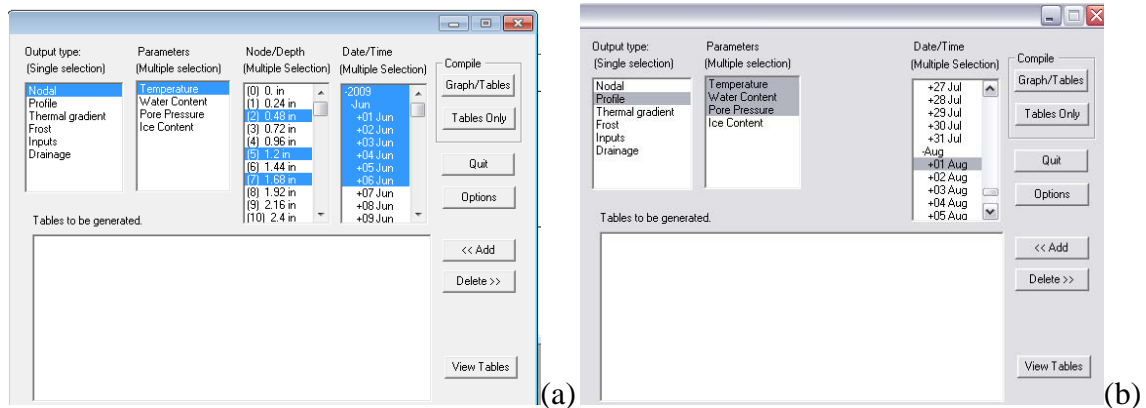


Figure E.13: Output data screens: (a) Nodal; (b) Profile

The output data can be viewed in either graphic form or raw data form. For the duration of this report, the results will be discussed in the form of plots and tables derived from the raw data. The raw data is obtained by selecting “Tables Only” from the output data window. This selection opens a folder where each output file is placed and the user can choose what data should be viewed. Plots are formed for this report by executing the following: open the data in Microsoft’s Excel; highlight the column of data; select “Data-Text to Columns”; choose option “fixed width”; and click at locations of the data to create a break. After this is done, a column is inserted for cumulative time elapsed. Next plots are inserted and data selected to model a representative amount of nodes. A representative amount of nodes contained in this report include a minimum of the upper node, lowest node, and intermediate node of each layer. Also the minimum amount of time series in each plot has been determined to be 10 data sets equally spaced throughout the year. Creating these plots may require a large processing speed due to the large file size.